

Medical University of South Carolina

MEDICA

MUSC Theses and Dissertations

2015

Stimulation of Mitochondrial Biogenesis through Induction Of cGMP Promotes Recovery of Mitochondrial and Renal Function Following Acute Kidney Injury

Ryan Michael Whitaker
Medical University of South Carolina

Follow this and additional works at: <https://medica-musc.researchcommons.org/theses>

Recommended Citation

Whitaker, Ryan Michael, "Stimulation of Mitochondrial Biogenesis through Induction Of cGMP Promotes Recovery of Mitochondrial and Renal Function Following Acute Kidney Injury" (2015). *MUSC Theses and Dissertations*. 488.

<https://medica-musc.researchcommons.org/theses/488>

This Dissertation is brought to you for free and open access by MEDICA. It has been accepted for inclusion in MUSC Theses and Dissertations by an authorized administrator of MEDICA. For more information, please contact medica@musc.edu.

Stimulation of Mitochondrial Biogenesis through Induction of cGMP Promotes Recovery of Mitochondrial and Renal Function Following Acute Kidney Injury

By

Ryan Michael Whitaker

A dissertation submitted to the faculty of the Medical University of South Carolina in partial fulfillment of the requirements for the degree of Doctor of Philosophy in the College of Graduate Studies.

Program in Drug Discovery and Biomedical Sciences

2015

Approved by:

Dr. Rick Schnellmann, Chairman, Advisory Committee

Dr. James Chou, Member, Advisory Committee

Dr. Craig Beeson, Member, Advisory Committee

Dr. Robin Muise-Helmericks, Member, Advisory Committee

Dr. Doug Pittman, Member, Advisory Committee

ADVISORY COMMITTEE



The image shows four handwritten signatures in blue ink, each written over a horizontal line. The signatures correspond to the names listed on the left: Rick Schnellmann, James Chou, Robin Muise-Helmericks, and Doug Pittman.

ACKNOWLEDGEMENTS

I would like to acknowledge the guidance that Dr. Rick G. Schnellmann provided that enabled me to complete this project. I would also like to thank my committee members: Dr. Craig Beeson, Dr. James Chou, Dr. Robin Muise-Helmericks, and Dr. Doug Pittman for their support and direction. I would like to acknowledge all the members of Dr. Schnellmann's laboratory who have assisted and supported me along the way. Finally, I would like to thank my beautiful and loving wife, Marie, for her neverending love and support, without which I would not be where I am today.

TABLE OF CONTENTS

Chapter 1: ACUTE KIDNEY INJURY AND MITOCHONDRIAL BIOGENESIS .1

Renal anatomy	2
Overview	2
The nephron	2
Renal vasculature.....	5
The glomerulus.....	5
The proximal tubule	6
Loop of Henle, distal tubule, and collecting duct	7
Acute kidney injury.....	7
Definition	7
Incidence, mortality, and cost.....	10
Types of AKI	12
Causes of AKI.....	12
Pathophysiology of ischemia/reperfusion-induced AKI	13
Animal models of AKI.....	21
Biomarkers	22
Pharmacological treatment of AKI.....	26
Mitochondrial dysfunction in disease	27
Mitochondrial homeostasis.....	27
Mitochondrial dysfunction in acute disease	30
Mitochondrial dysfunction AKI	34

Mitochondrial dysfunction in chronic disease.....	38
Mitochondrial biogenesis	41
Definition and overview	41
Physiological and pathophysiological activation of mitochondrial biogenesis.....	41
Pharmacological activation of mitochondrial biogenesis	48
Screening and validation of mitochondrial biogenics.....	56
Chapter 2: cGMP-SELECTIVE PHOSPHODIESTERASE INHIBITORS STIMULATE MITOCHONDRIAL BIOGENESIS AND PROMOTE RECOVERY FROM ACUTE KIDNEY INJURY	62
Abstract.....	63
Introduction.....	64
Experimental Procedures	67
Reagents	67
Animal care and use	67
Isolation and culture of proximal tubules.....	67
Oxygen consumption.....	68
Testing of compounds in C57BL/6 mice.....	68
Folic acid animal model	69
Quantitative real-time polymerase chain reaction	69
mtDNA content.....	70
cAMP and cGMP enzyme-linked immunosorbent assay	70
Tissue ATP levels.....	70
Data and statistical analysis.....	71
Results	72
Discussion.....	84
Chapter 3: EVALUATION OF PHOSPHODIESTERASE INHIBITORS IN A MODEL OF ACUTE-TO-CHRONIC KIDNEY DISEASE CHARACTERIZED BY MITOCHONDRIAL DYSFUNCTION.....	88

Abstract	89
Introduction	90
Experimental Procedures	93
Animal model	93
Histological analysis.....	94
mRNA analysis	94
Immunoblot analysis	95
Mitochondrial DNA content.....	95
Data and statistical analysis.....	96
Results	97
Discussion	109

**Chapter 4: THE GUANYLYL CYCLASE ACTIVATOR BAY 58-2667
STIMULATES MITOCHONDRIAL BIOGENESIS AND PROMOTES RECOVERY
FROM ISCHEMIA/REPERFUSION-INDUCED AKI..... 111**

Abstract	112
Introduction	113
Experimental Procedures	116
Isolation and culture of RPTCs.....	116
Measurement of oxygen consumption rate.....	116
Animal care and use	117
Testing of compounds in naïve mice	117
Ischemia/reperfusion (I/R)-induced AKI mouse model	117
Renal histology.....	118
Quantitative real-time PCR for mRNA and mtDNA expression.....	118
Immunoblotting for protein expression.....	119
Renal ATP levels.....	119
8-OH-dG and cGMP ELISA.....	120
Data and statistical analysis.....	120
Results	122

Discussion.....	141
------------------------	------------

Chapter 5: URINARY ATP SYNTHASE SUBUNIT β IS A NOVEL BIOMARKER OF RENAL MITOCHONDRIAL DYSFUNCTION IN ACUTE KIDNEY INJURY ... 147

Abstract.....	148
----------------------	------------

Introduction.....	149
--------------------------	------------

Experimental Procedures	151
--------------------------------------	------------

Mouse renal I/R-induced AKI model	151
---	-----

Mouse nonalcoholic steatohepatitis model	151
--	-----

Human urine samples	152
---------------------------	-----

Chemicals.....	154
----------------	-----

Oxygen consumption in isolated tubular segments	154
---	-----

Renal ATP levels.....	155
-----------------------	-----

Renal and urinary immunoblots	155
-------------------------------------	-----

ATPS β immunoprecipitation	156
--	-----

Urinary ATPS β identification with LC-MS/MS.....	156
--	-----

Data and statistical analysis.....	157
------------------------------------	-----

Results	158
----------------------	------------

Discussion.....	169
------------------------	------------

Chapter 6: URINARY MITOCHONDRIAL DNA IS A BIOMARKER OF MITOCHONDRIAL DISRUPTION AND RENAL DYSFUNCTION IN ACUTE KIDNEY INJURY 173

Abstract.....	174
----------------------	------------

Introduction.....	175
--------------------------	------------

Experimental Procedures	178
--------------------------------------	------------

Human urine samples	178
Animals and treatment.....	178
Quantitative reverse transcription polymerase chain reaction.....	179
Renal mtDNA content	179
Isolation and quantification of urinary mtDNA.....	179
Data and statistical analysis	180
Results	181
Discussion.....	197
Chapter 7: CONCLUSIONS, UNANSWERED QUESTIONS AND FUTURE DIRECTIONS	203
Conclusions.....	204
Unanswered questions.....	214
Future Directions.....	216
References.....	230

LIST OF FIGURES

Chapter 1

Figure 1.1: Kidney gross anatomy.....	3
Figure 1.2: Nephron structure and blood supply.....	4
Figure 1.3: AKI classification schemes.....	9
Figure 1.4: Mean hospital costs associated with change in serum creatinine.....	11
Figure 1.5: Pathogenesis of ischemic AKI.....	14
Figure 1.6: Effects of sub-lethal injury to tubular cells and their recovery.....	20
Figure 1.7: Biomarkers of AKI.....	25
Figure 1.8: Mitochondrial homeostasis is maintained through balanced biogenesis of new mitochondria, mitochondrial fission and fusion, and mitochondrial turnover by mitophagy.....	29
Figure 1.9: Mitochondrial ultrastructural changes.....	36
Figure 1.10: Sustained depletion of mitochondrial proteins after I/R AKI.....	37
Figure 1.11: Diverse physiological signals regulate mitochondrial biogenesis in a tissue-specific manner.....	42
Figure 1.12: Induction of PGC-1 α protein.....	45
Figure 1.13: Overexpression of PGC-1 α after oxidant injury.....	46
Figure 1.14: Formoterol stimulates mitochondrial biogenesis and promotes recovery of renal and mitochondrial function after I/R.....	47
Figure 1.15: Identification of stimulators of mitochondrial biogenesis with high-throughput respirometry and virtual screening.....	61

Chapter 2

Figure 2.1: PDE3 inhibitors, but not PDE4 inhibitors, increase FCCP-induced uncoupled mitochondrial respiration in RPTCs.....	73
Figure 2.2: PDE3 inhibitors, cilostamide or trequinsin, induce mitochondrial gene expression in RPTC.....	74
Figure 2.3: PDE inhibitor-induced increases in cGMP, but not cAMP, stimulate MB in RPTCs.....	76
Figure 2.4: The PDE5 inhibitor sildenafil stimulates MB in RPTCs.....	78
Figure 2.5: PDE3 inhibitors, cilostamide and trequinsin, induce mitochondrial gene expression and mtDNA copy number in mouse renal cortex.....	79
Figure 2.6: Sildenafil induces mitochondrial gene expression, mtDNA copy number, and ATP levels in mouse renal cortex.....	81
Figure 2.7: Sildenafil stimulates MB after FA-induced AKI.....	83

Chapter 3

Figure 3.1: Folic acid (FA) causes AKI.....	98
Figure 3.2: Histopathology of progressive FA nephropathy.....	99
Figure 3.3: Mitochondrial biogenesis is persistently down-regulated during FA nephropathy..	101
Figure 3.4: Time-matched control study.....	102
Figure 3.5: Early fibrosis and CKD in FA nephropathy.....	104
Figure 3.6: Measurement of urinary albumin and protein in FA nephropathy.....	106
Figure 3.7: Sildenafil does not promote recovery of mitochondrial biogenesis or limit fibrosis in FA-induced AKI.....	108

Chapter 4

Figure 4.1: BAY 41-2272 and BAY 58-2667 increase FCCP-uncoupled OCR in RPTC.....	123
Figure 4.2: BAY 58-2667, but not BAY 41-2272, stimulates mitochondrial biogenesis in mouse renal cortex.....	125
Figure 4.3: BAY 58-2667 promotes recovery from ischemia-reperfusion (I/R)-induced AKI..	127
Figure 4.4: BAY 58-2667 reduces renal tubular necrosis following I/R-induced AKI.....	129
Figure 4.5: BAY 58-2667 stimulates recovery of mitochondrial gene expression and mtDNA copy number following renal I/R.....	132
Figure 4.6: BAY 58-2667 promotes recovery of renal mitochondrial protein expression and ATP levels.....	133
Figure 4.7: BAY 58-2667 reduces renal fibrotic development following I/R.....	135
Figure 4.8: BAY 58-2667 reduces renal inflammatory cytokine expression.....	137
Figure 4.9: BAY 58-2667 reduces renal oxidative damage.....	138
Figure 4.8: BAY 58-2667 promotes recovery of renal eNOS expression, but has no effect on renal cGMP.....	140

Chapter 5

Figure 5.1: Urinary ATP synthase subunit β (ATPS β) is increased following I/R-induced AKI.....	160
Figure 5.2: Representative renal histology from various ischemia times.....	161
Figure 5.3: Renal cortical mitochondrial protein expression is reduced after I/R-induced AKI.....	162
Figure 5.4: Mitochondrial function is reduced after mild, moderate, or severe I/R-induced AKI.....	163
Figure 5.5: Urinary ATP synthase subunit β (ATPS β) expression time course in mice after I/R-induced AKI.....	165
Figure 5.6: Cleaved urinary ATP synthase subunit β (ATPS β) but not full length is elevated in a NASH model.....	166
Figure 5.7: Urinary ATP synthase subunit β (ATPS β) is elevated in human patients following cardiac surgery-induced AKI.....	168

Chapter 6

Figure 6.1: Urinary mtDNA copy number is not correlated with AKIN stage following cardiopulmonary bypass (CPB)-induced AKI in humans.....	183
Figure 6.2: Urinary mtDNA copy number is associated with progression of renal dysfunction from collection in patients with CPB-induced AKI.....	185
Figure 6.3: Urinary mtDNA copy number is not correlated with degree of CPB-induced AKI in humans.....	187
Figure 6.4: Urinary mtDNA levels are increased in mice following renal I/R.....	189
Figure 6.5: Total urinary output of mtDNA is correlated with degree of ischemia, but not BUN.....	190
Figure 6.6: Urinary mtDNA levels corrected for urinary creatinine are a marker of renal injury in mice.....	191
Figure 6.7: Total 18h urinary output of mtDNA is a biomarker of renal injury following I/R in mice.....	193
Figure 6.8: Total 18 h urinary output of mtDNA correlates with reductions in renal mtDNA copy number and mitochondrial gene expression.....	195
Figure 6.9: Urinary mtDNA levels corrected for urine creatinine correlate with a reduction of renal mitochondrial DNA copy number and mitochondrial gene expression in mice.....	196

Chapter 7

Figure 7.1: PGC-1 α and Tfam are suppressed 3 h after I/R injury.....	218
Figure 7.2: mtDNA copy number is suppressed 3 h after I/R injury.....	219
Figure 7.3: Mitochondrial-encoded mitochondrial genes are suppressed at 3 h after I/R.....	220
Figure 7.4: Nuclear-encoded mitochondrial genes are suppressed at 3 h after I/R.....	221
Figure 7.5: Renal cortical TNF- α is upregulated at 3 h after I/R.....	223
Figure 7.6: Renal mir-494 and mir-696 are upregulated after I/R.....	224
Figure 7.7: Sample of new ATP5 β antibody clone immunoblot results.....	226
Figure 7.8: mtDNA is released after oxidant injury and is associated with suppression of cellular mtDNA content and PGC-1 α expression.....	228
Figure 7.9: Effect of TLR9 agonists on mitochondrial gene expression in TKPTS cells.....	229

LIST OF TABLES

Table 1.1: Select listing of acute and chronic diseases implicating mitochondrial dysfunction...	31
Table 1.2: Select listing of pharmacological activators of mitochondrial biogenesis.....	49
Table 5.1: Sample clinical characteristics from cardiac surgery patients with AKI or no AKI..	153
Table 6.1: Patient demographics and clinical characteristics of cardiac surgery patients.....	182

ABBREVIATIONS

ADH = antidiuretic hormone
AKI = acute kidney injury
AKIN = Acute Kidney Injury Network
ALT = alanine transaminase
 α SMA = alpha smooth muscle actin
AMP = adenosine monophosphate
AMPK = AMP-activated protein kinase
ANP = atrial natriuretic peptide
ARF = acute renal failure
ATP = adenosine triphosphate
ATPS β (or ATP β) = ATP synthase subunit beta
AUC = area under curve
BAT = brown adipose tissue
 β 2AR = beta 2 adrenergic receptor
BNP = brain natriuretic peptide
BUN = blood urea nitrogen
CABG = coronary artery bypass graft
cAMP = cyclic adenosine monophosphate
cGMP = cyclic guanosine monophosphate
CHF = congestive heart failure
CKD = chronic kidney disease
COL1A2 = collagen 1A2
COXI = cytochrome c oxidase subunit 1
COXIV = cytochrome c oxidase subunit 4
CREB = cAMP-response element-binding protein
CSA = cyclosporine A
DA = dopaminergic
DAMPs = damage-associated molecular patterns

DEPC = diethylpyrocarbonate
Drp1 = dynamin related protein 1
EGF = epidermal growth factor
EGFR = epidermal growth factor receptor
ELISA = enzyme-linked immunosorbent assay
EMT = epithelial to mesenchymal transition
eNOS = endothelial nitric oxide synthase
ERK1/2 = extracellular signal-related kinases
ERR = estrogen-related receptor
ESRD = end stage renal disease
ETC = electron transport chain
FA = folic acid
FAO = fatty acid oxidation
FCCP = carbonylcyanide-p-trifluoromethoxyphenylhydrazone
FENa = fractional excretion of sodium
GC = guanylyl (or guanylate) cyclase
GFR = glomerular filtration rate
H&E = hematoxylin & eosin
HAVCR1 = hepatitis A virus cellular receptor 1
HBSS = Hank's buffered salt solution
HSC = hematopoietic stem cell
ICU = intensive care unit
IL-1 β = interleukin 1 beta
IQR = interquartile range
I/R = ischemia/reperfusion
KDIGO = Kidney Disease Improving Global Outcomes Consortium
KIM-1 = kidney injury molecule-1
LC-MS/MS = liquid chromatography-tandem mass spectrometry
LR = likelihood ratio
MB = mitochondrial biogenesis
MCP-1 = monocyte chemoattractant protein 1
MFN1/2 = mitofusin 1/2
MI = myocardial infarction
miRNA = microRNA
MnSOD = manganese superoxide dismutase
MPTP = mitochondrial permeability transition pore
MSC = mesenchymal stem cell
mtDNA = mitochondrial DNA
NADH = nicotinamide adenine dinucleotide
NASH = nonalcoholic steatohepatitis

NDUFB8 = NADH dehydrogenase (ubiquinone) 1 beta subcomplex 8
ND1 = NADH dehydrogenase 1
ND6 = NADH dehydrogenase 6
nDNA = nuclear DNA
NGAL = neutrophil gelatinase-associated lipocalin
NO = nitric oxide
NRF1/2 = nuclear respiratory factor 1/2
NSAIDs = non-steroidal anti-inflammatory drugs
OCR = oxygen consumption rate
OPA1 = optic atrophy 1
OXPHOS = oxidative phosphorylation
PAS = Periodic Acid Schiff
PCNA = proliferating cell nuclear antigen
PD = Parkinson's disease
PDE = phosphodiesterase
PGC-1 α = Peroxisome proliferator activated receptor gamma-coactivator-1-alpha
PKA = protein kinase A
PKG = protein kinase G
PPAR = peroxisome proliferator-activated receptor
p38 MAPK = p38 mitogen-activated protein kinase
qRT-PCR = quantitative reverse transcription polymerase chain reaction
RIFLE = Risk, Injury, Failure, Loss and End-stage renal disease
RMSD = root mean square deviation
ROC = receiver operator curve
ROS = reactive oxygen species
RPTC = renal proximal tubular cell
RRT = renal replacement therapy
RTK = receptor tyrosine kinase
SAKInet = Southern Acute Kidney Injury Network
SCr = serum creatinine
SEM = standard error of mean
sGC = soluble guanylyl cyclase
SIRT1 = sirtuin 1
SIRT3 = sirtuin 3
SN = substantia nigra
TBHP = tert-butyl hydroperoxide
TCA = tricarboxylic acid cycle
TFAM = mitochondrial transcription factor A
TFB1M = mitochondrial transcription factor B 1
TFB2M = mitochondrial transcription factor B 2

TGF- β = transforming growth factor β
TIF = tubulointerstitial fibrosis
TIM = translocase of inner membrane
Tim-1 = T-cell immunoglobulin and mucin domain 1
TLR = toll-like receptor
TNF α = tumor necrosis factor alpha
TOM = translocase of outer membrane
UCP1 = uncoupling protein 1
UmtDNA = urinary mtDNA
VEGF = vascular endothelial growth factor
WBC = white blood cell
ZDF = Zucker diabetic fatty rats
5HT = serotonin
8-OH-dG = 8-hydroxy-deoxyguanosine

ABSTRACT

RYAN MICHAEL WHITAKER, Stimulation of Mitochondrial Biogenesis through Modulation of cGMP Promotes Recovery of Mitochondrial and Renal Function Following Acute Kidney Injury (under the direction of Dr. Rick Schnellmann, PhD)

Mitochondrial damage and dysfunction are major pathophysiological mechanisms underlying acute kidney injury (AKI). Following various forms of AKI, mitochondrial biogenesis, the *de novo* generation of new, functional mitochondria, is suppressed. Pharmacological stimulation of PPAR γ -coactivator-1 α (PGC-1 α), the master regulator of mitochondrial biogenesis, promotes recovery of mitochondrial and renal function after AKI. The primary goals of this project were the evaluation of renal cGMP as a modulator of mitochondrial biogenesis in AKI, and the assessment of phosphodiesterase (PDE) inhibitors and guanylyl cyclase (GC) activators as novel agents to induce mitochondrial biogenesis and promote renal recovery.

cGMP has been demonstrated to stimulate mitochondrial biogenesis and function. Both cGMP generation through guanylyl cyclase and degradation through PDEs are highly regulated processes. Compounds that regulate cGMP levels, including the PDE3 inhibitors cilostamide and trequinsin, and the PDE5 inhibitor sildenafil, increased mitochondrial gene expression, and

elevated mitochondrial respiration in renal proximal tubule cell (RPTC) cultures. Furthermore, these compounds increased renal cortical mitochondrial gene expression and mtDNA copy number in naïve mice. PDE4 inhibitors, which regulate only cAMP levels had no effect. Treatment of mice with sildenafil in a folic acid model of AKI promoted recovery of mitochondrial gene expression, increased mtDNA content, and reduced expression of the tubular injury marker, kidney injury molecule-1 (KIM-1).

An occurrence of AKI is a strong risk factor for the development of chronic kidney disease (CKD) and end stage renal disease (ESRD). Following folic acid-induced AKI, mice developed renal fibrosis and early signs of CKD. These changes were associated with a chronic suppression of mitochondrial gene expression and mtDNA copy number. Treatment of mice with trequinsin or sildenafil failed to restore mitochondrial gene expression, and failed to prevent the progression of fibrosis.

Induction of cGMP through activation of guanylyl cyclase by the compound BAY 58-2667 increased mitochondrial respiration in RPTC, and additionally, increased mitochondrial gene and protein expression, and mtDNA copy number in mouse renal cortex. Daily treatment of mice with BAY 58-2667 beginning 24 h after renal ischemia-reperfusion (I/R) injury promoted renal functional and morphological recovery at 144 h after reperfusion. Renal inflammation and oxidative stress were also reduced. Renal recovery was associated with recovery of mitochondrial gene and protein expression, and mtDNA content in the renal cortex.

Taken together, we have demonstrated that cGMP is a regulator of mitochondrial biogenesis in the kidney, and activation of mitochondrial biogenesis through modulators of cGMP can promote recovery of renal function following AKI. PDE inhibitors and guanylyl cyclase

activators represent novel therapeutics that warrant further evaluation as potential interventions to treat AKI and other diseases characterized by mitochondrial dysfunction. To provide a platform for clinical evaluation of mitochondrial biogenics in renal disease in humans, we examined urinary ATP synthase subunit beta and urinary mtDNA as non-invasive biomarkers of renal mitochondrial dysfunction. These markers were shown to be efficacious as diagnostic and/or prognostic biomarkers of renal damage and mitochondrial dysfunction, and will aid in future development of mitochondrial-targeted renal therapies.

CHAPTER 1:

Acute kidney injury and mitochondrial biogenesis

RENAL ANATOMY AND PHYSIOLOGY

Overview

The kidneys serve a critical role in the maintenance of fluid homeostasis through regulation of filtration, reabsorption and secretion of substances in the blood. The kidney serves as the central regulator of body fluid volume, maintains electrolyte balance, including sodium, potassium and calcium, and blood pH, and clears the body of harmful metabolic waste products, including urea and ammonia, as well as various toxins and xenobiotics. The kidney also serves as a major regulator of blood pressure both through its regulation of fluid volume and through secretion of the hormone renin and activation of the renin-angiotensin-aldosterone signaling cascade. The kidney is divided into three distinct zones: the outermost region called the renal cortex, the renal medulla (consisting of the outer medulla composed of the outer and inner stripe regions and the inner medulla), and innermost renal papilla (Figure 1.1). These zones differ significantly in their morphology, function and extracellular conditions (i.e. pH and oxygen tension).

The nephron

The nephron is the basic functional unit of the kidney involved in the process of urine generation for excretion (Figure 1.2). The nephron prepares urine through a complex series of processes involving the filtration, secretion and reabsorption of fluid and electrolytes. The nephron is composed of the glomerulus, the site of renal filtration, and the renal tubule (comprised of the proximal tubule, the ascending and descending limbs of the loop of Henle, the distal tubule and the collecting duct). The following section will provide a detailed discussion of structure and function of the various sections of the nephron.

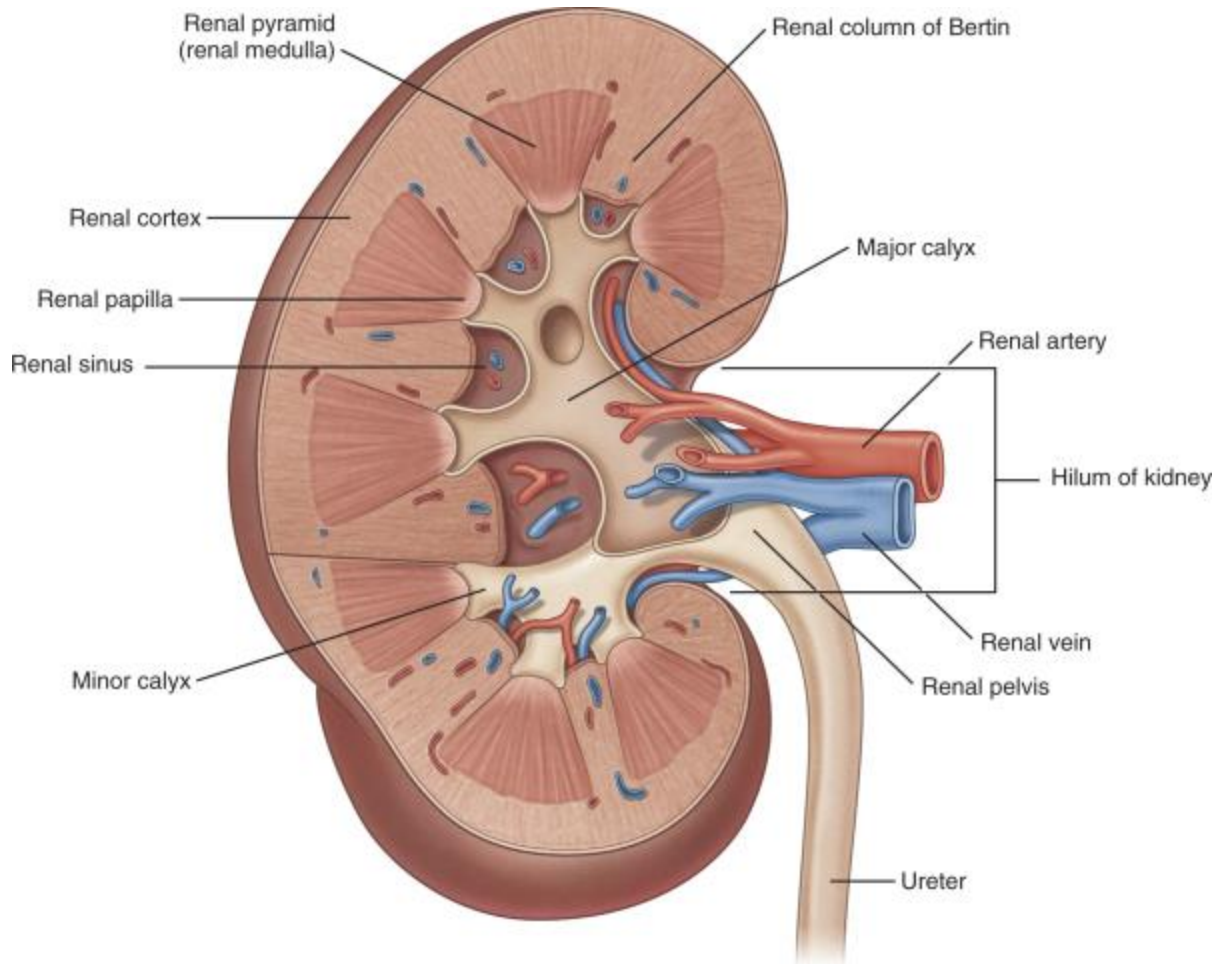


Figure 1.1: Kidney gross anatomy.

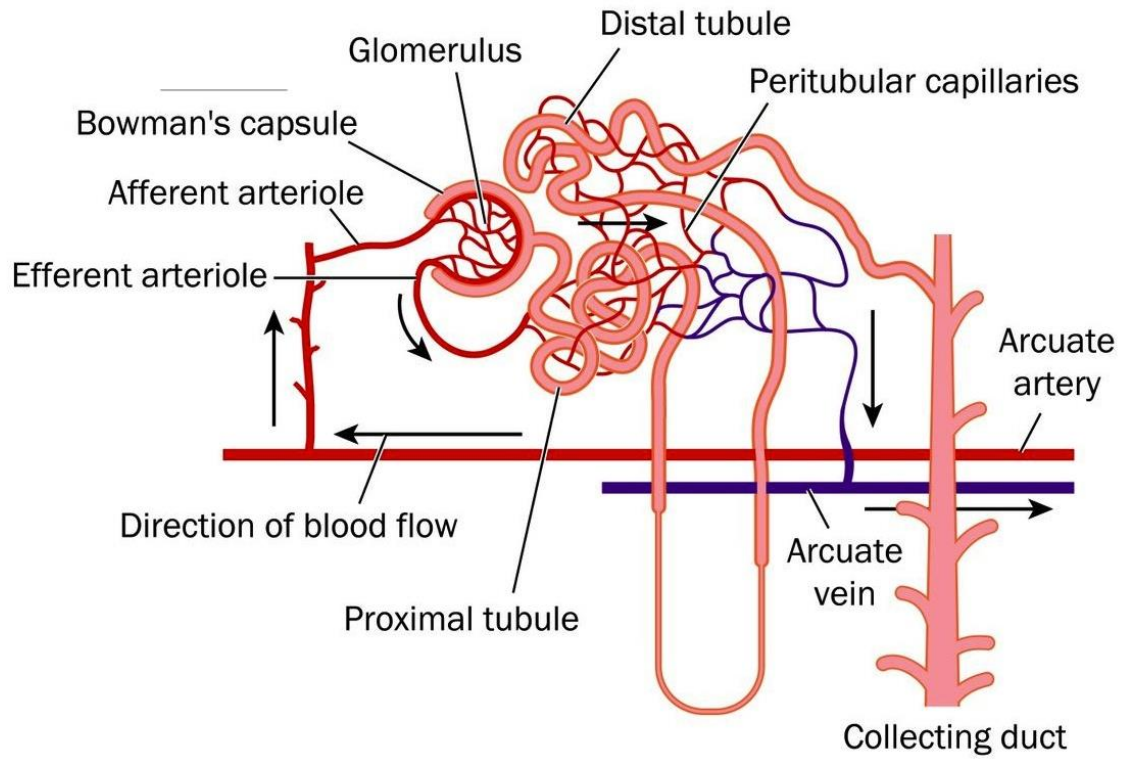


Figure 1.2: Nephron structure and blood supply.

Renal vasculature

Blood is supplied to the kidney via the renal artery, a branch of the descending aorta, which enters at the renal pelvis. The renal artery divides into 4-5 segmental branches supplying various regions of the kidney. These further subdivide into the afferent arterioles which supply the blood to the capillary bed of the glomerulus. Efferent arterioles carry blood away from the glomerulus. Regulation of vascular tone in the afferent and efferent arterioles affects renal filtration by modulating renal blood flow and hydrostatic pressure. Afferent and efferent arterioles are regulated via the autonomic nervous system as well as a variety of paracrine and endocrine signals including angiotensin, ADH, endothelin, adenosine and norepinephrine. After exiting the glomerulus via the efferent arterioles, blood is carried to the peritubular network supplying the renal cortex, or the vasa recta supplying the renal medulla. The renal cortex, which is highly dependent on oxidative phosphorylation for energy, receives approximately 90% of renal blood flow, while the renal medulla and papilla, which rely primarily on glycolytic metabolism receives the remaining 10%. These capillary networks converge to renal venules which combine to form segmental renal veins. These segmental veins converge to the renal vein which carries filtered, deoxygenated blood away from the kidney.

The glomerulus

The glomerulus serves as the site of plasma filtration in the nephron. Plasma components pass through a barrier consisting of the renal capillary endothelium, the vascular basement membrane, and the glomerular epithelium made up of cells called podocytes, into a cavity called Bowman's space. Fluid readily passes across this barrier (normally 20% of renal plasma flow is filtered); however, the passage of plasma solutes is restricted in a size- and charge-dependent

manner. Generally, small molecules (<60 kDA, or approximately the size of plasma albumin) are freely filtered, while larger molecules, i.e. large proteins and polysaccharides, remain in the blood due to the pore size created by the direct interaction of podocytes with the glomerular endothelium. Additionally, the movement of highly anionic molecules into the glomerular filtrate is limited by electrostatic repulsion with the anionic glomerular basement membrane. Glomerular filtration rate (GFR), the rate at which fluid moves from the blood to the renal filtrate at the glomerulus, serves as a measure of glomerular functional capacity. Normal GFR is approximately 180 mL/min; however, much of this filtrate is reabsorbed in the renal tubules to prevent excessive fluid loss in the urine.

The proximal tubule

The renal filtrate from the glomerulus passes first to the proximal tubule. The proximal tubule is the primary site of reabsorption of both fluid and electrolyte components of the renal filtrate. In fact, >75% of the water filtered at the glomerulus is reabsorbed in the proximal tubule. Additionally, 65% of filtered Na^+ , as well as other ions including Cl^- , Ca^{2+} , PO_4^{3-} and HCO_3^- are highly reabsorbed back into the blood through various ion transporters. Furthermore, larger molecules including glucose and other carbohydrates, amino acids and oligopeptides are reabsorbed through active and facilitated transport. Activity of these various transporters places high oxygen and energy demands on the proximal tubule, the primary consumer of ATP in the kidney. The proximal tubule can be subdivided into 3 structurally and functionally distinct regions: S1, S2 and S3. Structurally the segments can be identified by distinct brush border morphology, as well as significant differences in mitochondrial and lysosomal content. Furthermore, each section is characterized by differential transporter expression leading to distinctions in the reabsorptive capacity for various solutes. The S1 segment serves as the

primary site of HCO_3^- transport, as well as small proteins, amino acids and carbohydrates. Both the S1 and S2 segments contain cation active transporters, while the S2 and S3 sections contain multiple organic anion transporters involved in the secretion of various endogenous substrates including cyclic nucleotides, urate and folate, as well as pharmacological agents, including antibiotics and non-steroidal anti-inflammatory drugs (NSAIDs).

Loop of Henle, distal tubule and collecting duct

The loop of Henle is comprised of the thin descending and ascending limbs and the thick ascending limb. Much of the remaining water, Na^+ and K^+ is reabsorbed at this site. Urine filtrate is concentrated in the descending limb due to the reabsorption of water and impermeability to ions. Na^+ , K^+ and Cl^- are secreted in the ascending limb through activity of the $\text{Na}^+ - \text{K}^+ - \text{Cl}^-$ co-transporter. Secretion of ions into the renal medulla creates the osmotic gradient required for concentration of urine in the collecting duct. The distal tubule and collecting duct serve as the final sites of solute and water reabsorption for generation of concentrated urine. The distal tubule also directly interacts with a specialized group of cells called the juxtaglomerular apparatus composed of juxtaglomerular cells and the macula densa. This structure produces renin in response to decreased filtrate pressure causing increased renal blood flow and GFR.

ACUTE KIDNEY INJURY

Definition

Acute kidney injury (AKI) is the abrupt (occurring in less than 7 days) loss of renal function characterized by reduced urine output and an increase in the serum waste products, creatinine and urea [1]. The classical term acute renal failure (ARF), defined by a sudden

reduction in GFR, was replaced by AKI to provide a more encompassing definition to include renal damage that does not result in changes in GFR. In 2012, the KDIGO (Kidney Disease Improving Global Outcomes) consortium introduced specific guidelines for the diagnosis of AKI (Figure 1.3) [2]. AKI can be diagnosed if one of the following is present: an increase in serum creatinine (SCr) by ≥ 0.3 mg/dL within 48 hours, an increase in SCr ≥ 1.5 times baseline within 7 days, or a urine output of < 0.5 mL/kg/hr for 6 hours. The term renal failure is more narrowly used to define conditions requiring the application of renal replacement therapy (RRT) or dialysis. Additional classification schemes have been developed including the Acute Kidney Injury Network (AKIN) staging system, and the Risk, Injury, Failure, Loss and End-stage renal disease (RIFLE) criteria (Figure 1.3). The RIFLE criteria provides a classification scheme to follow the progression from mild, subclinical renal injury to significant, clinical renal dysfunction to permanent loss of renal function and need for dialysis. The RIFLE criteria defines Risk as a 1.5-fold increase in SCr or a 25% decrease in GFR, Injury as a 2-fold increase in SCr or 50% reduction in GFR, Failure as a 3-fold increase in SCr or a 75% reduction in GFR. Loss of kidney function is classified as persistent renal failure, and end-stage renal disease when renal replacement therapy is needed. AKIN classifies AKI in 3 stages similar to KDIGO staging. Use of classification systems has aided in standardization of patient populations allowing for greater comparison of diagnostic, prognostic and therapeutic renal studies.

Urine output (common to all)	KDIGO stage ^{198, 199} Serum creatinine		AKIN stage Serum creatinine		RIFLE class Serum creatinine or GFR	
<0.5 mL/kg/h for 6 h	Stage 1	Increase of 1.5–1.9 times baseline or $\geq 27 \mu\text{mol/L}$ ($\geq 0.3 \text{ mg/dL}$) increase	Stage 1	Increase to >150–200% (1.5–2-fold) from baseline or $\geq 27 \mu\text{mol/L}$ ($\geq 0.3 \text{ mg/dL}$) increase	Risk	Increase in serum creatinine $\times 1.5$ or GFR decrease >25%
<0.5 mL/kg/h for 12 h	Stage 2	Increase of 2–2.9 times baseline	Stage 2	Increase to >200–300% (>2–3-fold) from baseline	Injury	Increase in serum creatinine $\times 2$ or GFR decreased >50%
<0.3 mL/kg/h for 24 h or anuria for 12h	Stage 3	Increase of >3 times baseline or increase in serum creatinine to $\geq 354 \mu\text{mol/L}$ ($\geq 4 \text{ mg/dL}$) or initiation of RRT	Stage 3	Increase to >300% (>3-fold) from baseline or $\geq 354 \mu\text{mol/L}$ ($\geq 4 \text{ mg/dL}$) with an acute increase of $>44 \mu\text{mol/L}$ ($>0.5 \text{ mg/dL}$) or initiation of RRT	Failure	Increase in serum creatinine $\times 3$ or serum creatinine $\geq 354 \mu\text{mol/L}$ ($>4 \text{ mg/dL}$) with an acute rise $\geq 44 \mu\text{mol/L}$ ($>0.5 \text{ mg/dL}$) or GFR decreased >75%
ESRD					ESRD >3 months	

Figure 1.3: AKI classification schemes. KDIGO, Kidney Disease Improving Global Outcomes, AKIN, Acute Kidney Injury Network, RIFLE, Risk, Injury, Failure, Loss, End Stage Renal Disease [3].

Incidence, mortality and cost

AKI is an under-recognized condition that affects a significant portion of hospitalized patients. AKI is estimated to occur in 3-7% of all hospitalized patients, rising to 25-30% in patients admitted to the intensive care unit (ICU) [4-6]. Due to an array of increasing risk factors including an aging population, increased use of nephrotoxic medications, and higher rates of metabolic and cardiovascular disease, the rates of AKI continue to increase. AKI is associated with high rates of morbidity and mortality [7-9]. Among ICU patients, mortality rates are estimated to be as high as 80%. Patients that recover from AKI are often plagued by an array of chronic sequelae, including a highly elevated risk of development of chronic kidney disease (CKD) [10, 11]. Due to the need for aggressive treatment and application of renal replacement therapy (RRT), the cost of treatment of AKI is high. Annual U.S expenditures associated with the treatment of AKI are estimated to exceed \$9 billion per year; however, the exact costs associated with AKI are difficult to determine due to the presence of underlying conditions and AKI complications. Stratification of patients by degree of AKI and evaluation of additional consequences attributed to incremental increases in severity of AKI has shed some light on the overall impact of AKI on patient outcomes and healthcare cost. Even a moderate, yet clinically relevant, increase in serum creatinine levels (0.3-0.4 mg/dL) results in a 70% increase in the risk of death, an increase in the length of hospital stay of 3.5 days, and an added cost of \$9000 per patient [9]. Larger increases in SCr lead to exponential increases in morbidity and mortality, and healthcare costs (Figure 1.4A, B). These results further highlight the importance of standardized AKI classification systems, including the RIFLE and AKIN criteria, to provide better data for correlation of degree of renal injury with outcomes, and a platform to better compare data across clinical studies with diverse patient populations.

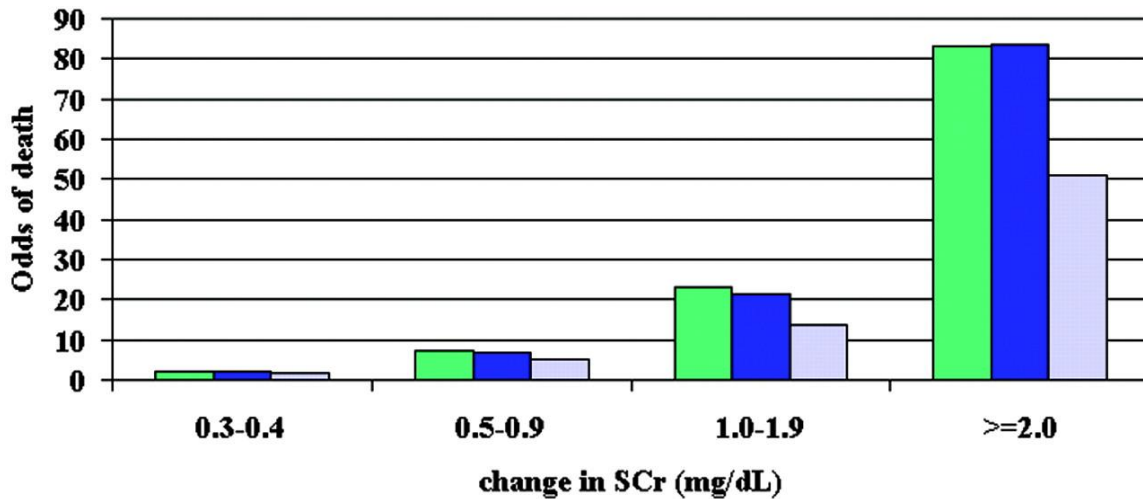


Figure 1.4A: Mortality associated with change in serum creatinine. Green bars are unadjusted, blue bars are age and gender adjusted, and gray bars are multivariable adjusted. Multivariable analyses adjusted for age, gender, diagnosis-related group (DRG), weight, chronic kidney disease (CKD) status, and ICD-9-CM codes for respiratory, gastrointestinal, malignant, and infectious diseases; n=1564, 885, 246, and 105 for change in SCr 0.3-0.4, 0.5-0.9, 1-1.9, and ≥2.0 mg/dL[9].

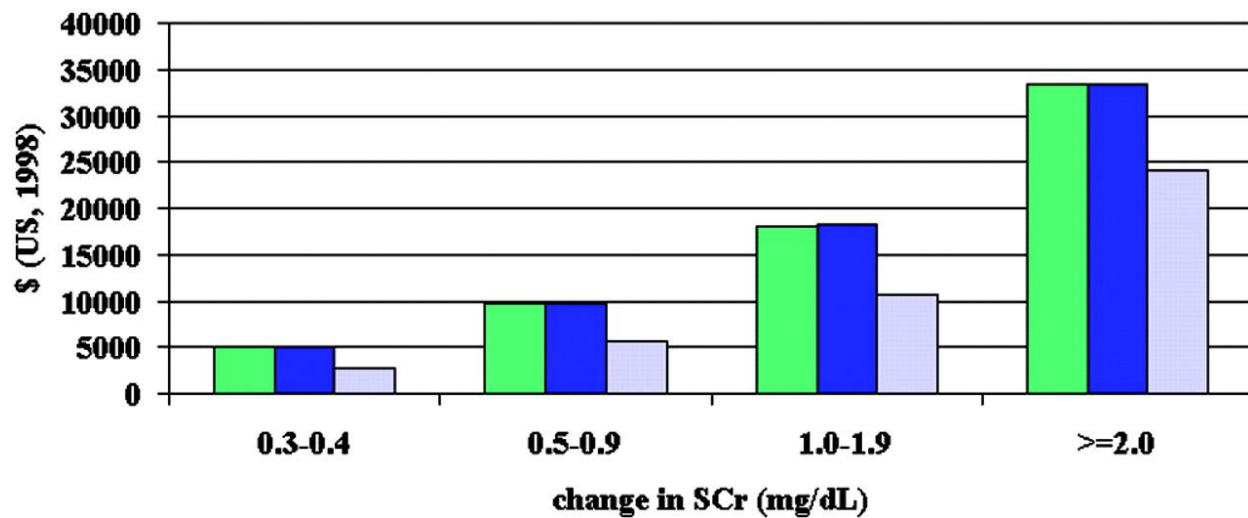


Figure 1.4B: Mean hospital costs associated with change in serum creatinine. Green bars are unadjusted, blue bars are age and gender adjusted, and gray bars are multivariable adjusted. Multivariable analyses adjusted for age, gender, diagnosis-related group (DRG), weight, chronic kidney disease (CKD) status, and ICD-9-CM codes for respiratory, gastrointestinal, malignant, and infectious diseases; n=1564, 885, 246, and 105 for change in SCr 0.3-0.4, 0.5-0.9, 1-1.9, and ≥2.0 mg/dL [9].

Types of AKI

AKI can be subclassified by its origin as prerenal, renal (or intrinsic), or postrenal AKI. Prerenal AKI, which accounts for ~60% of cases, occurs due to a reduction or complete loss of renal blood, observed in cardiac surgery, septic shock and vascular disease. Loss of renal blood flow causes ischemic injury and cell death in the kidney. The proximal tubule is heavily affected due to its reliance on oxygen for oxidative phosphorylation [12]. Intrinsic renal injury occurs when there is direct damage to a component of the nephron, typically as a result of xenobiotic or ischemic injury. Intrinsic AKI accounts for 35-40% of cases observed, and when examined together, pre-renal causes with ischemic ATN account for approximately 75% of AKI cases [13]. Finally, post-renal injury is caused by an obstruction of urinary outflow causing increased pressure in the kidney and hydronephrosis.

Causes of AKI

AKI is caused by a diverse array of insults including septic shock, major surgery, cardiogenic shock, and drug/toxicant exposure. Sepsis is the most common cause of AKI in critically ill patients accounting for nearly half of all cases [14]. Various pharmacological agents have been identified as nephrotoxics, including aminoglycoside antibiotics, various chemotherapeutic agents, radiocontrast media, and non-steroidal anti-inflammatory drugs (NSAIDs). Aminoglycosides preferentially accumulate in the renal proximal tubule and mediate nephrotoxicity through disruption of phospholipid metabolism and renal perfusion. Assessment in ICU patients demonstrated that administration of aminoglycosides caused renal toxicity in ~60% of patients [15]. Cisplatin, an effective platinum-based chemotherapeutic agent, is associated with high rates of renal toxicity. Cisplatin causes AKI through direct toxicity to renal tubules by disrupting mitochondrial function causing ATP depletion, and increased oxidative and

inflammatory tissue damage [16, 17]. Radiocontrast media are commonly used in various forms of tissue imaging, but are a frequent cause of AKI in hospitalized patients [18]. Pre-existing renal dysfunction sensitizes certain populations to radiocontrast nephrotoxicity. Radiocontrast agents cause renal damage through direct tubular injury, as well as through the reduction of renal blood flow and glomerular filtration [19]. Various NSAIDs, including acetaminophen and aspirin, are common causes of renal damage, particularly in aged and sensitive populations. Acetaminophen induces tubular necrosis through induction of renal oxidative stress and depletion of renal anti-oxidative mechanisms [20, 21].

Pathophysiology of ischemia/reperfusion-induced AKI

Renal ischemia/reperfusion (I/R) is a common cause of AKI. Ischemia occurs when blood flow to the kidney is reduced as a consequence of various insults including drug/toxicant exposure, cardiovascular disease, sepsis or surgery [22, 23]. Ischemic AKI is a multi-factorial disorder characterized by prominent microvascular and tubular dysfunction (Figure 1.5) [24]. Following ischemia, renal vessels become constricted reducing microcirculation. Additionally, endothelial damage and leukocyte infiltration are prominently observed [22, 25, 26]. Renal tubular damage is marked by breakdown of cytoskeletal components and a loss of renal tubular polarity. Epithelial cells undergo varying degrees of apoptotic and necrotic cell death and are sloughed into the renal tubular lumen resulting in tubular obstruction [12, 22, 27]. Each of these pathophysiological mechanisms are described in more detail in the following sections.

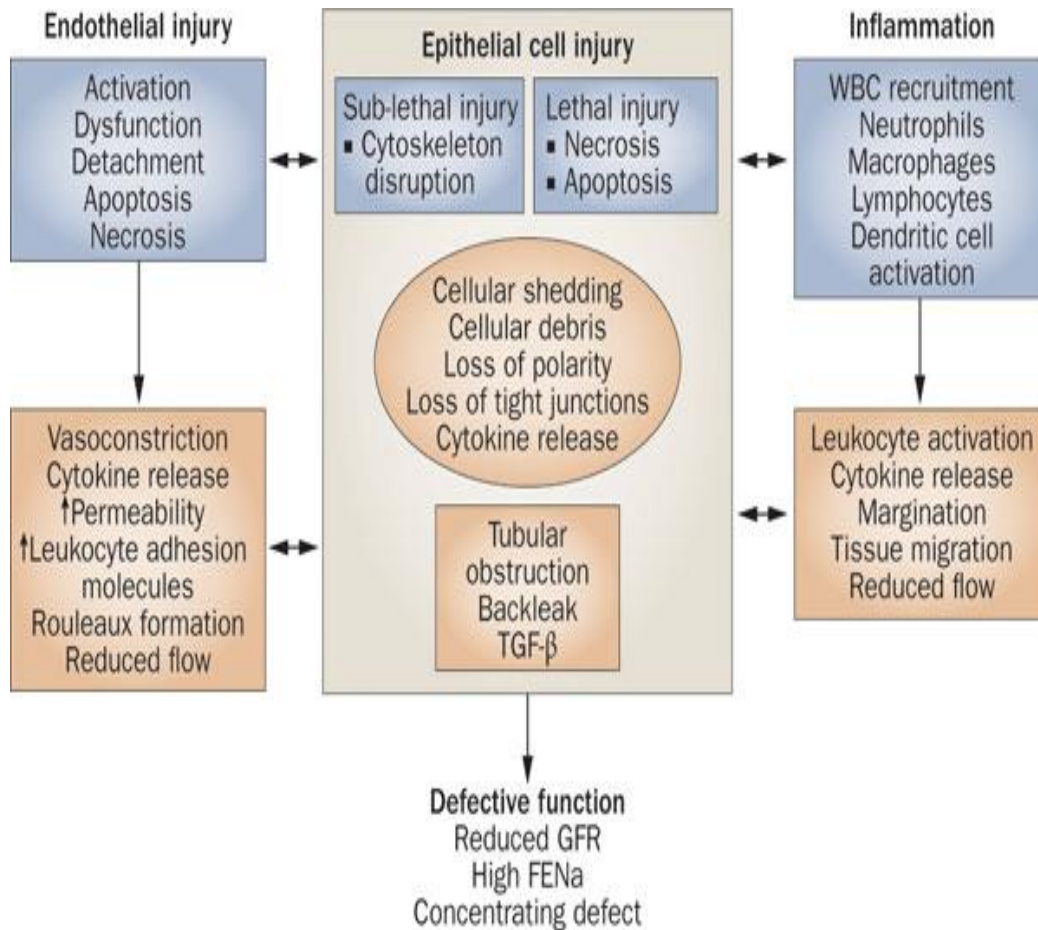


Figure 1.5: Pathogenesis of ischemic AKI. The major pathways of GFR impairment in ischemic acute tubular injury are caused by ATP depletion in vascular and tubular cells. Numerous interactions exist between endothelial cells, WBCs, and epithelial cells in the pathophysiology of ischemic AKI. These interactions are bidirectional between the cells involved, and result in specific functional and structural alterations. Inflammatory mediators released from proximal tubular cells influence endothelial cell processes (e.g. increase vasoconstriction and expression of cell adhesion molecules) that in turn influence the interactions between WBCs and endothelial cells, leading to reduced microvascular flow and continued hypoxia within the local environment. Additional functional changes occur, such as a marked reduction in production of erythropoietin and 25-hydroxylation of vitamin D. Electrolyte accumulation can rapidly lead to requirement of renal replacement therapy. Metabolic acidosis as a consequence of AKI must also be carefully monitored. Abbreviations: AKI, acute kidney injury; FENa, fractional excretion of sodium; GFR, glomerular filtration rate; TGF-β, transforming growth factor β; WBC, white blood cell [24].

Spatial and temporal pattern

The acute effects of I/R injury due to disrupted renal perfusion and ATP depletion are most prominently observed in the proximal tubule due to high energy demands [12, 22]. Following reperfusion, the extension phase of I/R is characterized both by renal recovery due to restoration of oxygen and nutrients to damaged tissue, but also by further oxidative injury. Damage to the vascular endothelium creates pockets of localized ischemia causing further progression of injury. During this phase, injury is observed primarily in the S3 segment of the proximal tubule and the medullary thick ascending limb at the border of the cortex and the medulla [28]. This region is very sensitive in this period due to a highly developed network of small vessels and high oxygen demands of the outer stripe of the medulla [29, 30]. The final, maintenance phase of AKI, is also characterized by mixed recovery and further injury. Further cellular injury occurs as the result of chronic inflammation and response to apoptotic stimuli.

Vascular injury

Microvascular injury following I/R is characterized by damage to endothelial cells and vascular smooth muscle cells. Damage is primarily confined to the glomerulus and outer stripe of the medulla. Differential morphology of the renal capillaries in these regions make them particularly sensitive. Autonomic nervous system dysfunction and release of paracrine signals promoting vasoconstriction (endothelin, adenosine, angiotensin II and thromboxane), and a reduced response to vasodilators (nitric oxide, PGE₂, acetylcholine and bradykinin) reduce blood flow to these regions [25].

Tubular cell death

Both apoptotic and necrotic cell death are observed following ischemic AKI. The degree of each type is dependent upon the severity of the injury and the region of the kidney which is affected. Prolonged ischemia leads to depletion of ATP causing necrotic cell death, primarily in the renal proximal tubule [31-33]. Furthermore, ATP depletion disrupts cellular ion transport and causes disruption of cellular protein structure and function [34-36]. Apoptosis is also observed in ischemic injury in both animal models and humans [37-40]. However, the contribution of cellular apoptosis to overall renal function is questionable as only a small portion of tubular cells undergo apoptosis. Additionally, apoptosis is primarily observed in the distal tubules, while the loss of tubular cells is primarily confined to the proximal tubule. Furthermore, ATP is a requirement for initiation of apoptotic cell death, and is severely depleted during and acutely following ischemia. Expression of apoptotic proteins, including Bax, Bad, Bak and various caspases, increases over time following renal ischemia due to the influence of prolonged oxidative stress, DNA damage and inflammation, potentially implicating apoptosis in the recovery phases of ischemic AKI [41].

Sub-lethal tubular injury

Renal tubular cells that do not undergo cell death still experience an array of morphological and functional changes following ischemia. The tubular cytoskeleton is severely disrupted resulting in loss of epithelial polarity [12, 22, 27]. Disruption of the actin cytoskeleton is an early consequence of ischemia. ATP is required for the dynamic formation and turnover of actin, and for the interaction of actin with myosin [42, 43]. Additionally, post-ischemic elevations of tubular Ca^{2+} levels disrupt actin-myosin interactions and microtubule formation

[44]. Ca^{2+} elevation also leads to the activation of the Ca^{2+} -dependent proteases, calpains. Calpains degrade actin and various actin binding proteins, as well as integral membrane proteins, membrane associated-proteins and cross linking proteins [24, 45-47]. Membrane phospholipids interacting with the cytoskeleton, including diacylglycerol and palmitic acid, are also disrupted following ischemia [47]. Finally, excessive ROS production leads to cross linking of actin and actin-binding proteins, disrupting cytoskeletal integrity [48-50].

Cytoskeletal disruption and subsequent loss of epithelial polarity has profound impacts on renal tubular structure and function, including loss of the apical brush border and redistribution of membrane proteins. Microvilli present on the apical membrane are shed into the tubular lumen following injury resulting in a reduction in functional renal surface area required for water and solute reabsorption [24, 51-53]. The redistribution of membrane proteins is best illustrated by the movement of the $\text{Na}^+\text{-K}^+$ ATPase from the basolateral to the apical membrane of the renal tubule following injury. Under physiological conditions, Na^+ enters the renal tubule via facilitated diffusion at the apical membrane. Na^+ is then pumped out of the cell against its concentration gradient across the basolateral membrane via the $\text{Na}^+\text{-K}^+$ ATPase. Movement of Na^+ out of the cell is required to maintain the gradient for tubular uptake of water and solutes. Relocalization of the $\text{Na}^+\text{-K}^+$ ATPase to the apical membrane inhibits Na^+ and water reabsorption by establishing a cycle where Na^+ is both reabsorbed and secreted into the tubular lumen [45, 54-56]. Tubular epithelial cells are held in place by their attachment to the extracellular matrix through integrins and to each other by adherens. Disruption of these adhesion complexes following ischemia leads to sloughing of renal tubular cells into the lumen. These cells appear as casts in the tubular lumen causing obstruction of flow of the luminal filtrate [45, 57].

Tubular repair

The renal tubular epithelium has an extensive capacity to repair itself following injury. Following ischemic injury, a host of renal repair mechanisms are activated. Renal cell turnover is markedly increased due to cell death and enhanced proliferation of renal epithelial cells, particularly in the S3 segment of the proximal tubule [58]. The generation of new renal epithelial cells replaces the cells lost due to apoptotic and necrotic cell death. However, the source of these cells is still under debate. Numerous origins have been suggested including bone marrow stromal cells [59, 60], a resident renal stem cell population [61], or proliferation of surviving renal epithelial cells [12]. Studies have shown that both hematopoietic stem cells (HSCs) and mesenchymal stem cells (MSCs), can replace renal epithelial cells following injury [61-65]. Additionally, administration of exogenous MSCs has been demonstrated to promote the repair of the renal epithelium and enhance renal recovery; however, other studies have contradicted these claims [61, 63, 66]. Other studies have demonstrated that surviving renal tubular cells do proliferate after ischemic insult [23]. Following injury with loss of renal epithelial cells, the surviving cells undergo a process of dedifferentiation [67]. These cells then migrate to areas of epithelial cell loss before undergoing proliferation. This proliferating cell population expresses various development markers including the proliferation marker PCNA and the mesenchymal marker vimentin [68]. The epithelial to mesenchymal transition (EMT) in these cells is mediated by signaling through the EGF receptor [69]. These cells lack the developed cytoskeleton and polarization of an intact renal epithelium [70-72]. Following migration and proliferation, mesenchymal tubular cells re-differentiate and reestablish polarity by inactivation of EGF signaling evidenced by regeneration of the actin cytoskeleton and localization of the Na⁺-K⁺ ATPase to the basolateral membrane (Figure 1.6) [24].

Abnormal repair and progression to CKD.

Even with the activation of renal repair processes described above, repair of the renal tubular epithelium is often incomplete. AKI is a major risk factor for the development of CKD, and there is increasing evidence that the two diseases are closely linked [10, 73, 74].

Microvascular damage causing persistent hypoxia, chronic inflammation, persistent oxidative stress and proliferation of resident fibroblasts contributing to extracellular matrix deposition causing renal fibrosis and failed renal recovery. The fate of the tubules may lie in the relative activation of pro-repair vs. pro-fibrotic signaling cascades; however, the mechanisms underlying the regulation of these processes post-ischemic AKI are still poorly understood. Evidence exists for the arrest of renal epithelial cells in the G2/M phase of the cell cycle following ischemia as a contributing factor to fibrosis, although further investigation is needed [75]. The source of the fibroblasts contributing to renal fibrosis after AKI has been debated. Some suggest that the damaged renal epithelial cells themselves cause fibrosis after undergoing EMT; however, conflicting evidence suggests that the fibroblasts arise from resident perivascular populations [76-81].

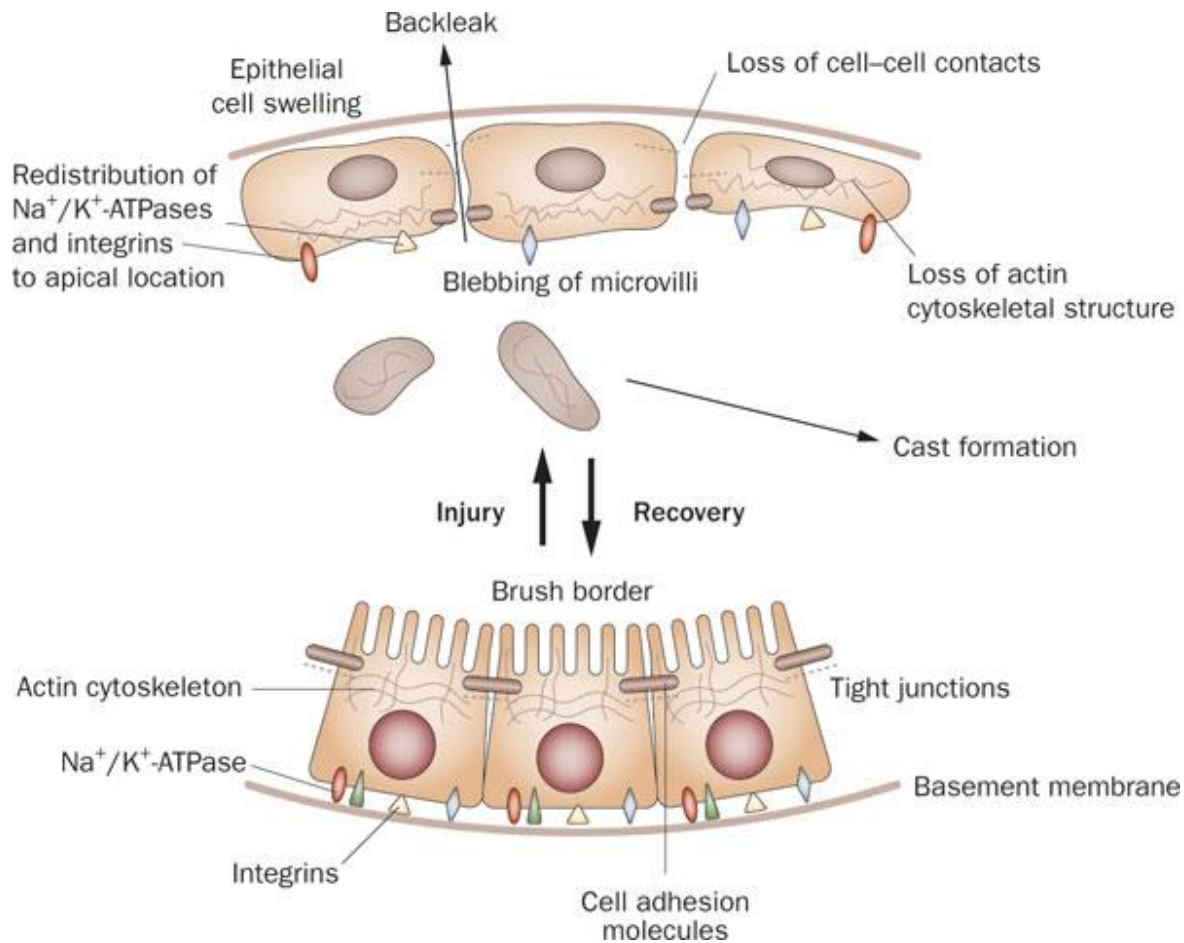


Figure 1.6: Effects of sub-lethal injury to tubular cells and their recovery. Damage to epithelial cells occurs early during ischemia and involves alterations to the cytoskeleton and in surface membrane polarity. ATP depletion induces rapid disorganization of the actin cytoskeleton structure, which disrupts tight junctions and in turn leads to backleak of tubular filtrate. Loss of cell-cell contacts and cell adhesion molecules results in flattened nonpolarized epithelial cells, denuded basement membranes, and expression of mesenchymal markers. Na⁺/K⁺-ATPase pumps normally located at the basolateral membrane and tethered by the actin-spectrin cytoskeleton, redistribute to the apical membrane of the proximal tubular cell and are internalized into the cytosol during ischemic injury. Morphologically, proximal tubular cells lose their brush borders, undergo swelling, and blebbing of microvilli during injury, leading to cast formation. Severely injured proximal tubular cells undergo mesenchymal differentiation and subsequent re-epithelization. Recovery of proximal tubular cells begins with integrin reattachment, reassembly of the actin cytoskeleton, repolarization of the surface membranes, and redistribution of the sodium pumps back to their basolateral location [24].

Animal models of AKI

Due to the complex nature of the disease and the lack of availability of human renal tissue for study, the use of relevant animal models has been vital to the study of the underlying pathophysiology of AKI. While existing animal models of AKI fail to completely mimic human disease, several models have proven reliable to study the underlying mechanisms of renal injury and repair, and serve as platform for testing of new therapeutics.

I/R model of AKI

Renal I/R can be induced in an array of animal systems; however, rats and mice are most commonly used. Ischemia is induced by unilateral or bilateral clamping of the renal artery or renal pedicle to obstruct blood flow to the kidney. Following clamping for a prescribed period of time, the clamps are released allowing blood to reperfuse the ischemic tissue. Ischemia times needed to induce injury vary widely, primarily based on the temperature at which the animals were maintained during ischemia [82]. Bilateral clamping of the renal pedicles for 60 min followed by 24 h of reperfusion in rats has been previously reported to induce severe AKI [83]. Unilateral clamping for 45-60 min has also been shown to be sufficient to induce renal failure. Mice tend to be relatively more sensitive to ischemia and require shorter ischemic periods to induce similar degrees of renal damage [84]. Following experimental I/R, cellular necrosis is observed primarily in renal epithelial cells in the outer stripe region of the medulla [85]. Some apoptotic cell death is also observed. Histological evaluation reveals dilated tubules, loss of brush border integrity with flattened renal epithelial cells, and cast formation causing tubular lumen obstruction [85].

Folic acid model of AKI

A single bolus overdose of folic acid has been used as a model of AKI in rats and mice [86-88]. The doses required to induce renal injury are not clinically relevant in humans; however, the model provides a simple, reproducible method of induction of both acute and chronic renal disease in animals. The model is characterized by both direct damage to the renal tubular epithelium and tubular obstruction [87]. After acute administration, animals demonstrate elevated renal injury biomarkers and reduced urine output. Folic acid is often used as a method of induction of CKD as proliferation of renal interstitial connective tissue (fibrosis) is prominently observed late after folic acid overdose [89].

Biomarkers

Serum creatinine and blood urea nitrogen (BUN) have long been the gold standard markers of renal function. However, poor sensitivity and kinetic profiles of these markers has created increased interest for the development of new markers of renal injury and dysfunction. Over the past 10 years, an array of promising new renal biomarkers have emerged with greater sensitivity, site specificity and enhanced diagnostic and prognostic potential (Figure 1.7) [90]. A sampling of these biomarkers is discussed below.

Creatinine and BUN

Serum creatinine is a standard clinical measure of renal function that has been traditionally used in the diagnosis of AKI. Measurement of creatinine concentration in the urine additionally allows for the measurement of creatinine clearance and estimation of GFR. Despite its universal usage as a marker of renal function, creatinine has numerous limitations. Baseline serum creatinine levels vary widely depending on population, degree of muscle and hydration status. Therefore, absolute serum creatinine concentrations are

difficult to interpret. Baseline creatinine measurements are needed in order to monitor increases, which may correspond to reduced renal function. Additionally, increased serum creatinine levels are noted only in patients who have lost a significant proportion of their baseline renal function, making creatinine a poor marker of early and/or mild AKI. BUN has also been used extensively as a renal functional marker and diagnostic tool for the detection of AKI. However, BUN suffers from the same lack of sensitivity and specificity as serum creatinine.

Kim-1

Kidney injury molecule-1 (Kim-1) is a type 1 transmembrane protein containing a mucin and immunoglobulin domain. Kim-1 was originally identified as a hepatitis A virus receptor (HAVCR1, or Tim-1). Kim-1 was demonstrated to be markedly upregulated in the kidney following renal ischemia/reperfusion injury in the rat [91]. Kim-1 has several advantages as a biomarker over traditional markers of renal dysfunction. Kim-1 is not expressed in normal, healthy kidney. Following injury, its expression becomes highly elevated, particularly in the apical membrane of renal tubules, and its expression is maintained throughout cellular recovery. Following its upregulation, the ectodomain of Kim-1 is shed into the tubular filtrate and excreted into the urine simplifying its assessment. Additionally, this shed domain has been found to be very stable in urine even at room temperature. Assessment of Kim-1 in pre-clinical animal models has demonstrated that Kim-1 is an early, sensitive and specific predictor of tubular damage that is elevated even in the absence of clinically detectable renal dysfunction by SCr and BUN [92-94]. The diagnostic and prognostic potential of Kim-1 has also been demonstrated in clinical populations following cardiac surgery, renal transplant, obstructive nephropathy, sepsis, chronic kidney disease and other disease states [95-98].

NGAL

Neutrophil gelatinase-associated lipocalin (NGAL) is a 25 kDa protein discovered in neutrophils, which plays a role in innate immunity through sequestration of iron. NGAL is expressed at very low levels in normal epithelial tissues including the respiratory tract, prostate and kidney. Following renal injury, NGAL expression is markedly upregulated in damaged renal tubular epithelial cells. NGAL has been demonstrated as a highly effective marker of early AKI in multiple animal models and human disease cohorts. NGAL is rapidly upregulated – less than 2 h – following renal I/R [99, 100]. NGAL has also been shown to be an effective predictor of patient outcomes, including need for renal replacement therapy, length of hospital stay and patient mortality [101-103].

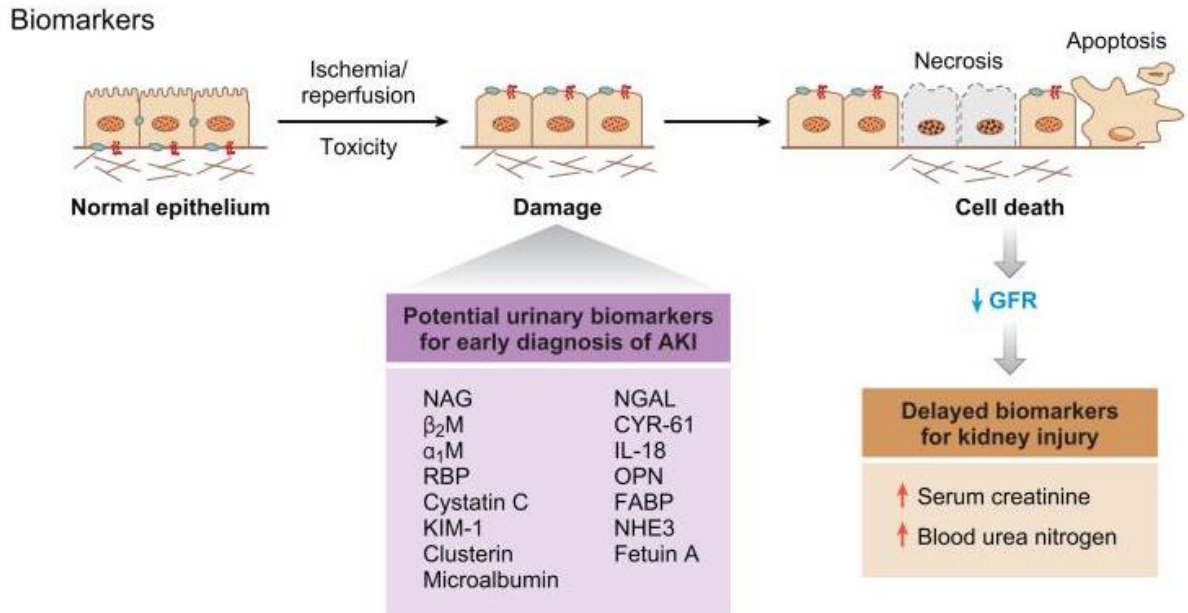


Figure 1.7. Biomarkers of AKI: Traditionally used markers, such as blood urea nitrogen (BUN) and creatinine (CR), are insensitive, nonspecific, and do not adequately differentiate between the different stages of AKI. A delay in diagnosis prevents timely patient management decisions, including administration of putative therapeutic agents. Urinary biomarkers of AKI will facilitate earlier diagnosis and specific preventative and therapeutic strategies, ultimately resulting in fewer complications and improved outcomes [90].

Pharmacological treatment of AKI

Many drugs been evaluated as prophylactic measures in patients at risk for the development of AKI, or as stimulators of renal recovery following injury. Primary targets of investigation include stimulators of naturesis and renal blood flow, or inhibitors of renal inflammation and oxidative stress. Tested therapies that have failed in human trials include the vasoactive drugs dopamine [104], fenoldopam [105] and theophylline [106], as well as anti-inflammatory drugs and antioxidants including aspirin, clonidine [107], dexamethasone [108] and N-acetylcysteine [109]. Several studies have shown promise with the use of sodium bicarbonate [110], statins [111], erythropoietin [112], naturetic peptides [113], fenoldopam [114], nitroprusside sodium [115] and clonidine [116] in various AKI patient cohorts; however, all of these drugs require further studies for validation. Despite the serious nature of AKI, there still exists no highly effective therapies that can protect against or promote recovery from AKI. The complexity of the pathophysiological mechanisms underlying AKI has made therapeutic development difficult. Multiple mechanisms including apoptotic and necrotic cell death, inflammation, oxidative stress and bioenergetic dysfunction occur simultaneously during the onset and progression of AKI. Future successful therapies will likely rely on a multi-targeted approach to address these various mechanisms. Additionally, the use of novel renal biomarkers with enhanced sensitivity and prognostic power in future AKI interventional studies to stratify patient cohorts will likely lead to enhanced success.

MITOCHONDRIAL DYSFUNCTION IN DISEASE

Mitochondrial homeostasis

Mitochondria are uniquely situated at a crossroads between multiple cellular processes critical to human health. As the site of aerobic respiration, mitochondria are primarily responsible for regulation of cellular energetics. However, mitochondria also serve as signaling organelles that can orchestrate complex cellular responses to both internal and external stimuli [117]. The mitochondrion is the only organelle that contains its own DNA (mtDNA) outside the nucleus, thus, regulation of mitochondrial function requires coordination of two distinct genomes [118]. The complex regulation of mitochondrial assembly and function, as well as the intricate nature of the tasks performed by mitochondria, provides myriad opportunities to derail mitochondrial homeostasis and facilitate onset of pathology.

Mitochondria are by nature plastic organelles, existing in a constant state of flux. This plasticity allows mitochondria to adapt to stark changes in cellular energy demands, as well as adapt to and mitigate cellular stress. As the site of oxidative phosphorylation, mitochondria are the chief consumers of intracellular oxygen, and thus are also a main source of reactive oxygen species (ROS). Under physiological conditions, mitochondrial-derived ROS serve as key second messengers to help coordinate cellular responses, including adaptation to hypoxia, cellular division, and complex responses to external stimuli, such as regulation of vascular tone [117, 119]. However, even under normal conditions oxidative damage inevitably occurs.

Mitochondria mitigate this stress through quality control measures, including balanced biogenesis of new mitochondria, autophagic degradation of dysfunctional mitochondria, mitochondria-specific protein refolding/turnover pathways and mitochondrial fission/fusion events (Figure 1.8) [120].

Disruption of mitochondrial homeostasis through perturbation of any of these quality control processes has been implicated in disease [121-124]. Due to the requirement of mitochondrial homeostasis for normal cellular function, mitochondria have received increasing attention as a therapeutic target [125]. More specifically, compounds capable of stimulating mitochondrial biogenesis (MB) have shown potential as a treatment for a wide range of diseases involving mitochondrial dysfunction, both acute and chronic.

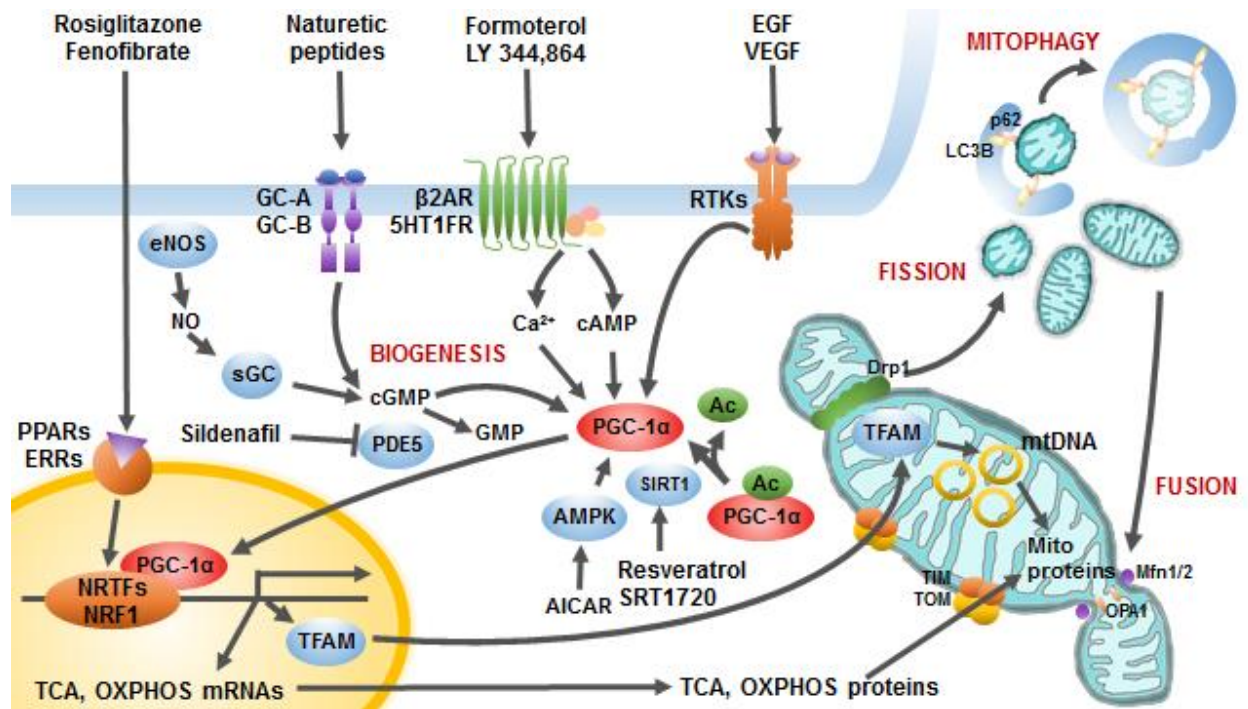


Figure 1.8: Mitochondrial homeostasis is maintained through balanced biogenesis of new mitochondria, mitochondrial fission and fusion, and mitochondrial turnover by mitophagy. Mitochondrial biogenesis (MB), the *de novo* generation of new mitochondria, is a highly regulated cellular process controlled by the central mediator and transcriptional coactivator PGC-1 α . PGC-1 α expression and activity is regulated through diverse pathways including receptor tyrosine kinases, G-protein coupled receptors, naturetic peptide receptors and nitric oxide synthase through cGMP, as well as AMPK activation, and SIRT1-mediated deacetylation. In response to various stimuli, mitochondria can undergo the process of fusion (enlargement by combination with other mitochondria) via mitofusin proteins, such as MFN1/2 and OPA1, or fission (size reduction by budding off of mitochondrial contents) via fission proteins, such as Drp1. Damaged mitochondria are eliminated by selective degradation in lysosomes. EGF, epidermal growth factor; VEGF, vascular endothelial growth factor; RTKs, receptor tyrosine kinases; β 2AR, β 2-adrenergic receptor; 5HT α R, serotonin receptor; GC-A/B, guanylyl cyclase A/B; eNOS, endothelial nitric oxide synthase; NO, nitric oxide; sGC, soluble guanylate cyclase; cGMP, cyclic guanosine monophosphate; cAMP, cyclic adenosine monophosphate; AMPK, AMP-activated kinase; SIRT1, sirtuin 1; PPAR, peroxisome proliferator-activated receptor; ERR, estrogen related receptor; NRF1, nuclear respiratory factor-1; PGC-1 α , peroxisome proliferator-activated receptor gamma coactivator-1 alpha; Ac, acetyl; TCA, tricarboxylic acid cycle; OXPHOS, oxidative phosphorylation; TOM, translocase of the outer membrane; TIM, translocase of the inner membrane; MFN2, mitofusin 2; OPA1, optic atrophy 1; DRP1, dynamin-related protein 1; mtDNA, mitochondrial DNA.

Mitochondrial dysfunction in acute disease

Mitochondrial dysfunction has been characterized as an important pathophysiological mechanism in many acute conditions including drug/toxicant exposure, sepsis, and ischemia/reperfusion (I/R) injury (Table 1.1) [126]. Given that the damage caused by tissue ischemia is most directly the result of mitochondrial dysfunction and energetic deficits, this section will focus on common hallmarks of I/R injury, as well as provide examples of mitochondrial directed interventions improving outcomes following I/R in various organ systems.

Acute ischemia most severely affects organs with large ATP requirements and limited regenerative potential, such as heart, kidney, and brain. Ischemia can occur following surgical intervention, or as a component of drug/toxicant exposure, systemic infection, or multi-organ failure [126]. However, regardless of the cause or site, the mechanisms underlying tissue damage and organ dysfunction following ischemia are conserved. Persistent ischemia causes blockade of oxidative phosphorylation, loss of mitochondrial membrane potential, and decreased cellular ATP levels. In addition, acidification of the tissue occurs as glycolytic flux increases and the metabolic waste products including protons and lactate accumulate. As intracellular ATP levels decrease, ATP-dependent ion channel function is impaired. This is critical, as the organ systems most severely affected by ischemia also require precise regulation of multiple ions, including Na^+ , Ca^{2+} , Cl^- and K^+ , for proper function, including conduction of action potentials in nervous tissue, muscle contraction/relaxation in the heart, and blood filtration in the kidney [126-128]. The loss of bioenergetic homeostasis following ischemia thus ultimately directly contributes to organ dysfunction.

Disease	Mitochondrial effect	References
Acute diseases		
Ischemia/reperfusion injuries: Myocardial Infarction ¹ Stroke ² Acute kidney injury ³ Spinal cord injury ⁴	Ischemia: ↓ATP and ATP-dependent cell functions, ↑ion imbalance (Na ⁺ , K ⁺ , Ca ²⁺), ↑reducing equivalents, ↓tissue pH. Reperfusion: ↑ ROS, ↑oxidative stress, and ↑increased apoptosis/necrosis.	¹ [128] ² [127] ³ [126] ⁴ [129]
Drug/toxin induced injuries: Nephrotoxicity ⁵ Acute liver injury ⁶	↑apoptosis/necrosis, ↑mtDNA release, ↑ oxidative stress and ↑systemic inflammatory responses.	⁵ [130] ⁶ [131]
Chronic diseases		
Type II diabetes ⁷	↓metabolic capacity, ↓PGC-1α-dependent gene expression, and ↑ lipids. Mitochondrial dysfunction possibly contributes to insulin resistance.	⁷ [132]
Neurodegenerative diseases: Alzheimer's disease (AD) ⁸ Parkinson's disease (PD) ⁹ Huntington's disease (HD) ¹⁰ Amyotrophic Lateral Sclerosis (ALS) ¹¹	AD: ↓mitochondrial proteostasis, ↓cellular ATP and ↑oxidative stress result in neuron loss and microvascular dysfunction. PD: Defective mitophagy and fission/fusion dynamics, ↑oxidative stress, ↓energetics, and ↑neuron loss. HD: ↓ETC complex numbers and activity. Mutant Huntingtin disrupts mitochondrial trafficking and ↑mitochondria fragmentation. Ca ²⁺ handling is disrupted, ↑ MPTP opening and apoptosis. ALS: ↓ATP from ETC, ↑ROS and oxidative stress, ↑ Ca ²⁺ imbalance	⁸ [133] ⁹ [134] ¹⁰ [135] ¹¹ [136]

Table 1.1: Select listing of acute and chronic diseases implicating mitochondrial dysfunction.

Following ischemia, restoration of blood flow leads to re-oxygenation and delivery of critical nutrients to the damaged tissue. However, reintroduction of oxygenated blood into the ischemic zone causes a secondary complication, termed reperfusion injury, characterized by inflammation and oxidative damage [137]. Reperfusion injury primarily affects the peripheral regions of an ischemic core, as cells in the central area of ischemia often undergo necrotic cell death due to sustained ATP depletion. However, cells in the peripheral zone of the ischemic site are not completely dependent upon the occluded vessel, and although hypoxic, are able to receive partial perfusion from collateral vessels. Upon reperfusion of the blocked vessel, the spike in oxygen introduced into the hypoxic environment of the peripheral zone causes a host of unintended reactions that create tremendous amounts of ROS [128]. A chief source of ROS during reperfusion comes from electrons mishandled in the electron transport chain (ETC) of dysfunctional mitochondria [127]. The sudden increase in ROS overwhelms endogenous antioxidant defenses, and can culminate in opening of the mitochondrial permeability transition pore (MPTP) subsequent to Ca^{2+} overload. Opening of the MPTP can lead to release of mitochondrial cytochrome c and initiate apoptotic cell death [138]. Additionally, leak of mitochondrial ROS into the cytosol causes damaging oxidative modifications to proteins and lipids, severely affecting cellular function. Early intervention during this critical period could limit damage and promote recovery following ischemia. Therapies capable of modulating and rescuing mitochondrial homeostasis upon reperfusion could restore redox balance, ameliorate cellular damage, and prevent initiation of cell death cascades, preserving organ function.

Efforts to target specific aspects of mitochondrial dysfunction, including oxidative and nitrosative stress, have had limited success [138, 139]. Indeed, multiple studies have targeted oxidative stress through administration of direct antioxidants, including MitoQ, an antioxidant

designed to accumulate in mitochondria [140], or with compounds that fuel endogenous antioxidant production, such as N-acetylcysteine, which is converted to cysteine to produce glutathione [141]. Although pretreatment strategies have shown efficacy, administration during or following organ reperfusion has been relatively ineffective [138]. Despite the deleterious effects of ROS following reperfusion, some level of physiological ROS is required for proper recovery to occur, and administration of a pan-antioxidant may potentially disrupt the beneficial effects of physiological ROS. In contrast, pharmacological blockade of MPTP using cyclosporine A (CSA) has shown some benefit in multiple organ systems, including brain, and heart, following I/R injury through prevention of apoptosis and preservation of mitochondrial function [142, 143]. CSA is currently in clinical trials for use in treatment of myocardial infarction (MI). Despite the positive effects of CSA on preservation of mitochondrial membrane potential, it is also known to induce oxidative stress and contribute to hepatic and renal toxicity, limiting its therapeutic application [144]. These studies illustrate that more global therapies targeting the restoration of mitochondrial homeostasis through enhanced MB (Figure 1.8) of mitochondria could accelerate the restoration of the physiologic balance of ATP and ROS production, limiting cell death and tissue loss.

Multiple studies provide evidence for the benefit of augmented MB in ischemic injury. A recent study by Jiang et al found that increased MB induced by exercise was able to attenuate adverse left ventricular remodeling and oxidant stress post-MI in rats [145]. Furthermore, overexpression of mitochondrial transcription factor A (TFAM), a transcription factor regulating mtDNA transcription and replication, in a transgenic mouse model correlated with increased survival, and decreased ventricular remodeling following permanent coronary artery ligation [146]. In a separate study, TFAM overexpression was also shown to decrease reperfusion injury

in a transient ischemic stroke model [147]. Due to the energy dependence of organ repair mechanisms, enhancement of MB has potential benefit in accelerating the recovery of organ structure and function. We have previously demonstrated that pharmacological activation of MB via 3 distinct pathways following onset of maximal acute ischemic kidney injury in mice accelerates recovery of kidney function [148-150], highlighting the critical need for MB to improve recovery. In addition, activation of MB has been demonstrated to block apoptotic cell death [151]. Collectively, these data suggest that restoration of mitochondrial homeostasis via increased MB could serve as platform for the development of meaningful therapeutics for acute organ injury and failure.

Mitochondrial dysfunction in AKI

Mitochondrial damage and dysfunction is a major underlying mechanism of lethal and sublethal cellular injury in the initiation and progression of AKI [152-156]. Increased production of reactive oxygen and nitrogen species, predominantly within the mitochondria, as well as compromised antioxidant mechanisms following renal ischemia make the mitochondria extremely susceptible [157-159]. Oxidative damage and disruption of the mitochondrial electron transport chain, mitochondrial membrane depolarization, ATP depletion, lipid peroxidation, activation of the mitochondrial permeability transition and release of apoptotic proteins contribute to mitochondrial and cellular injury in AKI [22, 34, 153]. Loss of mitochondrial polarity leads to the influx of Ca^{2+} and other ions into the mitochondria causing swelling. This phenomenon has been clearly demonstrated following hypoxia/reoxygenation via electron microscopy (Figure 1.9) [156].

Mitochondria are dynamic organelles and undergo dramatic changes in structure and organization following acute insult. Mitochondria become highly fragmented through the

process of mitochondrial fission following multiple forms of AKI [160]. Inhibition of fragmentation through the use of a dominant-negative Drp1 prevented mitochondrial fragmentation, inhibited the release of apoptotic proteins from the mitochondria, and attenuated renal dysfunction following I/R. Pharmacological inhibition of Drp1 by mdivi-1 before ischemia reduced renal morphological changes and renal dysfunction by preserving mitochondrial morphology [160]. Despite these results, the role of mitochondrial dynamics, including mitochondrial fission and fusion, in the onset, progression and recovery of AKI is still poorly understood and warrants further investigation.

Mitochondrial biogenesis has been shown to be chronically suppressed in multiple models of AKI, including I/R and myoglobinuric renal injury [161]. In both models, mitochondrial gene and protein expression is suppressed as early as 24 h after injury, and remains suppressed as late as 144 h after injury (Figure 1.10) [162]. The failure to recover mitochondrial gene and protein expression mirrored the incomplete recovery of renal glomerular and tubular function. This data indicates that re-activation of mitochondrial biogenesis is vital for renal recovery and re-establishment of a functional renal tubular epithelium.

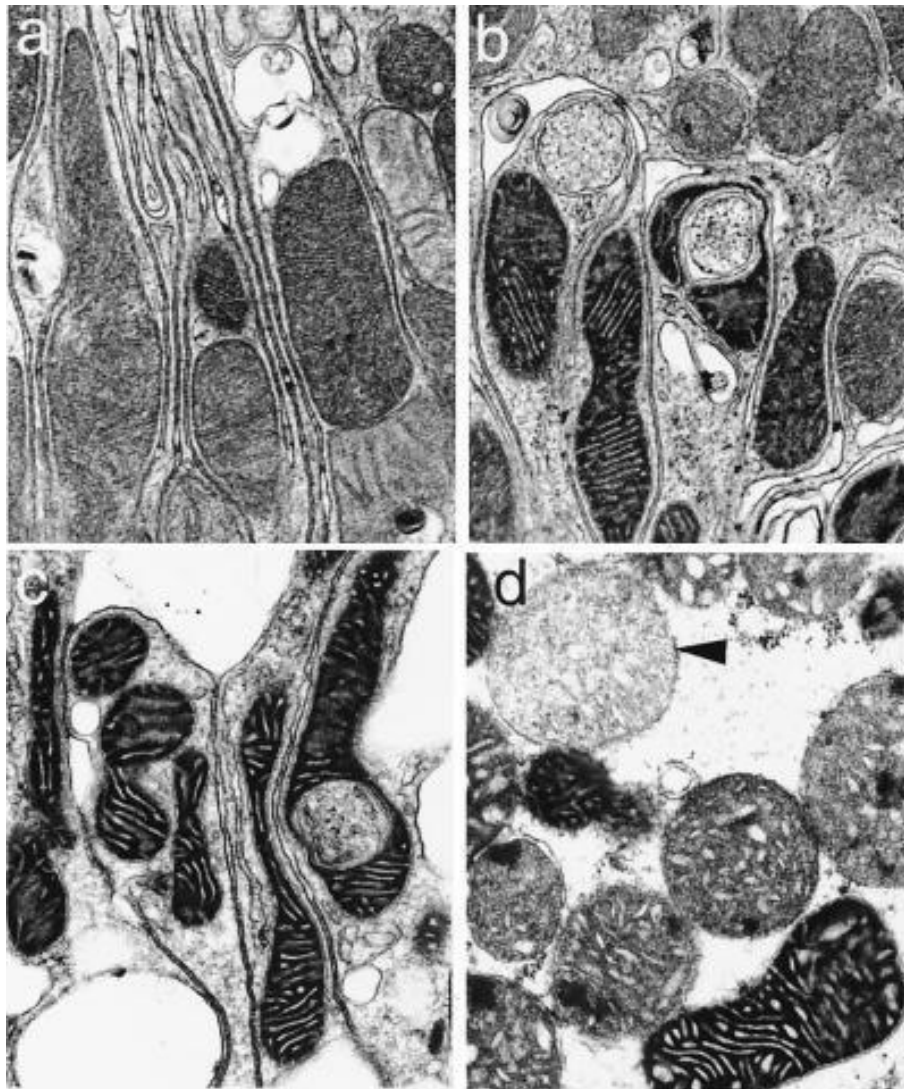


Figure 1.9. Mitochondrial ultrastructural changes. (a) Control. (b) Sixty-minute hypoxia. (c and d) Sixty-minute hypoxia followed by 60-min reoxygenation. Arrowhead, mitochondrion with high-amplitude swelling. ($\times 24,100$.) [156].

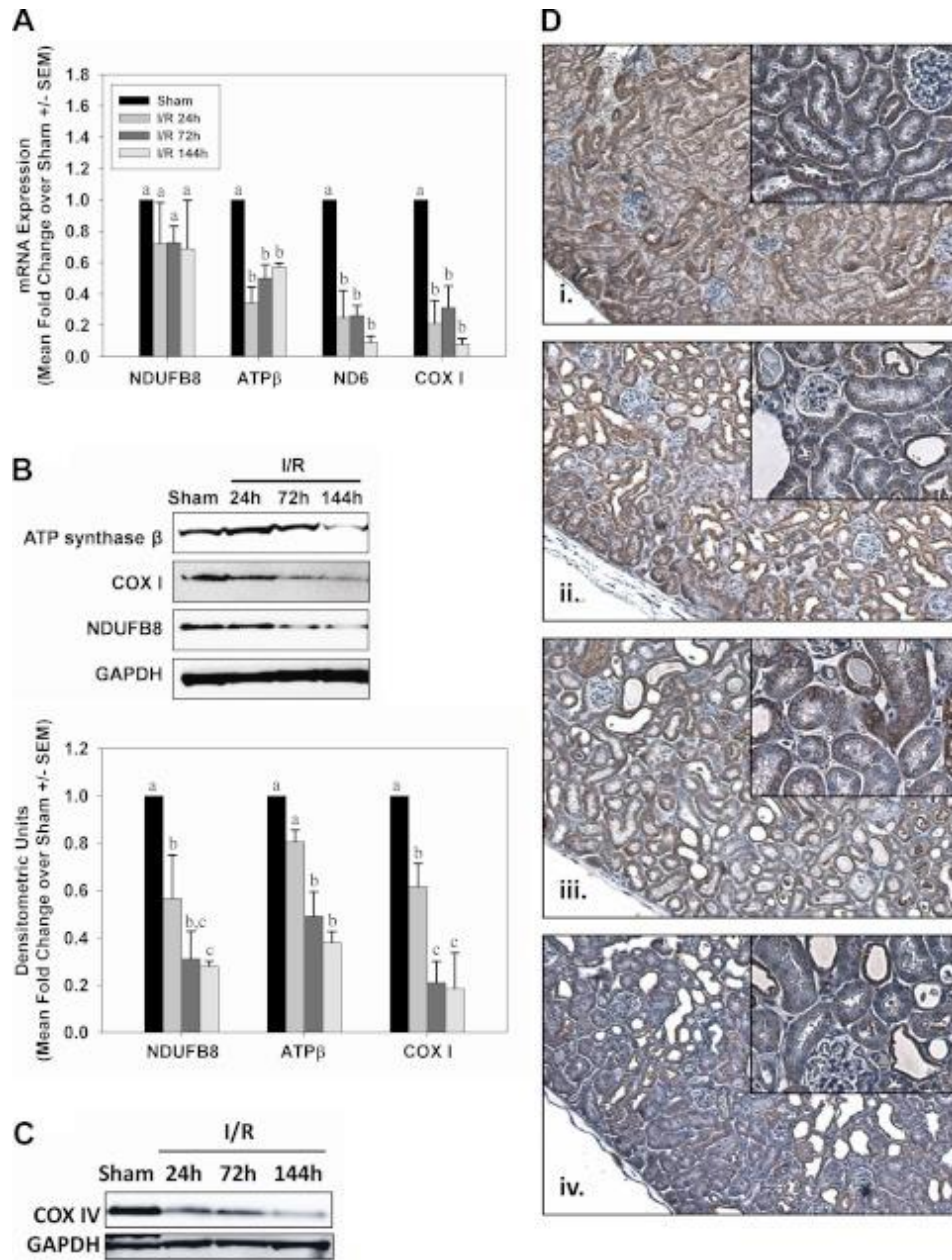


Figure 1.10. Sustained depletion of mitochondrial proteins after I/R AKI. *A*: mRNA from sham and I/R mice was analyzed by qRT-PCR for expression of nuclear-encoded respiratory genes NDUFB8 and ATP synthase β and the mitochondrial-encoded genes ND6 and COX I at 24, 72, and 144 h after injury. *B*: expression of mitochondrial respiratory proteins from kidneys of sham and I/R mice was examined by immunoblot analysis. Bars with different superscripts are significantly different from one another ($P < 0.05$). *C*: immunoblot analysis confirmed reduced COX IV protein expression in kidney cortex from mice 24, 72, and 144 h after I/R. *D*: COX IV immunohistochemistry (brown stain) in sham mice (*i*) or 24 h (*ii*), 72 h (*iii*), or 144 h (*iv*) after reperfusion in I/R mice, with hematoxylin counterstain. Low-magnification images were captured at $\times 10$ and higher-magnification *insets* were captured at $\times 40$ [161].

Mitochondrial dysfunction in chronic disease

Persistent mitochondrial dysfunction has been implicated in the initiation and progression of an array of chronic diseases and disorders, including neurodegeneration, type II diabetes mellitus, metabolic syndrome, and end stage renal disease (Table 1.1) [132, 134, 163]. As disease progresses mitochondria lose their ability to compensate for persistent stressors through regeneration and quality control measures leading to the development of tissue injury and dysfunction. Mitochondrial homeostasis (Figure 1.8), which occurs through the balance of biogenesis, fission/fusion events, and autophagic degradation of dysfunctional mitochondria, is essential to maintain tissue energetics and prevent chronic oxidative stress [164, 165]. Here we will highlight Parkinson's disease (PD) as an example of mitochondrial dysfunction in neurodegeneration, and discuss the role of mitochondrial dysfunction in the initiation and progression of type II diabetes mellitus and its secondary acute complications.

Parkinson's Disease

PD is the second most common neurodegenerative disease, affecting both motor and cognitive functions in the brain [166]. Current therapies for PD focus on symptomatic management, as there are no effective treatments to limit disease progression [167]. Multiple gene defects have been described for both familial and age-related forms of PD, several of which converge on pathways regulating mitochondrial homeostasis, implicating mitochondrial dysfunction in disease progression [134]. PD primarily affects dopaminergic (DA) neurons, which rely heavily on mitochondrial oxidative phosphorylation for energetic homeostasis. Additionally, DA neurons within the substantia nigra (SN) have limited antioxidant defense and are thus particularly sensitive to oxidative damage from mitochondrial-derived ROS [168].

Familial PD is associated with mutations in the proteins Parkin and Pink1, important components of mitophagy, leading to failed clearance of damaged and dysfunctional mitochondria.

Persistence of damaged mitochondria leads to chronically elevated ROS in the SN and ultimately DA neuron loss [135]. Maintenance of mitochondrial quality control through the proper balance of biogenesis and degradation within the SN, as well as other brain regions, are thus a primary concern in preventing the progression of both familial and age-related PD.

Indeed, increasing evidence suggests enhanced MB is a promising therapeutic target in PD [169, 170]. As shown in Figure 1, MB is governed in large part by peroxisome proliferator activated receptor coactivator-1 α (PGC-1 α). PGC-1 α , known as the master regulator on MB, is a transcriptional co-activator that interacts with multiple transcription factors and nuclear hormone receptors to regulate ~1500 nuclear-encoded mitochondrial genes to coordinate MB and oxidative metabolism [171]. Importantly, key PGC-1 α -dependent target genes are down-regulated in PD patients, and restoration of PGC-1 α *in vitro* protects DA neurons [172]. In addition, studies in animal models of PD have demonstrated that PGC-1 α is down-regulated [134], and PGC-1 α knockout mice are more susceptible to disease [173]. Subsequent studies have shown that pharmacological restoration of PGC-1 α expression by treatment with resveratrol or AICAR induce functional improvements in animal models of PD [174], suggesting that dysfunctional MB is a hallmark of PD and enhancement of PGC-1 α expression and function has potential as a therapeutic target.

Type II Diabetes

Though it is well established that mitochondrial dysfunction occurs in patients with Type II diabetes, it is currently not known whether mitochondrial dysfunction is a consequence or

cause of insulin resistance [175]. Type II diabetes is associated with decreased PGC-1 α expression, reduced PGC-1 α -dependent gene expression, and impaired ability to produce mitochondrial ATP [176]. Type II diabetes is also associated with systemic oxidative stress as a result of increased ROS production from mishandling of electrons in the ETC and endogenous oxidases. Indeed, oxidized proteins and lipids can be detected in the plasma of diabetic patients, suggesting that antioxidant defenses are overwhelmed or impaired [177].

Basal mitochondrial dysfunction and persistent oxidative stress, in the presence of hyperglycemia, culminates in conditions that exacerbate tissue injury in response to acute conditions, including MI, stroke, and acute kidney injury (AKI). During cerebral ischemia, hyperglycemia facilitates greater glycolytic flux than that observed in normoglycemic patients. This leads to the accumulation of multiple metabolic byproducts of glycolysis, including lactate, protons and NADH. Upon reperfusion, the spike in molecular oxygen, together with elevated levels of NADH, causes hyperpolarization of mitochondria and a rise in mitochondrial-derived ROS. Elevated tissue levels of ROS and increased inflammation contributes to decreased patient survival compared to non-diabetic patients [178]. Similar effects of hyperglycemia on patient outcomes are also seen in MI [179] and AKI [180], suggesting a conserved mechanism of dysfunction across organ systems. These data suggest that correction of baseline mitochondrial function in patients with metabolic disorders could both correct fundamental metabolic deficiencies involved in the chronic progression of disease, and could attenuate injury associated with acute diseases concurrent with Type II diabetes.

MITOCHONDRIAL BIOGENESIS

Definition and overview

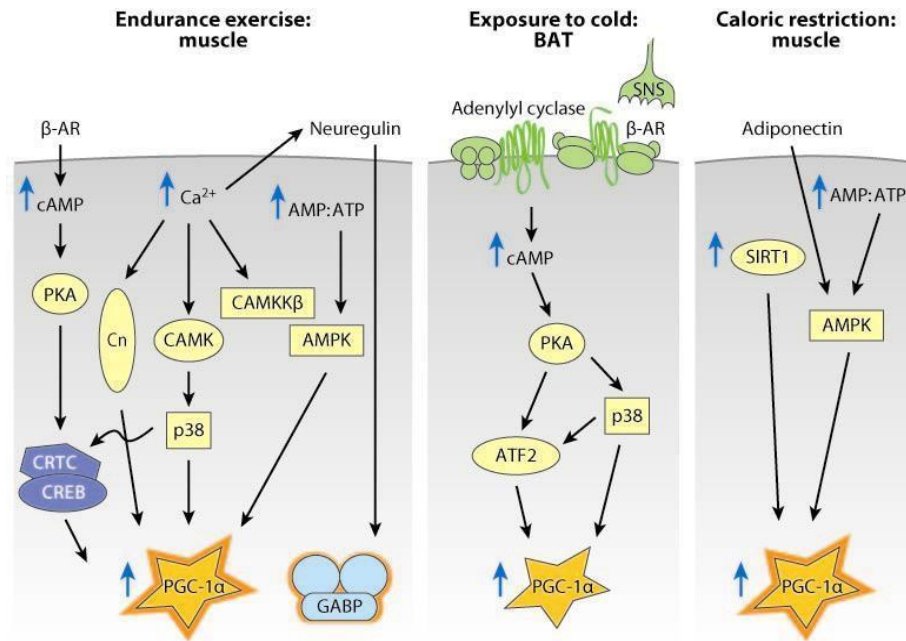
Mitochondrial biogenesis is an increase in cellular mitochondrial content through the growth of existing mitochondria or the generation of new, functional mitochondria [181].

Mitochondrial biogenesis can occur as a result of *de novo* synthesis of new mitochondria, the formation of mitochondria from other membranous structures, or the growth and/or division of existing mitochondria [182]. Mitochondrial biogenesis occurs under normal physiological conditions, but can be rapidly and potently induced in response to various stimuli with increased energy demands including repair responses to injury, cold exposure and caloric restriction [183-185]. Mitochondrial biogenesis is primarily regulated by the nuclear transcriptional coactivator peroxisome proliferator-activated receptor coactivator-1 alpha (PGC-1 α) (Figure 1.8). PGC-1 α exerts its effects through enhancing transcriptional activity of the nuclear transcription factors (NRF1 and NRF1) and the mitochondrial transcription factors TFAM, TFB1M and TFB2M [171, 186-188].

Physiological and pathophysiological activation of mitochondrial biogenesis

Signaling pathways promoting mitochondrial biogenesis are activated in response to a diverse array of physiological stimuli with increased energetic demand (Figure 1.11).

Mitochondrial biogenic responses to exercise training in muscle cells, cold exposure to brown adipose tissue and caloric restriction are described below. Additionally, mitochondrial biogenesis has been shown to be upregulated in response to cellular injury, including renal cells, to meet the energetic demand of recovery and regeneration [189].



AR Hock MB, Kralli A. 2009. Annu. Rev. Physiol. 71:177–203

Figure 1.11. Diverse physiological signals regulate mitochondrial biogenesis in a tissue-specific manner. Shown are signaling pathways that induce mitochondrial biogenesis in skeletal muscle in response to endurance exercise or caloric restriction, in BAT in response to cold exposure, and in macrophages in response to signals promoting alternative activation. The signals enhance activity (*orange outlines*) and/or expression (*upward blue vertical arrows*) of transcriptional regulators PGC-1 α , GABP, or PGC-1 β [189].

Exercise.

Increased physical activity creates an increased energetic demand that in part is met by induction of mitochondrial biogenesis, particularly within the skeletal muscle. Induction of mitochondrial biogenesis in skeletal muscle is triggered by increased cytosolic Ca^{2+} levels occurring during muscle contraction and activation of AMPK in response to an energetic deficit [190]. Furthermore, activation of the sympathetic nervous system and subsequent adrenergic receptor stimulation activates cAMP signaling, a known inducer of mitochondrial biogenesis. Following even a single occurrence of intense exercise, mitochondrial gene expression is elevated, and continued exercise causes notable increases in cellular mitochondrial content [190-195].

Cold exposure.

PGC-1 α expression and activity is induced following cold exposure due to activation of the sympathetic nervous system and subsequent stimulation of adrenergic receptors, primarily in brown adipose tissue (BAT) [183]. Adrenergic receptor activation leads to increased cAMP levels causing activation of the protein kinases PKA and p38 MAPK, and the transcription factor cAMP-response element-binding protein (CREB). Additionally, induction of PGC-1 α stimulates the activity of uncoupling protein 1 (Ucp1), causing heat generation by uncoupling of the mitochondrial proton gradient from ATP generation [183, 196, 197].

Caloric restriction.

Mitochondrial biogenesis is highly induced in animals and humans when caloric intake is restricted. This effect is believed to be mediated primarily through the activation of AMPK and

sirtuin 1 (SIRT1) [198, 199]. Endothelial nitric oxide synthase (eNOS) has also been demonstrated to be induced by caloric restriction and involved in the mitochondrial biogenic response [200]. Activation of these pathways regulates PGC-1 α activity and expression and enhances the efficiency of nutrient utilization by the mitochondria for energy [201-203].

Mitochondrial biogenesis in renal injury.

Following acute oxidant exposure in renal proximal tubular cells (RPTC), mitochondrial function is severely compromised, evidenced by reductions in cellular ATP levels and mitochondrial oxygen consumption [204, 205]. Mitochondrial function recovers in this model spontaneously over the course of 6 d after exposure, and this recovery is mirrored by the induction of PGC-1 α through the Src-EGFR-p38 MAPK signaling pathway (Figure 1.12) [204, 206]. Furthermore, overexpression of PGC-1 α following oxidant injury promoted recovery of mitochondrial protein expression, cellular ATP levels and mitochondrial oxygen consumption (Figure 1.13) [207]. Finally, stimulation of mitochondrial biogenesis using the β 2-adrenergic agonist, formoterol accelerated recovery of renal and mitochondrial function after I/R-induced AKI in mice through the activation of mitochondrial biogenic signaling pathways (Figure 1.14) [148].

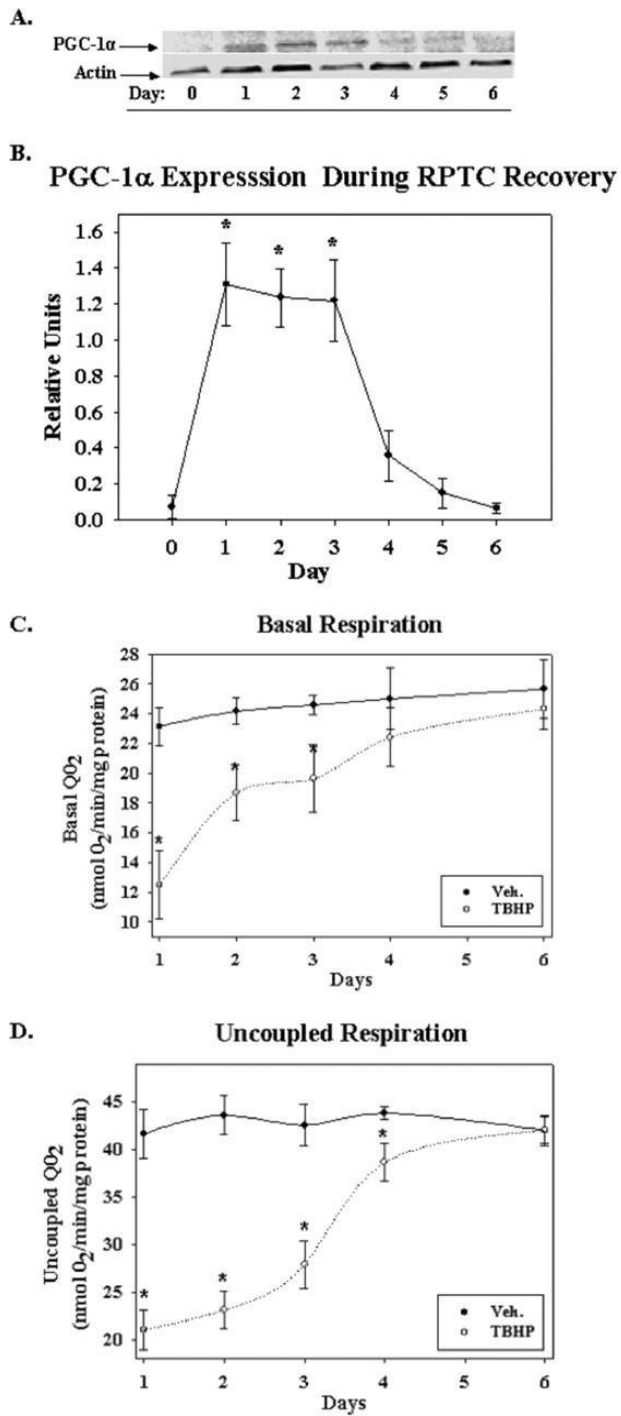


Figure 1.12. Induction of PGC-1 α protein (A,B) correlates with recovery of basal (C) and uncoupled (D) respiration after oxidant injury in RPTC [204].

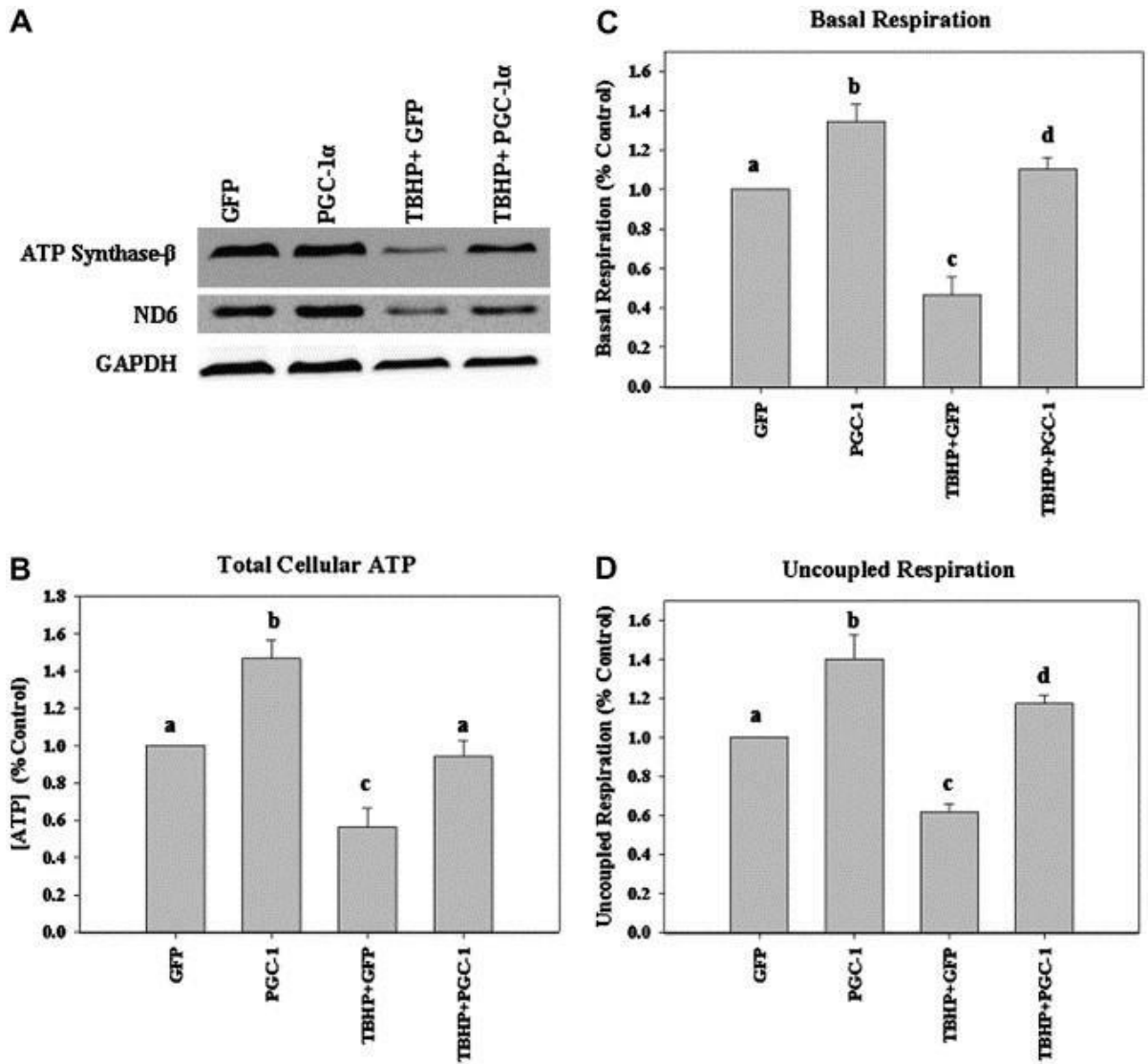


Figure 1.13. Overexpression of PGC-1 α after oxidant injury restored mitochondrial protein expression (A), as well as total cellular ATP (B) and basal (C) and uncoupled (D) oxygen consumption in RPTC exposed to *tert*butyl-hydroperoxide [207].

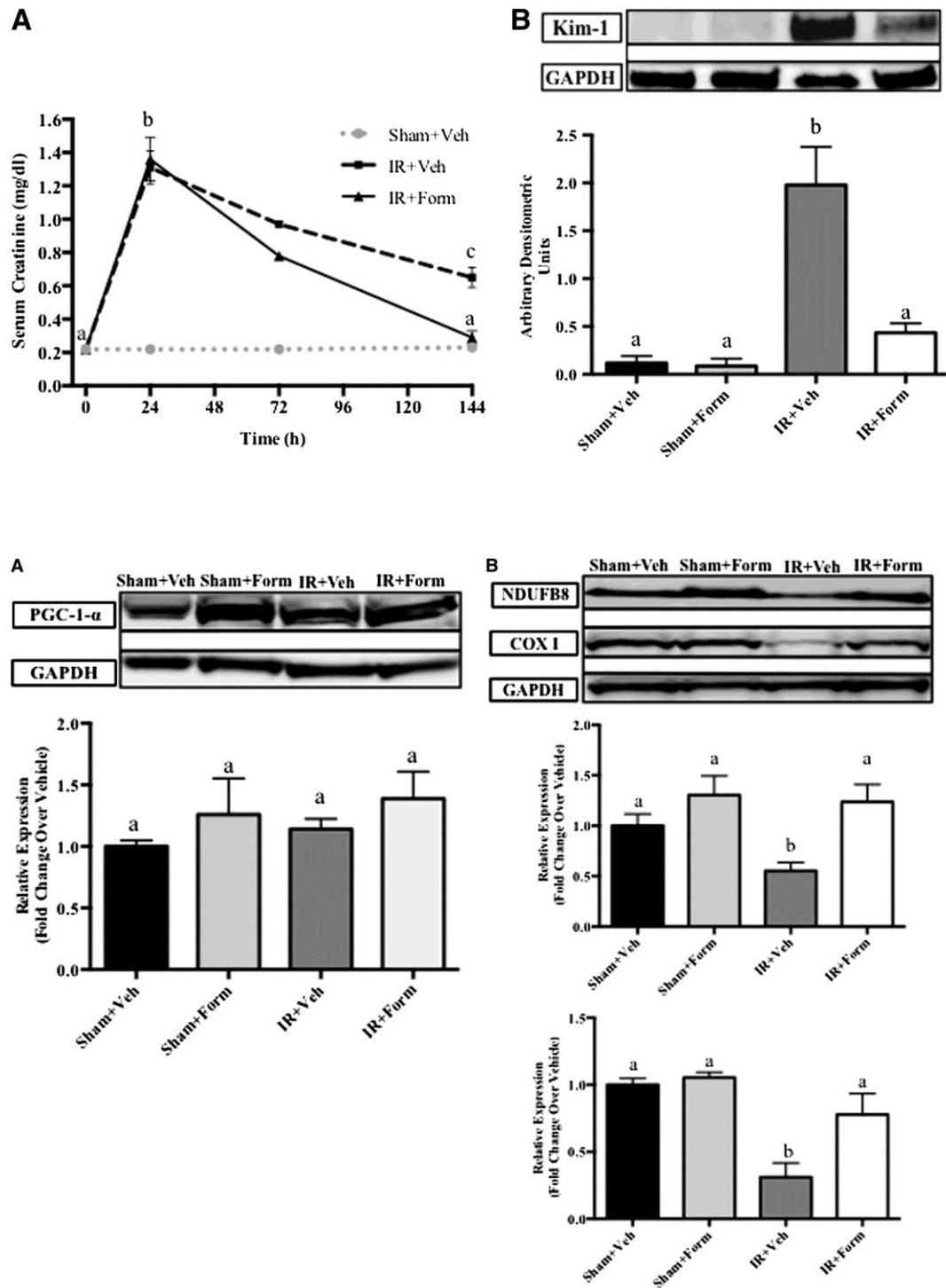


Figure 1.14. Formoterol stimulates mitochondrial biogenesis and promotes recovery of renal and mitochondrial function after I/R. Mice were subjected to sham surgery or I/R surgery and treated daily with saline vehicle or formoterol beginning at 24 h after reperfusion. Renal function and damage were assessed by serum creatinine and Kim-1 expression. Mitochondrial protein expression was measured by immunoblot [148].

Pharmacological activation of mitochondrial biogenesis

MB is a tightly controlled cellular process coordinated by several nuclear-encoded transcription factors, and a set of transcriptional co-activators and co-repressors [171, 188]. Identification of stimulators of expression or activity of PGC-1 α , a transcriptional co-activator of NRF-1 and master regulator of MB, has been a central focus of development of mitochondrial therapies. Modulation of MB has been accomplished through manipulation of an array of upstream energy sensing pathways including AMP kinase, sirtuins and cyclic nucleotides (cAMP and cGMP), as well as, through direct pharmacological activation of downstream effectors including peroxisome proliferator-activated receptors (PPARs) and estrogen-related receptors (ERRs) (Table 1.2).

Class	Drugs	Mitochondrial biogenic effects	References
AMPK activators	AICAR	↑PGC-1 α activity, ↑mito function in multiple tissues	[208-212]
SIRT1 activators	Resveratrol SRT1720, SRT1460, SRT2104, SRT2379	↑PGC-1 α activity, ↑mito function in multiple tissues	[162, 213-218]
GPCR modulators			
B2-adrenergic agonists	Formoterol	↑PGC-1 α , ↑mtDNA in RPTC, recovery of MB following mouse I/R	[148, 219]
5HT agonists	LY 344,864 DOI	↑PGC-1 α , ↑mtDNA in RPTC, recovery of MB following mouse I/R	[150, 220]
CB1 antagonists	Rimonabant	Activation of eNOS, ↑mtDNA, ↑ mito mRNA in mouse adipocytes	[221]
Nuclear receptor agonists			
PPAR α agonists	Fibrates	Activation of AMPK and PGC-1 α in multiple models	[222-226]
PPAR γ agonists	Thiazolidinediones	↑PGC-1 α , ↑mtDNA in adipose tissue in diabetes	[227, 228]
PPAR δ agonists	GW501516	↑PGC-1 α , ↑FAO in muscle and heart	[229]
Glucocorticoid agonists	Dexamethasone	↑PGC-1 α , ↑Tfam in liver, ↑MB in muscle with chronic administration	[230, 231]
cGMP modulators			
PDE inhibitors	Sildenafil Vardenafil	↑PGC-1 α , ↑mtDNA in RPTC, recovery of MB following FA AKI, ↑MB in adipose tissue	[149, 232]
Nitric oxide mimetics	DETA-NO	↑PGC-1 α , ↑mito mRNA, ↑ respiration in culture models	[233-236]
GC activators	BAY 41-2272 Cinaciguat Riociguat	↑PGC-1 α , ↑mito mRNA, ↑mito function in cell models and adipose tissue, protective in I/R and LPS models	[233, 237, 238]
Naturetic peptides	ANP BNP	ANP: ↑PGC-1 α , ↑UCP-1 in adipocytes BNP: ↑PGC-1 α , ↑mito content in muscle of HFD mice,	[239-241]
Natural products	Green tea polyphenols	↑PGC-1 α , ↑mtDNA following CsA toxicity in kidney	[242]
	Lipoamide	↑PGC-1 α , ↑mtDNA in adipocytes	[243]
	Isoflavones	SIRT1 activation, ↑PGC-1 α , ↑mito mRNA in RPTC	[244]
	Quercetin	↑PGC-1 α , ↑SIRT1, ↑mtDNA in heart and brain	[245, 246]
Genetic modulators	Recombinant Tfam	↑MB, ↑respiration in aged mice, LPS model	[247, 248]
	Donor mtDNA	↑MB, ↑respiration in LHON and LS cells	[249]

Table 1.2. Select listing of pharmacological activators of mitochondrial biogenesis.

AMPK Activators

AMP kinase (AMPK) is critical metabolic switch which is activated by an increased AMP/ATP ratio, indicating low cellular energy status. Activation of AMPK triggers increased glucose uptake, increased oxidative metabolism and MB [250]. AICAR acts as an AMP analog and has been used extensively as an AMPK activator and stimulator of MB [208-212]. AICAR has been described as an 'exercise mimetic' due to its ability to stimulate oxidative metabolism gene programs and increase endurance [251]. AICAR has also shown positive effects in both acute and chronic disease models characterized by mitochondrial dysfunction. Pre-conditioning of rats with AICAR was protective against cardiac I/R injury through enhancement myocardial glucose uptake [252]. AICAR was also shown to limit renal ischemia reperfusion injury in the rat kidney [253]. Chronic administration of AICAR prevented the development of hyperglycemia and insulin resistance in ZDF rats [254]. Finally, AICAR was shown to protect against cisplatin-induced renal injury in mice through SIRT3-mediated enhancement of mitochondrial dynamics and function [255].

Sirtuins

Sirtuins are a family of protein deacetylases that have been linked to MB and function. Of this family, SIRT1 has garnered the most interest due to its positive regulation by the oxidized coenzyme NAD⁺ and its ability to act as a positive transcriptional regulator of PGC-1 α and other mitochondrial associated genes through promoter deacetylation [211, 256]. Resveratrol, a stilbenoid found in red wine, has been extensively studied as a SIRT1 activator and stimulator of MB. Resveratrol has been shown to enhance MB and oxidative metabolism, and be protective in animal models of cardiovascular disease, neurodegeneration and metabolic

syndrome [257-263]. Evaluation of resveratrol in humans has shown positive effects on insulin resistance and glycemic control in diabetic patients [264]. Therapeutic application of resveratrol is limited by its low potency and poor bioavailability, which has led to the development of a new class of synthetic small molecule SIRT1 activators including SRT1720, SRT1460, SRT2104 and SRT237. These compounds have been shown to improve insulin resistance and lower plasma glucose in type 2 diabetic animals, while improving mitochondrial oxidative capacity [265]. SRT1720 significantly increased lifespan in obese mice fed a high fat diet [217]. Additionally, SRT1720 has been demonstrated to promote recovery from renal ischemia/reperfusion injury through activation of SIRT1/PGC-1 α and stimulation of MB [218]. In addition to resveratrol, several other natural products including quercetin, a flavonoid found in an array of different foods, and daidzein and genistein, isoflavones found in soybeans, can induce SIRT1 and positively regulate MB [244, 266].

In addition to SIRT1, SIRT3, which acts within the mitochondrial matrix, is critical for mitochondrial homeostasis. SIRT3 has been shown to regulate a wide range of mitochondrial processes, including ETC efficiency [267], maintenance of mtDNA integrity (30) and mitochondrial antioxidant status [121, 267]. Its reduction, at least in part, is thought to contribute to increased mitochondrial fission, a necessary event in mitochondrial turnover. As mentioned above, SIRT3 has been shown to be a critical downstream mediator of the protective effects of AICAR treatment in renal injury models. These data suggest sirtuins are critical mediators of mitochondrial homeostasis, and that direct or indirect pharmacological activation of sirtuins can positively affect disease outcomes through improved mitochondrial function.

β-adrenergic agonists and cAMP

Early work on the transcriptional regulation of PGC-1 α demonstrated a response to external stimuli including cold temperatures [197]. The transcriptional activation of PGC-1 α and associated MB was linked to activation of the sympathetic nervous system and subsequent release of endogenous adrenergic receptor agonists including norepinephrine. Release of norepinephrine leads to activation of β -adrenergic receptors, stimulation of adenylate cyclase and an increase in intracellular cAMP. Activation of protein kinase A (PKA) by elevated cAMP causes the phosphorylation and activation of cAMP response element-binding protein (CREB), which serves as a transcriptional activator of PGC-1 α . Thus, modulators of endogenous adrenergic ligands or use of pharmacological activators of adrenergic signaling could stimulate MB through this canonical pathway.

Formoterol, a long-acting β_2 -adrenergic receptor agonist, was shown to stimulate mitochondrial respiration and expression of PGC-1 α and PGC-1 α dependent gene expression in primary cultures of renal proximal tubular cells and mouse renal cortex [219]. Administration of formoterol 24 h after I/R-induced AKI in mice accelerated the recovery of mitochondrial and renal function through enhancement of MB [148]. Interestingly, another β_2 -adrenergic receptor agonist, clenbuterol, was shown to inhibit MB in muscle through activation of the negative regulator of MB, RIP140, and suppression of PGC-1 α [268]. These data suggest a functional selectivity of various β_2 -adrenergic agonists for activation of MB. Indeed, in a 2013 study by *Peterson et al.* a panel of β -adrenergic agonists, endogenous ligands of adrenergic receptors, and similar compounds were probed for their ability to stimulate MB in primary cultures of renal cells [269]. Three distinct phenotypes were observed: full MB, partial MB, and no MB among the panel of compounds. These data were used to construct pharmacophores for the

identification of spatial and chemical characteristics required for activation of MB in this class of compounds. These studies could guide the development of novel pharmacological activators of MB with structural similarity to a subset of classical β -agonists.

eNOS, natriuretic peptides and cGMP modulators

There is increasing evidence for a role of the second messenger cGMP in MB. Caloric restriction was demonstrated to induce MB in mice through the induction of endothelial nitric oxide synthase (eNOS) [200]. Furthermore, eNOS-deficient mice demonstrate reduced metabolic rates and increased weight gain compared to control mice [270]. Stimulation of eNOS leads to generation and release of NO from the endothelium causing the activation of soluble guanylate cyclase (sGC) and subsequent production of cGMP. Activation of the NO/cGMP signaling pathway through the use of NO donors, cGMP mimetics or sGC activators stimulates PGC-1 α associated MB and mitochondrial function *in vitro* [233]. Furthermore, the sGC activator, BAY 41-2272 increased brown fat differentiation through induction of UCP-1, PGC-1 α and other mitochondrial target genes. The sGC stimulator, cinaciguat (BAY 58-2667) was demonstrated to be protective in cardiac I/R injury through protein kinase G (PKG) dependent induction of H₂S, a known inducer MB [237].

Natriuretic peptides, including atrial natriuretic peptide (ANP) and brain natriuretic peptide (BNP), polypeptide hormones primarily responsible for vascular tone and natriuresis, exert their effects through activation of membrane bound guanylate cyclases (NPRA/GC-A and NPRB/GC-B) leading to the production of cGMP. Overexpression of brain natriuretic peptide (BNP) in mice fed a high fat diet reduced weight gain and insulin resistance, while partial knockdown of GC-A resulted in increased body fat and reduced insulin sensitivity [239].

Additionally, exercise induces the expression of NPRA/GC-A which correlates with the expression of PGC-1 α -dependent genes in muscle [240]. Finally, treatment of myotubes with ANP and BNP stimulates MB and mitochondrial respiration. Levels of cGMP can also be modulated by blunting its degradation. Sildenafil, a phosphodiesterase 5 (PDE5) inhibitor, which causes the accumulation of cGMP by blocking its conversion to GMP, stimulates PGC-1 α -dependent MB, mitochondrial function and ATP in renal proximal tubular cells and renal cortex of mice. Furthermore, post-treatment of mice with sildenafil after induction of folic acid-induced AKI promotes recovery of mitochondrial biogenic signaling, and reduces renal tubular injury [149]. While the mechanisms of cGMP-induced MB are still poorly understood, studies have implicated both SIRT1 and protein kinase G (PKG) as important downstream mediators of PGC-1 α expression and activity [271].

Transcription factor agonists

An array of nuclear receptors agonists, including peroxisome proliferator-activated receptors (PPAR) and estrogen-related receptors (ERR) have been evaluated for their ability to regulate cellular metabolism and mitochondrial function. Modulation of these pathways have demonstrated positive effects on MB and mitochondrial function, and disease outcomes in multiple animal and cellular models. Treatment with PPAR γ agonists, pioglitazone and rosiglitazone, stimulates MB and protects SH-SY5Y neuronal cells from glucose deprivation-induced cell death [272]. Additionally, the compounds bardoxolone and gallic acid exert a protective effect in renal I/R injury through activation of PPAR γ -dependent transcriptional programs [273, 274]. Finally, agonism of PPAR γ using rosiglitazone has shown efficacy in the treatment of type II diabetes mellitus, potentially through its effects on MB and oxidative metabolism [228].

Activation of PPAR α using fibrates positively modulates mitochondrial function and biogenesis through complex signaling pathways involving several protein kinases, sirtuins and interaction with the transcriptional co-activators PGC-1 α and PGC-1 β . Despite positive results in several model systems, use of these highly active nuclear receptors agonists has been limited by safety concerns. Recent efforts have also been made to directly target the replication of mtDNA using a membrane-penetrant recombinant human Tfam protein (rhTfam) designed with a mitochondrial targeting sequence. Treatment of aged mice with rhTfam stimulates MB in heart, brain and muscle, and slows the progression of cognitive decline [248]. Additionally, rhTfam reduced mortality in mice in an endotoxin-induced sepsis model, which is characterized by profound effects on MB signaling [247]. Use of rhTfam provides a highly specific strategy to stimulate mtDNA transcription and potentially activate biogenesis of mitochondrial-encoded proteins; however, it is unclear how it would exert an effect on the biogenesis of nuclear-encoded mitochondrial proteins, and further validation of its role in MB is needed.

Targeting negative regulators of MB

MB is a tightly regulated process involving both positive and negative regulators. Suppression of MB signaling pathways and reduction in mitochondrial number has been observed in various acute and chronic disease states. In multiple forms of AKI, including I/R injury, folic acid nephropathy and sepsis, mitochondrial gene and protein expression is rapidly and persistently suppressed [126, 161, 275, 276]. Failure of recovery of MB signaling mirrors the incomplete recovery of renal function in these models. Additionally, MB is suppressed in adipose tissue of obese, diabetic mice [277]. MB has also been demonstrated to decline in various tissues in an age-dependent manner [278, 279]. Numerous negative regulators of MB

have been described, including the transcriptional co-repressor, RIP140, HIF-1 α , and several kinases including ERK1/2 and p38 MAPK. However, the upstream mechanisms of suppression of MB following injury are still poorly understood. A link between inflammation and the negative regulation of MB has recently been explored. The pro-inflammatory cytokine, TNF- α was shown to reduce PGC-1 α expression in the heart through activation of NF-kappaB and p38 MAPK [280]. Furthermore, TNF- α suppresses eNOS expression and MB in fat and muscle of obese mice, which is recovered by administration of NO donors [234]. Interestingly, MB signaling has also been linked to the expression of anti-inflammatory genes through dual regulation by heme oxygenase-1 [185].

Damaged mitochondria themselves may provide the signal for the activation of inflammation in a diseased tissue. After tissue injury, damaged mitochondria release various proteins and mtDNA, which are recognized by innate immune cells through toll-like receptors (TLRs) [281]. Thus, mitochondrial damage leads to a vicious cycle of inflammation that may suppress the generation of new, functional mitochondria needed for tissue recovery. These data suggest that attenuation of inflammatory signaling in a diseased tissue may support sustained MB and cellular recovery. While significant work is still needed in this area, targeting inflammation through the use of anti-inflammatory agents including anti-TNF- α blocking antibodies, inhibitors of NF-kappaB, or blockade of specific TLRs may be an effective method to re-activate MB in the setting of injury.

Screening and validation of mitochondrial biogenics

While significant work has been performed in the identification and evaluation of diverse classes of drugs to stimulate MB, many of the identified compounds are limited by 1) poor

pathway specificity, 2) off-target toxicities, 3) adverse interactions with existing standard of care or morbidities, and/or 4) limited potency and efficacy. Therefore, continued identification of novel compounds targeting canonical and non-canonical pathways to MB is essential. To accomplish this goal, new, high-throughput cellular screening methods are required with outputs that accurately reflect increases in mitochondrial content and function that correlates with increased bioenergetic capacity of the cell or tissue. We will discuss the advantages and limitations of a high-throughput genetic-based PCR screening procedure for PGC-1 α transcription, as well as, a physiological-based respirometric screening technique that have both led to the identification of positive stimulators of MB.

Gene expression-based screening

As discussed above, PGC-1 α is a critical transcriptional co-regulator of mitochondrial content and oxidative metabolism. MB is highly dependent upon its expression and activity. Therefore, identification of potent stimulators of PGC-1 α would likely yield highly active MB agents. Studies performed by the Spiegelman group, used a gene-expression based screening technique to identify activators of PGC-1 α transcription and mitochondrial metabolism in cultured adipocytes and primary skeletal muscle cells [282, 283]. Briefly, cells were cultured in 384-well plates, treated with compounds of interest and analyzed for PGC-1 α mRNA expression by real time RT-PCR. This technique was used to screen ~3000 unique compounds including nearly 40% of all FDA-approved drugs. 82 compounds were identified as inducers of PGC-1 α in cultured myotubes, including glucocorticoids, tubulin inhibitors and protein synthesis inhibitors. Screening results from cultured adipocytes identified the CB1 receptor antagonist, AM-251, as a potent inducer of PGC-1 α mRNA expression. However, additional CB1 antagonists, SLV319

and CAY10505, failed to induce PGC-1 α expression. Examination of alternate targets of AM-251 led to the identification of antagonism of the Transient Receptor Potential Vanilloid (TRPV) family of ion channels as a strategy for induction of PGC-1 α . As PGC-1 α mRNA expression does not directly indicate increased mitochondrial content and function and changes in PGC-1 α mRNA and protein over time, confirmatory assays measuring mitochondrial protein expression and mitochondrial respiration were performed for hits from both screens. Evaluation of TRPV4 antagonism in mouse model of diabetes and metabolic syndrome demonstrated decreased weight, improved insulin sensitivity and decreased systemic inflammation. These results demonstrate that gene expression-based screening using PGC-1 α can be a simple and efficient technique for identification of MB agents in cultured cells that are applicable to more complex models. While the technique is useful as an initial screen, any hits require extensive further evaluation to demonstrate if increased PGC-1 α expression correlates with increased mitochondrial gene and protein expression, and if the compounds tested have direct effects on mitochondrial function and homeostasis. Furthermore, this assay would fail to detect any compounds capable of inducing MB through PGC-1 α independent mechanisms.

High-throughput respirometry and virtual screening

The goal of MB is not merely to increase mitochondrial content, but increase the functional mitochondrial capacity of a cell or tissue. Therefore, measurement of mitochondrial respiration may be a useful indicator of MB. However, application of this technique as a screen of compound libraries has been limited by the altered mitochondrial phenotypes of cultured cells and lack of instrumentation for high-throughput respirometry. Our lab developed a culture model of renal proximal tubular cells (RPTCs) that exhibit high, physiological levels of aerobic

metabolism, and adapted this model to a 96-well plate respirometric assay using the Seahorse Bioscience XF96 Extracellular Flux Analyzer (Figure 2). Assessment of FCCP-uncoupled respiration was shown to be a marker of maximal mitochondrial ETC activity and was increased in RPTC with increased MB induced by administration of DOI, SRT1720, resveratrol, daidzein, and metformin [284].

Using the assay, we screened a library of ~2000 compounds from the Sigma LOPAC and ChemBridge DIVERSet libraries for MB by measuring FCCP-uncoupled mitochondrial respiration. This led to the identification of several new classes of compounds that increase mitochondrial function (e.g. β_2 -adrenergic receptor agonists). Changes in mitochondrial respiration were confirmed to be due to activation of MB by evaluation of the induction of mitochondrial gene and protein expression, and mtDNA copy number in cellular and animal models.

One of the classes of compounds identified were agonists of the 5-hydroxytryptamine (serotonin)-1F receptor (5HT-1F), including LY334370 and LY344864 which have no previous association with known pathways of MB or mitochondrial function. Validation studies of the agonist LY344864 demonstrated its ability to induce PGC-1 α and PGC-1 α -dependent gene and protein expression both in RPTCs and *in vivo*. Furthermore, treatment of mice following I/R-induced AKI with LY344864 promoted recovery of mitochondrial content and accelerated recovery of renal function [150]. Identification of novel stimulators of MB that function in disease models demonstrates the efficacy of high-throughput respirometry to screen large chemical libraries for the identification of non-canonical regulatory pathways of mitochondrial function. Combining this phenotypic screen with a virtual screening procedure would provide the benefit of a physiological readout duplexed with the computational power to evaluate

millions of compounds. Development of pharmacophore models based on the structures of known MB agents could be used to screen large virtual libraries for chemical similarity to identify novel compounds. Further analysis of identified hits by clustering based on Tanimoto coefficient, determination of root mean square deviation (RMSD) and molecular docking could act as screens to identify additional lead compounds for evaluation by respirometry. In addition to identifying MB agents, similar procedures can be used to identify mitochondrial toxicants. Use of high-throughput respirometry, high-content imaging for cell viability, and chemoinformatic analysis in RPTC allowed for the construction of a mitochondrial toxicophore, which could have application in the prediction of mitochondrial toxicity for existing and new application therapeutics [285].

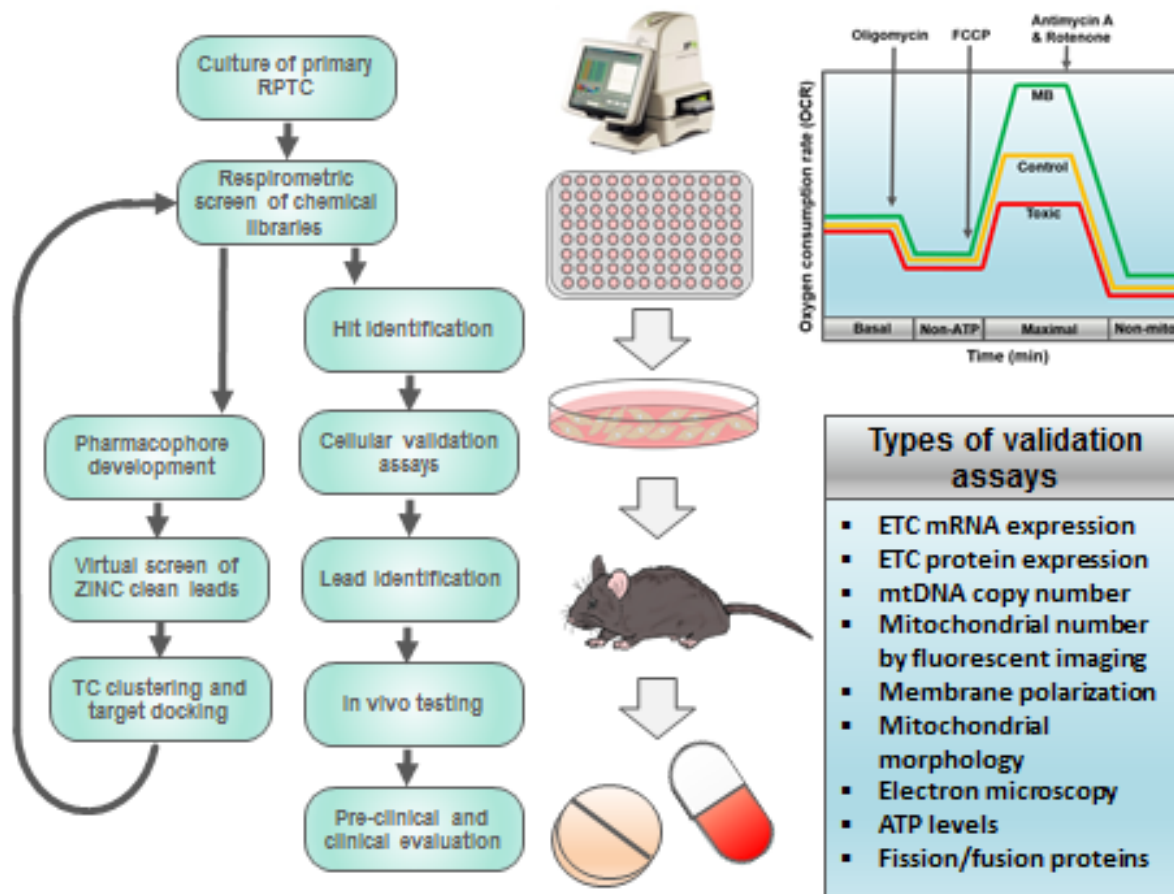


Figure 1.15: Identification of stimulators of mitochondrial biogenesis with high-throughput respirometry and virtual screening. High-throughput screening for potential mitochondrial biogenic agents was performed using a primary rabbit renal proximal tubular cell (RPTC) culture model with the Seahorse Bioscience XF96 Extracellular Flux Analyzer. Screening was performed for compounds in the Sigma LOPAC1280 and Chembridge DIVERset chemical diversity libraries. High-throughput screening was duplexed with computational techniques by construction of pharmacophores used for screening of the ZINC Clean Leads virtual library allowing for the identification of novel chemical hits. Hits from the high throughput screen were validated as mitochondrial biogenic agents by various assays before evaluation in naïve and diseased animal models. Successful agents will proceed into pre-clinical and clinical evaluation for safety and efficacy in human disease. FCCP, Carbonyl cyanide-4 (trifluoromethoxy) phenylhydrazone; ETC, electron transport chain; ATP, adenosine triphosphate.

CHAPTER 2:

**cGMP-selective phosphodiesterase inhibitors stimulate mitochondrial
biogenesis and promote recovery from acute kidney injury**

ABSTRACT

Recent studies demonstrate that mitochondrial dysfunction is a mediator of acute kidney injury (AKI). Consequently, restoration of mitochondrial function after AKI may be key to the recovery of renal function. Mitochondrial function can be restored through the generation of new, functional mitochondria in a process called mitochondrial biogenesis (MB). Despite its potential therapeutic significance, very few pharmacological agents have been identified to induce MB. To examine the efficacy of phosphodiesterase (PDE) inhibitors (PDE3: cAMP and cGMP activity; and PDE4: cAMP activity) in stimulating MB, primary cultures of renal proximal tubular cells (RPTCs) were treated with a panel of inhibitors for 24 hours. PDE3, but not PDE4, inhibitors increased the FCCP-uncoupled oxygen consumption rate (OCR), a marker of MB. Exposure of RPTCs to the PDE3 inhibitors, cilostamide and trequinsin, for 24 hours increased peroxisome proliferator-activated receptor γ coactivator-1 α , and multiple mitochondrial electron transport chain genes. Cilostamide and trequinsin also increased mRNA expression of mitochondrial genes and mitochondrial DNA copy number in mice renal cortex. Consistent with these experiments, 8-Br-cGMP increased FCCP-uncoupled OCR and mitochondrial gene expression, whereas 8-Br-cAMP had no effect. The cGMP-specific PDE5 inhibitor sildenafil also induced MB in RPTCs and in vivo in mouse renal cortex. Treatment of mice with sildenafil after folic acid-induced AKI promoted restoration of MB and renal recovery. These data provide strong evidence that specific PDE inhibitors that increase cGMP are inducers of MB in vitro and in vivo, and suggest their potential efficacy in AKI and other diseases characterized by mitochondrial dysfunction and suppressed MB.

INTRODUCTION

Mitochondrial dysfunction is increasingly recognized as an important pathophysiological mediator of a variety of disease states, including neurodegeneration, cardiovascular disease, metabolic syndrome and acute organ injury [125, 286-292]. Mitochondrial dysfunction is an established component of the pathogenesis of acute kidney injury (AKI) and a cause of renal tubular dysfunction and cell death [153-155, 293, 294]. Our group has demonstrated persistent disruption of mitochondrial homeostasis and inhibition of mitochondrial biogenesis (MB) after ischemia-reperfusion (I/R), rhabdomyolysis-induced AKI, and folic acid (FA)-induced AKI [161]. Restoration of mitochondrial number and function is thought to be required for recovery from AKI due to the high energy requirements of tissue repair. These data provide support for development of pharmacological agents that induced MB for treatment of AKI and other pathologies characterized by mitochondrial dysfunction.

Mitochondria are dynamic organelles that are continuously regenerated through the processes of biogenesis, mitophagy, fission, and fusion [160, 161, 295, 296]. MB is the assembly of new mitochondria from existing mitochondria, occurring under basal conditions to replace damaged mitochondria, but is rapidly induced in response to both physiological and pathophysiological stimuli, including sepsis, exercise, fasting, hypoxia, and cellular injury [197, 297-299]. The primary regulator of MB is the transcriptional coactivator peroxisome proliferator-activated receptor γ coactivator-1 α (PGC-1 α). PGC-1 α exerts its functions by activating the transcription factors, nuclear respiratory factors 1 and 2 (Nrf1 and Nrf2). Nrf1 controls the expression of mitochondrial transcription factor A (Tfam), which regulates the transcription of mitochondrial DNA (mtDNA) [183, 187, 188, 300]. PGC-1 α is enriched in tissues with high metabolic demand, including heart, muscle, and kidneys [301]. The ability of

PGC-1 α to respond to a variety of stimuli and its importance in cellular bioenergetics make it an ideal target for pharmacological intervention in disease states characterized by mitochondrial disruption.

Despite the promise of PGC-1 α and MB as a therapeutic target, there is a paucity of pharmacological agents capable of stimulating PGC-1 α expression and activity. Activators of silent mating type information regulation 2 homolog 1 (SIRT1), including isoflavones, resveratrol, and N-[2-[3-(piperazin-1-ylmethyl)imidazo[2,1-b][1,3]thiazol-6-yl]phenyl]quinoxaline-2-carboxamide (SRT1720), have been demonstrated to induce PGC-1 α and promote increased mitochondrial number and function [162, 214, 244]. Our laboratory also identified the 5-hydroxytryptamine type 2 agonist, 1-(2,5-dimethoxy-4-iodophenyl)-2-aminopropane hydrochloride (DOI), and the β 2-adrenergic receptor agonist, formoterol, as potent inducers of PGC-1 α and MB [219, 220]. Stimulation of MB after injury accelerates recovery of cellular morphology and function [162, 207, 220]. These data demonstrate the importance of MB in recovery of renal tubular epithelial cells after injury and suggest that agents that stimulate MB could serve as viable therapies after AKI.

Because of the importance the cAMP/protein kinase A (PKA)/cAMP-response element-binding protein (CREB) axis in PGC-1 α regulation, drugs that increase cellular cAMP may induce MB. The β 2-adrenergic signaling cascade, which upon activation increases intracellular cAMP through G_s-mediated activation of adenylyl cyclase, was shown to regulate oxidative metabolism and energy expenditure [302, 303]. Formoterol induces MB in renal proximal tubular cells (RPTCs), and mice treated with formoterol demonstrated increased mitochondrial gene expression and mtDNA copy number in renal cortex and heart [219]. cGMP levels have also been shown to regulate PGC-1 α expression and MB. Pharmacologically induced generation

of nitric oxide (NO) via endothelial nitric oxide synthase (eNOS) and subsequent NO-dependent activation of guanylyl cyclase led to MB in U937, L6 and PC12 cells [233].

Both cAMP and cGMP levels are tightly regulated through cleavage to AMP and GMP, respectively, by a class of enzymes called cyclic nucleotide phosphodiesterases (PDEs). The PDE superfamily consists of 11 families differing in tissue distribution, regulation and substrate affinity (e.g., cAMP versus cGMP) [304]. Potent, selective inhibitors of nearly all family members are available [305]. Inhibition of PDEs could serve as a novel and potentially efficacious drug target to induce MB. As such, we studied inhibitors of PDE3, PDE4, and PDE5 for their ability to induce MB in the kidney and promote recovery from FA-induced AKI.

EXPERIMENTAL PROCEDURES

Reagents

Cilostamide, trequinsin, (R)-(-)-rolipram, 4-(3-butoxy-4-methoxyphenyl)methyl-2-imidazolidone (Ro 20-1724), sildenafil, 8-Br-cAMP, and 8-Br-cGMP were purchased from Tocris Bioscience (Ellisville, MO). All other chemicals were obtained from Sigma-Aldrich (St. Louis, MO).

Animal Care and Use

Studies were carried out in strict accordance with the recommendations in the Guide for the Care and Use of Laboratory Animals of the National Institutes of Health. All protocols were approved by the Institutional Animal Care and Use Committee at the Medical University of South Carolina and all efforts were made to minimize animal suffering.

Isolation and Culture of Proximal Tubules

Female New Zealand white rabbits (1.5–2.0 kg) were purchased from Charles River Laboratories (Wilmington, MA). RPTCs were isolated using the iron oxide perfusion method previously described[306]. For respirometry experiments, cells were plated on 100-mm culture-grade Petri dishes at 37°C in a 5% CO₂/95% air environment. Dishes were continuously swirled on an orbital shaker at 80 rpm. Cell culture media consisted of a 1:1 mixture of Dulbecco's modified Eagle's essential medium and Ham's F-12 (lacking glucose, phenol red, and sodium pyruvate; Invitrogen, Carlsbad, CA), supplemented with HEPES (15 mM), glutamine (2.5 mM), pyridoxine HCl (1 μM), sodium bicarbonate (15 mM), and lactate (6 mM). Hydrocortisone (50 nM), selenium (5 ng/ml), human transferrin (5 μg/ml), bovine insulin (10 nM), and L-ascorbic

acid-2-phosphate (50 μM) were added daily to fresh culture media. After 3 days of culture, dedifferentiated RPTCs were trypsinized and replated on XF-96 polystyrene cell culture microplates (Seahorse Bioscience, North Billerica, MA) at a concentration of 18,000 cells per well. Cells were maintained at 37°C for an additional 2 days before experimentation [284]. For all other RPTC experiments, cells were plated and cultured in 35-mm dishes in the above-described media. Experiments were performed on the sixth day after plating when cells had formed a confluent monolayer. RPTCs were treated with various compounds for 24 hours unless otherwise noted.

Oxygen Consumption

The oxygen consumption rate (OCR) of RPTCs was measured using the Seahorse Bioscience XF-96 Extracellular Flux Analyzer according to a previously described protocol[284]. Each assay plate was treated with vehicle control (dimethylsulfoxide <0.5%), and increasing concentrations of the compounds of interest. Basal OCR was measured before injection of carbonyl cyanide 4-(trifluoromethoxy)phenylhydrazone (FCCP) (0.5 μM), allowing for the measurement of uncoupled OCR.

Testing of Compounds in C57BL/6 Mice

Male C57BL/6 mice (aged 6–8 weeks) were obtained from the National Institutes of Health National Cancer Institute (Bethesda, MD). Mice were housed individually in a temperature-controlled room under a 12-hour light/dark cycle. Mice were randomly assigned to saline control, cilostamide (0.3 or 3 mg/kg), trequinsin (0.3 or 3 mg/kg), or sildenafil (0.3 or 3 mg/kg) treatment groups. Mice were given a single intraperitoneal injection of saline or compound at the above-described doses. Mice were euthanized by CO₂ asphyxiation followed by cervical dislocation 24

hours after treatment. Kidneys were removed and preserved by flash-freezing in liquid nitrogen. Tissues were stored at -80°C for later analysis.

Folic acid animal model

Male C57BL/6 mice (aged 8–10 weeks) were given a single intraperitoneal injection of 250 mg/kg FA dissolved in 250 mM sodium bicarbonate or saline control based on previous literature[88]. Mice were injected with sildenafil (0.3 mg/kg) or diluent every 24 hours beginning 1 day after FA injection. Mice were euthanized at 7 days via isoflurane asphyxiation and cervical dislocation. Kidneys were removed and preserved by flash-freezing.

Quantitative Real-Time Polymerase Chain Reaction

Total RNA was extracted from RPTCs or renal cortex samples using TRIzol reagent (Invitrogen) according to the manufacturer's protocol. cDNA was synthesized via reverse transcription using the iScript Advanced cDNA synthesis kit (Bio-Rad, Hercules, CA) with 2 μg of RNA. Quantitative real-time polymerase chain reaction (qPCR) analysis was performed with cDNA using SsoAdvanced SYBR Green Supermix (Bio-Rad) at a concentration of $1\times$ and primers at a concentration of 750 nM (Integrated DNA Technologies, Coralville, IA). mRNA expression of all genes was calculated using the $2^{-\Delta\Delta\text{CT}}$ method normalized to tubulin in RPTCs or β -actin in renal cortical tissue. Primer sequences for PGC-1 α , NADH dehydrogenase 6 (ND6), NADH dehydrogenase [ubiquinone] 1 β subcomplex subunit 8 (NDUF β 8), and tubulin were described previously[161]. Primer sequences for NADH dehydrogenase 1 (ND1) and β -actin were as follows: ND1, sense 5'-TAGAACGCAAAATCTTAGGG-3' and antisense 5'-

TGCTAGTGTGAGTGATAGGG-3'; and β -actin, sense 5'- GGGATGTTTGCTCCAACCAA-3' and antisense 5'-GCGCTTTTGACTCAAGGATTTAA-3'.

mtDNA Content

Real-time PCR was used to determine the relative quantity of mtDNA in both RPTC and mouse renal cortical tissue samples. After treatment, DNA was extracted from cells or tissue using the DNeasy Blood and Tissue Kit (QIAGEN, Valencia, CA) and 5 ng of cellular DNA was used for qPCR. For RPTC samples, mitochondrial-encoded ND6 was used to measure mitochondrial copy number and was normalized to nuclear-encoded tubulin expression. For renal cortex, ND1 was used as the mitochondrial gene and expression was normalized to nuclear-encoded β -actin expression.

cAMP and cGMP Enzyme-Linked Immunosorbent Assay

RPTCs in 35-mm dishes were treated with vehicle control (dimethylsulfoxide) or the compound of interest for 20 minutes. RPTCs were then harvested according to the manufacturer's protocol and cAMP or cGMP levels were measured using a commercially available enzyme-linked immunosorbent assay kit (Cayman Chemical, Ann Arbor, MI).

Tissue ATP Levels

ATP was isolated from renal cortical tissue via phenol-Tris-EDTA extraction as previously described[307]. In brief, freshly prepared tissue was homogenized in 3.0 ml ice-cold Tris-EDTA saturated phenol. One milliliter of the homogenate was combined with 200 μ l chloroform and 150 μ l of deionized water and vortexed and centrifuged at 10,000g for 5 minutes at 4°C. An aliquot

from the supernatant was diluted 200-fold in deionized water, and ATP levels were measured using a luciferin-luciferase-based ATP determination kit (Invitrogen).

Data and Statistical Analysis

Data are presented as the mean \pm S.E.M. Single comparisons were performed using the t test. Multiple comparisons were subjected to one-way analysis of variance followed by the Newman-Keuls test, with $P < 0.05$ considered to be a statistically significant difference between means. RPTCs isolated from a single rabbit represented an individual experiment ($n = 1$) and were repeated until $n \geq 4$ was obtained. Mouse studies were repeated until $n \geq 3$ was obtained.

RESULTS

PDE3 Inhibitors, but not PDE4 Inhibitors, Increase FCCP-Uncoupled OCR in RPTCs.

We treated RPTCs in XF-96 culture plates with the PDE3 inhibitors cilostamide or trequinsin, the PDE4 inhibitors (*R*)-(-)-rolipram or Ro 20-1724, or vehicle control for 24 hours. PDE3 hydrolyzes both cAMP and cGMP to their noncyclic forms, AMP and GMP, whereas PDE4 specifically hydrolyzes cAMP to AMP [304]. FCCP-OCR increased in RPTCs compared with vehicle control after 24-hour exposure to cilostamide (25–100 nM) and trequinsin (30–100 nM) (Figure 2.1A, 2.1B), but no significant changes were observed in FCCP-OCR after treatment with (*R*)-(-)-rolipram (0.5–50 μ M) or Ro 20-1724 (5–20 μ M) (Figure 2.1C, 2.1D). These data suggest a functional selectivity for the MB response between PDE3 and PDE4 inhibition in RPTCs.

PDE3 Inhibitors Induce MB in RPTCs.

To validate that the increased FCCP-OCR observed in RPTCs after treatment with PDE3 inhibitors was due to MB, mRNA levels for PGC-1 α , the mitochondrial-encoded complex I protein ND6, and the nuclear-encoded complex I protein NDUFB8 were measured via qPCR. Gene expression was normalized to tubulin. PGC-1 α levels increased versus control after treatment with cilostamide (1.8-fold) or trequinsin (2.5-fold) (Figure 2.2). In addition, mRNA expression of mitochondrial-encoded ND6 and the nuclear-encoded NDUFB8 mitochondrial proteins were increased versus control with cilostamide (1.5- and 2.2-fold, respectively) and trequinsin (1.8- and 2.4-fold, respectively). These data provide strong evidence that inhibition of PDE3 causes functional MB in RPTCs.

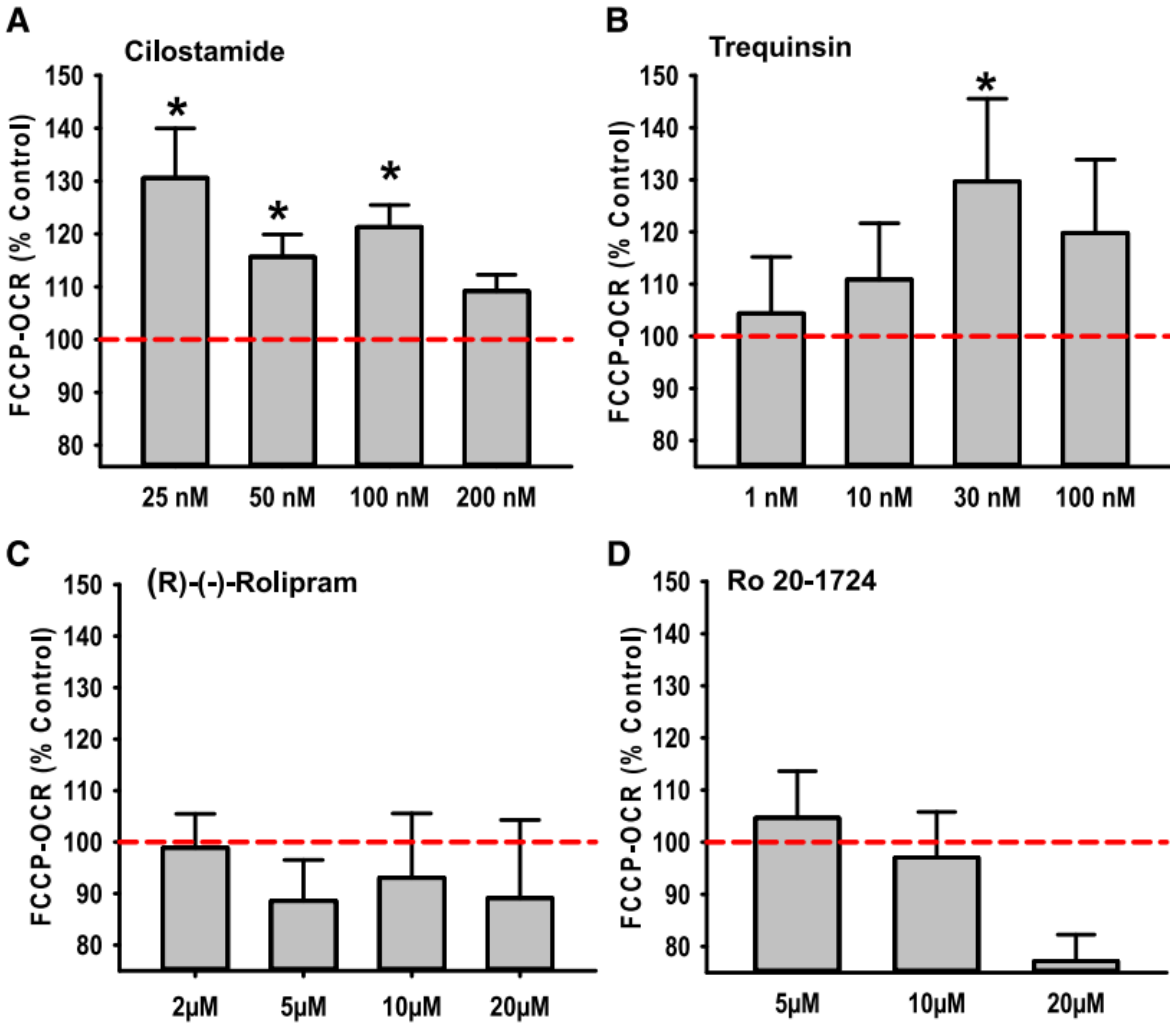


Figure 2.1: PDE3 inhibitors, but not PDE4 inhibitors, increase FCCP-induced uncoupled mitochondrial respiration in RPTCs. RPTCs were treated with cilostamide (A), trequinsin (B), (R)-(-)-rolipram (C), or Ro 20-1724 (D) for 24 hours. FCCP-uncoupled mitochondrial respiration was measured using the Seahorse XF-96 instrument. Data are presented as the mean \pm S.E.M. ($n \geq 3$). * $P < 0.05$ vs. vehicle control.

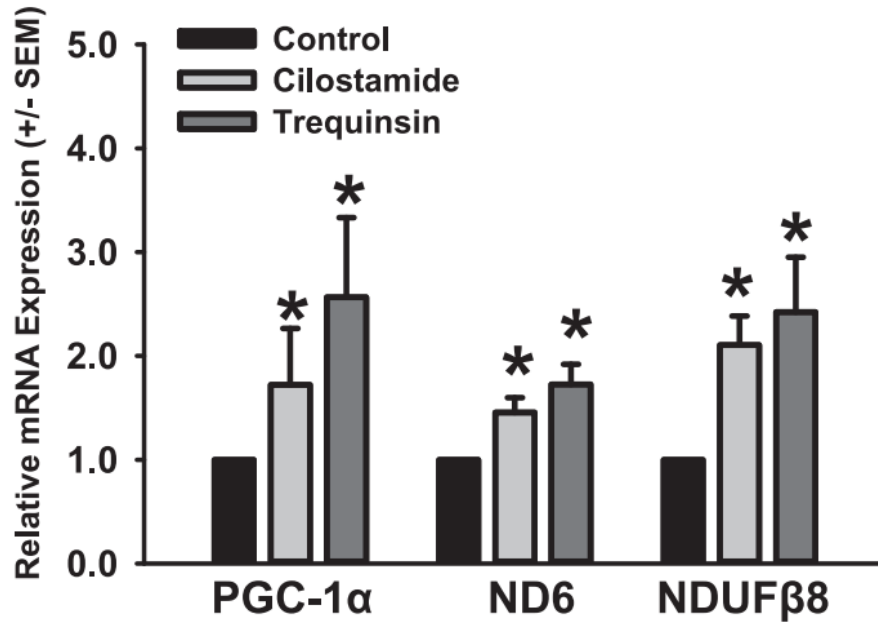


Figure 2.2: PDE3 inhibitors, cilostamide or trequinsin, induce mitochondrial gene expression in RPTCs. RPTCs were exposed to cilostamide (25 nM) or trequinsin (30 nM) for 24 hours and evaluated for changes in mRNA expression of PGC-1 α , ND6, and NDUF β 8 relative to dimethylsulfoxide controls. Data are presented as the mean \pm S.E.M. ($n \geq 4$). * $p < 0.05$ vs. vehicle control.

Increased cGMP, but Not cAMP, Induces MB in RPTCs.

To examine the functional selectivity of PDE3 and PDE4 inhibitors under conditions that induce MB, RPTCs were treated with the PDE3 inhibitors cilostamide and trequinsin, the PDE4 inhibitor (*R*)-(-)-rolipram, or vehicle control for a period of 20 minutes. Sildenafil, a specific inhibitor of PDE5 (cGMP-specific PDE), was included as a control. Both cAMP and cGMP levels increased in response to cilostamide and trequinsin compared with vehicle control, whereas cAMP only increased in RPTCs treated with rolipram (Figure 2.3A, 2.3B). RPTCs treated with sildenafil resulted in increased cGMP, but not cAMP. These data agree with the classic mechanisms of PDE3 (hydrolyzes both cAMP and cGMP), PDE4 (hydrolyzes only cAMP), and PDE5 (hydrolyzes only cGMP) [305]. The inability of rolipram and other PDE4 inhibitors tested to induce MB suggests that cGMP may be the primary mediator of MB in RPTCs.

To test this hypothesis, we treated RPTCs with the cell-permeable cyclic nucleotide analogs, 8-Br-cAMP and 8-Br-cGMP for a 24-hour period. RPTCs treated with 8-Br-cGMP (10–300 μ M) showed an approximately 20% increase in FCCP-uncoupled OCR at all concentrations tested, whereas treatment with 8-Br-cAMP resulted in no change (Figure 2.3C). To validate that this increase in FCCP-OCR is due to stimulation of MB, mRNA expression of PGC-1 α , ND6, and NDUFB8 was measured by qPCR. RPTCs treated with 8-Br-cGMP had elevated mRNA levels of PGC-1 α (2.2-fold), ND6 (1.7-fold), and NDUFB8 (1.9-fold). 8-Br-cAMP had no effect on mitochondrial gene expression (Figure 2.3D).

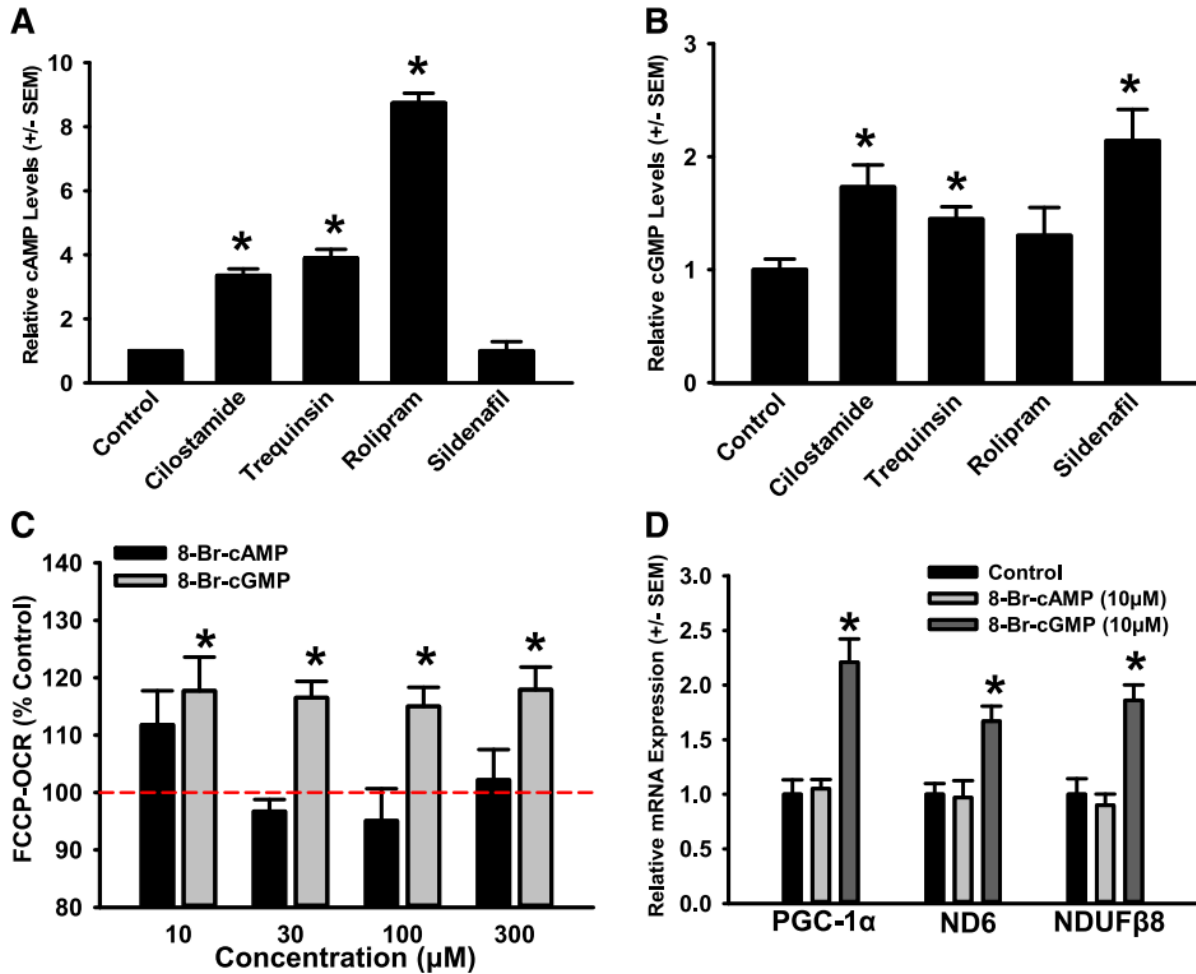


Figure 2.3: PDE inhibitor–induced increases in cGMP, but not cAMP, stimulate MB in RPTCs. cAMP (A) and cGMP (B) levels were measured in RPTCs by enzyme-linked immunosorbent assay 20 minutes after treatment with dimethylsulfoxide, cilostamide (25 nM), trequinsin (30 nM), rolipram (0.5 μM), or sildenafil (10 nM). (C) FCCP-uncoupled mitochondrial respiration was measured using the Seahorse XF-96 instrument after 24-hour treatment with 8-Br-cAMP or 8-Br-cGMP. (D) RPTCs were exposed to 8-Br-cAMP (10 μM) or 8-Br-cGMP (10 μM) for 24 hours and evaluated for changes in mRNA expression of PGC-1α, ND6, and NDUFB8 relative to dimethylsulfoxide controls. Data are presented as the mean ± S.E.M. ($n \geq 3$). * $P < 0.05$ vs. vehicle control.

Furthermore, to test the ability of a PDE5 inhibitor to induce MB in vitro, RPTCs were treated with sildenafil for 24 hours (1 nM–1 μ M) and FCCP-OCR was measured using the Seahorse XF96. RPTCs treated with sildenafil showed an approximately 20% increase in FCCP-uncoupled OCR versus controls (Figure 2.4A) at 10 and 100 nM. To validate that the increase in respiration was due to MB, mRNA levels of PGC-1 α , ND6, and NDUFB8 were measured and were found to increase 1.8-, 2.0-, and 1.5-fold, respectively (Figure 2.4B).

PDE3 Inhibitors Induce MB in Mouse Renal Cortex.

In kidneys of cilostamide-treated mice, PGC-1 α was induced 2- and 2.7-fold at doses of 0.3 and 3 mg/kg, respectively. Trequinsin induced PGC-1 α 2.7- and 2.8- fold in the kidney at doses of 0.3 and 3 mg/kg. mRNA expression of the nuclear-encoded mitochondrial genes NDUFB8 and ATP5 β both increased greater than 2-fold in kidneys of mice treated with either cilostamide or trequinsin at 0.3 or 3 mg/kg (Figure 2.5A, 2.5B). The mitochondrial-encoded mitochondrial genes ND1 and cytochrome *c* oxidase subunit I (COX1) increased in the kidneys of these mice. The mtDNA copy number was also increased in the kidneys of mice treated with cilostamide at 0.3 mg/kg, whereas mice treated with 3 mg/kg cilostamide had no effect (Figure 2.5C). Trequinsin increased mtDNA copy number in the kidneys 1.6- and 2-fold at doses of 0.3 and 3 mg/kg, respectively (Figure 5D). These data provide strong evidence that pharmacological inhibition of PDE3 induces MB in the kidney of naïve mice.

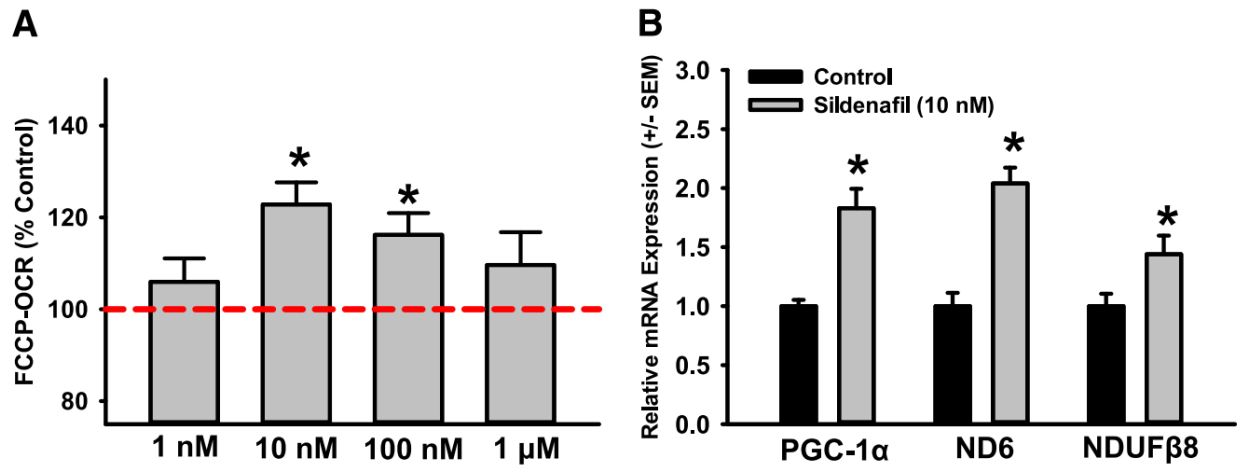


Figure 2.4: The PDE5 inhibitor sildenafil stimulates MB in RPTCs. Sildenafil increases FCCP-uncoupled mitochondrial respiration at various doses (A) and mitochondrial gene expression at 10 nM (B) in RPTCs. mRNA expression of PGC-1 α , ND6, and NDUF β 8 is presented as the mean \pm S.E.M. of at least three biologic replicates. * $P < 0.05$ vs. vehicle control.

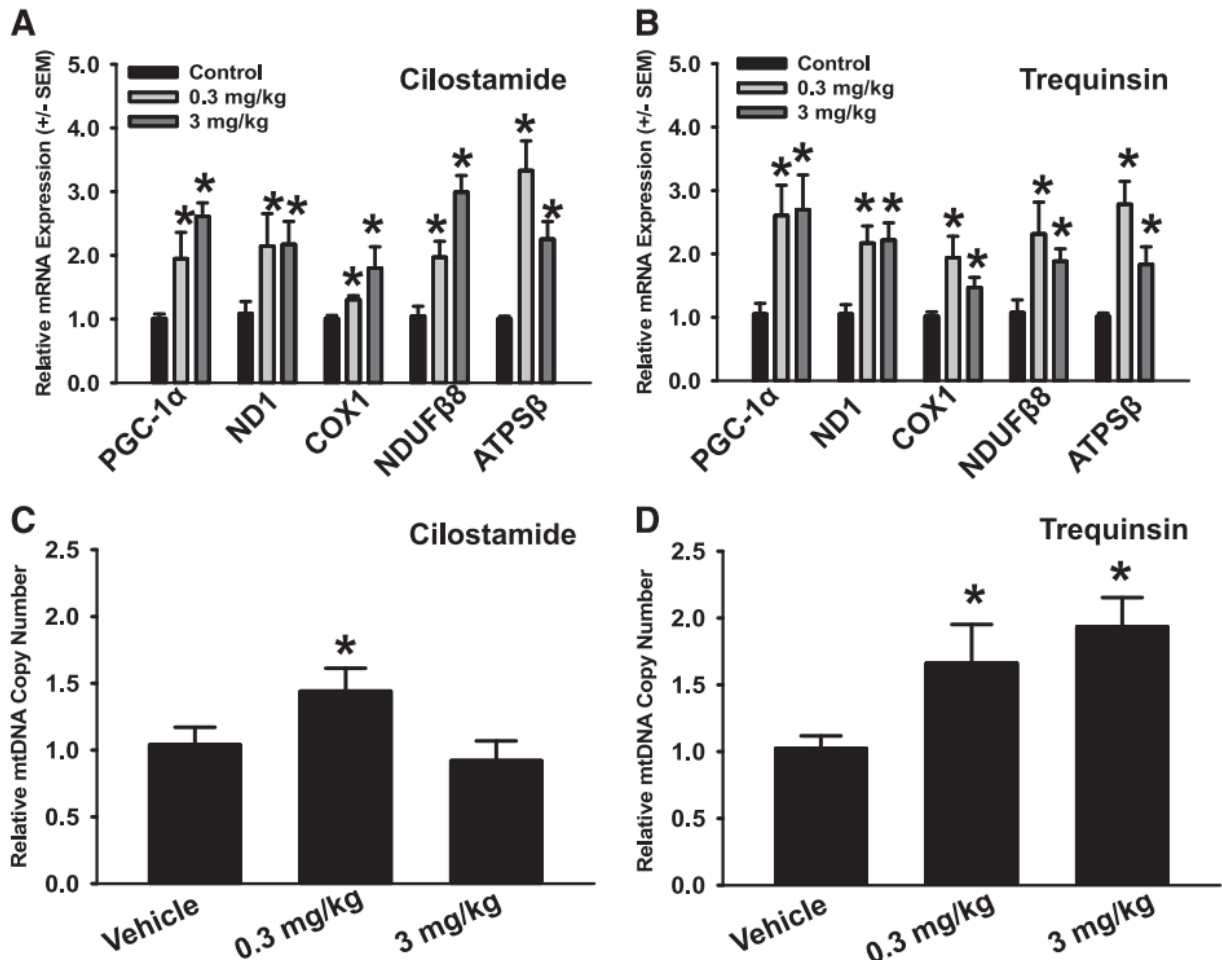


Figure 2.5: PDE3 inhibitors, cilostamide and trequinsin, induce mitochondrial gene expression and mtDNA copy number in mouse renal cortex. mRNA expression and mtDNA copy number were evaluated in the renal cortex of mice 24 hours after a single intraperitoneal injection of cilostamide (A and C) or trequinsin (B and D). Values indicate fold change relative to dimethylsulfoxide controls. Data are presented as the mean \pm S.E.M. ($n \geq 4$). * $P < 0.05$ vs. vehicle control.

Sildenafil Induces MB in Mouse Renal Cortex.

The selectivity of the MB response for cGMP in RPTCs indicates that inhibitors of cGMP-specific PDEs, such as PDE5, may in fact be a better therapeutic target and could eliminate off-target effects due to the accumulation of cAMP. PDE5 inhibitors also have a much more favorable safety protocol than PDE3 inhibitors, particularly for extended administration [308].

To determine whether PDE5 inhibition is capable of inducing MB in the kidney in vivo, mice were given a single intraperitoneal injection of sildenafil (0.3 or 3 mg/kg) or saline control. Mice were euthanized and kidneys were harvested 24 hours after treatment. mRNA levels of PGC-1 α , NDUFB8, ND1, ATP β , and COX1 were measured by qPCR. All mitochondrial genes, except for COX1 and ATP β , were increased in mice treated with 3 mg/kg sildenafil versus saline-treated animals (Figure 2.6A). mtDNA copy number was assessed by qPCR in kidneys of sildenafil-treated mice and was found to increase 1.6-fold in mice treated with 0.3 mg/kg sildenafil. No change in mtDNA copy number was observed in mice treated with 3 mg/kg sildenafil (Figure 2.6B).

To assess whether sildenafil-induced MB increased mitochondrial function in the kidney cortex, we measured ATP levels. ATP levels increased 32% in mice treated with 0.3 mg/kg sildenafil compared with control mice (Figure 2.6C). These data strongly support our hypothesis that PDE5 inhibitors induce MB and mitochondrial function in vitro and in vivo.

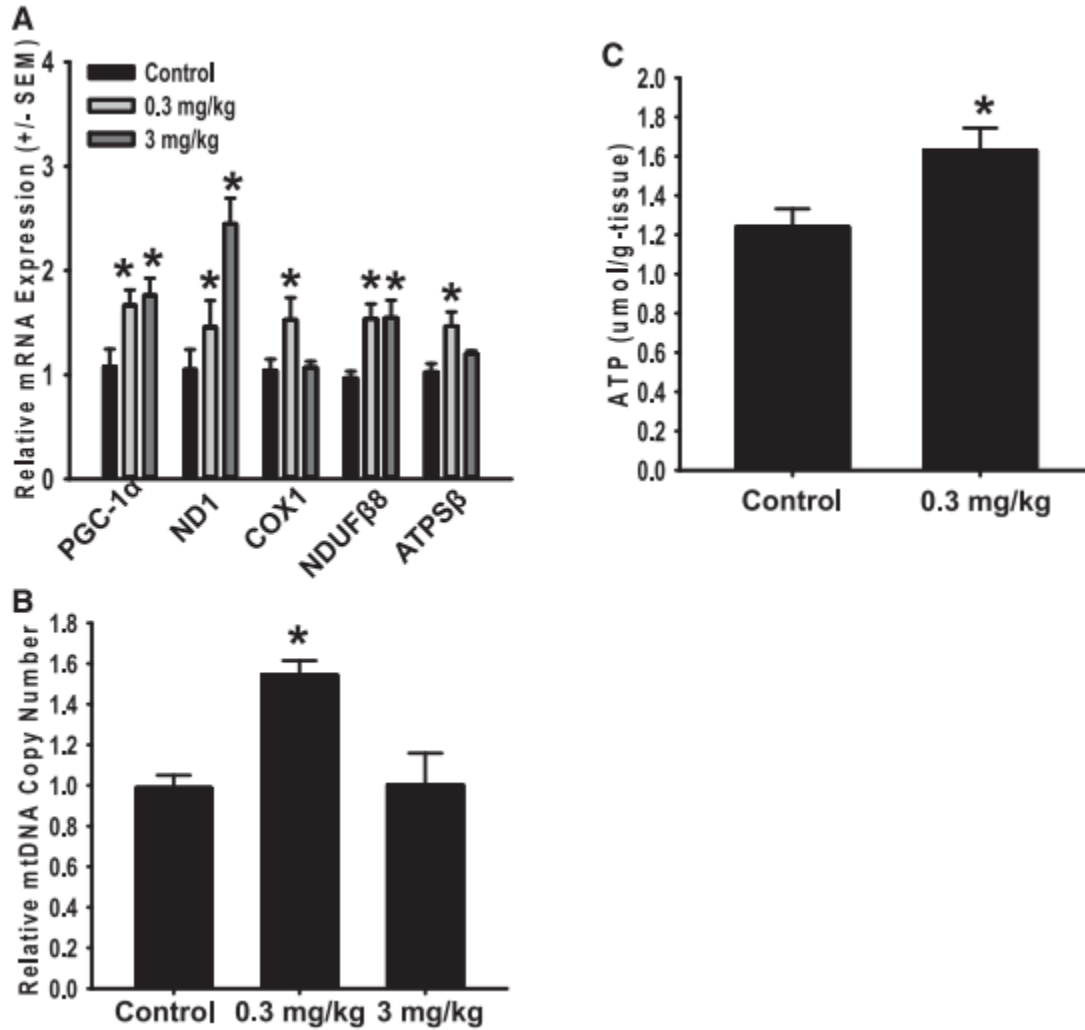


Figure 2.6: Sildenafil induces mitochondrial gene expression, mtDNA copy number, and ATP levels in mouse renal cortex. mRNA expression (A), mtDNA copy number (B), and ATP levels (C) were evaluated in the renal cortex of mice 24 hours after a single intraperitoneal injection of sildenafil. Values indicate fold change relative to dimethylsulfoxide controls. Data are presented as the mean \pm S.E.M. ($n \geq 4$). * $P < 0.05$ vs. vehicle control.

Sildenafil Promotes Recovery of MB and Renal Function after FA-Induced AKI.

To test the hypothesis that sildenafil-induced MB will accelerate recovery of mitochondrial and renal function after AKI, we induced AKI by injecting FA and then treated these mice with sildenafil or vehicle once daily starting at 24 hours after injury for 6 days. mRNA expression of COX1 and Tfam were reduced to 27 and 36% of control, respectively, in FA-treated mice receiving vehicle control at 6 days. Sildenafil-treated FA mice demonstrated a 1.6-fold increase in mRNA COX1 expression to 43% of control mice, and a 1.4-fold increase in Tfam expression to 50% of control (Figure 2.7A). mtDNA copy number was reduced to 36% of animals receiving FA alone, and treatment with sildenafil caused an approximately 2-fold induction to 63% of control (Figure 2.7B). These data demonstrate that sildenafil can induce MB in a model of AKI.

To examine whether MB promoted renal recovery, kidney injury molecule-1 (KIM-1), a specific marker of tubular injury, was measured in renal cortex. KIM-1 levels were markedly increased (approximately 6-fold) in FA-treated animals compared with control animals and treatment of FA mice with sildenafil restored KIM-1 expression to control levels (Figure 2.7C, 2.7D). These data demonstrate that sildenafil promotes renal recovery with its induction of mitochondrial gene expression and mtDNA copy number.

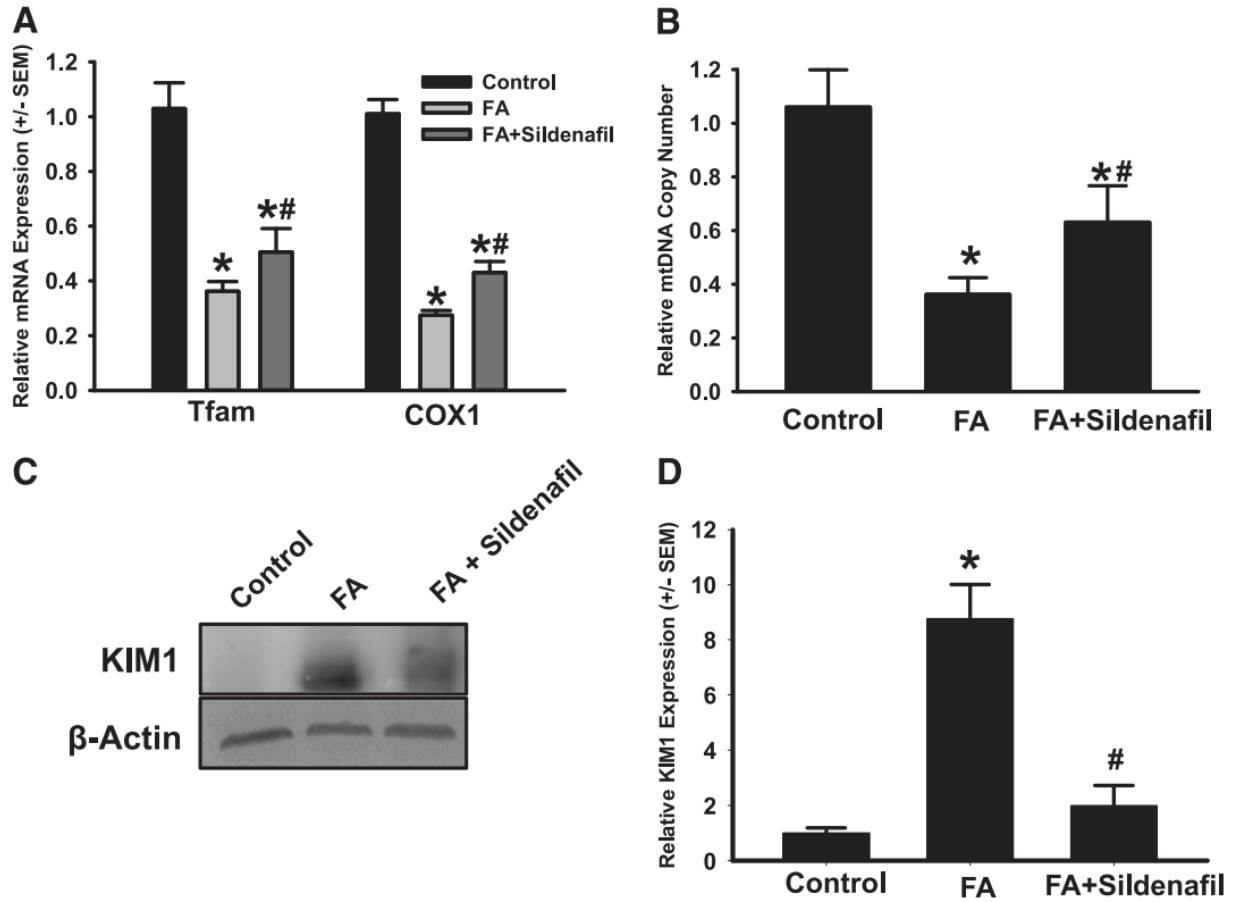


Figure 2.7: Sildenafil stimulates MB after FA-induced AKI. AKI was induced in C57BL/6 by a single intraperitoneal injection of FA. Mice received daily injections of sildenafil (0.3 mg/kg) or saline vehicle beginning 24 hours after FA. Mice were killed and kidneys were collected 7 days after FA administration. mRNA expression (A) and mtDNA copy number (B) were evaluated in the renal cortex. Immunoblotting was performed for renal cortical assessment of KIM-1 expression (C) and quantified via densitometry (D). Data are presented as the mean \pm S.E.M. ($n \geq 3$). * $P < 0.05$ versus vehicle control; # $P < 0.05$ vs. FA.

DISCUSSION

Mitochondria are highly regulated organelles whose function is tightly linked to the metabolic demands and health of a cell [160, 161, 295, 296]. Mitochondrial function is necessary for normal cell and tissue function, and is critical in energy-dependent repair processes. A wide array of disease states are characterized by mitochondrial dysfunction, including diabetes, neurodegenerative disease, traumatic brain injury, and acute organ injury [287, 289, 291, 292, 309]. I/R and drug/toxicant-induced renal injury demonstrate mitochondrial dysfunction and suppression of MB, and recovery of renal function is tightly linked to the restoration of mitochondrial number and function [161]. This suggests that development of therapies capable of inducing MB may have great potential in the treatment of a broad range of disease states.

Despite strong evidence supporting mitochondria as a therapeutic target, there are very few drugs/chemicals available that promote mitochondrial function or MB. Many of the agents that are available suffer from lack of specificity, low potency, or poor toxicity profiles. There is a clinical need to develop new pharmacological agents or identify existing therapeutics that induce MB. Because of the role of cyclic nucleotides as regulators of PGC-1 α , in this study, we sought to determine the efficacy of various classes of PDE inhibitors at stimulating MB.

The cAMP/PKA/CREB signaling cascade is a well characterized regulator of PGC-1 α expression and activity [310]. Increases in intracellular cAMP levels cause activation of PKA and subsequent phosphorylation and activation of CREB, an important transcriptional regulator of PGC-1 α . Induction of cAMP levels in the cell occurs after activation of various G protein-coupled receptors. Our laboratory recently identified the β 2-adrenergic agonist, formoterol, as a potent inducer of MB in the kidney and heart [219]. β -agonism was previously shown to induce

PGC-1 α in skeletal muscle of treated mice [311]. In addition, exercise-induced MB can be blocked by treatment with β -receptor antagonists, propranolol and ICI-118,551. cAMP levels in the cell are controlled both by the rate of synthesis and the rate of turnover by cyclic nucleotide PDEs. Therefore, inhibition of PDEs that hydrolyze cAMP may serve as a viable intervention to induce MB.

To test this hypothesis, we screened a panel of PDE3, PDE4, and PDE5 inhibitors using a phenotypic respirometric assay. FCCP-uncoupled OCR was used as a marker of increased energetic capacity and MB. Interestingly, PDE3 and PDE5 inhibitors increased FCCP-uncoupled OCR in RPTCs, whereas none of the PDE4 inhibitors tested caused an increase (Figures 2.1 and 2.4). To further probe the functional selectivity of PDE3, PDE4, and PDE5 inhibition in promoting MB, cAMP and cGMP levels were measured in RPTCs after treatment with the PDE3 inhibitors cilostamide and trequinsin, the PDE4 inhibitor rolipram, or the PDE5 inhibitor sildenafil. PDE3 inhibition led to increases in levels of both cAMP and cGMP in RPTCs, whereas rolipram increased only cAMP levels and sildenafil increased only cGMP levels (Figure 2.3). These data correspond with the classic substrate affinities of the various PDE family members: PDE3 hydrolyzes both cAMP and cGMP with nearly equal affinity, PDE4 specifically hydrolyzes cAMP, and PDE5 specifically hydrolyzes cGMP [304, 305]. Finally, 8-Br-cGMP increased FCCP-uncoupled OCR in the respirometric assay and increased mRNA expression of mitochondrial genes after 24-hour treatment. 8-Br-cAMP had no effect on respiration of mitochondrial gene expression in RPTCs. This multipronged approach strongly supports our hypothesis that cGMP, rather than cAMP, is important for regulation of MB in renal tubules.

cGMP was previously demonstrated to induce MB through the eNOS/NO soluble guanylate cyclase/cGMP signaling cascade. In 2004, Nisoli et al. [233] showed that long-term administration of NO mimetics, guanylyl cyclase activators, or 8-Br-cGMP increased mRNA expression of mitochondrial genes, mtDNA copy number, mitochondrial respiration, and ATP levels in multiple cell lines. eNOS-deficient mice have a reduction in metabolic rate and accelerated weight gain, which has been correlated with reduced mitochondrial content and function [270].

Both the PDE3 inhibitors cilostamide or trequinsin (0.3–3 mg/kg) and the PDE5 inhibitor sildenafil (0.3–3 mg/kg) when administered to naïve mice induced renal cortical mRNA expression of PGC-1 α , nuclear-encoded mitochondrial genes (NDUFB8 and ATP5 β), and mitochondrial-encoded mitochondrial genes (ND1 and COX1). mtDNA copy number was also increased in the renal cortex of these mice (Figures 2.5 and 2.6). Sildenafil increased the number of functional mitochondria in the renal cortex as evidenced by a significant increase in tissue ATP levels (Figure 6). These data confirm that PDE3 and PDE5 inhibitors are capable of inducing MB both in vitro in RPTCs and in vivo in mouse kidney.

Cyclic nucleotides including both cAMP and cGMP were shown to be activators of signaling pathways promoting MB in various model systems [233, 270, 302, 303]. Acute ex vivo administration of the PDE5 inhibitor vardenafil to human skeletal muscle stimulated MB as evidenced by increases in mitochondrial gene expression and mtDNA copy number [232]. This is the first report of pharmacological induction of MB in vivo by inhibition of either PDE3 or PDE5, and could represent a novel use for these classes of compounds. Despite the evidence of their role in MB, these compounds have yet to be evaluated as potential therapies for mitochondrial damage and dysfunction.

Previous studies reported the ability of various classes of PDE inhibitors to protect against AKI. Pretreatment with rolipram, a specific PDE4 inhibitor, blunted I/R-induced renal dysfunction in rat kidney and reduced oxidative damage [312]. Sildenafil was shown to be protective in cisplatin-induced AKI, whereas tadalafil, a long-acting PDE5 inhibitor, protected against early I/R injury in rats[313, 314] However, limitations of these studies have been the lack of a clear mechanism for the renoprotective effects and the use of pretreatment protocols. To address these issues, we examined the ability of sildenafil to promote recovery from FA-induced AKI by administering the drug 24 hours after induction of injury, and examined the effects of FA and sildenafil on both renal and mitochondrial function. Sildenafil promoted recovery mitochondrial gene expression (i.e., COX1 and Tfam) and mtDNA copy number. In addition, renal KIM-1 expression was reduced in sildenafil-treated mice, indicating an enhanced recovery from the renal injury. These results demonstrate that sildenafil accelerates recovery from AKI by activating MB pathways.

Our results indicate that PDE inhibitors that are capable of increasing tissue levels of cGMP, including sildenafil, are promising treatments for diseases characterized by mitochondrial dysfunction and suppression of MB, including AKI.

CHAPTER 3:

Evaluation of phosphodiesterase inhibitors in a model of acute-to-chronic kidney disease characterized by mitochondrial dysfunction

ABSTRACT

Acute kidney injury (AKI) is a disease with mitochondrial dysfunction and a newly established risk factor for the development of chronic kidney disease (CKD) and fibrosis. We examined mitochondrial homeostasis in the folic acid (FA)-induced AKI model that develops early fibrosis over a rapid time course. Mice given a single dose of FA had elevated serum creatinine (3-fold) and urine glucose (2.2-fold) 1 and 2 d after injection that resolved by 4d. In contrast, peroxisome proliferator gamma coactivator 1 α (PGC-1 α) and mitochondrial transcription factor A (TFAM), critical transcriptional regulators of mitochondrial biogenesis (MB), were down-regulated ~80% 1d after FA injection and remained depressed through 14 d. Multiple electron transport chain and ATP synthesis genes were also down-regulated from 1 to 14 d after FA, including NADH dehydrogenase (ubiquinone) 1 beta subcomplex 8 (NDUF β 8), ATP synthase subunit β (ATPS β), and cytochrome C oxidase subunit I (COXI). Mitochondrial DNA copy number was reduced ~50% from 2 to 14 d after FA injection. Protein levels of early fibrosis markers α -smooth muscle actin and transforming growth factor β 1 were elevated at 6 and 14 d after FA. Picrosirius red staining and collagen 1A2 (COL1A2) IHC revealed staining for mature collagen deposition at 14 d. We propose that mitochondrial dysfunction induced by AKI is a persistent cellular injury that promotes progression to fibrosis and CKD. Treatment of mice for 1 week following FA administration with the PDE5 inhibitor sildenafil failed to recover mitochondrial gene expression or attenuate fibrotic progression.

INTRODUCTION

Acute kidney injury (AKI) is defined as a rapid and reversible decline in renal function. AKI affects 40–60% of intensive-care unit patients and incidence rates remain unchanged [23, 315]. Drugs, toxicants, ischemia/reperfusion (I/R), and sepsis are common causes of AKI and lead to reduced glomerular filtration and tubular necrosis. One mechanism of drug and toxicant-induced renal injury is crystal formation in the lumen, as observed with uric acid, acyclovir, and calcium oxalate, the molecule responsible for renal toxicity of ethylene glycol [23]. When given intraperitoneally at high doses (e.g. 250 mg/kg), folic acid (FA) causes AKI in rodents [316, 317]. The mechanism of FA nephropathy may be due to the formation of luminal crystals at these doses [318]; however, FA also has direct toxicity on the tubular epithelium at high doses [87]. The Reference Daily Intake for adult humans provided by the Food and Drug Administration is 400 µg. While renal toxicity of FA has not been reported in humans, FA-induced nephrotoxicity has been used as a model of AKI.

CKD is defined as a consistent reduction in the glomerular filtration rate and typically progresses to end stage renal disease (ESRD) [319]. CKD affects over 750,000 people in the US and the incidence is rising due to increasing rates of diabetes and hypertension [319]. Tubulointerstitial fibrosis (TIF) is the best predictive marker of progression to ESRD [320] and development of TIF is observed following I/R- and toxicant-induced AKI [75, 321]. Fibrotic lesions damage the peritubular vasculature, and lead to a state of chronic hypoxia in the nephron, promoting sustained oxidative stress [321, 322].

Recent advances in nephrology research demonstrate a causal role for AKI in CKD development. For example, AKI is a major risk factor for CKD, increasing the risk of progression to CKD as much as 28-fold [323]. In addition, the severity of injury in the acute

phase of AKI is a highly effective indicator of progression to CKD [10]. In mice, CKD and fibrosis have been shown to follow AKI caused by FA, I/R, and aristolichic acid [75, 324]. CKD progression in the models is dependent upon the extent of AKI[75] and preventable with therapeutic intervention during the acute phase [325]. These studies form the basis of our analysis of mitochondrial dysfunction in the AKI to CKD continuum.

Mitochondrial dysfunction is a recognized pathogenic element of AKI and cause of tubular cell dysfunction and death. Increased reactive oxygen species (ROS) and reactive nitrogen species (RNS) production, decreased ATP production, and cytochrome *c* release are frequently associated with epithelial cell injury in AKI [157, 326, 327]. Our group recently reported persistent disruption of mitochondrial homeostasis and suppression of mitochondrial biogenesis (MB) following I/R- and glycerol-induced AKI [161]. In both models, renal mitochondrial proteins cytochrome *c* oxidase subunit I (COXI), ATP synthase subunit β (ATPS β) and NADH dehydrogenase (ubiquinone) 1 beta subcomplex 8 (NDUF β 8) were depleted, indicative of mitochondrial damage and suppressed MB [161]. Over-expression of PGC-1 α , the master regulator of MB, in renal proximal tubule cells restored mitochondrial and cellular functions after oxidant exposure, demonstrating the importance of MB in recovery from cellular injury [207]. While the mechanisms of maladaptive repair of the tubular epithelium after AKI are still unclear, it can lead to TIF through paracrine activation of resident fibroblasts and epithelial-mesenchymal transition (EMT) of renal epithelial cells [78, 328]. Interestingly, mitochondrial-derived ROS can induce EMT in renal tubular cells *in vitro*, and restoration of functional mitochondria and antioxidant mechanisms by induction of PGC-1 α attenuates this transition [67, 329]. However, little is known about the role of mitochondrial function in renal

fibrosis. Here we report that persistent mitochondrial dysfunction is linked to early renal fibrosis in a model of FA-induced AKI.

EXPERIMENTAL PROCEDURES

Animal Model

This study was carried out in strict accordance with the recommendations in the Guide for the Care and Use of Laboratory Animals of the National Institutes of Health. The protocol was approved by the Institutional Animal Care and Use Committee at the Medical University of South Carolina and all efforts were made to minimize animal suffering. Male CD-1 mice (8–10 weeks of age, Harlan Laboratories) were injected with a single intraperitoneal dose of 250 mg/kg FA (Sigma) dissolved in 300 mM NaHCO₃ as previously described [330]. At 0, 1, 2, 4, 6, 10, and 14 d after treatment, serum and urine samples were collected. Urine was collected overnight from mice housed in metabolic cages (18 h collection period). Serum and urine creatinine, blood urea nitrogen (BUN), and urine glucose levels were measured using Quantichrom Assay Kits (BioAssay Systems). Urine glucose was normalized to urine creatinine. Urine osmolality was measured using the 5004 Micro-Osmette (Precision Systems). Mice were euthanized 0, 1, 2, 6, and 14 d after treatment by CO₂ asphyxiation. These time points were chosen to capture the acute, recovery and chronic phases of FA-induced AKI. Kidneys were removed and preserved either by snap freezing or formalin fixation and paraffin embedding. For drug studies with sildenafil, male C57BL/6 mice aged 8-10 weeks were used. Mice received daily injections of saline vehicle or sildenafil (0.3 mg/kg) beginning at 1 d after induction of FA nephropathy until 7 d. Mice were sacrificed at 14 d after FA administration and kidneys were collected for biochemical analyses.

Histological Analysis

Kidneys were sectioned and stained with Periodic Acid Schiff (PAS) for the evaluation of histology. Fibrillar collagen content was evaluated using picro-sirius red staining. Briefly, slides were deparaffinized and rehydrated, stained with Weigert's Iron hematoxylin for 10 min, and washed with water for 10 min. Slides were then stained with picro-sirius red (0.1% direct red 80 CI#35780 in saturated aqueous picric acid) for 1 h, washed twice in 1% glacial acetic acid, dehydrated, cleared with xylene, mounted with Permount and examined under plane polarized light. Immunohistochemistry was performed as previously described using the collagen 1A2 (COL1A2) antibody (Santa Cruz) [331].

mRNA Analysis

Total RNA was isolated from renal cortex with Trizol (Invitrogen) and reverse transcription was performed using the iScript Advanced cDNA Synthesis Kit (Bio-Rad) with 2 μ g RNA. qPCR was performed using SsoAdvanced SYBR Green Supermix (Bio-Rad). mRNA expression of all genes was calculated using the $2^{-\Delta\Delta CT}$ method normalized to β -actin. Primer sequences for PGC-1 α , TFAM, NDUFB8, COX1, and ATP5B were described previously [161]. Additional primer sequences were as follows: COL1A2: sense 5'-TGTTGGCCCATCTGGTAAAGA-3', antisense 5'-CAGGGAATCCGATGTTGCC-3'; β -actin: sense 5'-GGGATGTTTGCTCCAACCAA-3', antisense 5'-GCGCTTTTGACTCAAGGATTTAA-3'.

Immunoblot Analysis

Protein lysates were isolated from renal cortex using RIPA buffer containing mammalian protease inhibitor cocktail, 1 mM sodium orthovanadate, and 10 mM sodium fluoride (Sigma). Proteins were separated on a 4–15% SDS-PAGE gel and transferred to a nitrocellulose membrane before blocking in 2.5% BSA. Membranes were incubated with primary antibody at 4°C overnight. Primary antibodies used were α -smooth muscle actin (α -SMA) (1:1000, Sigma), transforming growth factor β_1 (TGF- β_1) (1:1000, Abcam), neutrophil gelatinase-associated lipocalin 2 (NGAL) (1:1000, Abcam) and β -actin (1:500, Santa Cruz). Membranes were then incubated with an appropriate horseradish peroxidase (HRP)-conjugated secondary antibody for 1 h. Bound antibody was imaged following chemiluminescent visualization using a GE ImageQuant LAS4000 standalone imaging system. Densitometry of Western blots was performed using NIH Image J software.

Mitochondrial DNA Content

qPCR was used to determine relative quantities of mitochondrial DNA content in renal cortex as previously described[162]. Briefly, the DNeasy Blood and Tissue kit (QIAGEN, Valencia, CA) was used for genomic DNA extraction and 5 ng of total DNA was used for qPCR. Mitochondrially encoded NADH dehydrogenase 1 (ND1) was used to measure mitochondrial copy number and was normalized to nuclear β -actin. Primer sequences were as follows: ND1: sense 5'-TAGAACGCAAAATCTTAGGG-3', antisense 5'-TGCTAGTGTGAGTGATAGGG-3'; β -actin: sense 5'-GGGATGTTTGCTCCAACCAA-3', antisense 5'-GCGCTTTTGA CTCAAGGATTTAA-3'.

Data and Statistical Analysis

Data are presented as means \pm SEM and were subjected to one-way analysis of variance (ANOVA). Multiple means were compared using Student-Newman-Keuls test with $p < 0.05$ considered to be a statistically significant difference between means.

RESULTS

FA Induces AKI with Rapid Functional Recovery

FA decreased glomerular function as serum creatinine levels increased ~3-fold versus controls 1–2 d after FA injection and returned to control levels at 4 d (Figure 3.1A). BUN concentrations increased ~8-fold versus controls 1–2 d after FA injection, and did not return to control levels until 10 d (Figure 3.1B). Over 90% of mice developed AKI, defined as a doubling of serum creatinine or BUN levels at 2 d. As an indicator of tubular function we measured urinary glucose concentrations, which increased 2-fold over controls 1–2 d after FA injection (Figure 3.1C). Urinary glucose concentrations returned to control levels at 4 d. Renal NGAL protein levels also increased ~4-fold 1–2 d after FA injection and returned to control levels at 6 d (Figure 3.1D).

Renal histopathology was examined using PAS staining at 2, 6, and 14 d. At 2 d the renal cortex displayed tubular dilatation, brush border loss, cast formation, and accumulation of debris in the lumen. At 6 d there was a partial restoration of normal renal architecture characterized by repopulation of the tubular epithelial cells, but brush border restoration remained incomplete at 14 d (Figure 3.2).

In summary, peak renal dysfunction occurred 2 d after FA administration, as indicated by maximal levels of serum creatinine, BUN, urine glucose, and the injury marker NGAL. All markers returned to control levels by 4 d except BUN, which gradually decreased over time and returned to control levels at 10 d. In contrast to the recovery of glomerular and tubular function, persistent disruption of normal tubular morphology was observed in PAS-stained kidneys through 14 d, revealing incomplete recovery.

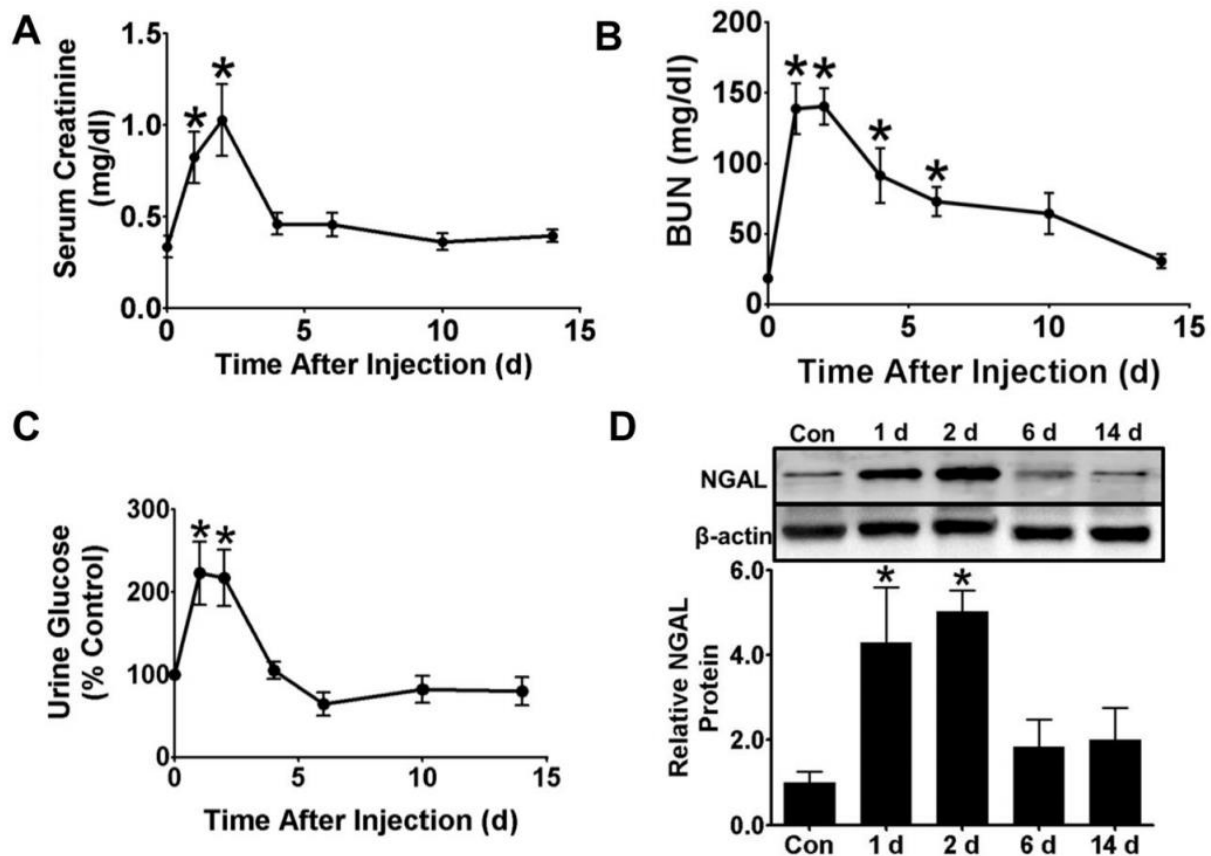


Figure 3.1: Folic acid (FA) causes AKI. Two days after a 250 mg/kg intraperitoneal dose of FA, serum creatinine (A), BUN (B), and urine glucose (C) levels were maximally elevated. Both serum creatinine and urine glucose concentrations returned to control levels at 4 d. BUN concentrations returned to control levels at 10 d. Protein levels of renal NGAL increased at 1 and 2 d but returned to control levels at 6 and 14 d (D). Data are represented as mean \pm SEM. *, $p < 0.05$ vs control. N = 8–19 (A and B), 7–21 (C), 4–7 (D).

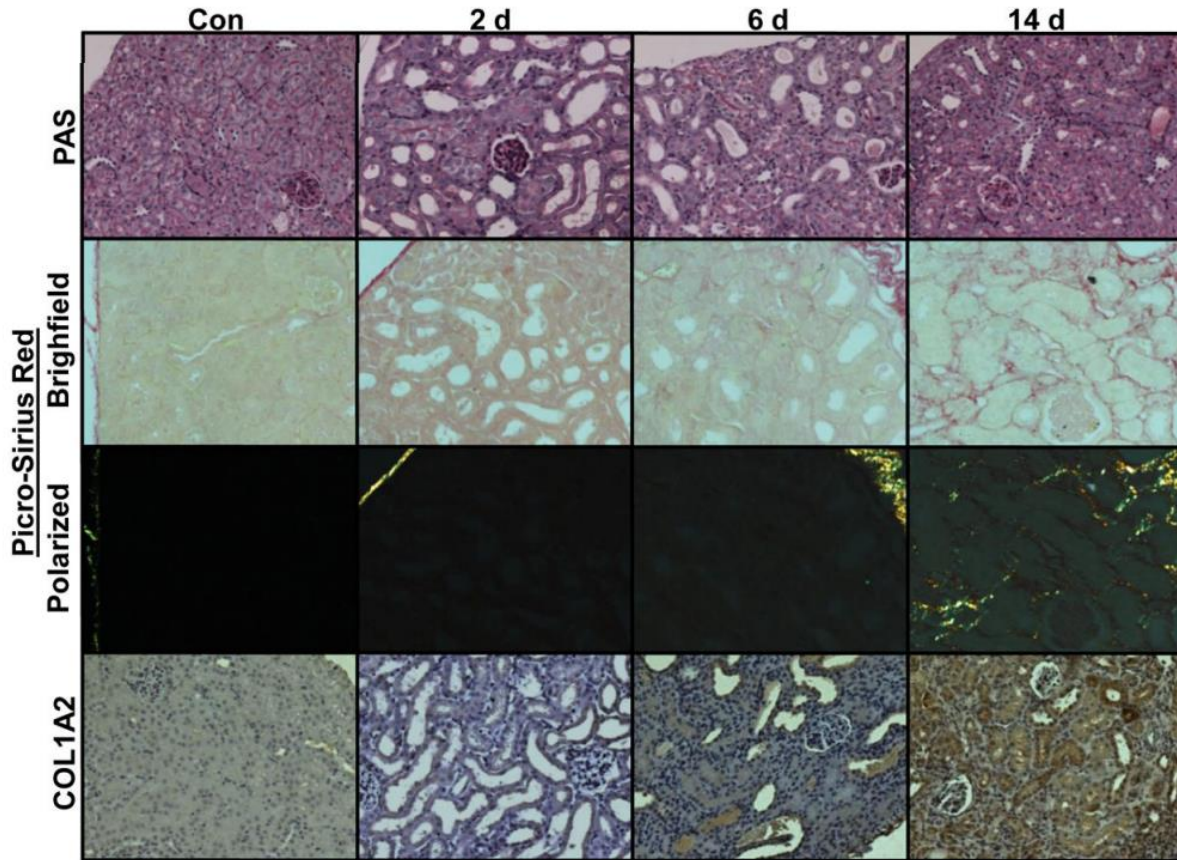


Figure 3.2: Histopathology of progressive FA nephropathy. Kidneys display massive tubular dilatation and brush border loss at 2 d via PAS staining (top row) that partially recovered at 6 and 14 d. Picro-sirius red staining showed deposition of fibrillar collagen at 14 d using brightfield (second row) and polarized (third row) light microscopy. Immunohistochemical detection of COL1A2 (bottom row) showed strong staining only at 14 d after FA injection. Representative images shown, N = 3–8.

FA-Induced AKI Suppresses Mitochondrial Homeostasis and Biogenesis Rapidly and Persistently

To determine if FA nephrotoxicity disrupts mitochondrial homeostasis and biogenesis, transcript levels of mitochondrial markers of homeostasis and biogenesis were measured in renal cortex over time. mRNA levels of the transcription factor coactivator PGC-1 α and mitochondrial transcription factor A (TFAM) decreased by ~80% 1 d after FA treatment (Figure 3.3A, 3.3B). PGC-1 α levels remained reduced throughout the 14 d experiment while TFAM levels partially recovered to ~60% of controls at 2 d and remained depressed at 6 and 14 d. One day after FA injection, transcript levels of NDUFB8, ATP5B, and COX1 decreased 85%, 83%, and 72%, respectively (Figure 3.3C-E). NDUFB8 levels partially recovered at 6 d but remained depressed at 14 d. COX1 and ATP5B transcript levels remained depressed throughout the 14 d of the experiment. Finally, we measured mitochondrial DNA copy number as an indicator of mitochondrial content. Mitochondrial DNA copy number was reduced ~50% 2 d after FA injection and remained depressed through 14 d (Figure 3.3F). To control for possible variation in expression of the mitochondrial markers over the course of the study, a separate experiment was performed using time-matched controls. Over 14 d mRNA expression did not change in control mice, while mitochondrial markers were suppressed in FA-treated mice (Figure 3.4).

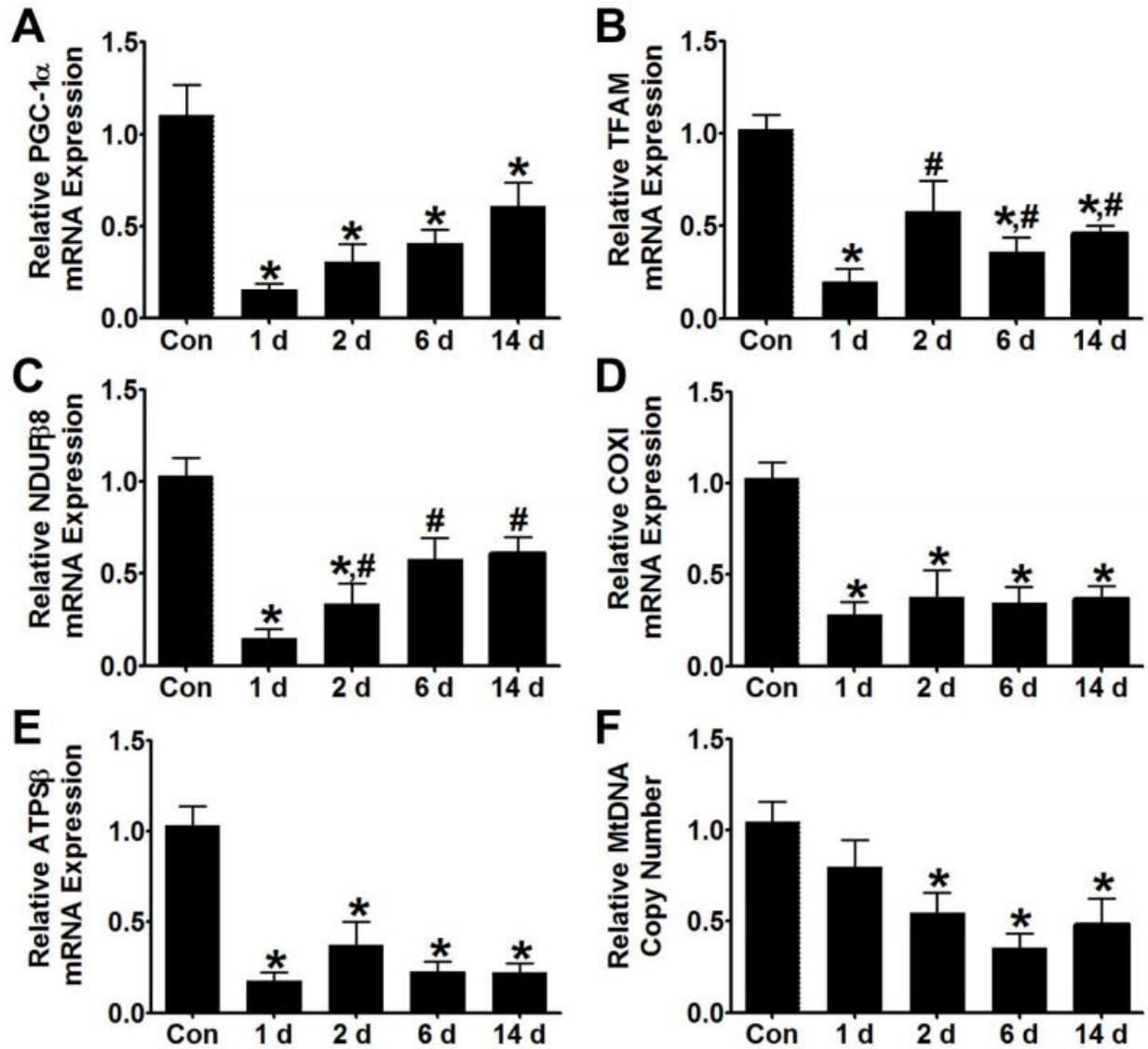


Figure 3.3: Mitochondrial biogenesis is persistently down-regulated during FA nephropathy. mRNA levels of PGC-1 α (A) and TFAM (B) were reduced 1 d after FA injection. PGC-1 α remained depressed while TFAM mRNA partially recovered at 2 d and did not increase further through 14 d. Expression of mitochondrial homeostasis markers NDUF β 8 (C), COX1 (D), and ATP5 β (E) was also strongly suppressed at 1 d, and only NDUF β 8 reached a partial recovery at 6 and 14 d. Mitochondrial copy number was reduced by ~50% 2 d after FA injection and remained persistently depressed at 6 and 14 d (F). Data are represented as mean \pm SEM. *, $p < 0.05$ vs control, # $p < 0.05$ vs 1 d. N = 4–8.

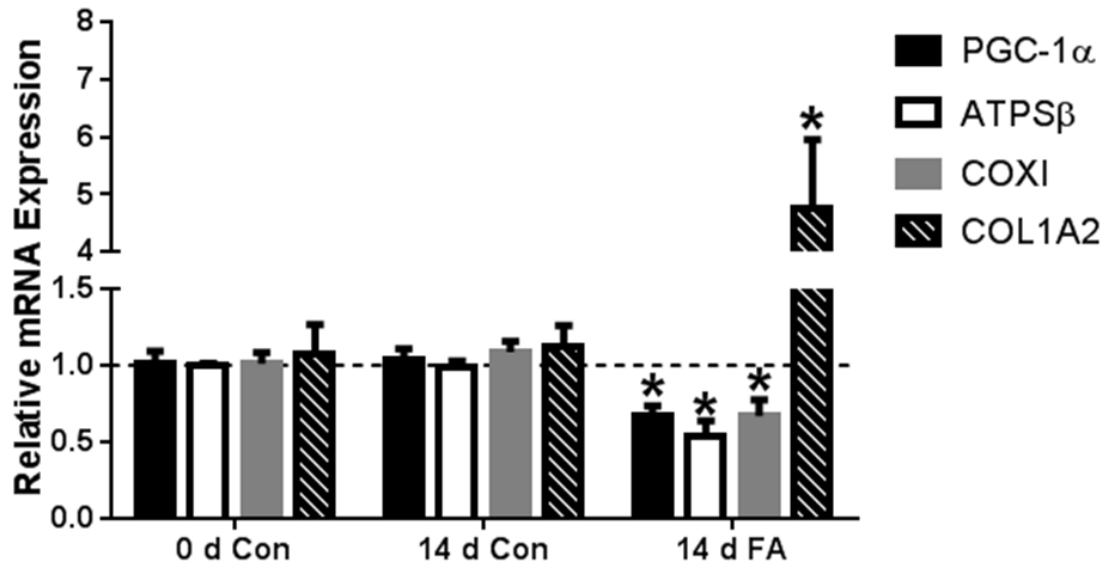


Figure 3.4: Time-matched control study. mRNA levels of mitochondrial genes PGC-1 α , ATP5 β , and COXI were equivalent in control mice at day 0 and day 14, and decreased in FA mice at day 14. The fibrosis marker COL1A2 increased 14 d after FA (B). Data are represented as mean \pm SEM. *, $p < 0.05$ vs 0 d and 14 d Con. N = 5–6.

In summary, numerous markers of mitochondrial homeostasis were strongly suppressed at 1 d and remained suppressed through 14 d. It should be noted that TFAM and NDUF β 8 partially recovered to 50% and 60% of control, respectively. Importantly, mitochondrial DNA copy number, an indirect marker of mitochondrial content was also decreased from 2–14 d. These data reveal that the disruption of mitochondrial homeostasis and content begins with the onset of AKI and persists, consistent with the disruption of tubular morphology. The persistent loss of mitochondrial homeostasis in this model is similar to that reported in AKI caused by I/R and myoglobulinuria [161]. Furthermore, it is interesting that the early recovery of glomerular and tubular function is not dependent on the up-regulation of these genes.

FA-Induced AKI and Mitochondrial Dysfunction is Followed by Fibrosis

Protein levels of early fibrosis markers TGF- β ₁ and α -SMA increased at 6 and 14 d after FA injection with a maximum induction of ~4- and ~9-fold, respectively (Figure 3.5A). Transcript levels of COL1A2 (Figure 3.5B), a primary transcriptional target of TGF- β ₁ and pathological molecule in fibrosis, increased at 6 and 14 d, in concert with the increases in TGF- β ₁. COL1A2 mRNA also increased versus 14 d controls in the separate time-matched study (Figure 3.4). We measured urine output and osmolality as indicators of CKD. Urine output was similar to controls from 1–6 d after FA injection but increased at 10 and 14 d. (Figure 3.5C). Urine osmolality decreased 14 d after FA injection (Figure 3.5D).

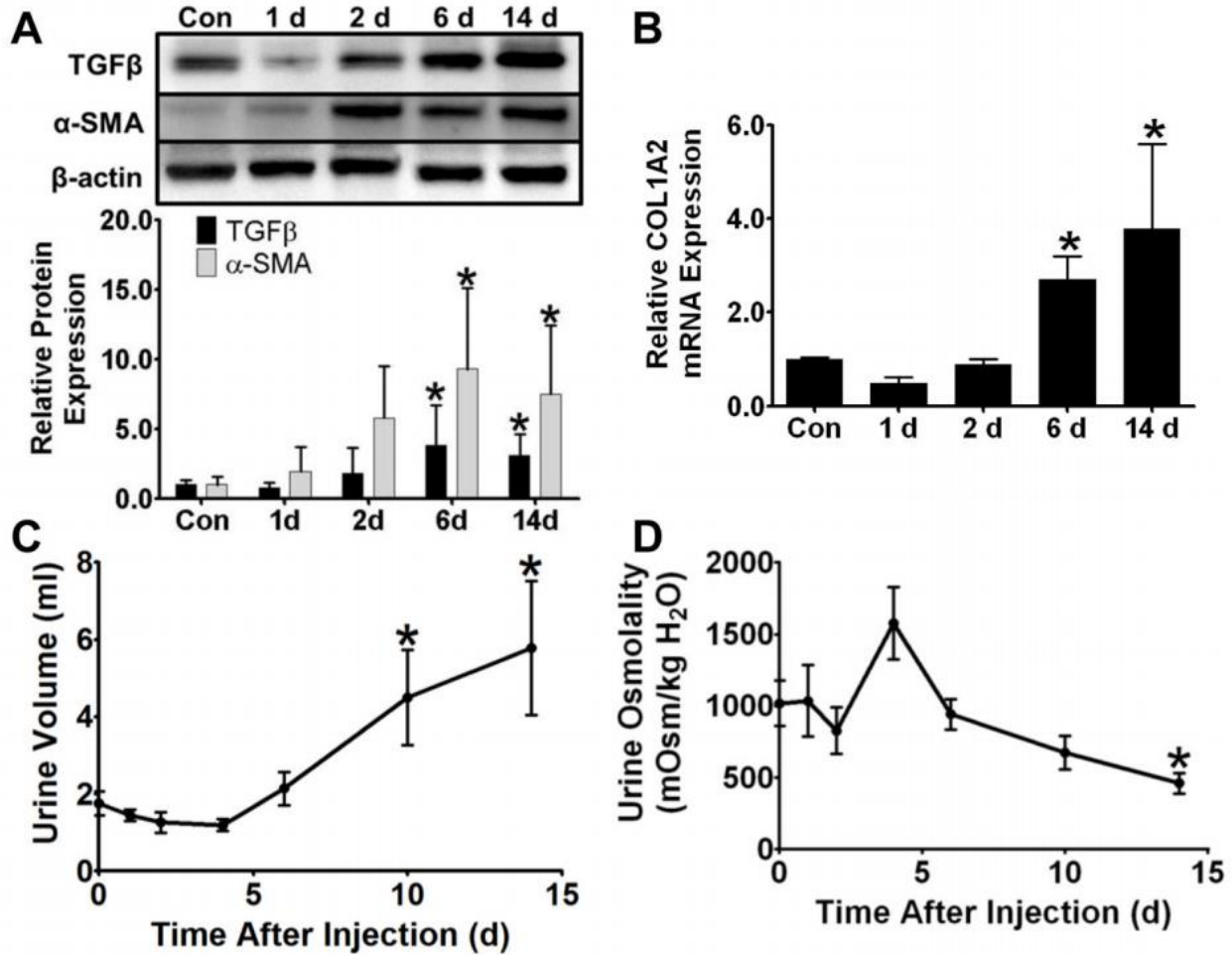


Figure 3.5: Early fibrosis and CKD in FA nephropathy. TGF- β_1 and α -SMA protein remained at control levels through 2 d but increased at 6 and 14 d (A). COL1A2 mRNA was significantly increased in renal cortex 6 and 14 d after FA treatment (B). Urine volume increased 10 and 14 d after FA injection (C), while urine osmolality decreased at 14 d (D). Data are represented as mean \pm SEM. *, $p < 0.05$ vs control. N = 5–8 (A), 4–10 (B), 8–20 (C), 6–7 (D).

Kidney sections were stained with picro-sirius red to examine the development of TIF. When examined using bright-field microscopy, the red staining is indicative of general ECM deposition (Figure 3.2). We observed very low levels of red staining in control kidneys and in kidneys 2 and 6 d after FA injection. However, at 14 d there was a marked increase in red staining in the tubulointerstitium. We also examined the picro-sirius red staining under polarized light, which allows specific visualization of fibrillar collagen [332]. There was no detectable kidney collagen staining in controls or at 2–6 d following FA treatment, but there was an intense tubulointerstitial staining pattern at 14 d (Figure 3.2). We used immunohistochemistry to examine the levels of COL1A2. Low levels of staining were observed through 6 d after FA injection, but at 14 d there was a strong increase in the COL1A2 positive staining in the renal cortex (Figure 3.2).

In conclusion, while glomerular and tubular function recovered, early fibrosis occurred at 6 d and continued through 14 d following FA treatment. Molecular markers of fibrosis including TGF- β_1 and α -SMA increased 6 and 14 d after FA, and picro-sirius red staining and IHC for COL1A2 showed increases in staining 14 d after FA injection. The changes in these markers are consistent with the persistent disruption of tubular morphology. Additionally, increases in urine volume were observed at 6 and 14 d, and urine osmolality decreased at 14 d. Decreased ability to concentrate the urine is seen in CKD patients [333]. CKD has been characterized in the FA model, with decreased glomerular function and microalbuminuria at 2 and 12 weeks [324, 334]. We did not detect increases in urinary albumin or total protein in FA-treated mice at 14 d (Figure 3.6). This finding could be due to the early stage of fibrosis at 14 d in this study. In summary, the FA model under these conditions represents early AKI with recovery of multiple functions within 4 d that is followed by early fibrosis and CKD.

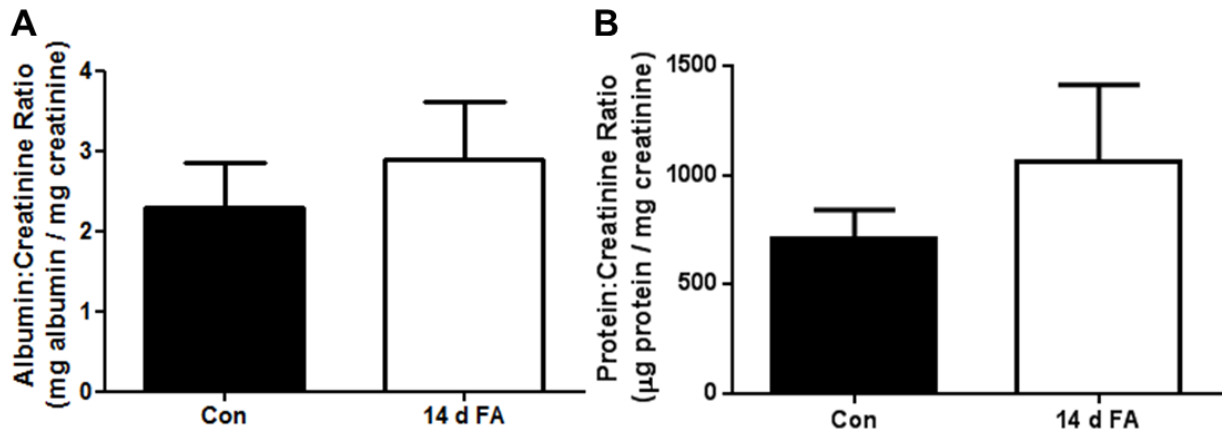


Figure 3.6: Measurement of Urinary Albumin and Protein in FA Nephropathy. There was no statistical change in the albumin:creatinine ratio (A) or protein:creatinine ratio (B) in the urine of mice 14 d after FA injection. Data are represented as mean \pm SEM. N = 4 (A) and 8 (B).

Sildenafil failed to stimulate mitochondrial biogenesis and prevent fibrosis in folic acid-induced CKD

To test whether stimulation of mitochondrial biogenesis can promote renal recovery and prevent development of renal fibrosis, mice received daily injection of sildenafil at a dose of 0.3 mg/kg beginning at 1 d after folic acid administration for a period of 1 wk. Mice were then sacrificed at 14 d after folic acid administration and kidneys were collected. Expression of the mitochondrial genes COX, NDUFB8, PGC-1 α and Tfam remained suppressed in mice treated with folic acid at 14 d compared to control animals. Treatment with sildenafil failed to promote recovery of mitochondrial gene expression in these mice (Figure 3.7A-C). Furthermore, sildenafil treatment did not decrease COL1A2 expression in folic acid treated mice (Figure 3.7D). These data indicate that sildenafil may not be an effective therapy for limiting the progression to CKD following folic acid-induced AKI.

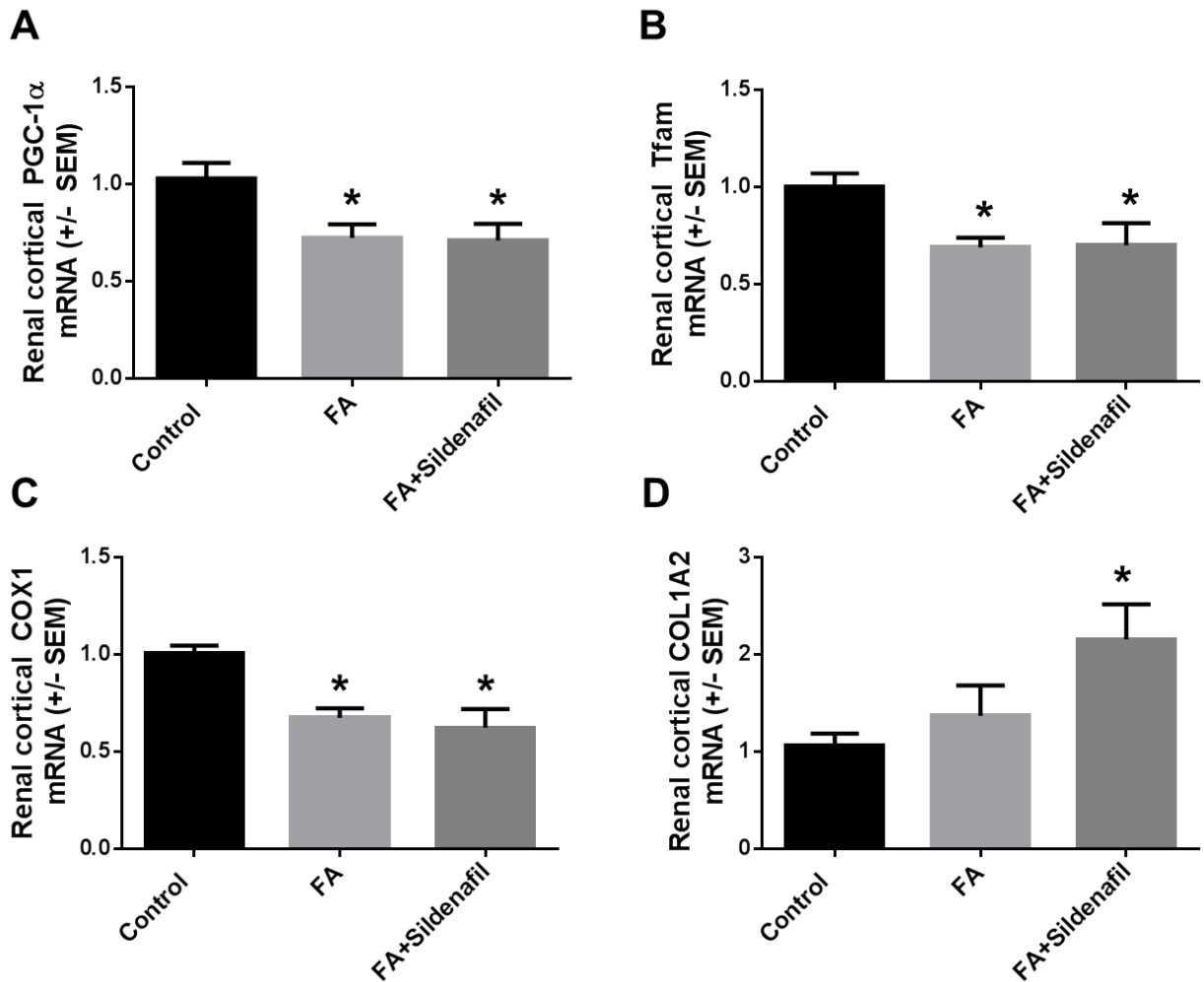


Figure 3.7: Sildenafil does not promote recovery of mitochondrial biogenesis or limit fibrosis in FA-induced CKD. Renal damage was induced by bolus injection of folic acid in C57BL/6 mice. Mice received daily treatment with saline vehicle or sildenafil (0.3 mg/kg) beginning at day 1 after FA until day 7. mRNA levels of PGC-1 α (A), Tfam (B), COX1 (C) and COL1A2 (D) were measured at 14 d after FA by real time PCR. Data are represented as mean \pm SEM. *, $p < 0.05$ vs control, N = 5-12.

DISCUSSION

The above studies provide the first evidence of a link between suppression of the MB program and the AKI to CKD continuum. However, while the sustained suppression of MB is correlated with development of early fibrosis and CKD, it is not clear if early fibrosis and CKD are dependent on MB suppression. Hickey *et al.*, in 2011, reported increased PGC-1 α protein in a unilateral ureteral obstruction (UUO) model of renal fibrosis [335]. However, the authors did not measure any PGC-1 α targets or functional mitochondrial parameters *in vivo*. In skeletal muscle, it has been shown that tissue-specific over-expression of PGC-1 α slows the age-dependent development of fibrosis [336]. In addition, the severe cardiomyopathy induced by anthracycline, which includes fibrosis as a hallmark, is associated with decreased cardiac MB and increased oxidative stress [337]. These studies support our findings that the suppression of MB by AKI is involved in the development of renal fibrosis.

The AKI-CKD continuum is recently established and many questions remain regarding clinical progression and pathophysiological mechanisms. A single episode of AKI is known to increase the risk of CKD [338, 339], and the severity of the acute injury is predictive of progression to CKD [10]. TIF, a pathological hallmark of CKD, is an effective predictor of declining renal function [340], and work in animal models has addressed mechanisms of fibrogenesis after AKI. Inhibition of prolyl-4-hydroxylase domain (PHD)-containing dioxygenases, which promote degradation of hypoxia inducible factors (HIF) 1 and 2, reduces I/R-induced AKI and subsequent fibrogenesis [325]. The effect was only observed when PHD inhibitors were administered before I/R [325] and suggests that the well-known activity of HIF in regulating cellular metabolism could be a critical factor in the early response to AKI and the maladaptive repair and fibrogenesis that develop afterwards. In addition, repeated, selective

injury of renal epithelial cells was sufficient to cause fibrosis using a genetically engineered model expressing the diphtheria toxin (DT) receptor in the renal epithelium [341]. This suggests a key role for epithelia in renal fibrogenesis. Finally, hyper-methylation of the promoter for *RASALI*, an inhibitor of the RAS oncoprotein, was also found to promote renal fibrosis after FA-induced AKI and was attenuated by 5-azacytidine or DNA methyltransferase 1 haploinsufficiency [342]. We did not examine promoter methylation in this study, but these findings raise the possibility that epigenetic mechanisms could play a role in silencing expression of MB pathway genes and progression to fibrosis.

CHAPTER 4:

The guanylyl cyclase activator BAY 58-2667 stimulates mitochondrial biogenesis and promotes recovery from ischemia-reperfusion induced AKI

ABSTRACT

Mitochondrial dysfunction is an important pathophysiological component of acute kidney injury (AKI). Following AKI, reduced mitochondrial function can impair energy-dependent renal repair processes. Thus, stimulation of mitochondrial biogenesis (MB), the generation of new, functional mitochondria, could promote renal recovery. We explored the ability of the guanylyl cyclase activator, BAY 58-2667, to induce MB and promote renal recovery following I/R-induced AKI. Treatment of renal proximal tubular cells (RPTCs) with BAY 58-2667 increased FCCP-uncoupled OCR. Furthermore, BAY 58-2667 increased mitochondrial gene and protein expression, and mtDNA content in the renal cortex of naïve mice. Beginning 24 h after I/R injury, daily treatment with BAY 58-2667 accelerated recovery of renal function evidenced by reduced BUN levels at 6 d. Additionally, renal expression of the tubular injury markers NGAL and Kim-1 were also decreased. Histological examination demonstrated reduced renal tubular necrosis in BAY 58-2667 treated mice. BAY 58-2667 blunted the progression of renal fibrosis evidenced by reduced COL1A2 and α SMA expression. Furthermore, BAY 58-2667 decreased renal expression of the inflammatory cytokines, TNF- α and IL-1 β , and reduced oxidative DNA damage. Finally, BAY 58-2667 promoted the recovery of renal mitochondrial biogenic signaling after I/R. Renal mRNA expression of PGC-1 α , NRF1, ND1, COX1 and ATP5 β were all increased over I/R+vehicle levels. mtDNA content and protein expression of PGC-1 α and COX1 were also induced. Finally, mitochondrial function was recovered evidenced by a return of ATP levels to sham control levels. These data demonstrate that activation of guanylyl cyclase by BAY 58-2667 promotes recovery from AKI by stimulation of mitochondrial biogenesis, and reduction of inflammatory and oxidative damage.

INTRODUCTION

Acute kidney injury (AKI) is a rapid loss of renal function characterized by reduced urinary output and increased serum biomarkers, including creatinine and urea. AKI is caused by a diverse array of insults including inflammatory renal disease, sepsis, obstruction, ischemia-reperfusion (I/R) injury, and drug or toxicant exposure [14, 45, 343]. AKI causes a host of systemic complications including disrupted acid-base and electrolyte homeostasis, and other organ damage [344]. AKI has a poor prognosis, particularly in intensive care patients, with mortality rates up to 80% [7]. Survivors of AKI are at a highly increased risk of development of chronic kidney disease (CKD) and ultimately progression to end stage renal disease (ESRD) requiring dialysis [10, 74]. Increased utilization of nephrotoxic agents, higher rates of metabolic syndrome and cardiovascular disease, and an aging population have led to an increased incidence of AKI. AKI also substantially increases healthcare costs due to extended hospital stays, increased ICU admissions and utilization of renal replacement therapy (RRT) [9]. Despite the serious nature of the disease and an increasing array of risk factors, there are still no highly effective therapies to prevent or promote recovery from AKI. Thus, the need exists to identify new targets and develop new pharmacological agents for its treatment.

The pathogenesis of AKI is complicated and multifactorial, which has made development of new therapies difficult. Following an acute insult, the renal tubular epithelium undergoes apoptotic and necrotic cell death with the shedding of damaged cells into the tubular lumen [22, 27]. Restoration of renal morphology and function requires the regeneration of functional tubules through the proliferation and differentiation of new renal epithelial cells. This process requires rapid and sustained activation of critical tissue repair mechanisms, which are highly energy dependent. The requirement of ATP for renal repair has highlighted mitochondrial

integrity and function as important factors in AKI pathogenesis and recovery. Following ischemia-reperfusion (I/R) injury, cells of the renal tubular epithelium experience profound mitochondrial dysfunction characterized by activation of the mitochondrial permeability transition, loss of membrane potential and swelling caused by uptake of cytosolic calcium [45, 153, 156, 345]. Loss of mitochondrial polarity impairs electron transport chain function causing depletion of renal ATP levels and increased production of reactive oxygen and nitrogen species. Furthermore, in the recovery phase following I/R-induced AKI, mitochondrial biogenesis (MB), the generation of new mitochondria, is persistently suppressed, and is associated with a failed recovery of renal tubular function [161]. Therefore, reactivation of the signaling cascades that induce MB could promote recovery of mitochondrial function and enhance renal repair. Use of various pharmacological activators of PGC-1 α -dependent MB has shown the efficacy of this therapeutic strategy. Treatment with the SIRT1 activator SRT1720, the 5HT-1F receptor agonist LY 344-864, or the β 2-adrenergic agonist formoterol, following renal I/R, accelerated recovery of MB and renal function [148, 150, 218]. Additionally, the PDE5 inhibitor sildenafil, stimulated MB and reduced renal cortical Kim-1 levels after folic acid-induced AKI [149]. These data highlight a potential for renal cGMP as a modulator of MB following AKI.

The cyclic nucleotide, cGMP, acts as an important signaling molecule linking membrane receptor activation to activation of intracellular kinases and other proteins, much like cAMP. cGMP levels are regulated both by their generation by guanylyl cyclases (GC), as well as their degradation by phosphodiesterases (PDE), providing two potential targets for therapeutic modulation. Previous studies have shown that cGMP regulates MB in a variety of model systems [271, 346]. Nisoli et al. in 2004, demonstrated that cGMP induction by nitric oxide or direct activation of GC stimulated MB and mitochondrial function *in vitro* [233]. Furthermore,

eNOS^{-/-} mice showed reduced tissue mitochondrial gene expression, mtDNA content, ATP levels and mitochondrial respiration. Transgenic mice overexpressing the natriuretic peptide, BNP, which signals through activation of GC, were protected against diet-induced obesity and metabolic dysfunction through effects on MB [239]. PDE5 inhibition has also been shown to induce mitochondrial biogenesis in renal tissue and fat [149, 232].

Recently, novel, potent, NO-independent inducers of GC activity have been identified. Screening for more potent and specific GC activators based on the imidazole scaffold of the GC inducer YC-1, led to the identification of the compounds BAY 41-2272 and BAY 41-8543 [347, 348]. Further work has led to the identification of a number of other compounds in this class and has led to the division of these compounds into 2 subclasses: GC stimulators and GC activators, which target 2 different redox states of GC. GC stimulators act upon GC containing a reduced heme moiety which is NO-sensitive. GC activators, however, can activate GC when this heme becomes oxidized and is no longer responsive to NO [349]. Several of these compounds have shown promise in the treatment of pulmonary arterial hypertension and cardiovascular disease; however, no studies have examined their effects on mitochondrial biogenesis in disease models [350-352]. For these studies, we sought to evaluate the efficacy of the small molecule GC stimulator, BAY 41-2272, and the GC activator, BAY 58-2667, to stimulate mitochondrial biogenesis and promote recovery of renal function in a mouse model of I/R-induced AKI.

EXPERIMENTAL PROCEDURES

Isolation and culture of RPTCs.

Female New Zealand white rabbits (1.5 – 2.0 kg) were obtained from Charles River Laboratories (Wilmington, MA). RPTCs were isolated using the iron oxide perfusion method as previously described. Cells were incubated at 37 °C in a 5% CO₂/95% air environment with continuous swirling. Cells were cultured using 100 mm dishes in a 1:1 mixture of Dulbecco's modified Eagle's essential medium and Ham's F-12 without glucose, phenol red or sodium pyruvate (Mediatech, Manassas, VA) supplemented with HEPES (15 mM), glutamine (2.5 mM), pyridoxine HCl (1 μM), sodium bicarbonate (15 mM), and lactate (6 mM). Further supplements including hydrocortisone (50 nM), selenium (5 ng/mL), human transferrin (5 μg/mL), bovine insulin (10 nM) and L-ascorbic acid-2-phosphate (50 μM) were added fresh daily to culture media. Following 3 days in culture, RPTCs were trypsinized and replated in XF-96 polystyrene cell culture microplates (Seahorse Bioscience, North Billerica, MA) at a density of 18,000 cells per well. Cells were maintained in culture for an additional 2 days before treatment with vehicle or compounds of interest.

Measure of oxygen consumption rate.

The oxygen consumption rate (OCR) of RPTCs was measured using the Seahorse Bioscience XF-96 Extracellular Flux Analyzer as previously described. Plates were treated with vehicle control (DMSO < 0.5% v/v), or increasing concentrations of BAY 41-2272 or BAY 58-2667. Basal OCR was measured before injection of 0.5 μM carbonyl cyanide 4-(trifluoromethoxy)phenylhydrazone (FCCP) for measurement of uncoupled (maximal) OCR.

Animal care and use.

Studies were carried out in strict accordance with the recommendations in the *Guide for the Care and Use of Laboratory Animals* from the National Institutes of Health. All protocols were approved by the Institutional Animal Care and Use Committee at the Medical University of South Carolina. All efforts were made to minimize animal pain and suffering.

Testing of compounds in naïve mice.

Male C57BL/6 mice (8-10 weeks old) were obtained from the Charles River Laboratories (Wilmington, MA). Mice were housed individually in a temperature controlled room under a 12-hour light/dark cycle. Mice were given a single intraperitoneal injection of BAY 41-2272 (100 µg/kg or 1 mg/kg), BAY 58-2667 (10 µg/kg or 100 µg/kg), or saline vehicle. Mice were euthanized 24 h after treatment by isoflurane inhalation and cervical dislocation. Kidneys were removed, preserved by flash-freezing in liquid nitrogen and stored at -80 °C for later analysis.

Ischemia-reperfusion (I/R)-induced AKI mouse model.

For the I/R model of AKI, mice were subjected to bilateral renal pedicle ligation as described previously [148, 353]. In brief, renal artery and vein were isolated and blood flow was occluded with a vascular clamp for 19 minutes. Mice were maintained at 37°C throughout the procedure using a homeothermic heating system. Sham surgery mice received all manipulations with the exception of clamping of the renal pedicles. Mice were treated once daily beginning at 24 hours after reperfusion with saline vehicle, sildenafil (1 mg/kg) or BAY 58-2667 (0.1 mg/kg). Blood was collected from mice via retro-orbital bleed at 24 and 144 hours after surgery. Blood urea nitrogen (BUN) levels were measured using a QuantiChrom Urea Assay Kit (BioAssay Systems, Hayward, CA) according to the manufacturer's protocol. Urine was collected at 72 h

and 144 h after surgery using metabolism cages for monitoring of urine volume. Mice were euthanized at 144 hours after the procedure, at which time kidneys were harvested for molecular analyses.

Renal histology.

Formalin-fixed kidney sections approximately 5–6 microns from mice at 144 hours after I/R or sham surgery were stained with hematoxylin and eosin, and the degree of morphologic changes was determined by light microscopy in a blinded fashion. Degree of tubular necrosis was evaluated on a scale from 0 to 4, which ranged from not present (0), mild (1), moderate (2), severe (3), and very severe (4).

Quantitative real-time PCR for mRNA and mtDNA expression.

Total RNA was extracted from renal cortical samples using Trizol reagent (Life Technologies, Carlsbad, CA). cDNA was synthesized via reverse transcription using the iScript Advanced cDNA synthesis kit (Bio-Rad, Hercules, CA) with an input of 2 µg of RNA. qPCR was performed using SSoAdvanced SYBR Green Supermix (Bio-Rad) at a concentration of 1x and primers at a final concentration of 750 nM (Integrated DNA Technologies, Coralville, IA). mRNA expression was calculated using the $2^{-\Delta\Delta CT}$ method normalized to β -actin. Primer sequences for COL1A2 [275], PGC-1 α , NRF-1, COX1, ND1, ATP5 β , Kim-1, NGAL, TNF- α , IL-1 β , and β -actin were previously described [276]. Additional primer sequences used were as follows: MCP-1: F: 5'- ACCACAGTCCATGCCATCAC-3', R: 5'- TTGAGGTGGTTGTGGAAAAG-3'; F4/80: F: 5'- CTTTGGCTATGGGCTTCCAGTC-3', R: 5'- GCAAGGAGGACAGAGTTTATCGTG-3'; Catalase: F: 5'- GCAGATACCTGTGAACTGTC-3', R: 5'- GTAGAATGTCCGCACCTGAG-3'; MnSOD: F:

5'- ACACATTAACGCGCAGATCA-3', R: 5'- AGCCTCCAGCAACTCTCCTT-3'; eNOS: F: 5'- TCTGCGGCGATGTCACTATG-3', R: 5'- CATGCCGCCCTCTGTTG-3'. qPCR was used to determine the relative quantity of mtDNA in mouse renal cortical tissue. DNA was extracted from tissue using the DNeasy Blood and Tissue Kit (Qiagen, Valencia, CA). qPCR was performed as described above using 5 ng of cellular DNA. The mitochondrial gene ND1 was used as an indicator of mtDNA content and was normalized to nuclear-encoded β -actin expression.

Immunoblotting for protein expression.

Renal lysates were prepared via homogenization and sonication in RIPA buffer. Samples were centrifuged at 10,000 x g for 10 min. to clear insoluble material. Protein concentrations were quantified via BCA assay (Life Technologies). Equal amounts of protein (10 μ g) were separated on 4%–20% gradient SDS-polyacrylamide gels and transferred to nitrocellulose membranes. Membranes were blocked with 2.5% BSA in TBST and incubated with anti-PGC-1 α (Calbiochem, 1:1000), anti-COX1 (Santa Cruz, 1:1000), anti- β actin (Santa Cruz, 1:1000), anti-Kim-1 (R&D Systems, 1:1000), anti-NGAL (Abcam, 1:1000), anti- α SMA (Sigma, 1:5000), or anti-GAPDH (Santa Cruz, 1:5000) overnight at 4°C. After incubation for 2 h at room temperature with secondary antibodies (1:5000) conjugated with horseradish peroxidase, membrane proteins were detected via chemiluminescence. Renal proteins were quantified via densitometry using NIH ImageJ.

Renal ATP levels.

ATP was isolated from fresh kidneys as described previously [307]. Briefly, renal cortical tissue was homogenized in phenol-TE. DEPC water and chloroform were added and the

suspension was vortexed. Samples were centrifuged at $10,000 \times g$ for 5 min at 4°C . The upper layer was diluted 1:100 in DEPC water and ATP was measured using the ATP Determination Kit (Invitrogen, Carlsbad, CA). ATP levels were normalized to tissue wet weight.

8-OH-dG and cGMP ELISA.

cGMP was isolated from flash frozen tissue via TCA extraction. Briefly, renal tissue was homogenized in 10 volumes ($\mu\text{L}/\text{mg}$ tissue) 5% TCA. Samples were centrifuged for 10 min at $1,500 \times g$ and the supernatant was collected. TCA was extracted 3x in water-saturated ether. Samples were heated at 70°C to remove residual ether. cGMP levels were then measured using a commercially available ELISA kit according to manufacturer's instructions (Cayman Chemical).

To prepare samples for measurement of 8-OH-dG, flash frozen tissue samples were homogenized in Homogenization buffer (PBS + 1 mM EDTA). Samples were centrifuged at $1,000 \times g$ to remove insoluble material. DNA was then purified using the DNeasy Blood and Tissue kit (Qiagen). Resultant DNA was digested with nuclease P1 (Sigma) according to manufacturer instructions. pH of the sample was then adjusted to 7.5-8.5 using 1 M Tris. Samples were incubated with alkaline phosphatase (1 U/100 μg DNA) at 37°C for 30 min. Samples were then boiled for 10 min and placed on ice. 8-OH-dG levels were measured using a commercially available kit according to manufacturer's instructions (Cayman Chemical).

Data and statistical analysis.

Data are expressed as means \pm SEM for parametric data, or median \pm IQR for non-parametric data. Multiple comparisons of normally distributed data were analyzed by one-way ANOVA and group means were compared using Fisher's LSD post-test. Non-parametric data were analyzed using a

Kruskal-Wallis test followed by a Dunn's test for multiple comparisons. The criterion for statistical differences was $p < 0.05$ for all comparisons.

RESULTS

BAY 58-2667 and BAY 41-2272 stimulate mitochondrial respiration in RPTC.

To evaluate the ability of GC activators and stimulators to stimulate mitochondrial biogenesis and increase mitochondrial function, RPTC were treated for 24 h with the GC stimulator, BAY 41-2272 (10 nM – 10 μ M) or the GC activator, BAY 58-2667 (10 nM – 10 μ M). Basal and FCCP-uncoupled (maximal) oxygen consumption rate (OCR) were determined using the Seahorse XF96 Extracellular Flux analyzer. Basal OCR was unchanged at any concentration tested for either BAY 41-2272 or BAY 58-2667 (Figure 4.1A-B). BAY 41-2272 increased FCCP-uncoupled OCR 25% and 30% at concentrations of 1 and 10 μ M, respectively. BAY 58-2667 significantly increased FCCP-uncoupled OCR at all concentrations tested from 21-26% above vehicle controls (Figure 4.1C-D). These data demonstrate that either GC activators or stimulators can increase maximal mitochondrial function, which could be due to activation of mitochondrial biogenic signaling.

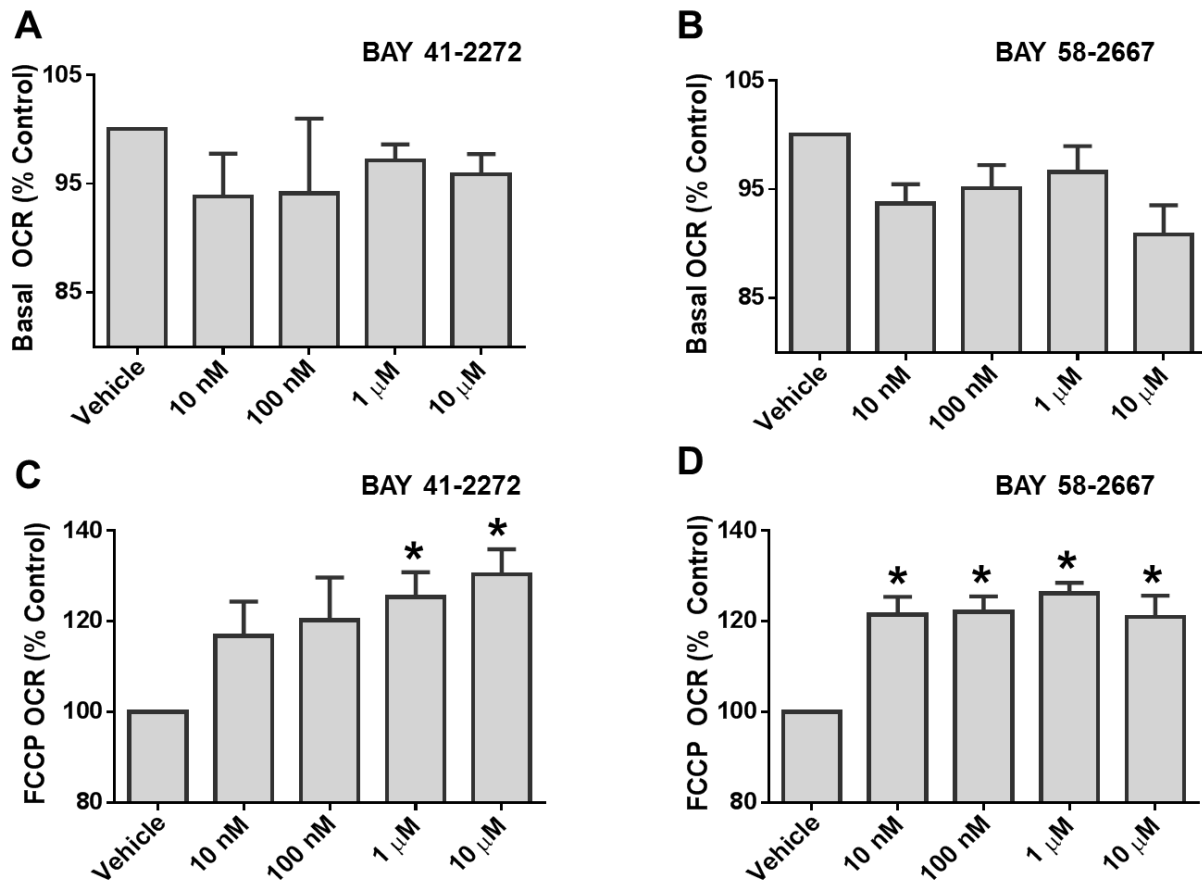


Figure 4.1: BAY 41-2272 and BAY 58-2667 increase FCCP-uncoupled OCR in RPTC. RPTC were treated with BAY 41-2272 (10 nM – 10 μ M) or BAY 58-2667 (10 nM – 10 μ M) for 24 h. Basal (A, B) and FCCP-uncoupled (C, D) OCR were measured using the Seahorse XF96 Extracellular Flux Analyzer. Data are expressed as % of vehicle control. * indicates significant difference from vehicle ($p < 0.05$), $n = 4$ per group.

BAY 58-2667, but not BAY 41-2272 stimulates mitochondrial biogenesis in mouse renal cortex.

To examine activation of pathways of mitochondrial biogenesis, BAY 41-2272 and BAY 58-2667 were evaluated in mouse renal cortex. Mice were administered BAY 41-2272 (100 µg/kg or 1 mg/kg), BAY 58-2667 (10 µg/kg or 100 µg/kg), or saline vehicle by intraperitoneal injection. Mice were sacrificed and kidneys were collected for biochemical analyses 24 h after dosing. mRNA expression of the mitochondrial-encoded mitochondrial genes COX1 and ND1 were evaluated by quantitative PCR (qPCR). COX1 and ND1 mRNA expression increased to 1.90 and 1.75-fold of control mice, respectively, in mice that were treated with BAY 58-2667 at 100 µg/kg (Figure 4.2A-B). No changes were observed in COX1 and ND1 expression for either dose of BAY 41-2272 or BAY 58-2667 at 10 µg/kg vs. vehicle control. Renal cortical mitochondrial DNA (mtDNA) copy number, an indicator of mitochondrial number, was increased to 1.35-fold of vehicle control in mice treated with BAY 58-2667 at 100 µg/kg (Figure 4.2C). No changes were observed in any of the other treatment groups vs. control. Finally, protein expression of PGC-1 α and COX1 were assessed by immunoblot (Figure 4.2D-F). PGC-1 α and COX1 protein were significantly increased in mice treated with either 10 µg/kg BAY 58-2667 (1.44- and 1.35-fold) or 100 µg/kg BAY 58-2667 (1.53- and 1.37-fold) vs. control. No changes were observed in PGC-1 α or COX1 protein expression with either dose of BAY 41-2272. These results indicate that the GC activator BAY 58-2667, but not the GC stimulator BAY 41-2272, is capable of inducing mitochondrial biogenesis in mouse renal cortex.

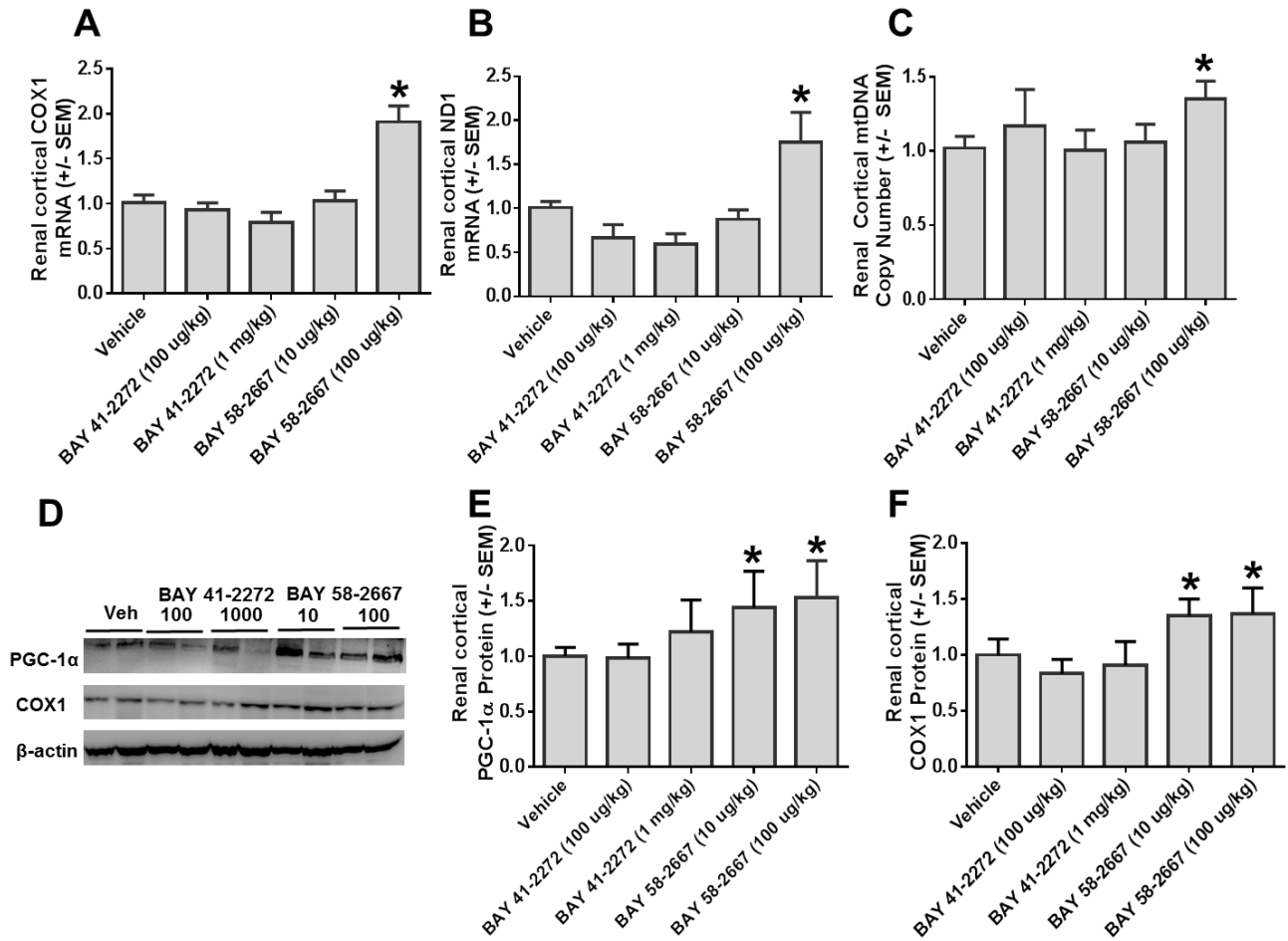


Figure 4.2: BAY 58-2667, but not BAY 41-2272 stimulates mitochondrial biogenesis in mouse renal cortex. Male C57BL/6 mice (8-10 weeks old) were administered BAY 41-2272 (100 μ g/kg or 1 mg/kg), BAY 58-2667 (10 μ g/kg or 100 μ g/kg) or saline vehicle by intraperitoneal injection. Mice were sacrificed 24 h after injection and kidneys were collected. Renal cortical mRNA expression of COX1 (A) and ND1 (B), and mtDNA copy number (C) were assessed by qPCR. Protein expression of PGC-1 α and COX1 were assessed by immunoblot (D). Blots were quantified by densitometry and corrected to β -actin (E-F). * indicates significant difference from vehicle ($p < 0.05$), $n = 4-8$ per group.

BAY 58-2667 promotes recovery of renal function and renal tubular damage markers following I/R-induced AKI.

In order to evaluate the efficacy of BAY 58-2667 in the setting of renal injury, AKI was induced in C57BL/6 mice by bilateral clamping of the renal pedicle for 19 minutes followed by reperfusion. Mice undergoing sham surgery served as controls. 24 h after I/R injury, mice displayed significant renal dysfunction evidenced by a ~4-fold increase (sham: ~25 mg/dL; I/R ~100 mg/dL) in blood urea nitrogen (BUN) levels. Beginning 24 h after reperfusion mice received daily injections with BAY 58-2667 (100 µg/kg) or saline control. Additionally, a group of mice were treated with sildenafil, a PDE5 inhibitor, at 1 mg/kg, as a positive control. Sildenafil has previously been demonstrated to induce mitochondrial biogenesis, and be protective and/or promote recovery in multiple models of AKI [149, 313, 354, 355]. BUN levels remained elevated at 6 d after I/R in mice treated with saline vehicle; however, treatment with either sildenafil or BAY 58-2667 reduced BUN levels indicating an acceleration of recovery of renal function (Figure 4.3A). We then assessed renal tubular damage by measuring renal cortical Kim-1 and NGAL mRNA and protein expression at 6 d after I/R. Renal Kim-1 and NGAL mRNA levels were increased to 150-fold and 25-fold of sham surgical levels, respectively (Figure 4.3B,C). Treatment with sildenafil or BAY 58-2667 significantly reduced renal Kim-1 levels, but had no effect on renal NGAL expression. Kim-1 and NGAL protein levels were measured by immunoblot in the renal cortex, and were increased to 120-fold and 23-fold of sham surgical levels, respectively (Figure 4.3D-F). BAY 58-2667, but not sildenafil significantly reduced renal Kim-1 levels. Both sildenafil and BAY 58-2667 reduced renal NGAL protein levels back to near sham surgical levels. These data indicate that induction of cGMP through either inhibition of PDE5 or activation of GC promotes recovery of renal function and reduces tubular damage markers after I/R-induced AKI.

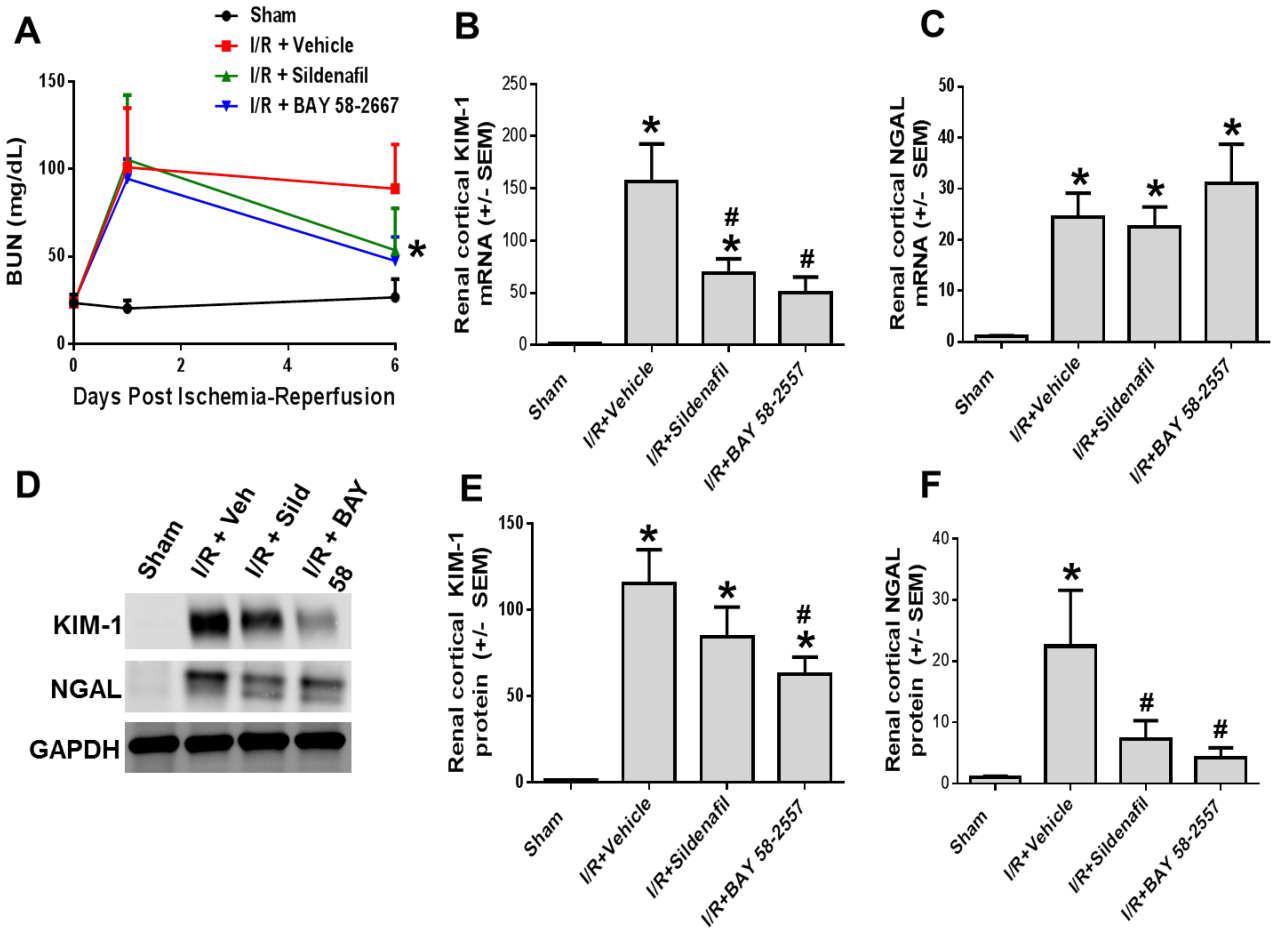


Figure 4.3: BAY 58-2667 promotes recovery from ischemia-reperfusion (I/R)-induced AKI. Male C57BL/6 mice (8-10 weeks old) underwent sham surgery or 19 minutes of ischemia by bilateral clamping of the renal pedicle followed by reperfusion. Mice were treated with saline vehicle, the PDE5 inhibitor sildenafil (1 mg/kg), or BAY 58-2667 (100 μ g/kg) daily beginning at 24 h after surgery. Blood was collected via retroorbital bleed at 1 and 6 d after surgery. Urine was collected using metabolism cages at 3 and 6 d after surgery. Mice were sacrificed 6 d after surgery for tissue collection. Renal function was monitored by assessment of BUN (A) and urine output (B). Renal damage was assessed biochemically by measurement of renal cortical KIM-1 and NGAL mRNA (C,D) and protein levels (E). * indicates significant difference from sham ($p < 0.05$), # indicates significant difference from I/R+vehicle ($p < 0.05$), $n = 5-17$ per group depending on assay.

BAY 58-2667 reduces renal morphological damage following I/R-induced AKI.

Formalin-fixed renal sections were stained with hematoxylin-eosin (H&E) for histological evaluation and were scored by a pathologist. At 6 d after I/R, kidneys continued to demonstrate severe morphological disruption characterized by tubular dilation, degeneration and necrosis, loss of tubular brush borders and inflammatory cell infiltration (Figure 4.4A). Mice treated with BAY 58-2667 showed a partial recovery of renal morphology evidenced by reduced histological score for tubular necrosis (Figure 4.4B).

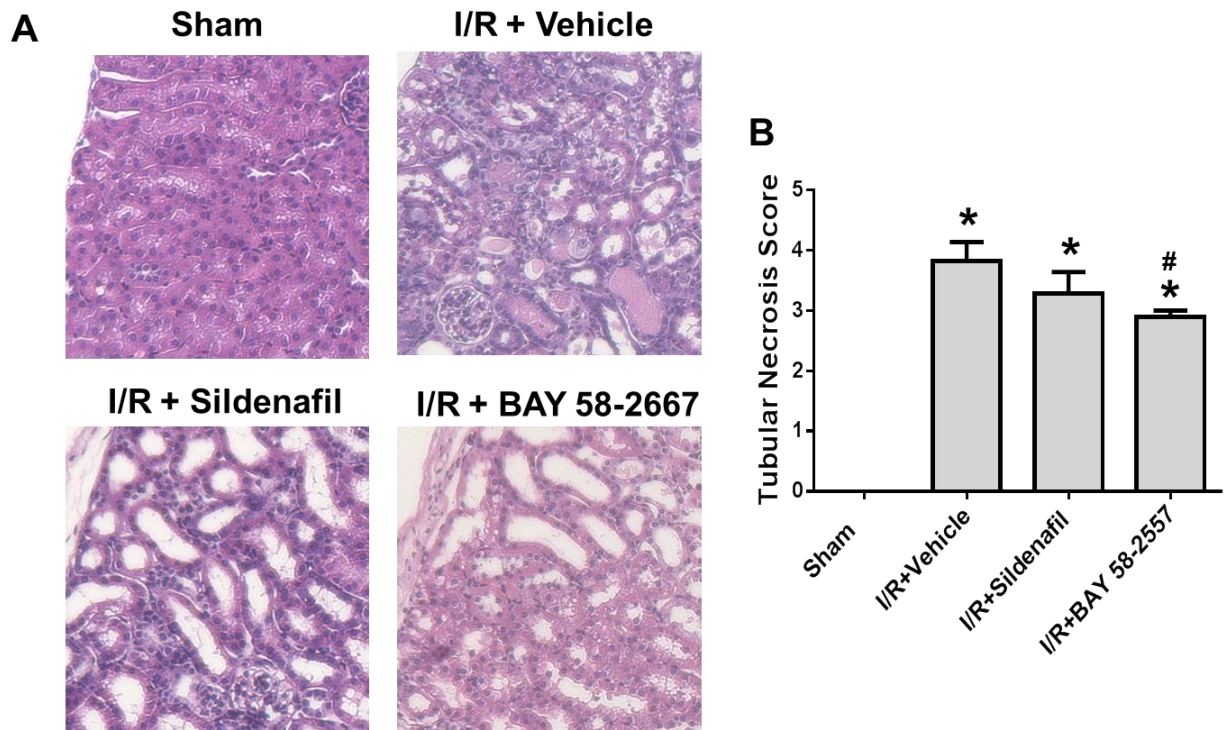


Figure 4.4: BAY 58-2667 reduces renal tubular necrosis following I/R-induced AKI.

Kidneys were stained for morphological assessment with hematoxylin & eosin (H&E) (A).

Kidneys were scored in a blinded fashion by pathologist for tubular necrosis on a scale from 0-4 (0=absent, 1=mild, 2=moderate, 3=severe, 4=very severe) (B). * indicates significant difference from sham ($p < 0.05$), # indicates significant difference from I/R+vehicle ($p < 0.05$), $n = 6-7$.

BAY 58-2667 stimulates mitochondrial biogenesis and promotes recovery of renal function following I/R-induced AKI.

Due to the importance of mitochondrial energetics in tissue repair and recovery, and our data demonstrating the efficacy of BAY 58-2667 in naïve mice as an inducer of MB, we examined mitochondrial biogenic signaling and its outcomes in the kidney after renal I/R. Previous studies have demonstrated that MB is potently and persistently suppressed in the kidney after various forms of AKI including I/R [161]. Our results concur with these previous data as mRNA expression of PGC-1 α , NRF-1, COX1, ND1 and ATP5 β were also suppressed to 30-50% of sham controls at 6 d after I/R injury (Figure 4.5A-E). Furthermore, mtDNA copy number was reduced to 34% of control levels (Figure 4.5F). Treatment with BAY 58-2667 promoted the recovery of PGC-1 α and NRF-1 back to control levels. Additionally, mRNA expression of COX1, ND1 and ATP5 β were also significantly increased. Finally, mtDNA content was restored back to near sham control levels. To examine whether these transcriptional changes manifested as increases in mitochondrial protein levels, we measured PGC-1 α and COX1 expression via immunoblot (Figure 4.6A-C). At 6 d after I/R injury, PGC-1 α protein expression was unchanged vs. sham controls. However, treatment with sildenafil or BAY 58-2667 increased PGC-1 α expression to ~1.8-fold of sham levels, indicating that MB is being driven above levels observed in healthy controls. COX1 expression was reduced to 34% of control levels in I/R mice, and treatment with either sildenafil or BAY 58-2667 restored expression to normal levels. Finally, as an assessment of renal mitochondrial function, we measured renal cortical ATP levels using a luminescence based assay (Figure 4.6D). Renal ATP levels were reduced to 39% of normal levels in I/R mice. Both sildenafil and BAY 58-2667 restored renal ATP levels back to control levels suggesting a restoration of mitochondrial content and/or

function. These data clearly demonstrate that BAY 58-2667 acts as a stimulator of MB after I/R-induced AKI.

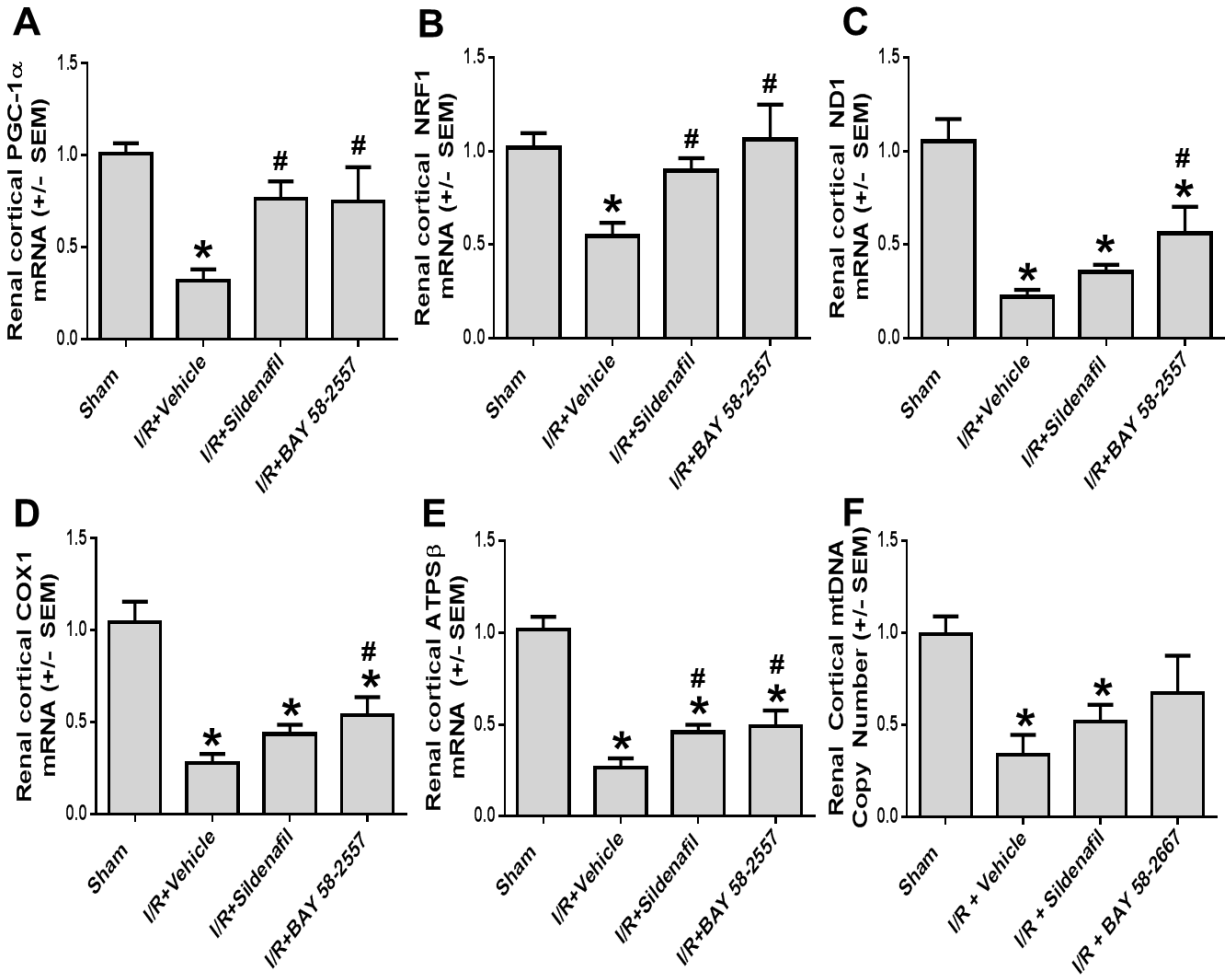


Figure 4.5: BAY 58-2667 stimulates recovery of mitochondrial gene expression and mtDNA copy number following renal I/R. Renal cortical mRNA expression of PGC-1 α (A), NRF1 (B), ND1 (C), COX1 (D), ATP5 β (E) and mtDNA copy number (F) were assessed by qPCR. * indicates significant difference from sham (p<0.05), # indicates significant difference from I/R+vehicle (p<0.05), n = 7-12.

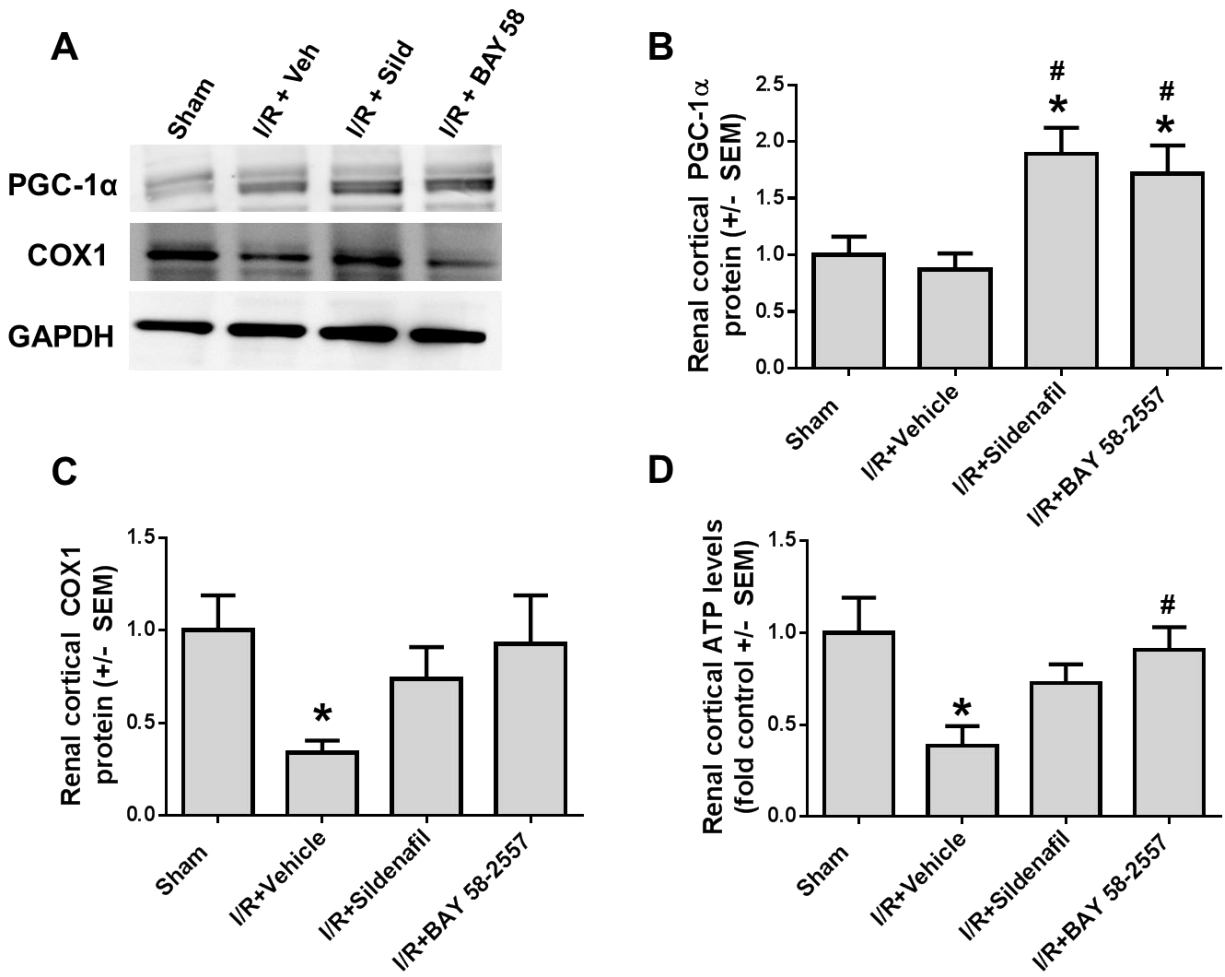


Figure 4.6: BAY 58-2667 promotes recovery of renal mitochondrial protein expression and ATP levels. . Renal cortical protein expression of PGC-1α and COX1 were assessed by immunoblot (A) and quantified by densitometry (B,C). ATP levels (D) were quantified using the ATP Determination Kit (Life Technologies) * indicates significant difference from sham (p<0.05), # indicates significant difference from I/R+vehicle (p<0.05), n = 7-12 for qPCR, n=7-8 for ATP levels.

BAY 58-2667 reduces development of renal fibrosis after I/R.

Increasing evidence points to AKI as a major risk factor for the development of chronic kidney disease (CKD) and end stage renal disease (ESRD) [10, 74, 356]. The failed repair of the renal tubular epithelium and chronic inflammation and oxidative stress may contribute to the development of fibrosis and chronic renal disease [27]. Furthermore, collagen deposition and fibrotic signaling have been prominently observed in animal models of I/R-induced renal injury [75, 357, 358]. In our model, early fibrotic development was observed following I/R, evidenced by a 5-fold induction in COL1A2 gene expression, and a 7.2-fold induction in renal cortical α SMA protein expression at 6 d after I/R (Figure 4.7A-C). Treatment with BAY 58-2667 reduced COL1A2 expression to 2.6-fold of sham controls, and α SMA to 3.7-fold of controls. As polyuria is often observed in patients with early CKD, we monitored urinary output in these mice following I/R. Urine output was significantly increased in I/R mice vs. sham controls at 6 d after I/R. Treatment with either sildenafil or BAY 58-2667 did not reduce urine output (Figure 4.7D).

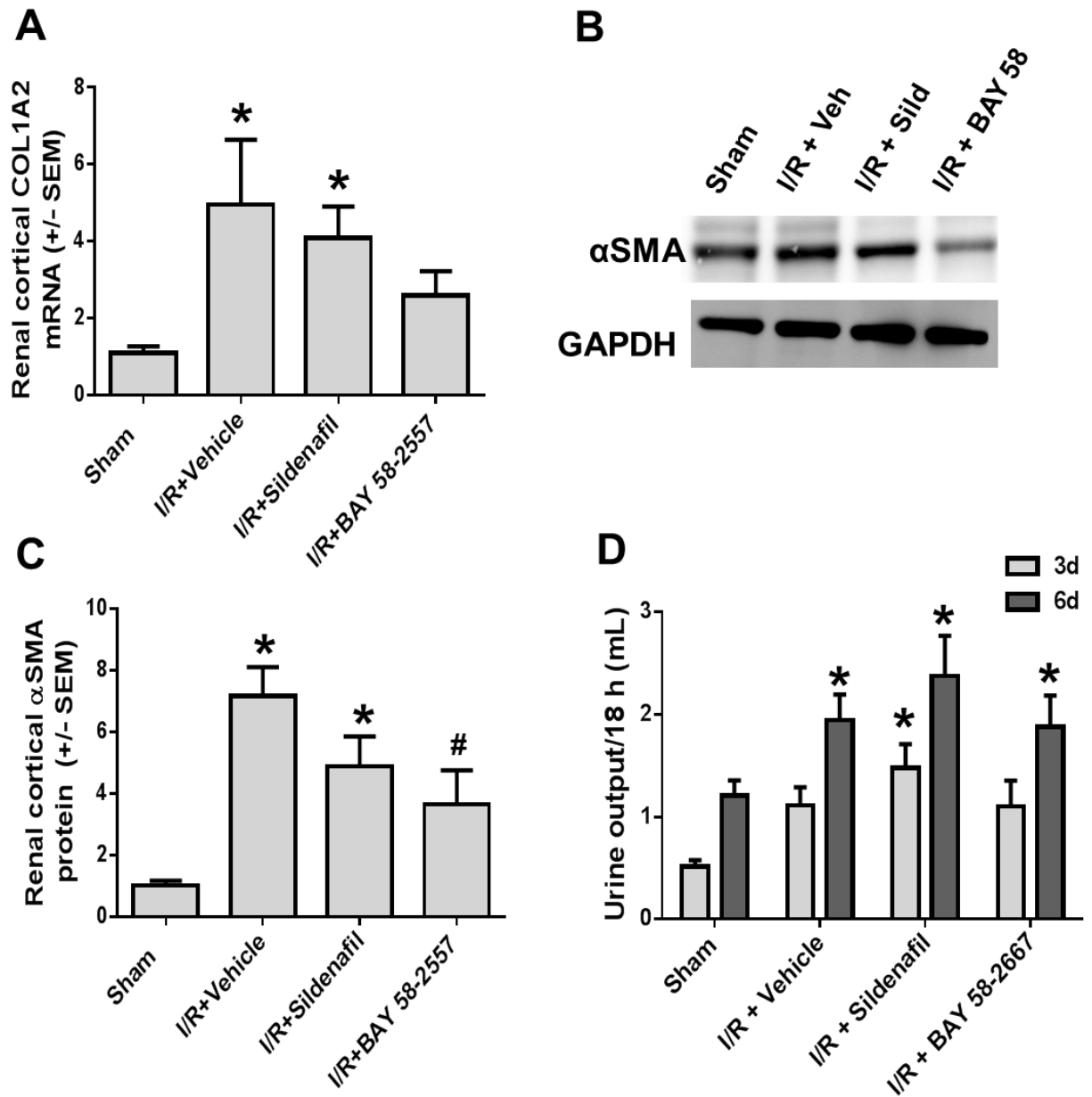


Figure 4.7: BAY 58-2667 reduces renal fibrotic development following I/R. Renal cortical mRNA expression COL1A2 (A) was assessed by qPCR. Renal cortical protein expression of α SMA was assessed by immunoblot and quantified by densitometry (B,C). Urine output was monitored by 18-h collection in metabolism cages (D). * indicates significant difference from sham ($p < 0.05$), # indicates significant difference from I/R+vehicle ($p < 0.05$), $n = 7-12$.

BAY 58-2667 reduces renal inflammatory cytokines and oxidative damage.

Inflammation and oxidative stress are key mediators of the initiation and progression of renal damage and dysfunction following I/R injury [359]. Additionally, inflammation and oxidative stress have been demonstrated to affect mitochondrial function [360]. We examined the effects of treatment with BAY 58-2667 on expression of inflammatory cytokines and chemokines, and markers of oxidative stress and antioxidant status. Following I/R injury, expression of the inflammatory cytokines TNF- α and IL-1 β were markedly upregulated in the renal cortex (Figure 4.8A-B). Treatment with sildenafil or BAY 58-2667 reduced expression of both markers to near sham control levels. Furthermore, mRNA expression of the macrophage marker F4/80 and the macrophage chemokine MCP-1 were upregulated 6-fold and 50-fold, respectively, 6 d after I/R, indicating profound macrophage infiltration (Figure 4.8C-D). Neither sildenafil nor BAY 58-2667 reduced the expression of these markers. Antioxidant status of the renal cortex was assessed by measurement of gene expression of catalase and the mitochondrial antioxidant manganese superoxide dismutase (MnSOD). At 6 d after I/R, catalase and MnSOD levels were suppressed to ~20% of control levels. Treatment with sildenafil and BAY 58-2667 appeared to modestly increase these expression levels, however, these changes were not significant (Figure 4.9A,B). Interestingly, despite having no significant effects on antioxidant status, sildenafil and BAY 58-2667 reduced 8-OH-dG levels (a marker of oxidative DNA damage) in the renal cortex back to sham control levels (Figure 4.9C). These data demonstrate that induction of cGMP has beneficial effects on renal inflammation and oxidative tissue damage after I/R.

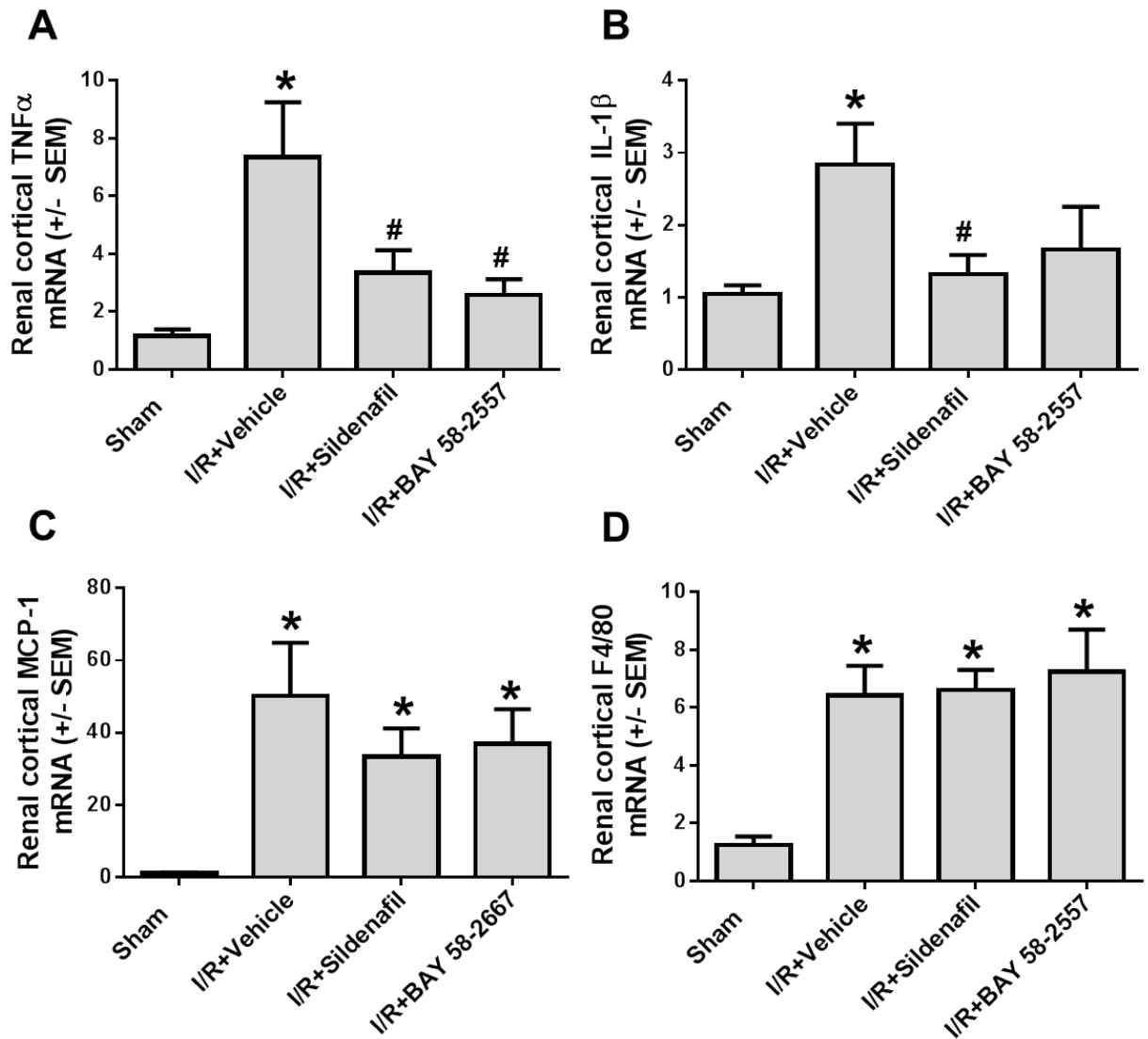


Figure 4.8: BAY 58-2667 reduces renal inflammatory cytokine expression. Renal cortical mRNA expression of TNF α (A), IL1 β (B), MCP-1 (C) and F4/80 (D) were assessed by qPCR. * indicates significant difference from sham ($p < 0.05$), # indicates significant difference from I/R+vehicle ($p < 0.05$), $n = 7-12$.

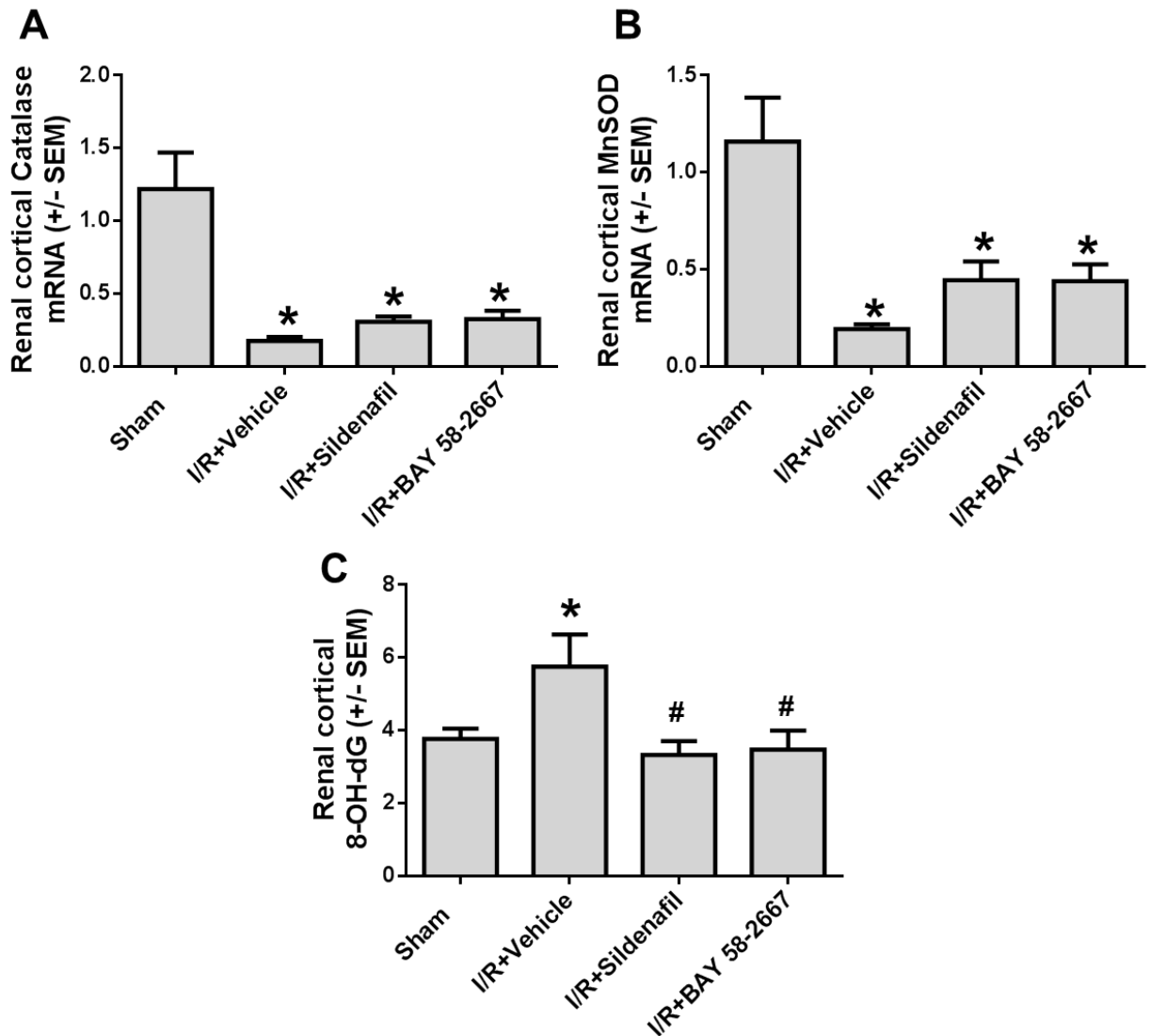


Figure 4.9: BAY 58-2667 reduces renal oxidative damage. Renal cortical mRNA expression of catalase (A) and MnSOD (B) were measure by qPCR. Renal 8-OH-dG levels were assessed by ELISA. * indicates significant difference from sham ($p < 0.05$), # indicates significant difference from I/R+vehicle ($p < 0.05$), $n = 6-12$ for qPCR, $n = 5-9$ for 8-OH-dG ELISA.

BAY 58-2667 stimulates renal eNOS expression.

Previous reports have demonstrated that pharmacological induction of cGMP can cause the upregulation of eNOS expression and NO production through a positive-feedback loop [361]. Additionally, eNOS expression and activity have been shown to be inhibited following I/R injury [362]. Furthermore, eNOS has been demonstrated to have an important role in MB [233, 270, 271]. We examined renal eNOS gene expression following I/R and the effects of sildenafil and BAY 58-2667 on its expression. eNOS expression was reduced to ~60% of controls at 6 d after I/R (Figure 4.10A). Treatment with sildenafil restored eNOS expression to sham levels, while BAY 58-2667 increased eNOS to 2-fold of sham controls. To determine the effect of BAY 58-2667 on renal cGMP levels both through its induction of GC activity and its effect on eNOS expression, we measured cGMP in the kidney via ELISA (Figure 4.10B). No changes were observed in cGMP levels following renal I/R vs. sham controls. Furthermore, treatment with sildenafil did not significantly increase renal cGMP. BAY 58-2667 did increase cGMP significantly over sham levels, but not I/R+vehicle levels, however, cGMP levels in all groups were quite variable.

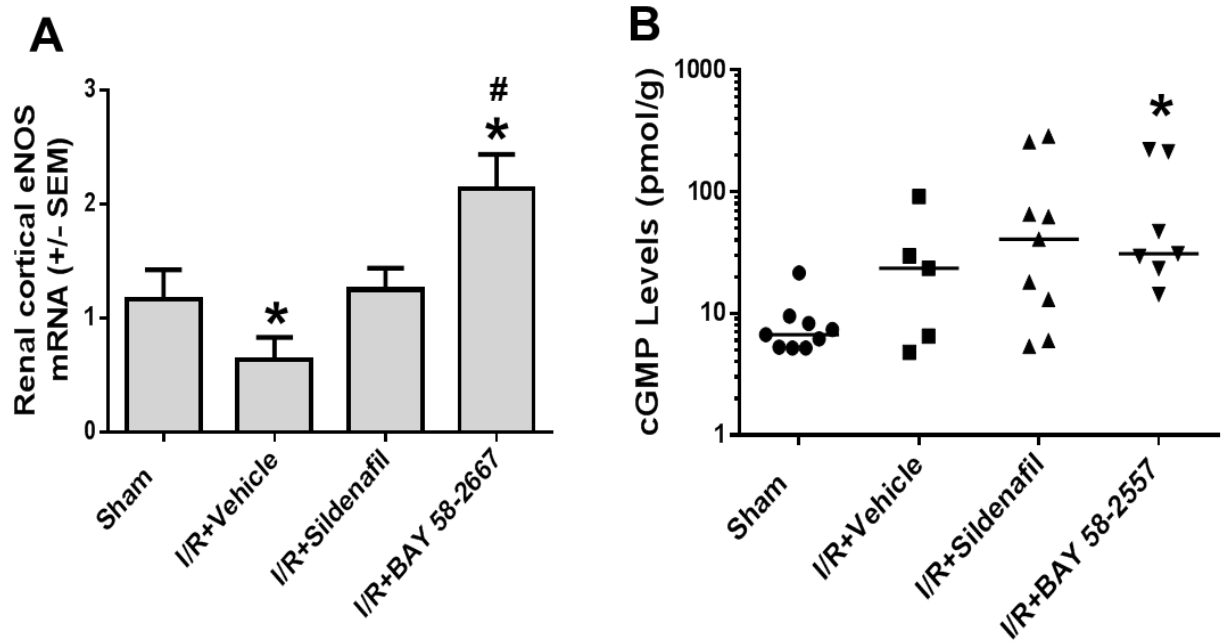


Figure 10: BAY 58-2667 promotes recovery of renal eNOS expression, but has no effect on renal cGMP. Renal cortical mRNA expression of eNOS (A) was measured by qPCR. Renal cGMP levels were measured by ELISA. * indicates significant difference from sham ($p < 0.05$), # indicates significant difference from I/R+vehicle ($p < 0.05$), $n = 7-12$ for qPCR, $n = 5-9$. Significance for cGMP was assessed using the Kruskal-Wallis analysis.

DISCUSSION

Mitochondria are dynamic organelles whose content, structure and function are regulated by the balance of mitochondrial degradation by mitophagy, mitochondrial fission and fusion processes, and the generation of new mitochondria through the process of mitochondrial biogenesis (MB) [125]. Mitochondrial function is required for the maintenance of normal cellular function, and is vital for tissue structural and functional repair following injury. Mitochondrial dysfunction is prominently observed in an array of both acute and chronic conditions including diabetes and metabolic syndrome, neurodegeneration, cardiovascular disease, and acute kidney injury (AKI) [153, 363-365]. Following renal ischemia-reperfusion (I/R)-induced AKI, renal tubular mitochondria undergo a number of pathological changes including loss of membrane potential, Ca^{2+} -induced swelling, and activation of the mitochondrial permeability transition [153, 156, 345]. These mitochondrial disturbances lead to tissue ATP depletion, release of apoptotic mediators and production of reactive oxygen species, furthering renal tissue damage. Furthermore, mitochondrial homeostasis following renal I/R injury remains persistently disrupted evidenced by disturbances in mitochondrial fission/fusion proteins, elevated mitophagy and suppressed mitochondrial biogenesis [126, 161]. Due to the energetic requirements of renal repair, this persistent mitochondrial dysfunction could limit renal recovery following AKI. Thus, induction of the generation of new, more functional mitochondria through the activation of MB could accelerate renal recovery.

Previous studies by our laboratory with inducers of MB including SRT1720, formoterol and LY 344-864 have shown restoration of renal mitochondrial content and function, and acceleration of renal functional recovery [148, 150, 218]. Additionally, cGMP has a well-characterized role in the regulation of MB. Induction of cGMP using PDE5 inhibitors has been

shown to protect against or promote recovery from AKI [149, 314, 354, 355]. Treatment of mice with sildenafil after folic acid-induced AKI stimulated the recovery of mitochondrial gene expression and mtDNA content, and reduced tubular injury evidenced by decreased Kim-1 expression. cGMP levels can also be regulated by controlling their generation by guanylyl cyclases (GCs). GCs are activated primarily through G-protein coupled membrane receptors or by naturetic peptides. Recent work has led to the development of novel small molecule GC stimulators (activated reduced GC) and activators (activate oxidized GC). In these studies, we examined the ability of BAY 41-2272, a GC stimulator, and BAY 58-2667, a GC activator, to stimulate MB *in vitro* and *in vivo* and to promote recovery renal and mitochondrial recovery after I/R-induced AKI.

Treatment of rabbit renal proximal tubular cells (RPTC) with BAY 41-2272 stimulated mitochondrial uncoupled OCR (FCCP-OCR) at concentrations of 1-10 μ M, while BAY 58-2667 increased FCCP-OCR at concentrations of 1 nM – 10 μ M. No changes were observed in basal oxygen consumption (Figure 4.1). Due to the high oxidative potential of these cells, a change in basal oxygen consumption is rarely observed with induction of MB. Increases in FCCP-OCR alone are indicative of increased mitochondrial content or function. We then treated naïve mice with BAY 41-2272 (0.1-1 mg/kg) and BAY 58-2667 (0.01-0.1 mg/kg) to assess their *in vivo* efficacy. BAY 58-2667 increased renal cortical expression of mitochondrial genes and proteins, and mtDNA copy number (Figure 4.2). Interestingly, BAY 41-2272 had no effect on renal MB signaling. The failure of BAY 41-2272 to induce MB could indicate that GC in the renal cortex is primarily present in the oxidized (or heme-free) form preventing the interaction of GC stimulators, but not activators. Due to the high levels of oxidative metabolism in the renal cortex this is likely a region that experiences relatively high levels of oxidative stress, perhaps leading

to GC oxidation. Further studies are needed to characterize the oxidative state of GC in the renal tubular epithelium.

Due to the efficacy of BAY 58-2667 in naïve mice, we tested its ability to promote mitochondrial and renal recovery after I/R-induced AKI in mice. MB is potently and chronically suppressed following renal I/R injury, thus reactivation of MB signaling could accelerate renal recovery. Mice were treated with BAY 58-2667 (0.1 mg/kg) at peak injury (24 h after I/R) to evaluate its role in renal recovery. Additionally, another group of mice were treated with the PDE5 inhibitor sildenafil due to its known role in the activation of MB and its ability to promote renal recovery in other models of AKI. Daily treatment with either sildenafil or BAY 58-2667 from 24-144 h promoted recovery of renal function evidenced by reduced BUN, and reduced tubular injury markers, Kim-1 and NGAL (Figure 4.3). Additionally, BAY 58-2667 reduced histological scores for renal tubular necrosis (Figure 4.4). Due to the delay in treatment, these changes in renal function and damage markers are indicative of a promotion of renal recovery, rather than a blunting of renal injury.

As previously described, mitochondrial function is critically important for renal repair. MB signaling has previously been shown to be persistently reduced, and vital for renal recovery. Mice treated with BAY 58-2667 demonstrated recovery of expression of PGC-1 α , NRF-1 and several mitochondrial and nuclear-encoded mitochondrial genes, as well as mtDNA content indicating a reactivation of MB (Figure 4.5). Furthermore, protein expression of PGC-1 α was induced over sham control levels promoting the recovery of COX1 protein expression, and renal function evidenced by renal cortical ATP levels (Figure 4.6). These data clearly demonstrate the ability of the GC activator BAY 58-2667 to promote MB in the injured kidney. Restoration of renal cortical ATP levels provides the energy necessary to power renal tissue repair mechanisms.

Recent work has elucidated the link between AKI and the development of CKD and ESRD [10, 74, 356]. Previously believed to be unique and independent disease states, AKI and CKD are now described on a continuum of renal dysfunction. Following an acute renal insult, activation of renal repair processes regenerate the renal tubular epithelium and restore renal function. However, failure of these processes can lead to tubular atrophy, secretion of pro-fibrotic signals, proliferation of resident or infiltrating myelofibroblasts, and ultimately chronic renal dysfunction [73]. We examined the effects of BAY 58-2667 treatment on early fibrotic development 144 h after I/R. Mice treated with BAY 58-2667 showed reduced expression of the fibrotic markers COL1A2 and α SMA (Figure 4.7). Urinary output was monitored as polyuria is observed early during CKD. BAY 58-2667 did not reduce urine output back to control levels; however, as cGMP is a crucial signal for naturesis, GC activation alone likely stimulates urine output making interpretation of this result difficult. Previous work has shown that NO-cGMP signaling is reduced in experimental models of renal fibrosis, and induction of cGMP using the GC stimulator BAY 41-2272 reduces fibrotic development [366, 367]. The efficacy of BAY 41-2272 in these models and the failure of BAY 41-2272 to induce MB in the renal cortex suggests a MB-independent mechanism for suppression of renal fibrosis. However, other studies have demonstrated the potential of BAY 41-2272 to stimulate MB in other tissues. Differences in dosing and timing of assessment of mitochondrial endpoints could yield different results, thus MB may still play a role in fibrotic suppression.

Mitochondrial function is closely linked with tissue inflammation and oxidative stress [360]. Mitochondrial dysfunction can lead to the release of inflammatory mediators, including mtDNA, and the production of reactive oxygen and nitrogen species. Contrarily, inflammatory signals can negatively impact mitochondrial function, and ROS can lead to damage of

mitochondrial proteins and lipids. Thus, activation of any one of these components can negatively impact the others creating a vicious cycle of elevated inflammatory signaling, compromised mitochondrial function and increased oxidative cellular damage. Due to the role of mitochondria in inflammation and oxidative stress, we measured inflammatory gene expression and markers of oxidative stress in I/R mice following treatment with BAY 58-2667. Expression of the inflammatory cytokines TNF- α and IL-1 β were potently induced following renal I/R, and treatment with both sildenafil and BAY 58-2667 reduced expression of these inflammatory signals (Figure 4.8). BAY 58-2667 additionally reduced renal oxidative damage assessed by 8-OH-dG levels independent of effects on antioxidant mechanisms (Figure 4.9). These data demonstrate that BAY 58-2667 has beneficial effects on renal recovery after I/R by reducing inflammatory signaling and oxidative stress. This effect could be a result of generation of better functioning mitochondria and thus reduced release of inflammatory mediators and ROS from dysfunctional mitochondria, or a direct effect of cGMP-induction on inflammatory or oxidative signaling. As cGMP has a well-known effect on vascular function and permeability [368], the positive effects observed in this study are likely caused by a mixed effect on renal tubular mitochondria, endothelial cells and resident inflammatory cells.

Previous work has shown that under certain conditions cGMP can promote its own generation through a positive feedback mechanism leading to enhanced production of NO via eNOS [361]. eNOS expression and activity has been shown to be disrupted in a number of acute conditions including I/R injury [369-371]. In our studies, we observed that eNOS expression was suppressed 6 d after I/R and that treatment with sildenafil promoted its recovery to control levels. BAY 58-2667 stimulated eNOS expression to 2-fold of control levels indicating a greater potency for GC activators vs. PDE inhibitors for this response (Figure 4.10). In addition to

potentially enhancing NO-cGMP-induced MB, induction of eNOS expression could have beneficial effects on vascular homeostasis. Assessment of renal cGMP levels via ELISA demonstrated that cGMP was unchanged following treatment with BAY 58-2667. However, this measurement was performed in tissue 24 h after the last dose of drug. Induction of cGMP via BAY 58-2667 is likely a transient response causing activation of more prolonged downstream signals. Induction of cGMP can lead to activation of PDEs through a negative feedback loop. Further studies are needed to evaluate acute changes in renal cGMP and associated signaling cascades.

Overall these studies demonstrate that induction of renal cGMP levels using the guanylyl cyclase activator BAY 58-2667 promotes recovery of renal function and structure, and limits fibrotic progression through activation of mitochondrial biogenesis, and reduction in renal inflammation and oxidative stress. These studies highlight the therapeutic potential for GC activators in AKI and other settings of acute organ injury.

CHAPTER 5:

Urinary ATP synthase subunit β is a novel biomarker of renal mitochondrial dysfunction in acute kidney injury

ABSTRACT

Although the importance of mitochondrial dysfunction in acute kidney injury (AKI) has been documented, noninvasive early biomarkers of mitochondrial damage are needed. We examined urinary ATP synthase subunit β (ATPS β) as a biomarker of renal mitochondrial dysfunction during AKI. Mice underwent sham surgery or varying degrees (5, 10, or 15 min ischemia) of ischemia/reperfusion (I/R)-induced AKI. Serum creatinine, BUN, and neutrophil gelatinase-associated lipocalin were elevated only in the 15 min I/R group at 24 h. Immunoblot analysis of urinary ATPS β revealed two bands (full length \sim 52 kDa and cleaved \sim 25 kDa), both confirmed as ATPS β by LC-MS/MS, that increased at 24 h in 10- and 15-min I/R groups. These changes were associated with mitochondrial dysfunction evidenced by reduced renal cortical expression of mitochondrial proteins, ATPS β and COX1, proximal tubular oxygen consumption, and ATP. Furthermore, in the 15-min I/R group, urinary ATPS β was elevated until 72 h before returning to baseline 144 h after reperfusion with recovery of renal function. Evaluation of urinary ATPS β in a nonalcoholic steatohepatitis model of liver injury only revealed cleaved ATPS β , suggesting specificity of full-length ATPS β for renal injury. Immunoblot analyses of patient urine samples collected 36 h after cardiac surgery revealed increased urinary ATPS β levels in patients with postcardiac surgery-induced AKI. LC-MS/MS urinalysis in human subjects with AKI confirmed increased ATPS β . These translational studies provide evidence that ATPS β may be a novel and sensitive urinary biomarker of renal mitochondrial dysfunction and could serve as valuable tool for the testing of potential therapies for AKI and chemical-induced nephrotoxicity.

INTRODUCTION

Acute kidney injury (AKI) is a significant clinical problem in hospitalized patients that is increasing in prevalence[372]. Furthermore, rates of adverse complications, mortality, and treatment costs are positively correlated with the severity of renal dysfunction[6]. Mitochondrial disruption is a key event promoting the progression of tubular cell injury/death during surgery, trauma, sepsis, ischemia/reperfusion (I/R), and drug/toxicant-induced AKI [152-154, 160, 163, 373]. Mitochondria play a major role in Ca^{2+} homeostasis, reactive oxygen species generation and redox balance, cellular proliferation, and apoptosis in AKI. Mitochondrial dysfunction is also a component of many chronic diseases including diabetes, neurodegeneration, and aging [163, 373].

Ischemia is a common pathophysiologic mechanism in many forms of AKI. Ischemic insult occurs when there is a reduced blood flow to the kidney which may occur after drug or toxicant exposure or as a component of vascular disease, sepsis, or volume depletion and hypotension [22, 27]. Mitochondrial damage is a major contributor to the tubular cell injury observed in the initiation and progression of ischemic AKI [22, 27, 152-154]. Following restoration of blood flow after ischemia, production of reactive oxygen and nitrogen species within the mitochondria is dramatically increased. Oxidative damage to mitochondrial proteins and lipids causes dysfunction of respiratory complexes, membrane depolarization, ATP depletion, and release of apoptotic proteins contributing to cellular injury and death.

Current organ injury biomarkers do not focus on mitochondrial dysfunction, and tests for mitochondrial integrity are limited to invasive procedures including muscle biopsies, organ ATP measurements, or respiratory measurements in isolated mitochondria [374]. While the importance of mitochondrial dysfunction during AKI in animals has been well documented [126, 149, 218,

275], similar data in humans is sparse as the availability of renal tissue for mitochondrial analysis is limited. Consequently, there is a significant need for early, specific and non-invasive biomarkers of mitochondrial dysfunction in AKI. Identification and validation of these markers could elucidate novel targets and mechanisms of renal mitochondrial dysfunction in AKI, and enable the development of new therapies.

We have previously reported that after I/R and glycerol-induced AKI, a time-dependent loss of renal cortical mitochondrial proteins including ATP synthase subunit β (ATPS β), a component of the electron transport chain (ETC), was indicative of renal mitochondrial dysfunction [126, 148, 161, 218]. Mitochondrial and renal function fail to fully recover after injury suggesting that mitochondrial function is a key component of the renal repair process. Thus, biomarkers of renal mitochondrial dysfunction may be a suitable proxy for monitoring mitochondrial and renal function in patients after AKI. In this study we validated urinary ATPS β as a potential translational biomarker of renal mitochondrial dysfunction following AKI.

EXPERIMENTAL PROCEDURES

Mouse renal I/R-induced AKI model

Eight-week-old male C57BL/6 mice (25–30 g) were divided into naïve, sham or I/R groups. Mice in the I/R group were subjected to bilateral renal pedicle clamping as described previously [148, 161]. Briefly, the renal artery and vein were isolated and blood flow was occluded with a vascular clamp for 5, 10, or 15 min. Mice were placed in metabolic cages 6 h after I/R until 24 h for 18 h urine collections. Urine was collected using a chilled collection system and protease inhibitors were added immediately after collection to prevent protein degradation. Mice were euthanized 24 h after surgery, at which time serum was collected and kidneys harvested for biochemical and histological analyses. For time course studies, urine, serum and kidneys were collected at 72 and 144 h. Renal function was monitored by serum creatinine and BUN using kits (BioAssay Systems, Hayward, CA) per the manufacturer's instructions. Urinary NGAL was measured by immunoblot and normalized to a standard sample. Renal tissues were fixed in 4.5% buffered formalin, dehydrated, and embedded in paraffin. For general histopathology, sections were stained with hematoxylin and eosin (H&E). All procedures involving animals were performed with approval from the IACUC in accordance with the NIH *Guide for the Care and Use of Laboratory Animals*.

Mouse nonalcoholic steatohepatitis model

Male C57BL/6 mice (8–9 weeks) were fed a liquid diet *ad libitum* containing 35% of calories from fat using corn oil with 0.5% (w/v) cholesterol for 5 months. Control mice were fed normal chow (Teklad Global 18% Protein rodent diet) containing 6.2% fat (18% of calories from fat) *ad libitum*. The fatty acid compositions in each diet were as follows: 16% saturated, 31% monounsaturated, 53% polyunsaturated in the nonalcoholic steatohepatitis (NASH) diet, and

32% saturated, 41% monounsaturated and 27% polyunsaturated for the control diet. Mice were placed in metabolic cages for 24 h for urine collection. Blood was collected under pentobarbital anesthesia (80 mg/kg, ip). Liver function was assessed by serum ALT determined using kits from Pointe Scientific (Lincoln Park, MI). For general histopathology, sections were stained with H&E.

Human urine samples

We used a subset of human urine samples from a recent study with published details of sample collection, processing, informed consent, and inclusion/exclusion criteria [375]. Urine samples were obtained as part of NIDDK-funded multicenter trial (NIH #DK080234) to identify prognostic urine markers from cardiac surgery patients who developed AKI. Protease inhibitors were added to each urine sample, and the supernatant was collected after centrifugation at 1,000 x g, and aliquots were frozen at -80 °C. Samples were shipped to the MUSC site on dry ice and kept frozen until use. Corresponding data including patient demographics, baseline chemistry measurements, urine collection and maximum values for serum creatinine, electrolytes, surgery type, cardiopulmonary bypass time, preexisting diseases, dialysis status, days to discharge and mortality status were provided (Table 1). Samples were also collected from patients who had cardiac surgery but did not develop AKI. These samples were collected by the MUSC CTSA Biobank and are linked to medical record numbers which provided subject demographic and clinical information.

TABLE 1. Characteristics of Patients With Urine Samples Obtained After Cardiac Surgery

Characteristics	AKI Status	
	No AKI	AKI
Number of patients	16	16
% Female	21	56
% Black	14	19
Age (years)	67	68
Weight (kg)	79	83
% CHF	55	13
% Diabetes	44	56
% CABG	88	88
% Valve replacement	44	19
% Bypass	86	75
Bypass time (min)	112	115
Baseline creatinine (mg/dl)	1.4	1.3
Collection creatinine (mg/dl)	1.4	2.7
Time to collection (days)	1.5	1.5
% Mortality	0	25
Days to discharge or death	10	19

Table 5.1: Sample clinical characteristics from cardiac surgery patients with AKI or no AKI. Data are shown as median (interquartile range), *n* (%), or mean \pm SD (*n* = 16 per group). AKIN, acute kidney injury network; CABG, coronary artery bypass graft; CHF, congestive heart failure.

Chemicals

Unless stated otherwise, all chemicals and biochemicals were purchased from Sigma Chemical Co. (St. Louis, MO). Rabbit polyclonal anti-NGAL and mouse monoclonal anti-ATPS β were purchased from Abcam Inc. (Cambridge, MA); mouse monoclonal anti-COX1 was purchased from Life Technologies (Carlsbad, CA); and the loading control glyceraldehyde 3-phosphate dehydrogenase (GAPDH) was obtained from Fitzgerald International Inc. (Acton, MA). Anti-rabbit and anti-mouse secondary antibodies conjugated with horseradish peroxidase were obtained from Pierce (Rockford, IL). All LC-MS/MS reagents were LC-grade pure and purchased from Waters (Milford, MA). Protein-A agarose beads used in the immunoprecipitation protocol were purchased from Roche (Indianapolis, IN).

Oxygen consumption in isolated tubular segments

Proximal tubules were isolated from fresh kidneys as previously described [32]. Briefly, renal cortical tissue was homogenized in Hanks Buffered Salt Solution (HBSS) containing collagenase (Worthington Biochemical Corp., Lakewood, NJ) and Soybean Trypsin Inhibitor (Sigma-Aldrich, St. Louis, MO). Tubules were incubated on a rocker at 37 °C for 30 min. Following digestion, horse serum was added and samples were vortexed for 30 s to inactivate collagenase. Samples were centrifuged at 200 x *g* for 5 min, the pellet was washed with HBSS and centrifuged at 200 x *g* again. Tubules were resuspended in RPTC culture media [149] and further diluted in media for respirometric analysis. Tubules were transferred to an XF-96 polystyrene cell culture plate (Seahorse Biosciences, North Bellerica, MA) and basal and FCCP-uncoupled oxygen consumption rate (OCR) were assessed in triplicate using the Seahorse XF96 Extracellular Flux Analyzer as previously described [284]. OCR was normalized to protein, assessed by BCA (Sigma-Aldrich, St. Louis, MO), using bovine serum albumin as the standard.

Renal ATP levels

ATP was isolated from fresh kidneys as previously described [307]. Briefly, renal cortical tissue was homogenized in phenol-TE. DEPC water and chloroform were added and the suspension was vortexed. Samples were centrifuged at 10,000 x *g* for 5 min at 4 °C. The upper layer was diluted 1:100 in DEPC water and ATP was measured using the ATP Determination Kit (Invitrogen, Carlsbad, CA). ATP levels were normalized to tissue wet weight.

Renal and urinary immunoblots

Immunoblots using mouse renal cortical tissue were performed as previously described [376, 377]. Urine samples from mice and humans were thawed and homogenized in 1 volume of protein lysis buffer (1% Triton X-100, 150 mM NaCl, 10 mM Tris-HCl, pH 7.4; 1 mM EDTA; 1 mM EGTA; 2 mM sodium orthovanadate; 0.2 mM phenylmethylsulfonyl fluoride; 1 mM HEPES, pH 7.6; 1 µg/ml leupeptin; and 1 µg/ml aprotinin) using a Polytron homogenizer. The homogenate was stored on ice for 10 min and then centrifuged at 1,000 x *g* for 2 min at 4 °C. The supernatant was collected and total urinary protein was determined as described above. Equal amounts of protein (10 µg) were separated on 4 to 20% gradient SDS-polyacrylamide gels and transferred to nitrocellulose membranes. Membranes were blocked either in 5% dried milk (for NGAL) or BSA in TBST (for all other antibodies) and incubated with 1:1,000 dilutions of anti-NGAL, anti-ATPSβ, anti-COX1 and anti-GAPDH overnight at 4 °C. After incubation for 2 h at room temperature with secondary antibodies (1:2,000) conjugated with horseradish peroxidase, membrane proteins were detected via chemiluminescence. Renal proteins were quantified and normalized with GAPDH. Urinary proteins were quantified and normalized to a standard sample and corrected to total urinary protein.

ATPS β immunoprecipitation

Immunoprecipitation was performed according to the method described by Abcam Inc. (Cambridge, MA). Briefly, mouse urine samples from the 15 min I/R (severe injury) group were homogenized in lysis buffer with protease inhibitor cocktail and then centrifuged to remove cell debris. Lysates were pre-cleared to reduce non-specific binding during the immunoprecipitation. Briefly, a non-ATPS β mouse IgG1 antibody (50 μ L) was added to urine lysates and incubated on ice for 1 h. Protein-A agarose bead slurry (100 μ L) was added and samples were incubated for 30 min at 4 °C with gentle agitation. Samples were centrifuged and the supernatant saved for immunoprecipitation. Protein concentration of the pre-cleared supernatant was determined by BCA as described above. A 500 μ g aliquot of pre-cleared protein was incubated with 10 μ g mouse monoclonal anti-ATPS β (Abcam Inc., Cambridge, MA) overnight at 4 °C with gentle agitation. Protein complexes were mixed with protein-A agarose bead slurry (70–100 μ l) on ice and incubated overnight at 4 °C under rotary agitation. After incubation, samples were centrifuged and the supernatant was collected and washed in lysis buffer three times via centrifugation at 4 °C. The final supernatant was removed and 25–50 μ l of 2x loading buffer was added. Samples were boiled at 95–100 °C for 5 min, centrifuged and the supernatant was separated by SDS-PAGE. The gel was stained with Coomassie blue and bands were excised for LC-MS/MS-based peptide identification as previously described [378].

Urinary ATPS β identification with LC-MS/MS

Frozen urine aliquots were thawed at 37 °C for 10 min and centrifuged for 10 min at 1,000 x g and 4 °C. Total urinary protein and creatinine values were measured. Sample volume used for trypsin digestion and subsequent proteomic analysis was calculated by normalizing total urinary protein to both urine volume and urine creatinine to eliminate biological variability. LC-

MS/MS analysis including ATPS β peptide identification and normalization of spectral counts with internal standard HIV gp160 protein for each sample was performed as previously described [375, 377].

Data and statistical analysis

Data are expressed as means \pm SEM for all experiments. Multiple comparisons of normally distributed data were performed by one-way ANOVA, as appropriate, and group means were compared using a Student-Newman-Keuls *post-hoc* test. Single comparisons were analyzed using the Student's *t*-test where appropriate. The criterion for statistical differences was $P < 0.05$ for all comparisons.

RESULTS

Urinary ATPS β correlates with the degree of renal injury following I/R-induced AKI in mice

Mice were subjected to sham or I/R surgery by bilateral renal pedicle ligation for 5, 10, or 15 min corresponding to mild, moderate, and severe injury, respectively. BUN and serum creatinine were increased only in mice with severe injury at 24 h after reperfusion (Figure 5.1A, 5.1B). Correlated with renal functional loss, mice in the severe injury group exhibited extensive proximal tubular necrosis throughout the corticomedullary region characterized by eosinophilic tubules with karyolytic nuclei (Figure 5.2). No histological renal damage was observed in mice after sham or mild I/R injury, whereas minimal proximal tubular vacuolization was observed in moderately injured mouse kidneys (Figure 5.2). Urinary NGAL, a renal tubular damage biomarker, was detected in severely injured mice only at 24 h (Figure 5.1C). Thus, this model demonstrates three distinct groups for evaluation with varying degrees of renal injury and functional loss.

Using these groups, we evaluated urinary ATPS β as a biomarker of renal mitochondrial dysfunction during I/R-induced AKI and correlated levels to the severity of renal dysfunction. We identified full length (~52 kDa) and cleaved fragments (~25 kDa) of urinary ATPS β protein via immunoblot (Figure 5.1D). Normalized to total urinary protein, full length ATPS β increased in mice after moderate and severe injury (Figure 5.1E). When normalized to total protein, expression of the cleaved fragment increased in mice only after severe injury (Figure 5.1F). The proposed full length and cleaved fragment of ATPS β were immunoprecipitated from urinary protein isolates (Figure 5.1G) and fragments were confirmed to be ATPS β by LC-MS/MS

analysis via identification of the peptide sequence VVDLLAPYAK, which is specific to the ATP5B N-terminal region.

Increases in urinary ATP5B are associated with renal mitochondrial protein loss and reduced mitochondrial function

We recently reported that renal mitochondrial disruption, including ATP5B loss, persists for at least 6 days after I/R-induced AKI [126, 148, 161, 218]. Confirming that renal cortical mitochondrial proteins decreased in conjunction with increased urinary ATP5B, we observed that renal COX1 decreased following moderate or severe injury, while ATP5B decreased in the severe injury group at 24 h (Fig. 2A-C). Thus, moderate or severe renal damage is associated with the loss of renal cortical COX1 and ATP5B and increased urinary ATP5B.

The loss of mitochondrial proteins has been reported to cause a reduction in mitochondrial function [148, 379]. Mitochondrial function was evaluated by assessment of basal and FCCP-uncoupled OCR in isolated proximal tubular segments. FCCP-uncoupled OCR, a mitochondrial stress test, was reduced 50% in mild, moderate and severe injury groups at 24 h compared to sham controls (Fig 3A). Basal respiration was not reduced in any group. To evaluate whether the observed decreases in OCR manifest as reduced renal energy content, renal cortical ATP levels were measured. ATP levels were reduced 30-40% following mild, moderate or severe I/R-induced AKI (Fig. 3B). These multiple mitochondrial markers demonstrate renal mitochondrial dysfunction in conjunction with increased urinary ATP5B.

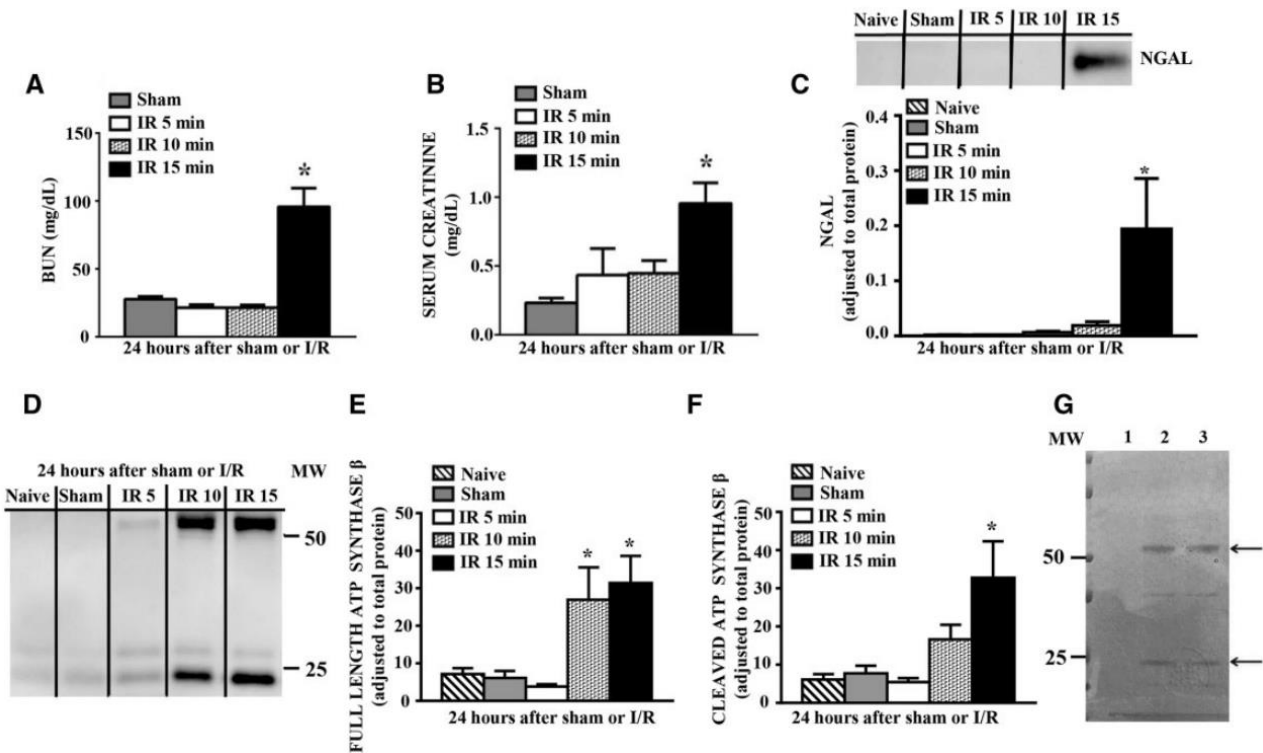


Figure 5.1: Urinary ATP synthase subunit β (ATPS β) is increased in mice following I/R-induced AKI. Male C57BL/6 mice (8–10 weeks old) were subjected to no surgery, sham, or renal I/R (5, 10, or 15 min) surgery. Mice were euthanized at 24 h after reperfusion, and blood, urine, and kidneys were collected. BUN (A), serum creatinine (B), and urinary neutrophil gelatinase lipocalin 2 (NGAL) (C) protein expression were measured as indicators of renal function and damage. Urinary ATPS β were measured via immunoblot (D). The ATPS β full length and cleaved fragments were quantified via densitometry (E, F) and normalized to a standard sample and total urinary protein. To validate the immunoblot results, ATPS β was immunoprecipitated from urinary isolates, purified via gel electrophoresis and analyzed by LC-MS/MS. A representative Coomassie gel for immunoprecipitated-urinary ATPS β with mouse monoclonal anti-mitochondrial ATPS β antibody is shown (G). Data are expressed as mean \pm SE ($n = 12$). *Difference from naïve and sham controls ($P < 0.05$).

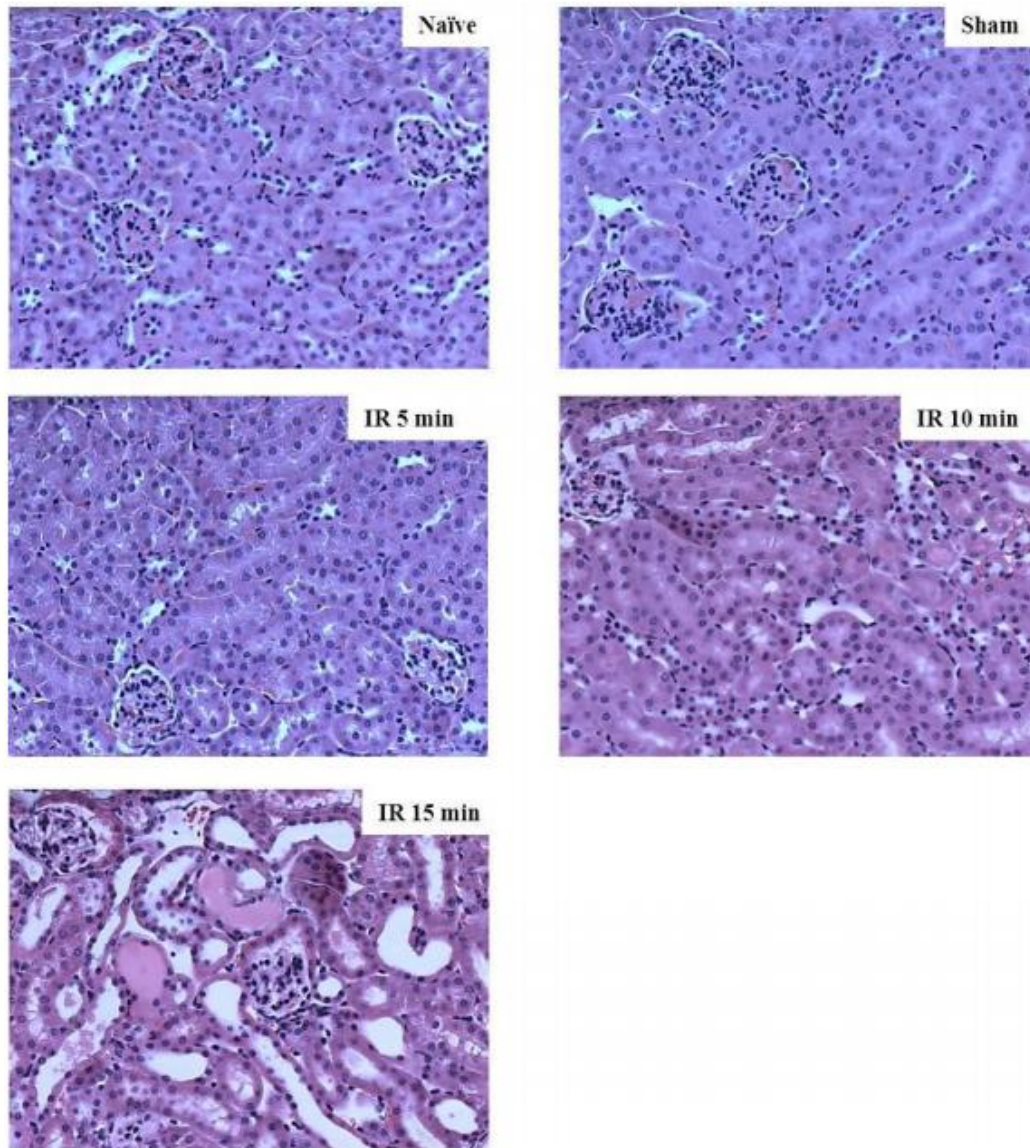


Figure 5.2: Representative renal histology from various ischemia times. Kidneys were collected from mice with no surgery, or 24 h after sham surgery or 5, 10 or 15 min of ischemia and fixed in formalin. Sections were stained with H&E for assessment of morphology. Images are representative of n=12.

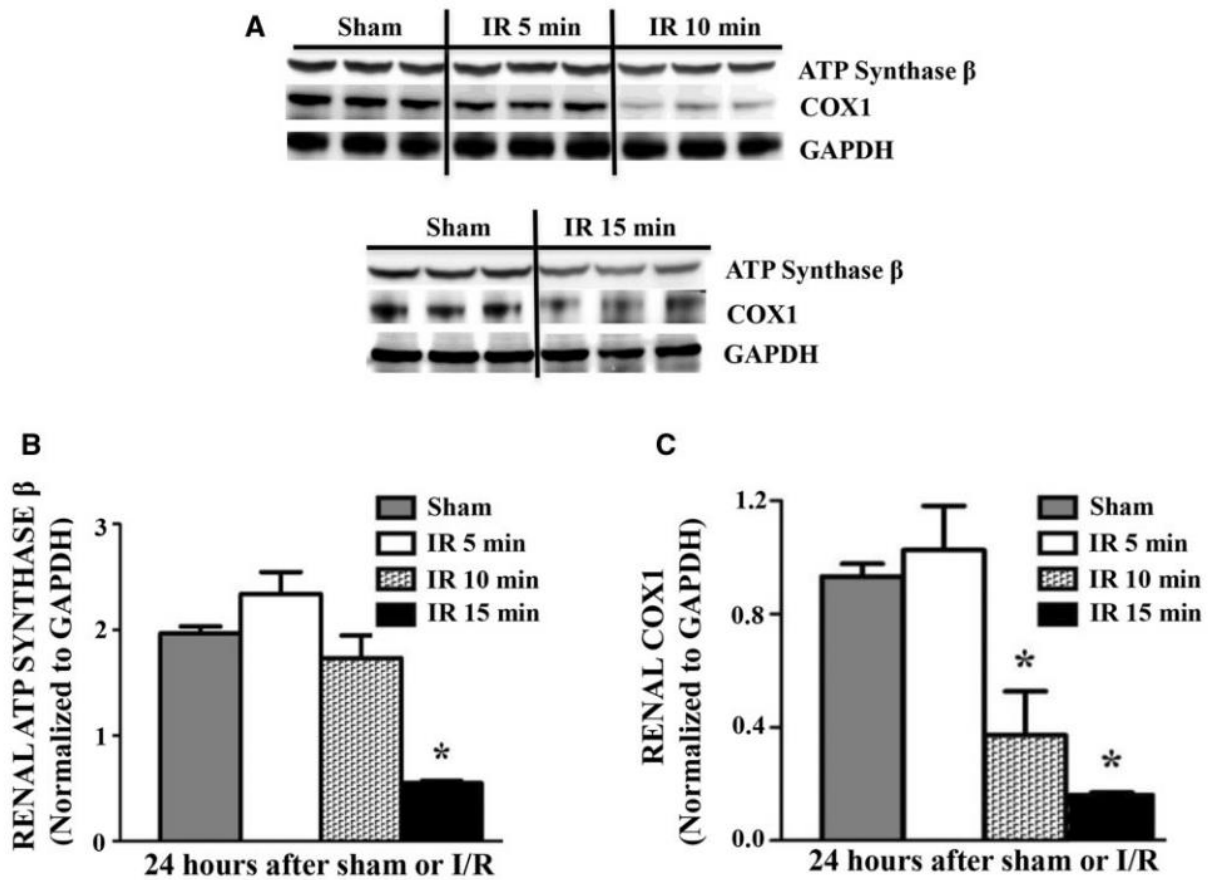


Figure 5.3: Renal cortical mitochondrial protein expression is reduced after I/R-induced AKI. Mouse renal cortical protein expression of ATP synthase subunit β (ATPS β) and COX1 (A) was measured by immunoblot and quantified via densitometry (B, C) at 24 h after sham surgery or ischemia. Expression was normalized to glyceraldehyde 3-phosphate dehydrogenase (GAPDH). Data are expressed as mean \pm SE ($n = 6$). *Difference from sham ($P < 0.05$).

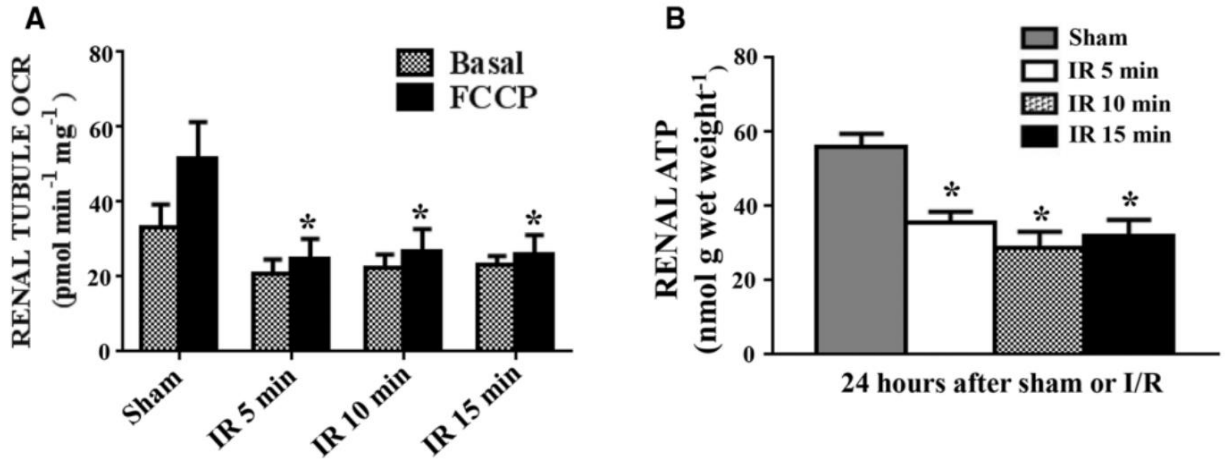


Figure 5.4: Mitochondrial function is reduced after mild, moderate, or severe I/R-induced AKI. Basal and FCCP-uncoupled oxygen consumption rate (OCR) was measured in freshly isolated mouse renal proximal tubules 24 h after sham surgery or 5, 10, or 15 min of ischemia followed by reperfusion (A). Rates were normalized to protein. ATP levels were determined and normalized to wet tissue weight (B). Data are expressed as mean \pm SE ($n = 6$). *Difference from sham ($P < 0.05$).

Urinary ATPS β levels are a marker of renal functional recovery after I/R-induced AKI

We then examined urinary ATPS β over time after AKI. Urinary full-length and cleaved ATPS β remained elevated 72 h after severe injury and returned to baseline at 144 h. (Fig. 5.5A-C). Renal function partially recovers 144 h after severe renal injury in this model [126, 148, 161, 218] and the return of ATPS β to baseline is consistent with this partial recovery of renal function.

Urinary full-length ATPS β is specific for renal mitochondrial dysfunction

ATPS β is a ubiquitously expressed component of the ETC; thus extra-renal sources of ATPS β in the urine cannot be excluded. To assess the specificity of urinary ATPS β for renal mitochondrial dysfunction, we evaluated its presence in the urine of mice with NASH. Mice exhibited liver damage and dysfunction evidenced by histological changes (*ie*, fat accumulation) and a rise of serum ALT (Figure 5.6A, 5.6B). No change in serum creatinine was observed suggesting that renal function was not disrupted (Figure 5.6C). Urinary immunoblot analysis detected the cleaved ATPS β fragment; however, no full-length protein was detected (Figure 5.6D). These data provide evidence that the full-length fragment may specifically arise from renal mitochondrial dysfunction, whereas the cleaved fragment may arise from renal or nonrenal tissues (*ie*, liver).

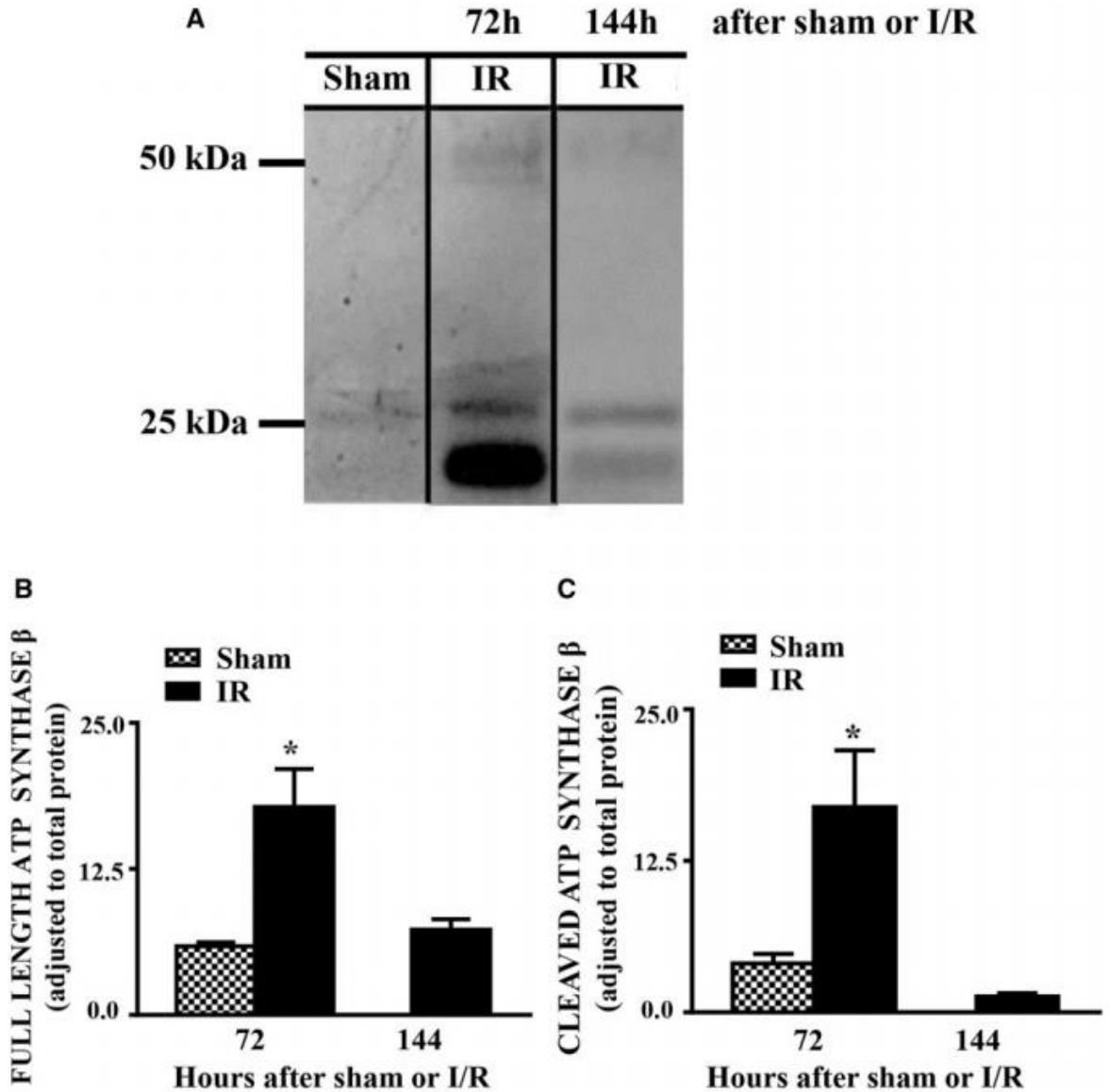


Figure 5.5: Urinary ATP synthase subunit β (ATPS β) expression time course in mice after I/R-induced AKI. Mice were subjected to sham surgery or bilateral renal pedicle ligation for 17 min. Urine was collected at 72 and 144 h after reperfusion. Urinary ATPS β protein expression was evaluated by immunoblot (A). The ATPS β full length and cleaved fragments were quantified via densitometry (B, C) and normalized to a standard sample and total urinary protein. Data are expressed as mean \pm SE ($n = 5-10$). *Difference from sham ($P < 0.05$).

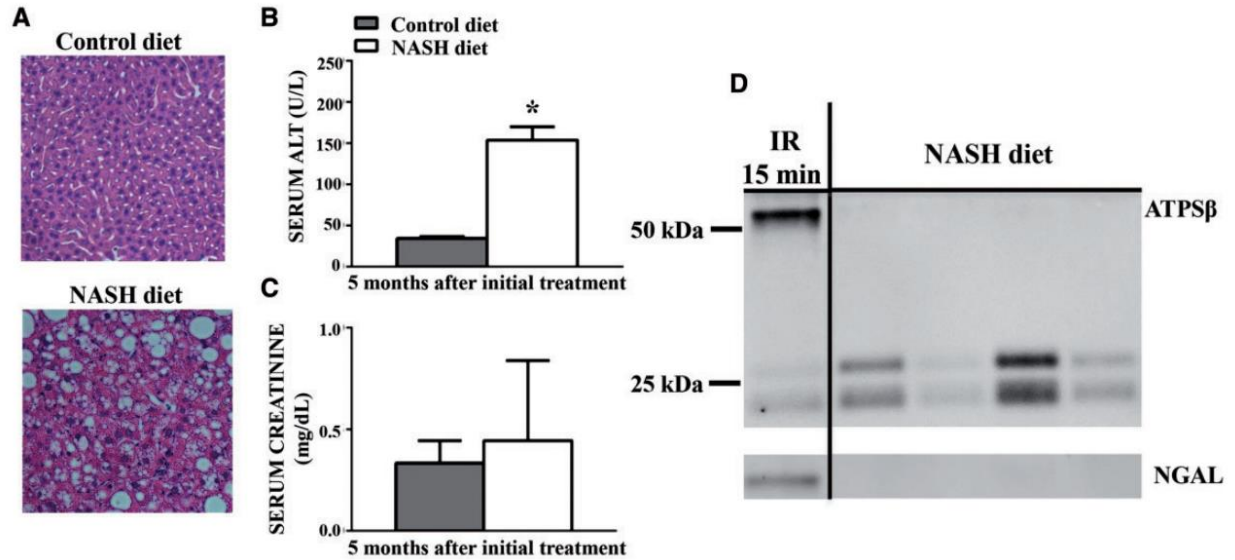


Figure 5.6: Cleaved urinary ATP synthase subunit β (ATPS β) but not full-length is elevated in a NASH model. C57BL/6 mice were fed a high fat/high cholesterol diet for 5 months to induce NASH. Controls were fed a normal chow diet. Liver damage was assessed histologically by hematoxylin and eosin (H&E) staining (A). Liver (B) and renal (C) function were assessed by serum ALT and creatinine, respectively. Data are expressed as mean \pm SE. Urinary ATPS β was measured via immunoblot analysis (D) ($N = 4$).

Urinary ATPS β levels are increased in human patients that developed postcardiac surgery AKI

To assess ATPS β as a renal mitochondrial dysfunction biomarker in humans, we analyzed urine collected from patients 36 h after cardiac surgery who either developed AKI or did not. Patient demographic and clinical parameters were collected (Table 5.1). Baseline and postsurgical renal function were evaluated by serum creatinine and patients who developed AKI showed a 2-fold increase in serum creatinine over baseline indicating severe injury (Figure 5.7D). We identified full length (~52 kDa) and cleaved fragments (~25 kDa) of urinary ATPS β protein in patients who developed AKI (Figure 5.7A). Normalization of full length and cleaved urinary ATPS β to total protein revealed increased full-length ATPS β in AKI patients (Figure 5.7B), but no changes were observed in cleaved ATPS β levels (Figure 5.7C). To validate immunoblot results, we conducted LC-MS/MS-analysis which confirmed increases in the same unique peptide (VVDLLAPYAK) identified in mouse urine isolates (Figure 5.7E).

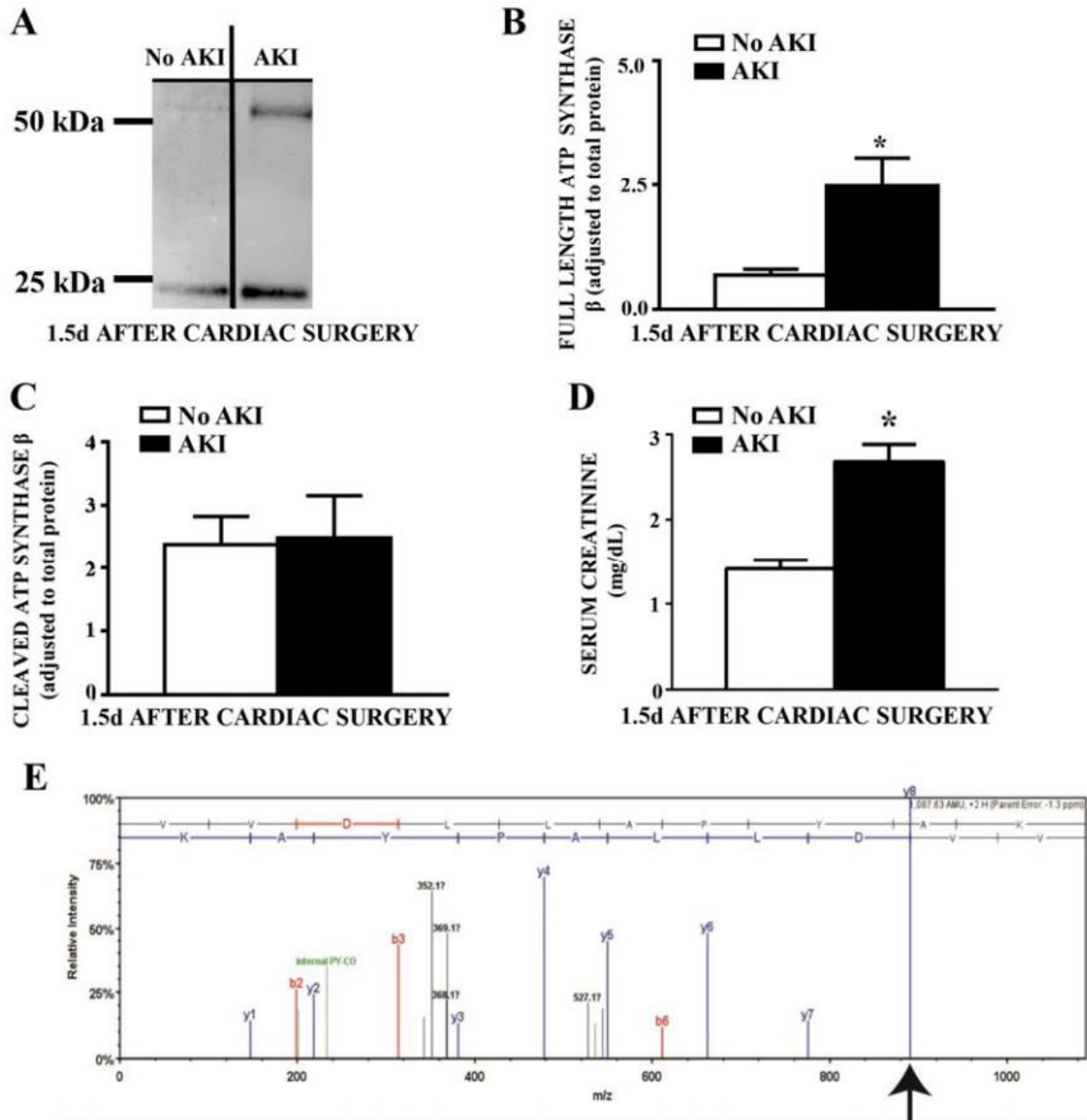


Figure 5.7: Urinary ATP synthase subunit β is elevated in human patients following cardiac surgery-induced AKI. ATPS β protein expression was measured via immunoblot in urine collected 36h after cardiac surgery in patient with either no AKI or AKI (A). The full length and cleaved fragments were quantified via densitometry (B, C) and normalized to total urinary protein. Renal function was assessed by serum creatinine (D). LC-MS/MS analysis from urine of AKI patients after cardiac surgery revealed a fragmentation pattern consistent with the tryptic peptide VVDLLAPYAK, unique for human ATPS β (E). Data are expressed as mean \pm SE (n = 16). * indicates different from no-AKI controls. (p<0.05).

DISCUSSION

Mitochondria have been characterized as central mediators of the pathophysiology of AKI resulting from a variety of insults including drug/toxicant exposure, ischemia-reperfusion injury and sepsis [152-154, 160, 163, 373]. Persistent disruption of mitochondrial dynamics, function and biogenesis has been well documented in animal models of renal injury [126, 148, 149, 161, 218, 275]. However, due to the limitations in the availability of renal tissue, little is known about the role of mitochondrial dysfunction in human AKI. Therefore, non-invasive biomarkers of renal mitochondrial dysfunction are needed to enhance our understanding of the role of mitochondria in the initiation and recovery from AKI. To this end, we examined urinary levels of ATP5B as a potential biomarker of renal mitochondrial dysfunction in a mouse model of I/R-induced AKI and in humans who developed AKI following cardiac surgery.

Mice underwent varying degrees of renal ischemia (5, 10 or 15 min) followed by reperfusion. These groups were characterized as representative of mild, moderate and severe renal injury by renal histology and by markers of renal function and damage including serum creatinine, BUN and renal NGAL expression (Fig. 1A-C; Suppl. 1). Immunoblot analysis demonstrated a full-length and cleaved form of ATP5B in the urine of mice following moderate or severe renal injury (Fig. 1D-F). The observed increase in urinary ATP5B after severe injury may arise from necrosis and epithelial cell sloughing into the tubular lumen due to profound renal injury consistent with observed increases in urinary NGAL [22, 27]. Interestingly, full-length urinary ATP5B was also elevated after moderate injury in the absence of increases in serum creatinine and urinary NGAL, indicating mitochondrial dysfunction prior to renal dysfunction (Fig. 1A-C; Suppl. 1). Thus, full-length urinary ATP5B increases with moderate and severe renal damage and this increase precedes elevations of other renal injury markers. In contrast, urinary cleaved ATP5B

increased only after severe injury. While immunoblot analysis is appropriate for biomarker discovery, use of this method for quantification of urinary proteins is neither as sensitive nor quantitative as ELISA, thus we are likely missing changes in urinary ATP5B.

At 52-56 kDa, ATP5B falls around the cutoff for glomerular filtration. Thus, ATP5B may be filtered, and extra-renal sources cannot be excluded. However, the potential that urinary ATP5B originates from an extra-renal source during AKI is low as levels are similarly elevated after moderate and severe injury despite significant differences in creatinine and NGAL levels between these groups (Fig. 1B). These results provide evidence that sub-lethal damage to mitochondria in the absence of necrotic cell death may result in the release of ATP5B; however, the exact mechanism of release is still unclear.

To validate renal specificity, we measured urinary ATP5B in a mouse model of NASH that exhibited liver injury without an increase in serum creatinine. We detected no full-length ATP5B in the urine from these mice; however, the cleaved fragment was detected (Fig. 5). These data support the idea that full-length ATP5B is a specific marker for renal mitochondrial damage, while the cleaved fragment may arise from renal and extra-renal sources. We hypothesize that the cleaved fragment is freely filtered due to its small size, while full-length ATP5B is not filtered as it is near the size exclusion limit for filtration, and it carries a significant negative charge at physiological pH. Our data from cardiac surgery patients also supports this hypothesis, as we observed both the cleaved fragment in AKI and no AKI samples, while only full-length ATP5B increased in AKI samples (Fig. 6). The cleaved fragment may be of renal or extra-renal origin in these patients (heart, liver, vasculature, etc.).

We have previously demonstrated a time dependent decrease in renal cortical mitochondrial protein expression following various forms of AKI in rodent models. In this study we observed a decrease in renal cortical expression of COX1 24 h after reperfusion in mice with moderate or severe renal injury, and ATP5B in mice with severe injury (Fig. 2). Furthermore, mitochondrial function was compromised 24 h after mild, moderate or severe I/R injury as assessed by isolated proximal tubule OCR and renal cortical ATP (Fig. 3). Reduction of renal mitochondrial function appears to precede the loss of renal mitochondrial proteins and elevations in urinary ATP5B in this model, although this may be due the sensitivity of immunoblot analysis. Overall, these results confirm renal mitochondrial dysfunction occurs with increased urinary ATP5B.

Evaluation of urinary ATP5B levels at 72 and 144 h after I/R in mice revealed a recovery of ATP5B levels to near control levels at 144 h after injury (Fig. 4). This recovery mirrors the partial recovery of renal function as measured by serum creatinine in this model indicating that urinary ATP5B may serve as a marker of renal functional recovery [148, 161]. Interestingly, the recovery of ATP5B precedes the recovery of renal cortical expression of mitochondrial proteins observed in this model. We postulate that this result may be due to either 1) the remaining mitochondria are functionally intact and are not shedding mitochondrial proteins, or 2) the severe reduction in mitochondrial number, evidenced by reduced renal cortical expression, creates an artificially low expression of shed mitochondrial proteins in the urine.

To examine the translational potential of urinary ATP5B, we measured levels in the urine of human patients 36 h after cardiac surgery (Fig. 6). Urinary excretion of ATP5B increased in patients that developed AKI following surgery as compared to those that did not. These human data suggest that increased urinary ATP5B in AKI patients predicts renal mitochondrial

dysfunction compared to subjects without AKI. Additional analyses are needed to correlate changes in ATPS β with other renal functional markers and patient outcomes. A large group of well-characterized samples in subjects with mild to moderate AKI, and AKI from other etiologies will enable us to elucidate confounding variables and enhance the predictive power of ATPS β in human AKI. However, as human renal cortical samples (e.g. biopsies) are not readily available it will be difficult to directly link urinary ATPS β with renal mitochondrial function.

These studies provide evidence that urinary ATPS β increases in mice subjected to I/R-induced AKI and that this increase correlates with renal mitochondrial dysfunction. Furthermore, urinary ATPS β has translational potential for detection of renal mitochondrial dysfunction in post-operative AKI in humans. There are no current reports of non-invasive biomarkers of renal mitochondrial dysfunction after AKI with the exception of urinary cytochrome c in drug-induced AKI [380]. However, use of cytochrome c is limited due to rapid, transient changes in tissue expression and poor renal specificity. Thus, our studies offer evidence that urinary full-length ATPS β may be the first sensitive and specific translational biomarker of renal mitochondrial dysfunction in AKI. However, additional validation is needed to ascertain its pre-clinical and clinical applicability. Characterization of ATPS β as a biomarker of renal mitochondrial disruption and the roles of miRNAs and proteolytic/autophagic pathways in the regulation of ATPS β and renal mitochondrial function in AKI will assist in the development of new therapeutic targets.

CHAPTER 6:

Urinary mitochondrial DNA is a biomarker of mitochondrial disruption and renal dysfunction in acute kidney injury

ABSTRACT

Recent studies demonstrate the importance of mitochondrial dysfunction in the initiation and progression of acute kidney injury (AKI); however, no biomarkers exist linking renal injury to mitochondrial function and integrity. To this end, we evaluated urinary mitochondrial DNA (UmtDNA) as a biomarker of renal injury and function in humans with AKI following cardiac surgery. mtDNA was isolated from urine of patients following cardiac surgery and quantified via qPCR. Patients were stratified into no AKI, stable AKI and progressive AKI groups based on Acute Kidney Injury Network (AKIN) staging. UmtDNA was elevated in progressive AKI patients, and was associated with progression of patients with AKI at collection to higher AKIN stages. To evaluate the relationship of UmtDNA to measures of renal mitochondrial integrity in AKI, mice were subjected to sham surgery or varying degrees of ischemia followed by 24 h reperfusion. UmtDNA increased in mice after 10-15 min ischemia and positively correlated with ischemia time. Furthermore, UmtDNA was predictive of AKI in the mouse model. Finally, UmtDNA levels were negatively correlated with renal cortical mtDNA and mitochondrial gene expression. These translational studies demonstrate that UmtDNA is associated with recovery from AKI following cardiac surgery by serving as an indicator of mitochondrial integrity. Therefore, UmtDNA may serve as valuable biomarker for the development of mitochondrial targeted therapies in AKI.

INTRODUCTION

Acute kidney injury (AKI) is a serious clinical problem, particularly among surgical and critically ill patients [6, 381]. Despite advances in diagnosis and patient management, incidence of AKI continues to increase and outcomes continue to be poor. An expanding array of risk factors for AKI and expanded use of nephrotoxic drugs have contributed to its increased incidence and prevalence. AKI is associated with high levels of short and long term mortality, and increases patient risk of progression to chronic kidney disease (CKD) and end stage renal disease (ESRD) [10, 382, 383]. Survivors of AKI, particularly those with ESRD requiring dialysis, are plagued by a variety of chronic sequelae contributing to decreased quality of life and increased utilization of healthcare resources.

Cardiac surgery requiring cardiopulmonary bypass (CPB) is a common cause of AKI in humans. Estimates of incidence of AKI in patients following cardiac surgery are as high as 30% [384, 385]. Furthermore, AKI is one of the most significant negative predictors of patient outcome in this population [386, 387]. Despite the high incidence and severity of CPB-induced AKI, methods for early detection following surgery remain poor. Additionally, there are no effective therapeutic strategies to prevent or promote recovery from AKI in these patients [1, 388, 389]. These facts highlight the need to better understand mechanisms of CPB-induced AKI and to develop novel diagnostic tools and therapies.

Renal injury following CPB is multifactorial and poorly understood; however, ischemia-reperfusion (I/R) injury is believed to play a significant role [390, 391]. Poor renal perfusion due to reduced cardiac output, increased systemic inflammation, hemodynamic alterations, volume depletion and perioperative administration of nephrotoxic drugs, contribute to I/R-induced renal injury following cardiac surgery [392, 393]. Mitochondrial damage and dysfunction is a key pathophysiological component of renal tubular injury during both the initiation and recovery

phases of ischemic AKI [154, 156]. Organ reperfusion following ischemia leads to rapid opening of the mitochondrial permeability transition pore (MPTP) causing mitochondrial membrane depolarization, increased production of reactive oxygen and nitrogen species, and release of apoptotic proteins. Oxidative damage of mitochondrial respiratory complexes and subsequent reduction in mitochondrial function contributes to tissue ATP depletion inhibiting energy-dependent cellular repair mechanisms [12]. Additionally, generation of new, functional mitochondria through the process of mitochondrial biogenesis (MB) is persistently suppressed following renal injury in mice [126, 148].

These reports highlight mitochondria as an intriguing diagnostic and therapeutic target for AKI in animals; however, correlative data in humans is limited due to limited availability of renal tissue for analysis. Current assays for mitochondrial function including tissue ATP and oxygen consumption measurements require invasive tissue biopsies [374]. Due to the profound role of mitochondria in tissue repair, biomarkers of mitochondrial dysfunction following CPB may serve as better prognostic measures of AKI progression and recovery compared to existing biomarkers, enabling modification of patient management and development of new mitochondrial-targeted therapies for AKI. To this end, we conducted proof of concept experiments that examine the efficacy of urinary mitochondrial DNA (UmtDNA) as a predictive biomarker of AKI development and progression in humans with CPB-induced AKI. Furthermore, we validated UmtDNA as a biomarker of renal mitochondrial integrity in a mouse model of renal I/R injury. Fragments of mtDNA, referred to as mtDNA damage associated molecular patterns (DAMPs), are released into circulation following injury [281, 394]. Released mtDNA can modulate oxidative and inflammatory injury at distant sites through activation of Toll-like receptor signaling [395]. While numerous studies have evaluated serum

and plasma levels of mtDNA as predictors of injury and disease progression, no reports exist of the evaluation of UmtDNA as a specific marker of renal damage/dysfunction.

EXPERIMENTAL PROCEDURES

Human urine samples

Human urine samples were obtained from a NIDDK-funded multicenter trial (DK080234) with the goal of identification of prognostic urine biomarkers of cardiac surgery-induced AKI. Patients were enrolled prior to undergoing cardiac surgery to determine baseline renal function. Urine was collected approximately 1 d following cardiac surgery (mean = 1.26, median = 1). Urine was collected from both patients who developed AKI and those that did not. Following collection, protease inhibitors were added to urine samples. Urine was centrifuged at 1,000 x g to remove intact cells and cellular debris, and supernatants were collected and kept frozen at -80°C until analysis. Urine supernatant was used rather than total urine as inclusion of the pellet would lead to the assessment of both soluble mtDNA and mtDNA contained in cells (including lymphocytes and damaged proximal tubular epithelial cells) that have been released into the urine.

Animals and treatment

Eight-week-old male C57BL/6 mice (20-25 g) were subjected to sham or I/R surgery by bilateral renal pedicle clamping for 5, 10 or 15 min. as described previously [148, 161]. Urine was collected for a period of 18 h from 6-24 h post-surgery. Mice were euthanized at 24 h after surgery, and blood and kidneys were collected for analysis. Renal function was evaluated by measurement of urine volume and BUN (Bioassay Systems, Hayward, CA). All procedures involving animals were performed in accordance with the NIH *Guide for the Care and Use of Laboratory Animals*.

Quantitative reverse transcription polymerase chain reaction

Total RNA was extracted from mouse renal cortex using TRIzol reagent (Life Technologies, Carlsbad, CA). cDNA was synthesized via reverse transcription (RT) using the

iScript Advanced cDNA synthesis kit (Bio-Rad, Hercules, Ca) with an input of 1 μ g RNA. Quantitative polymerase chain reaction (qPCR) analysis was performed using SsoAdvanced SYBR Green Supermix (Bio-Rad) at a concentration of 1x with primers at a concentration of 750 nM (Integrated DNA Technologies, Coralville, IA). mRNA expression was calculated using the $2^{-\Delta\Delta CT}$ method normalized to β -actin. Primer sequences for PGC-1 α , cytochrome c oxidase subunit 1 (COX1), and NADH dehydrogenase [ubiquinone] 1 β subcomplex subunit 8 (NDUFB8) were described previously [149, 150].

Renal mtDNA content

qPCR was used to determine the relative quantity of mtDNA in mouse renal cortical tissue samples. DNA was extracted using the DNeasy Blood and Tissue Kit (Qiagen, Valencia, CA). Total DNA (5 ng) was used for analysis. Mitochondrial-encoded NADH dehydrogenase 1 (ND1) was used to measure mitochondrial copy number and was normalized to nuclear-encoded β -actin. Primers used for ND1 and β -actin were described previously [396].

Isolation and quantification of urinary mtDNA

Human and mouse urine supernatants were concentrated using Amicon Ultracel-30k centrifugal filters (EMD Millipore, San Diego, CA). DNA was isolated and purified from the concentrate using a Viral RNA Mini Kit (Qiagen, Valencia, CA). Total DNA concentration was determined using the Quant-iT PicoGreen dsDNA reagent (Life Technologies, Carlsbad, CA). qPCR was used to determine UmtDNA content with a template input of 0.3-5 ng of total DNA. For human urine, absolute values of mtDNA and nDNA were determined by calculation from a standard curve of total DNA isolated from HK2 cells. Primer sequences for human ND1 and β -actin were as follows: ND1, sense 5'-ACACTAGCAGAGACCAACCG-3' and antisense 5'-

GAAGAATAGGGCGAAGGGGC-3'; and β -actin, sense 5'-TAAAGCGGCCTTGGAGTGTG-3' and antisense 5'-GAACACGGCTAAGTGTGCTG-3'. For mouse urine, absolute ND1 levels were determined by calculation from a standard curve of total DNA isolated from mouse kidney ranging from 0.1-10 ng. Primer sequences for mouse ND1 were: sense 5'-TCCGAGCATCTTATCCACGC-3' and antisense 5'-GTATGGTGGTAACTCCCGCTG-3'. Mouse UmtDNA levels were corrected for urine creatinine (Bioassay Systems, Hayward, CA).

Data and statistical analysis

Data are expressed as means \pm SEM for parametric data, or median \pm IQR for non-parametric data. Multiple comparisons of normally distributed data were analyzed by one-way ANOVA and group means were compared using a Newman-Keuls *post-hoc* test. Non-parametric data were analyzed using a Kruskal-Wallis test followed by a Dunn's test for multiple comparisons. Single comparisons were analyzed via a Mann-Whitney U-test where appropriate. Receiver operator characteristic (ROC) curve analysis was used to test the predictive ability of UmtDNA for AKI development and progression in mice and humans. Optimal cutoffs were by minimizing the geometric distance from the point representing 100% sensitivity and 100% specificity. Linear regression analyses were performed on multiple variables and correlations were determined by calculation of Spearman Rank order coefficients. The criterion for statistical differences was $p < 0.05$ for all comparisons.

RESULTS

UmtDNA is associated with AKI progression following cardiac surgery

To assess UmtDNA as a biomarker of renal dysfunction in humans, UmtDNA levels were measured by qPCR in urine collected as a component of an NIDDK-funded multicenter trial (NIH #DK080234) to determine prognostic biomarkers of AKI following cardiac surgery [375]. Samples were collected through the Southern Acute Kidney Injury Network (SAKInet) consortium. The patient cohort included both patients who developed AKI and those who did not develop AKI following surgery. Patients were enrolled before surgery for baseline measurements and urine was collected approximately 1 d following surgery (mean collection time = 1.26 d, median collection time = 1 d). Table 6.1 shows the demographic and clinical characteristics of the subjects. Renal function was evaluated at collection and during follow-up by serum creatinine, and patients were staged using the Acute Kidney Injury Network (AKIN) criteria. The urine mtDNA/nDNA ratio was not elevated in patients with AKI (AKIN 1 at the time of collection) (median=147, IQR 102-610) vs. no AKI (AKIN 0) (median=202, IQR 59-604), and no differences were observed in UmtDNA levels between healthy or any AKIN stage patients based on either AKIN at collection or maximum AKIN stage achieved (Figure 6.1).

AKI Status

<i>Patient demographics</i>	No AKI	Stable AKI	Progressive AKI	P-value
Total patients	17	59	31	
Female	3 (18 %)	13 (22 %)	15 (48 %)	0.02
Black	3 (18 %)	16 (27 %)	6 (19 %)	0.59
Age (years)	65 ± 16	66 ± 11	68 ± 12	0.66
Weight (kg)	81 ± 28	93 ± 20	85 ± 28	0.11
<i>History</i>				
CHF	6 (36 %)	14 (24 %)	11 (35 %)	0.42
Prev. cardiac surgery	2 (12 %)	9 (15 %)	10 (32 %)	0.10
Diabetes mellitus	8 (47 %)	20 (34 %)	14 (45 %)	0.45
COPD	2 (12 %)	3 (5 %)	4 (13 %)	0.39
Peripheral vascular disease	0 (0 %)	6 (10 %)	1 (3 %)	0.22
Stroke	0 (0 %)	4 (7 %)	2 (6 %)	0.55
<i>Surgical parameters</i>				
CABG	16 (94 %)	42 (71 %)	23 (74 %)	0.15
Valve replacement	4 (24 %)	22 (37 %)	15 (48 %)	0.23
Bypass	14 (82 %)	46 (78 %)	27 (87 %)	0.57
Bypass Time	117 ± 49	139 ± 65	150 ± 90	0.31
<i>Outcomes</i>				
Baseline creatinine	1.3 ± 0.4	1.2 ± 0.3	1.3 ± 0.5	0.41
Collection creatinine	1.4 ± 0.4	2.0 ± 0.7	1.8 ± 0.8	0.0083
Max creatinine	1.4 ± 0.4	2.1 ± 0.8	2.9 ± 1.5	<0.0001
RRT	1 (6 %)	1 (2 %)	5 (16 %)	0.031
Mortality	1 (6 %)	1 (2 %)	7 (23 %)	0.0029
Days to discharge	6.8 ± 2.6	9.3 ± 8.6	15.1 ± 11.4	0.0031
Days to max creatinine	5.6 ± 4.5	2.3 ± 1.7	4.1 ± 2.6	<0.0001

Table 6.1: Patient demographics and clinical characteristics of cardiac surgery patients. No AKI (AKIN 0 throughout follow-up), Stable AKI (\geq AKIN 1 at collection, collection AKIN = maximum AKIN), Progressive AKI (\geq AKIN 1 at collection, maximum AKIN > collection AKIN). CHF, congestive heart failure; COPD, chronic obstructive pulmonary disease; CABG, coronary artery bypass graft; RRT, renal replacement therapy. P-values were determined using the Chi-Square test or ANOVA, as appropriate.

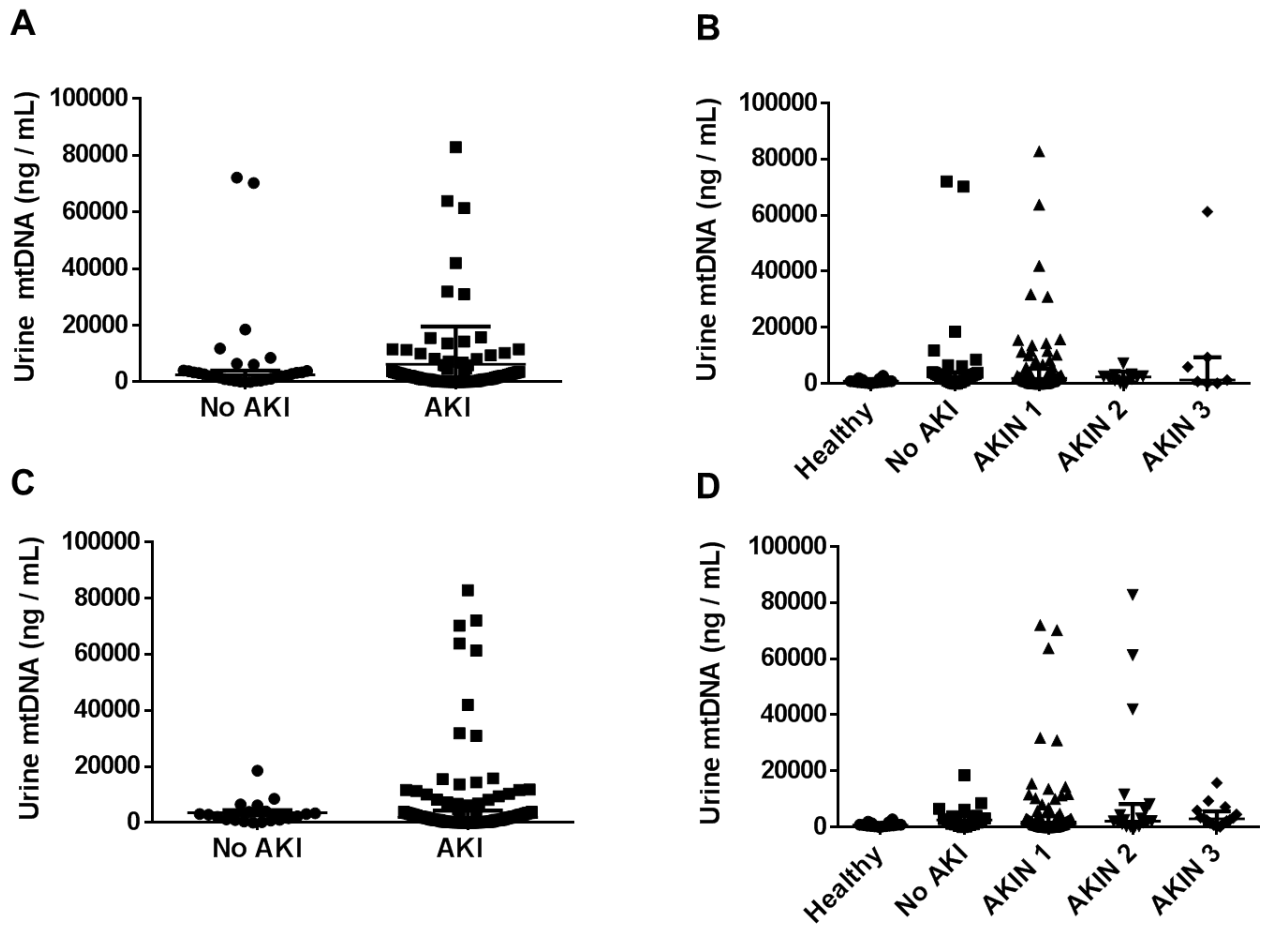


Figure 6.1: Urinary mtDNA copy number is not correlated with AKIN stage following CPB-induced AKI in humans. Patients were stratified into no AKI or AKI (AKIN 1+) groups by AKIN stage at collection (A) or maximum AKIN stage (B). Patients were further stratified into healthy, no AKI (AKIN 0), or AKIN stage 1, 2 or 3 by collection AKIN stage (C) or maximum AKIN stage (D). Data are expressed as median +/- IQR. Single comparisons were performed via Mann-Whitney U-test. Multiple comparisons were performed using a Kruskal-Wallis test followed by Dunn's test.

To assess the efficacy of UmtDNA in predicting worsening of AKI, patients were classified into 3 groups based on disease progression: no AKI (AKIN 0 throughout follow-up), stable AKI (\geq AKIN 1 at collection, maximum AKIN $>$ collection AKIN), or progressive AKI (\geq AKIN 1 at collection, maximum AKIN $>$ collection AKIN). Patients with AKIN 0 at collection that subsequently developed AKI were excluded from the progressive AKI group, although no patients displaying this behavior were observed in the cohort. UmtDNA was elevated in patients with progressive AKI (median = 353, IQR 187 - 1053) vs. no AKI (median = 118, IQR 26 - 517), or stable AKI (median = 104, IQR 50 - 340) (Figure 6.2A).

ROC curve analysis was performed to assess UmtDNA as a predictive test for AKI progression. There was no difference between no AKI and stable AKI patients (AUC=0.53, $p=0.73$) (Figure 6.2B). Elevated UmtDNA was a fair predictor of progressive AKI compared to no AKI (AUC=0.72, $p=0.012$) (Figure 6.2C) and stable AKI patients (AUC=0.72, $p=0.0008$) (Figure 6.2D). Evaluation of the primary endpoint of AKI progression in patients with established AKI at collection (stable vs. progressive AKI) revealed an optimal cutoff at 207 at which the test had a sensitivity and specificity of 71% and 71%, respectively. A cutoff of 899 yielded the highest positive likelihood ratio ($LR^+ = 3.0$). Seventeen of eighty-nine AKI patients had urinary mtDNA/nDNA ratios greater than 899, of which eight met the outcome of progressive AKI. The sensitivity and specificity of the test using this cutoff was 36% and 88%, respectively. The lowest negative likelihood ratio was achieved at a cutoff of 52 ($LR^- = 0.08$). Sixteen patients had urinary mtDNA/nDNA ratios less than 52, of which fifteen did not meet the outcome of progressive AKI. Using this cutoff, the test had a sensitivity and specificity of 97% and 41%, respectively.

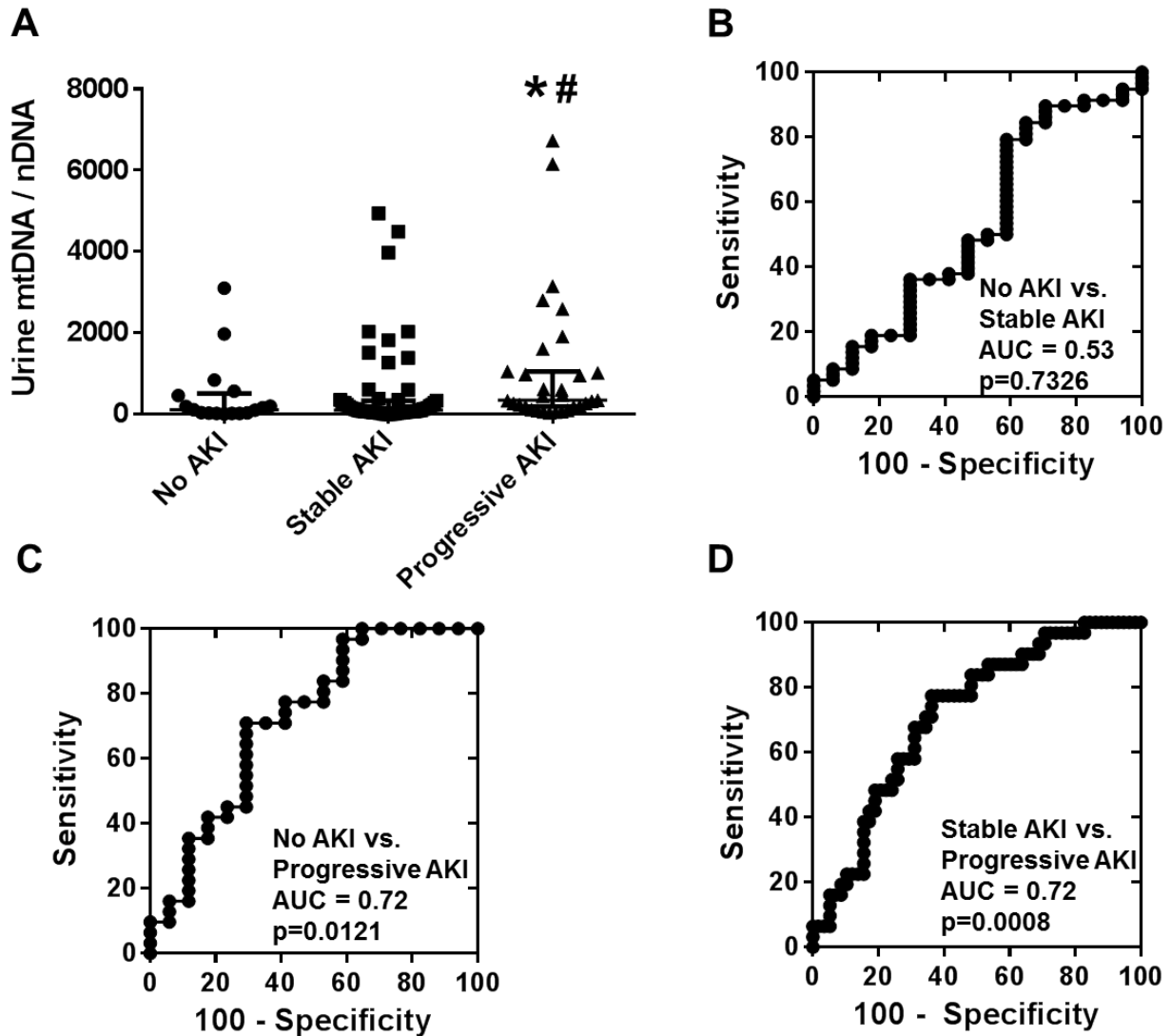


Figure 6.2: Urinary mtDNA copy number is associated with progression of renal dysfunction from collection in patients with CPB-induced AKI. Urine was collected from patients following CBP. Urinary mtDNA levels were measured via real time qPCR for ND1, and corrected to the nuclear control gene β -actin. Patients were stratified into 3 groups based on collection and maximum AKIN staging: no AKI (n=17), stable AKI (n=63) and progressive AKI (n=31) (A). Data are expressed as median +/- IQR. Multiple comparisons were performed using a Kruskal-Wallis test followed by Dunn's test. *p<0.05 vs. No AKI, #p<0.05 vs. stable AKI. AUROC analysis was performed comparing the 3 groups of patients (B-D).

UmtDNA does not correlate with existing markers of renal damage and dysfunction following cardiac surgery

To evaluate the performance of UmtDNA as an indicator of renal function, we compared UmtDNA with serum creatinine in the cohort. Correlation analysis of UmtDNA revealed no correlation with maximum serum creatinine (Figure 6.3A) ($r=0.0733$, $p=0.4533$), or maximum % change in serum creatinine from baseline (Figure 6.3B) ($r=-0.0013$, $r=0.9894$). Due to the limited sensitivity of serum creatinine as a marker of renal injury, we compared UmtDNA levels to levels of urinary angiotensinogen, a marker demonstrated to perform as well as urinary KIM-1 and NGAL as an indicator of renal damage and progression [375, 397]. UmtDNA was not correlated with urinary angiotensinogen levels following CPB (Figure 6.3C) ($r=0.0681$, $p=0.4877$). Furthermore, UmtDNA did not correlate with bypass time (Figure 6.3D) ($r=0.0370$, $p=0.7053$), days to maximum creatinine (Figure 6.3E) ($r=0.0190$, $p=0.8467$), or days to discharge (Figure 6.3F) ($r=0.0760$, $p=0.4546$).

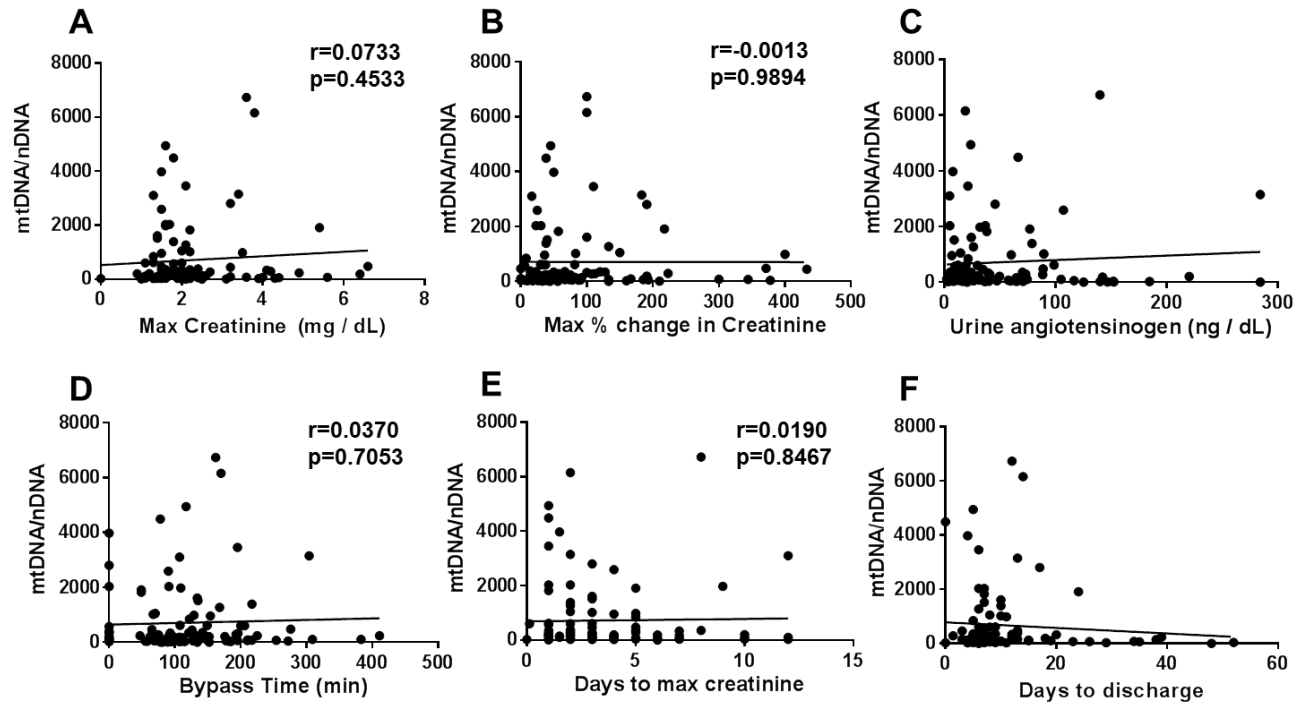


Figure 6.3: Urinary mtDNA copy number is not correlated with degree of CPB-induced AKI in humans. Urinary mtDNA/nDNA was not correlated with maximum serum creatinine (A), maximum % change in serum creatinine from baseline (B), urinary angiotensinogen levels (C), cardiopulmonary bypass time (D), days to maximum creatinine (E) and days to discharge (F) (n=111 for all analyses). Linear regression was performed and Spearman's Rank order coefficients were calculated.

UmtDNA is elevated in mice after I/R-induced AKI and correlates with ischemia time

To explore the biological correlates of UmtDNA in the kidney, we used a mouse model of renal I/R injury. Mice were subjected to sham surgery (n=12) or bilateral renal pedicle ligation for 5 (n=4), 10 (n=9) or 15 min (n=11) corresponding to mild, moderate and severe renal histological damage [398]. Mice that produced no or insufficient urine for detection of UmtDNA (n=6) were excluded from further analyses. BUN was elevated at 24 h only in the 15 min I/R group, and no difference was observed in urine output between all groups (Figure 6.4A, 6.4B). Total output of UmtDNA over the course of an 18 h collection period increased in the 10 or 15 min I/R groups (Figure 6.4C). UmtDNA was not normalized to nDNA due to undetectable levels of urinary β -actin in mice. Normalization of UmtDNA to urine creatinine demonstrated an increase vs. sham only in the 10 min I/R group (Figure 6.4D). UmtDNA correlated with time of ischemia ($r=0.63$, $p<0.0001$); however it did not correlate with renal function assessed by BUN (Figure 6.5A, 6.5B) ($r=0.17$, $p=0.33$). Correction of UmtDNA levels for urine creatinine did not alter/improve these correlations (Figure 6.6 A, 6.6B).

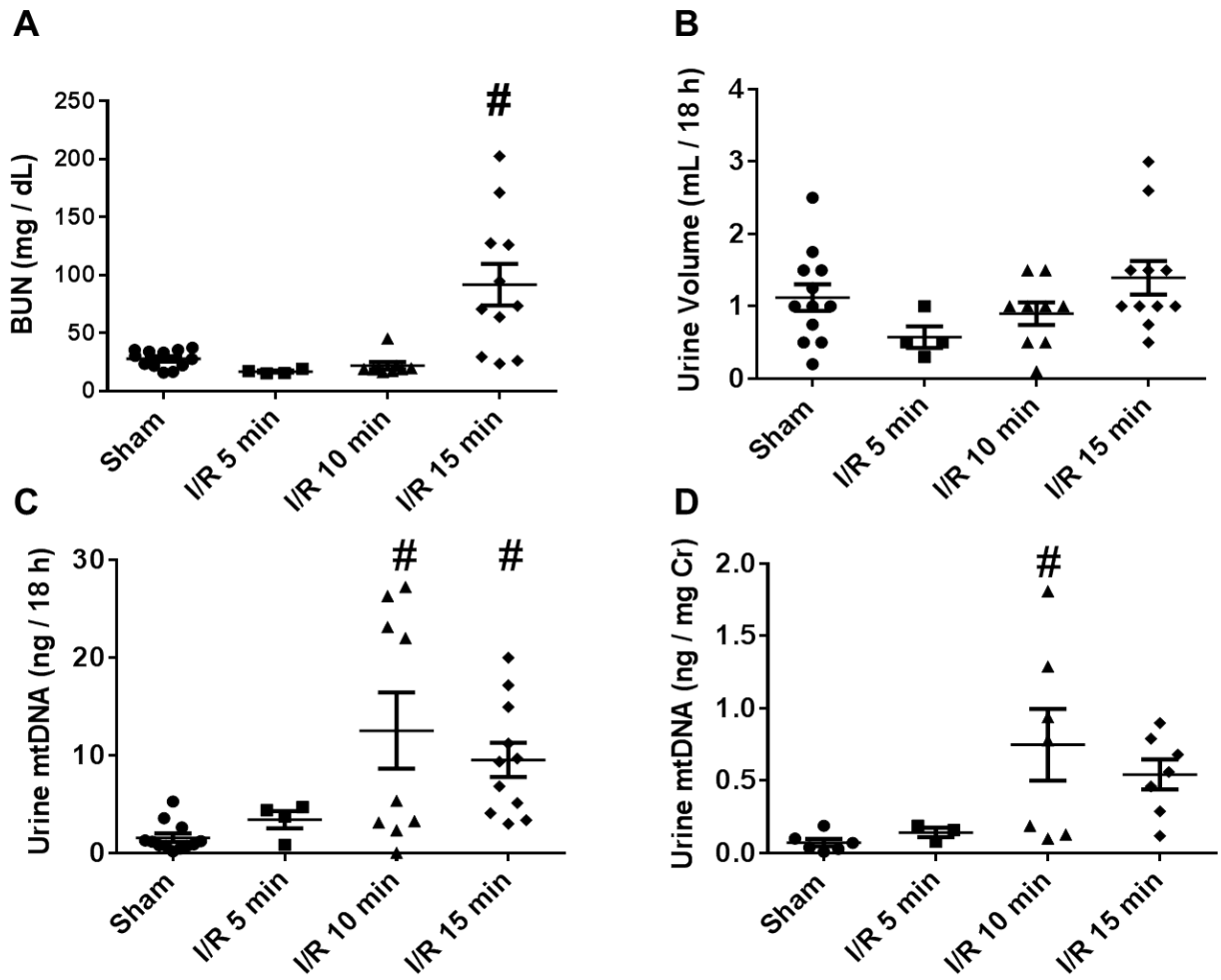


Figure 6.4: Urinary mtDNA levels are increased in mice following renal I/R. Male C57BL/6 mice underwent sham surgery or ischemia (5, 10 or 15 min) followed by reperfusion. Mice were placed in metabolic cages from 6-24 h after reperfusion for urine collection. Blood was collected and mice were euthanized 24 h after reperfusion. Renal function was evaluated by BUN (A) and 18 h urine output (B). Urinary mtDNA levels were measured by qPCR for ND1 and are expressed as total urinary output in 18 h (C) and urinary output corrected for urinary creatinine levels (D). Data are expressed as mean \pm SEM. # indicates statistical significance at $p < 0.05$; sham (n=12), 5 min I/R (n=4), 10 min I/R (n=9), 15 min I/R (n=11).

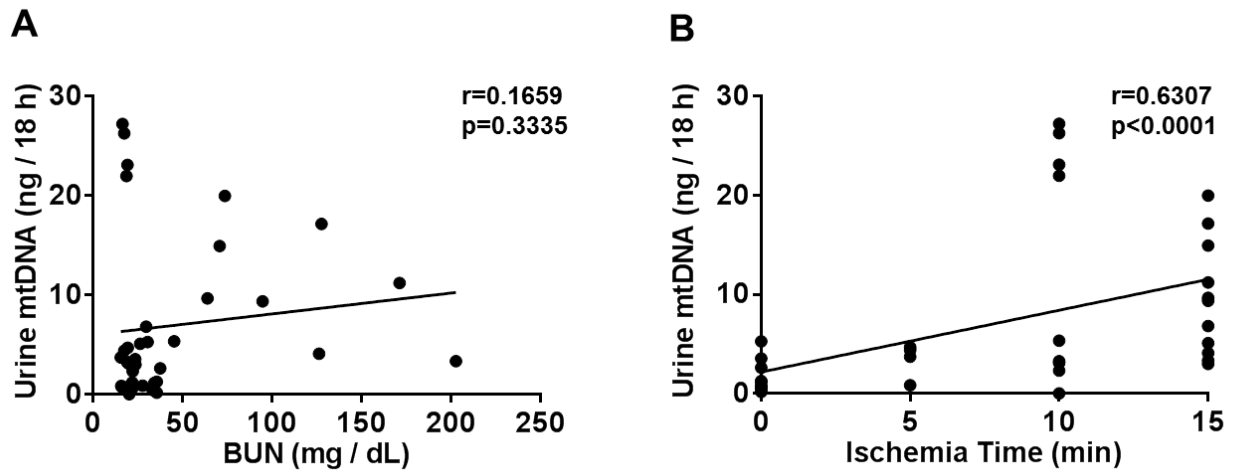


Figure 6.5: Total urinary output of mtDNA is correlated with degree of ischemia, but not BUN. Urinary mtDNA levels expressed as total urinary output per 18 h were correlated with BUN levels (A) or ischemia time (B) (n=36). Linear regression was performed and Spearman's Rank order coefficients were calculated.

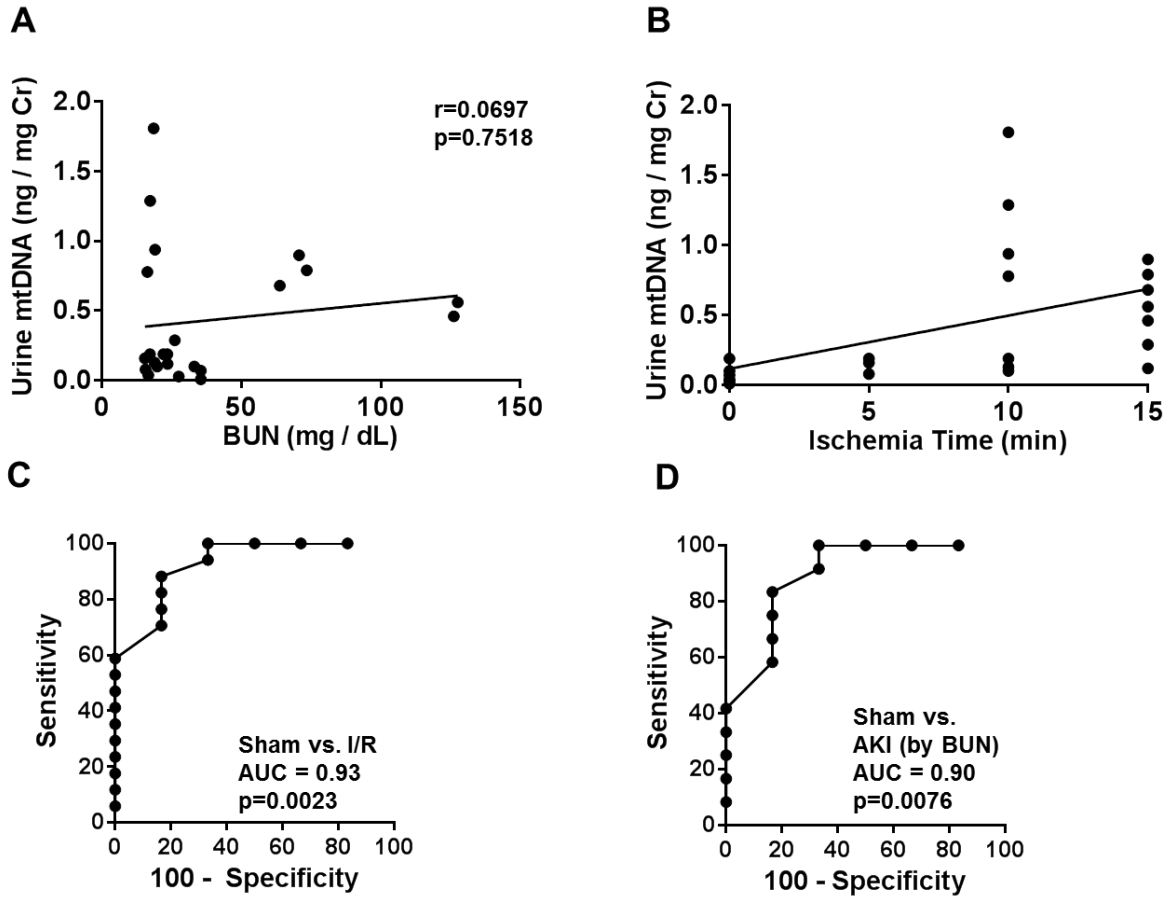


Figure 6.6: Urinary mtDNA levels corrected for urinary creatinine are a marker of renal injury in mice. Urinary mtDNA levels expressed as total urinary output corrected for urinary creatinine were not correlated with BUN (A) but were correlated with ischemia time (B) (n=36). Linear regression was performed and Spearman’s Rank order coefficients were calculated. ROC curves were constructed for urinary output of mtDNA corrected for urinary creatinine comparing sham mice (n=12) to all mice that had underwent I/R (n=24) (C) or mice reaching a cutoff value >2 SD above the historical sham average BUN (n=13) (D).

UmtDNA is predictive of AKI development in mice after I/R

ROC curve analysis was performed to assess the ability of UmtDNA to predict AKI development in mice following renal I/R. UmtDNA was predictive of AKI development in mice undergoing any degree of ischemia vs. sham control mice (AUC=0.88, p=0.0003) (Figure 6.7A). An optimal cutoff of 2.8 ng mtDNA/18 h yielded a sensitivity and specificity of 88% and 83%, respectively.

Several non-responders (no increase in BUN) were observed in the renal I/R group; therefore, mice were reclassified into no AKI and AKI groups based on an increase of >2 SD above our historical sham surgical BUN level (mean +/- SD = 24.0 +/- 9.7 mg/dL, BUN cutoff \geq 43.4 mg/dL). Mice with BUN levels below this cutoff were excluded from this analysis. ROC curve analysis demonstrated predictive power for AKI vs. no AKI using UmtDNA in mice after renal I/R (AUC=0.80, p=0.011) (Figure 6.7B). The optimal cutoff for this analysis was also determined to be 2.8 ng/18 h with a sensitivity and specificity of 77% and 83%, respectively. No differences were observed when analyses were performed corrected for urine creatinine (Figure 6.6C, 6.6D).

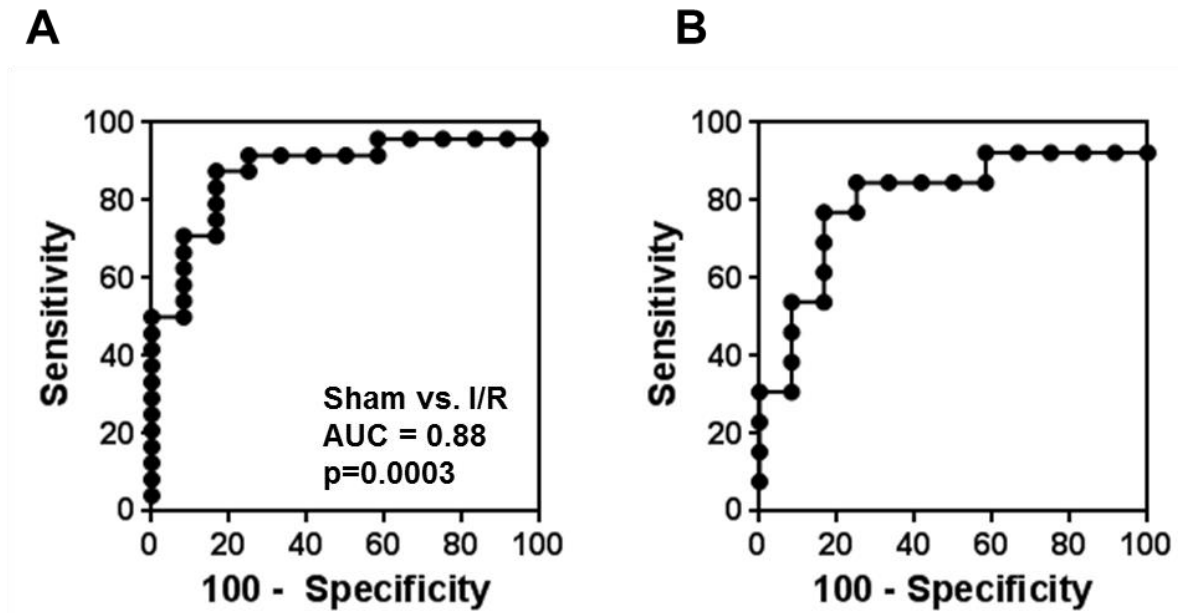


Figure 6.7: Total 18 h urinary output of mtDNA is a biomarker of renal injury following I/R in mice. ROC curves were constructed for total 18 h urinary output of mtDNA comparing sham surgical mice (n=12) to all mice that underwent I/R (n=24) (A) or only mice with BUN >2 SD above the historical sham average BUN (≥ 43.4 mg/dL) (n=13) (B).

Renal mitochondrial gene expression and mtDNA copy number are negatively correlated with UmtDNA levels

Renal cortical mtDNA copy number and mRNA expression of PGC-1 α , COX1 and NDUFB8 were assessed via qPCR and correlated to 18 h urinary output of mtDNA. Renal cortical mtDNA copy number decreased following I/R, and was negatively correlated with UmtDNA output ($r=-0.45$, $p=0.039$) (Figure 6.8A). Additionally, mRNA expression of PGC-1 α , COX1 and NDUFB8 decreased after I/R and their expression was also negatively correlated with UmtDNA output (PGC-1 α : $r=-0.48$, $p=0.034$; COX1: $r=-0.45$, $p=0.046$; NDUFB8: $r=-0.66$, $p=0.0015$) (Figure 6.8B-D). Analysis performed using UmtDNA corrected for urine creatinine produced modest improvements in these correlations (Figure 6.9).

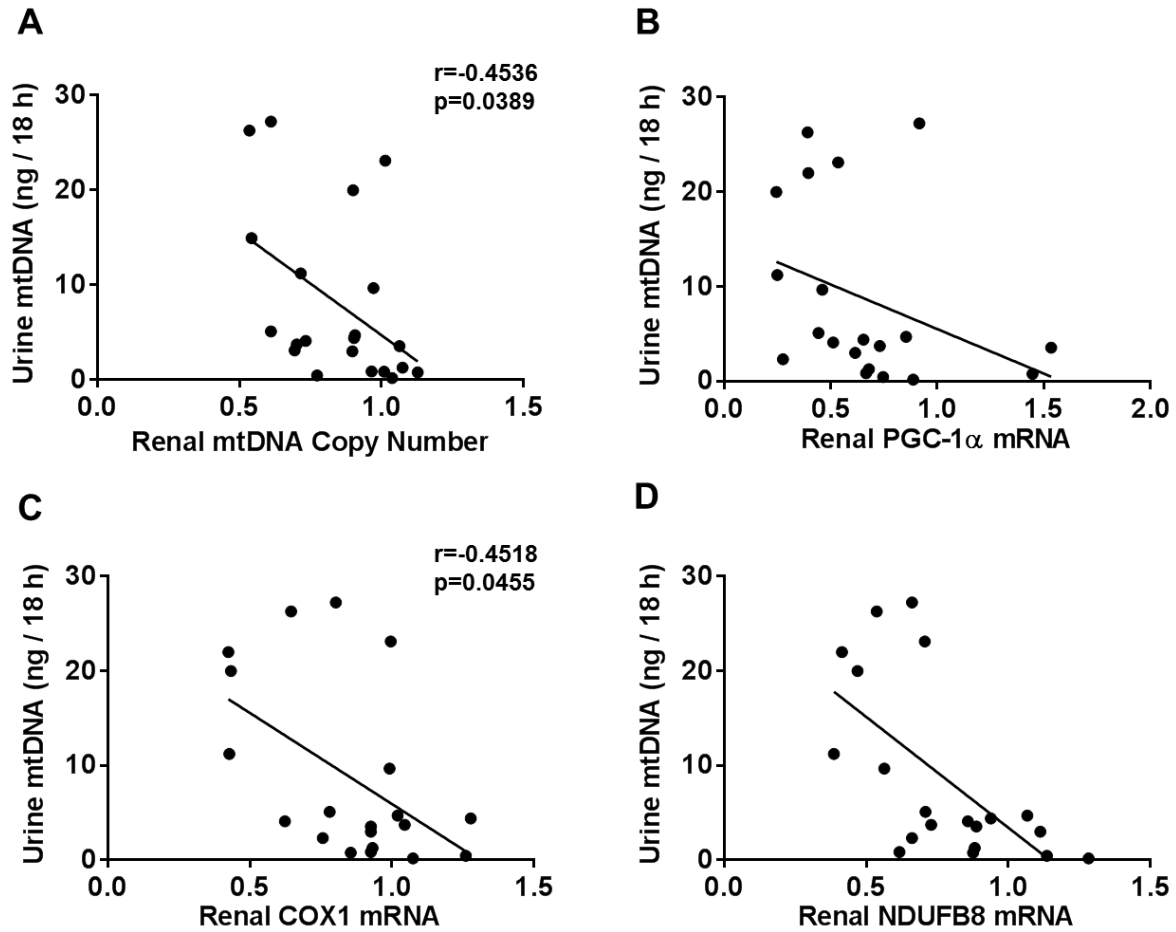


Figure 6.8: Total 18 h urinary output of mtDNA correlates with reductions in renal mtDNA copy number and mitochondrial gene expression. Urinary mtDNA levels expressed as total urinary output per 18 h were correlated with relative renal mtDNA copy number (A), PGC-1 α (B), COX1 (C) and NDUFB8 (n=36). Renal mtDNA and mRNA expression were corrected to the nuclear gene β -actin. Linear regression was performed and Spearman's Rank order coefficients were calculated.

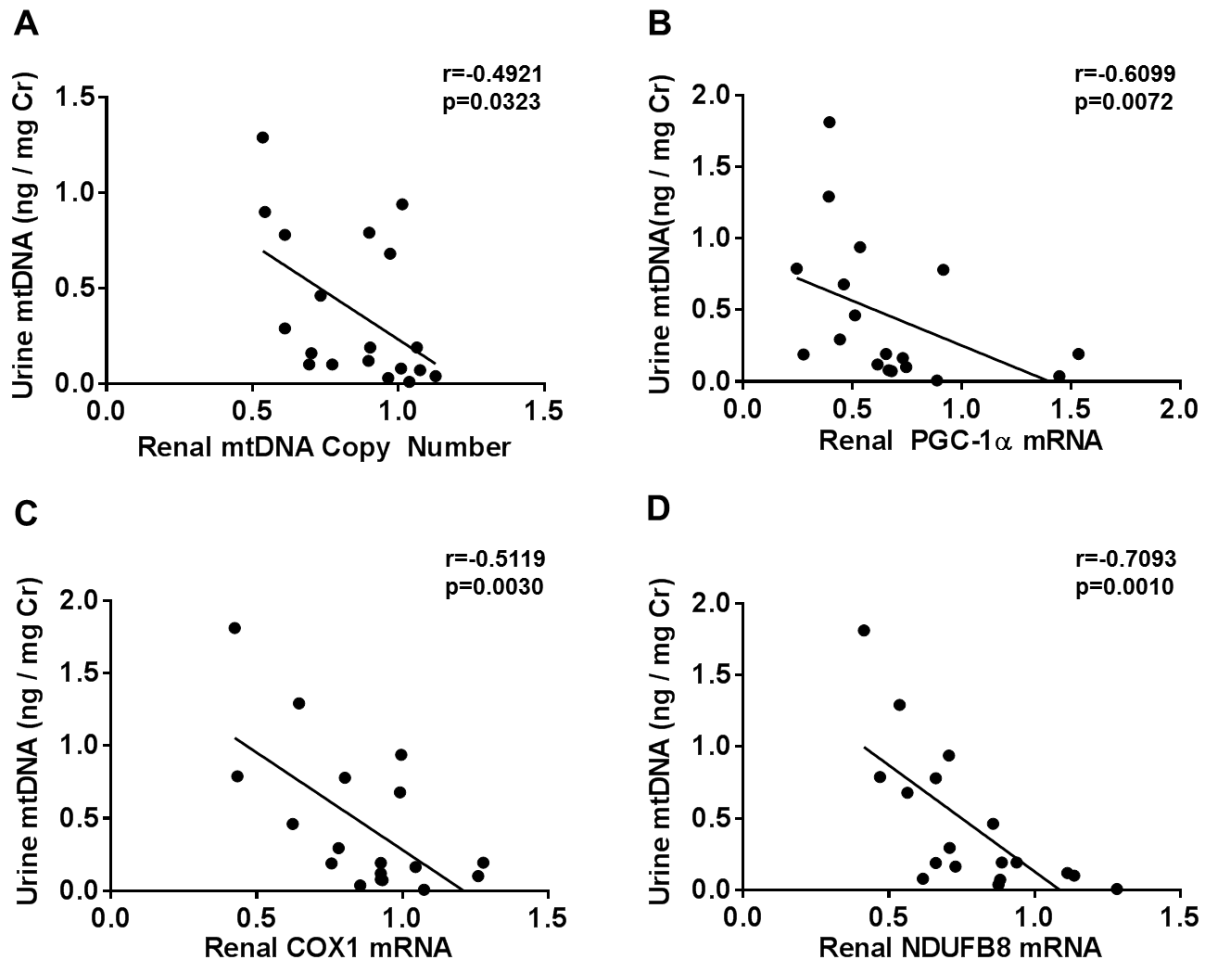


Figure 6.9: Urinary mtDNA levels corrected for urine creatinine correlate with a reduction of renal mitochondrial DNA copy number and mitochondrial gene expression in mice.

Urinary mtDNA levels expressed as total urinary output corrected for urinary creatinine were correlated with relative renal mtDNA copy number (A), PGC-1 α (B), COX1 (C) and NDUF8 (D) (n=36). Renal mtDNA and mRNA expression were corrected to the nuclear gene β -actin. Linear regression was performed and Spearman's Rank order coefficients were calculated.

DISCUSSION

Complete recovery from renal injury is dependent on a rapid and sustained activation of critical tissue repair processes, particularly of the renal proximal tubule [12, 399, 400]. Following injury, a coordinated tissue repair response is activated promoting recovery of sub-lethally injured cells, clearance of necrotic cells and debris, and re-establishment of an intact, polarized and functional renal epithelium. Repair of the renal tubular epithelium is highly energy dependent, thus mitochondrial function is crucial to the structural and functional recovery of the kidney. Due to the significant role of mitochondria in renal repair and recovery, biomarkers of renal mitochondrial function and integrity may be valuable prognostic tools of AKI progression. While the role of mitochondrial dysfunction in AKI in animals is clearly established, practical limitations of existing assays of mitochondrial function involving renal biopsy have limited our ability to study the link between mitochondrial dysfunction and renal injury in humans [12, 126, 148, 153, 156, 161, 401].

In the present study, we examined UmtDNA copy number as marker of renal injury in a cohort of patients who developed AKI following cardiac surgery. We found that UmtDNA was associated with an increased risk of worsening AKI following initial sample collection, and that UmtDNA is mildly predictive of AKI progression by ROC analysis (Figure 6.2). The power of these studies is limited by a small cohort size, and the practical limitations of stratification of patient data according to serum creatinine. AKI progression was based on an increase in AKIN stage as determined by serum creatinine from collection baseline. As serum creatinine is a poor early indicator of renal damage/dysfunction, it is possible that some patients classified as AKIN 0-1 at collection had more severe renal damage, potentially affecting the predictive value of UmtDNA for AKI progression in this cohort. Therefore, UmtDNA may simply serve as an

indicator of varying degrees of renal damage rather than a biological indicator of renal repair, recovery or progression. However, stratification of patients by AKIN stage at collection or maximum AKIN stage revealed no differences in UmtDNA between any groups suggesting that UmtDNA is not significantly associated with degree of renal damage, and notable increases in days to maximum creatinine and days to discharge occurred in the progressive AKI group (Table 6.1). This data suggests differences in recovery between these groups rather than initial injury; however, practical limitations of serum creatinine still temper these conclusions. Larger scale studies are needed in patients with AKI of various degrees and from multiple etiologies in order to validate the predictive power of UmtDNA. In this study we determined LR^+ and LR^- values to serve as maximum and minimum cutoff values to stratify patients into low and high risk groups. Analysis of our data set using the cutoffs demonstrated that risk of AKI progression could be evaluated with reasonable confidence. These cutoffs value could be used for patient screening for enrollment into future larger scale studies with AKI progression as an endpoint.

Traditional markers of renal dysfunction including serum creatinine and BUN have limited to no ability to predict progression of disease following CBP-induced AKI [402]. These limitations have led to the development of new renal injury markers with enhanced predictive power over existing clinical markers [403, 404]. However, the prognostic value of even these newer markers, including KIM-1 and NGAL, is still relatively weak [405, 406]. A recent study by Arthur *et al.* examined the ability of a panel of renal biomarkers including KIM-1, NGAL, L-FABP and IL-18 to predict the progression of AKI following cardiac surgery using a different subset of SAKInet patients than used in our study [407]. From this study, IL-18 was determined to be the best predictor of AKI progression (AKIN 1 to AKIN 2/3 or death) with an AUC of 0.74. While our definition of AKI progression differed slightly from that of this study, the

predictive performance of UmtDNA compared favorably (AUC = 0.72, stable vs. progressive AKI). Interestingly, in contrast to many of the markers assessed in the study by Arthur *et al.*, UmtDNA failed to correlate with traditional markers of renal damage and dysfunction (Figure 6.3) even in the acute injury phase. We compared UmtDNA levels to another candidate biomarker of AKI and AKI progression, urinary angiotensinogen. Urinary angiotensinogen has been shown to be a strong predictor of AKI progression in ICU patients [375]. Furthermore, urinary angiotensinogen measured on the first day of hospitalization predicted future development of AKI in patients with decompensated CHF with extremely high accuracy, and was superior to the performance of urinary NGAL [397]. Interestingly, UmtDNA was not correlated with urinary angiotensinogen in our cohort. These data may suggest that UmtDNA, a potential surrogate marker of renal mitochondrial integrity, is a biomarker of different cellular processes than urinary angiotensinogen and other candidate markers, and perhaps represents a more direct indicator of renal repair. The mechanistic relevance of UmtDNA levels in the status of renal mitochondria and renal repair processes warrants further investigation. Furthermore, failure of UmtDNA to correlate with urinary angiotensinogen could be useful in the development of a prognostic biomarker panel, as non-correlated biomarkers are superior for use in combinatorial predictive models such as a multivariable logistic regression models or classification trees [407].

As human renal cortical samples (e.g. biopsies) from AKI patients are not readily available we chose to explore the physiological link between UmtDNA and renal mitochondrial integrity in a mouse model of renal I/R. Our lab has demonstrated that mitochondrial homeostasis is persistently disrupted following I/R-induced AKI in rodents, and this persistent mitochondrial disruption is associated with an incomplete renal repair process [126, 161]. Mice were subjected

to varying degrees of ischemia (5, 10 or 15 min) followed by reperfusion for 24 h. UmtDNA levels increased in mice with moderate (10 min ischemia) or severe (15 min ischemia) renal injury (Figure 6.4), and correlated with degree of ischemia (and histological grade), but not renal function as assessed by BUN (Figure 6.5). These data differ from results from human cardiac surgery patients as no correlation was observed with bypass time during cardiac surgery. However, bypass time, while often a reasonable indicator of surgical complexity, is likely a poor surrogate marker of degree of ischemia or renal injury in humans due to heterogeneous patient characteristics and surgical parameters. UmtDNA levels were found to be associated with renal injury in mice (Figure 6.7). Of note, when mice without detectable renal injury by BUN were excluded, the predictive power of UmtDNA decreased in our studies. This is likely due to poor performance of BUN as a marker of renal injury. Based on data from figure 6.4, UmtDNA levels fail to correlate with BUN indicating that UmtDNA is not an indicator of renal function, but more likely a better indicator of degree of renal damage or progression in these mice. Limitations of BUN as a true marker of renal damage are likely leading to exclusion of mice that are truly injured, thus reducing the observed predictive power of UmtDNA. Overall, these data demonstrate that mouse I/R provides a reasonable model of the UmtDNA response observed in human patients following CBP, and provided a platform for examination of renal cortical mitochondrial parameters.

We evaluated mouse renal cortical mtDNA copy number and mRNA expression of PGC-1 α , COX1 and NDUFB8 (genes involved in mitochondrial biogenesis) as markers of mitochondrial integrity and biogenesis following renal I/R. Correlation of renal mtDNA copy number and mitochondrial genes with total UmtDNA output demonstrated negative correlations indicating that UmtDNA is reflective of renal mitochondrial disruption following I/R (Figure 6.8). Normalization of UmtDNA to urine creatinine showed modest improvements in these

correlations (Figure 6.9). Normalization to urine creatinine, commonly used to quantitate urine albumin, has been used inconsistently in biomarker evaluations. Systematic evaluation of the performance of urinary biomarkers as an absolute concentration, corrected for urine creatinine or as total urinary excretion, demonstrated improved predictive power of biomarkers when corrected to creatinine [408] however, we observed no substantial improvement in predictive power of UmtDNA when corrected for urine creatinine in our studies.

Correlations of UmtDNA with mitochondrial gene expression suggest that the predictive power of UmtDNA for AKI progression may arise from its ability to predict the degree of renal mitochondrial damage and disruption, which could inhibit renal repair processes. However, we cannot definitively conclude that UmtDNA is a marker of renal repair or recovery. Correlation of suppression of mitochondrial gene expression to elevations of UmtDNA fails to causally link mitochondrial integrity to recovery from AKI. Future mechanistic studies are needed to examine how modulation of UmtDNA levels correlates with renal repair and functional recovery after AKI. Additionally, regulation of renal mtDNA and mitochondrial mRNA expression is subject to complex regulatory processes. Changes in these indicators may not be truly reflective of mitochondrial damage or disruption. However, many previous studies have clearly demonstrated mitochondrial damage and dysfunction as key pathophysiological components of the initiation and recovery from I/R-induced AKI. Significant structural alterations, loss of mitochondrial membrane integrity, and decreases in mitochondrial function have been previously demonstrated in multiple models of renal injury [345, 398, 409].

Past reports of urinary markers of renal mitochondrial dysfunction are limited to urinary cytochrome c which is elevated following drug-induced AKI [380]. Cytochrome c is a poor renal biomarker as it is only transiently elevated following injury and thus likely serves as a better

predictor of degree of renal damage rather than recovery and disease progression. Our group recently published that urinary levels of the protein ATP synthase subunit β serve as a biomarker of CPB-induced AKI; however, its predictive value in this study was not assessed [398]. These studies provide preliminary evidence of UmtDNA as a novel biomarker reflective of AKI progression linked to renal mitochondrial integrity. The mitochondrial and energy dependence of renal repair processes and renal recovery make UmtDNA a promising tool for exploration of the role of mitochondrial damage and dysfunction in human renal disease and the development of new mitochondrial-targeted therapies.

CHAPTER 7:

Conclusions, Unanswered Questions and Future Directions

Conclusions

Sublethal and lethal injury to the renal proximal tubular cells of the kidney contributes to renal dysfunction following AKI [22, 27]. Following injury, the renal proximal epithelium has the capacity to repair itself through the activation of renal cell proliferation and repair processes. These repair processes are highly energy dependent, and thus rely on proper mitochondrial function for the supply of ATP. However, mitochondrial dysfunction is a common pathophysiological mechanism of various forms of AKI characterized by mitochondrial depolarization, reduced ATP output, increased oxidative stress, mitochondrial fragmentation and the suppression of mitochondrial biogenesis, thus limiting renal recovery [22, 156, 293, 410]. Therefore, re-activation of mitochondrial biogenic signaling pathways to generate new, functional mitochondria may serve as a novel therapeutic target for the promotion of renal recovery following AKI.

Cellular models of oxidant-induced proximal tubular injury using the model oxidant tert-butyl hydroperoxide (TBHP), demonstrated that mitochondrial biogenesis was induced following injury, and vital to the recovery of cellular function [204]. Furthermore, activation of mitochondrial biogenesis through the overexpression of PGC-1 α , the master regulator of mitochondrial biogenesis, accelerated recovery of renal proximal tubular cells (RPTC) following TBHP-induced damage [207]. This data suggested that activation of mitochondrial biogenesis through the induction of the transcriptional coactivator PGC-1 α could promote recovery of renal tubular cells. Thus, the need existed to identify pharmacological activators of PGC-1 α -dependent mitochondrial biogenesis.

Use of high throughput respirometry allowed for the identification and evaluation of several classes of compounds that could induce mitochondrial biogenesis in RPTC including the SIRT1 activators, resveratrol and SRT1720 [162, 284], isoflavones [244], the 5-

hydroxytryptamine IIB receptor agonist, DOI, and the long acting β 2-agonist, formoterol [219]. Further studies with SRT1720 and formoterol demonstrated their ability to induce mitochondrial gene and protein expression and mitochondrial function in RPTC [162, 219]. Additionally, treatment of RPTC with SRT1720 following oxidant damage with TBHP accelerated recovery of mitochondrial protein expression, uncoupled mitochondrial respiration and cellular ATP levels. Furthermore, treatment of mice following renal I/R injury with either SRT1720 or formoterol accelerated renal functional recovery through the activation of mitochondrial biogenic signaling, perhaps by enhancing the bioenergetic surplus needed for renal repair [148, 218]. These results provided strong evidence that pharmacological activation of mitochondrial biogenesis is a viable approach to stimulate renal recovery.

Exploration of additional druggable targets for the induction of mitochondrial biogenesis led us to explore the role of cyclic nucleotides, and pharmacological modulators of renal cyclic nucleotides levels. cAMP is a well-characterized inducer of PGC-1 α transcription through its activation of protein kinase A and subsequent phosphorylation of cAMP response element-binding protein (CREB). This signaling pathway was identified in early work examining the signaling pathways involved in the cold induction of PGC-1 α expression. Cold exposure causes the release of norepinephrine, activation of the sympathetic autonomic nervous system and increased levels of cAMP through G_s-receptor activation.

cAMP and cGMP levels are regulated both by their production, primarily through G-protein coupled receptors, and their degradation by phosphodiesterases (PDEs) to their non-cyclic forms, AMP and GMP. Inhibition of PDEs using various class specific inhibitors can lead to the accumulation of cAMP and/or cGMP and promote activation of their downstream signaling pathways. Due to the well-characterized role of cAMP in mitochondrial biogenesis,

we explored the efficacy of the PDE3 (degrades both cAMP and cGMP) inhibitors, cilostamide and trequinsin, and the PDE4 (degrades only cAMP) inhibitors, rolipram and Ro 20-1724.

Treatment of RPTC for 24 h demonstrated a dose-dependent increase in mitochondrial uncoupled OCR with the PDE3 inhibitors, cilostamide and trequinsin, while no change was observed in uncoupled OCR with either rolipram or Ro 20-1724, indicating a potential specificity of the mitochondrial biogenic response for cGMP in RPTC (Figure 2.1).

Additionally, cilostamide and trequinsin caused dose-dependent increases in the expression of PGC-1 α , and the mitochondrial genes NDUFB8 and COX1 in RPTC (Figure 2.2). Furthermore, mitochondrial gene expression and mtDNA copy number were increased in the renal cortex of mice 24 h after treatment with either cilostamide or trequinsin (Figure 2.5).

In order to explore the specificity of the activation of mitochondrial biogenesis in RPTC for either cAMP or cGMP, we measured the induction of cAMP and cGMP via ELISA in RPTC (Figure 2.3). The PDE3 inhibitors, cilostamide and trequinsin, demonstrated rapid and potent inductions of both cAMP and cGMP levels, while the PDE4 inhibitor, rolipram, induced only cAMP, and the PDE5 (degrades only cGMP) inhibitor, sildenafil, increased only cGMP levels. Furthermore, treatment with the cell permeable cyclic nucleotide analogs, 8-Br-cAMP and 8-Br-cGMP, revealed that only 8-Br-cGMP induced mitochondrial uncoupled OCR and mitochondrial gene expression in RPTC. This data provided strong evidence that the mitochondrial biogenic response was cGMP-specific in renal tubular cells.

cGMP has previously been characterized as an inducer of mitochondrial biogenesis in other model systems. The nitric oxide (NO) mimetic DETA-NO, 8-Br-cGMP, and the guanylyl cyclase stimulator, BAY 41-2272, all were shown to stimulate mitochondrial biogenesis and increase mitochondrial function after 6 d treatment in U937 monocytes, L6 myoblasts, and PC12

neurosecretory cells [233]. Vardenafil, a long-acting PDE5 inhibitor, stimulated mitochondrial biogenesis in cultured adipocytes [232]. Treatment with naturetic peptides, activators of membrane bound guanylyl cyclases, induced muscle mitochondrial content and function and fat oxidation in diabetic mice [239]. Finally, caloric restriction was demonstrated to induce expression of endothelial nitric oxide synthase (eNOS) and subsequently mitochondrial biogenesis, and eNOS-knockout mice demonstrated reduced mitochondrial content and metabolism, and increased weight gain [271].

Treatment of RPTC with the PDE5 inhibitor sildenafil increased mitochondrial uncoupled OCR and mitochondrial gene expression (Figure 2.4). Additionally, mice treated with sildenafil showed increased mitochondrial gene expression, mtDNA content and renal ATP levels 24 h after treatment (Figure 2.6). To determine the efficacy of sildenafil in a model of AKI, renal injury was induced in mice via bolus injection of folic acid. Mitochondrial gene expression and mtDNA content were rapidly and potently suppressed following injury; however, treatment with sildenafil promoted the recovery of mitochondrial markers, and furthermore, reduced renal tubular injury demonstrated by reduced renal cortical expression of Kim-1 (Figure 2.7). These data provide strong support for the efficacy of induction of cGMP through inhibition of cGMP regulatory PDEs as a novel approach to induce mitochondrial biogenesis and accelerate renal recovery following AKI.

Increasing evidence suggests that failed renal recovery after AKI is a significant risk factor for the progression to chronic kidney disease (CKD) and end stage renal disease (ESRD) [10, 74, 356]. Due to the energetic demands of renal repair, compromised mitochondrial function could play a significant role in the inability of the renal tubular epithelium to fully repair after AKI. Pharmacological stimulation of mitochondrial biogenesis and recovery of renal

bioenergetics could enhance renal recovery and limit the development of renal fibrosis and CKD progression.

To evaluate this hypothesis, we first examined the chronic effects on mitochondrial biogenesis in a folic acid-induced model of renal injury. Treatment of mice with high dose folic acid caused a rapid AKI with peak injury at 24 h after injection, characterized by elevations in serum creatinine, BUN, urinary glucose levels and renal cortical NGAL expression (Figure 3.1). These biomarkers recovered over the course of 14 d after injection. However, during this recovery phase, kidneys demonstrated signs of fibrotic development and progression to early CKD (Figure 3.5). Renal expression of the growth factor TGF β was elevated, as well as the fibrotic markers α SMA and COL1A2. Marked collagen deposition was demonstrated by picrosirius red staining and polarized microscopy. Furthermore, mice demonstrated progressive increases in urinary output and decreases in urine osmolality all indicative of CKD development. Correlated with the apparent failure of renal repair and fibrotic development was a persistent suppression of mitochondrial gene expression, including PGC-1 α , Tfam, COX1, NDUFB8, and ATP5B, and mtDNA copy number (Figure 3.3). These data support a potential role for the suppression of mitochondrial biogenesis and persistent mitochondrial dysfunction in the failure of renal repair.

We hypothesized that stimulation of mitochondrial biogenesis using the PDE5 inhibitor, sildenafil, could promote recovery of these mitochondrial parameters and slow the progression of renal fibrosis. Mice were treated daily beginning at 24 h after folic acid for a period of a 1 wk. Sildenafil failed to promote recovery of renal mitochondrial gene expression and mtDNA content (Figure 3.7). Furthermore, sildenafil failed to limit the progression of renal fibrosis in this model. Failure of sildenafil to promote recovery in FA-induced CKD could be the result of

attenuation of the mitochondrial biogenic response to chronic PDE inhibition, and/or chronic inhibitory signals that cannot be overcome by exogenous activation of mitochondrial biogenic signaling. The fibrotic response observed following folic acid administration is quite potent, and perhaps the failure of sildenafil was model dependent.

Due to the lack of efficacy of cGMP modulation in the folic acid model, we chose to evaluate the effect of cGMP-induced mitochondrial biogenesis following renal I/R injury. Additionally, we sought to examine the efficacy of activation of cGMP production through guanylyl cyclase (GC) stimulation by the GC stimulator, BAY 41-2272, or the GC activator, BAY 58-2667. Treatment of RPTC with either BAY 41-2272 or BAY 58-2667 caused a dose-dependent increase in mitochondrial uncoupled OCR, indicating that these compounds are affecting mitochondrial content or function (Figure 4.1). Injection of mice with BAY 58-2667 (10-100 $\mu\text{g}/\text{kg}$) increased renal cortical mitochondrial gene and protein expression and mtDNA copy number, however, BAY 41-2272 (0.1-1 mg/kg) had no effect (Figure 4.2). BAY 41-2272, classified as a GC stimulator functions by activating GC through interaction with its reduced heme moiety. In contrast, BAY 58-2557, a GC activator, increases GC activity without interacting with the heme moiety and thus can activate the oxidized form of GC. BAY 58-2667 can activate GC synergistically with nitric oxide. The ability of BAY 58-2667, but not BAY 41-2272 to stimulate mitochondrial biogenesis could thus be due to the ability to activate oxidized or non-heme containing GC. As the proximal tubule is highly dependent upon oxidative phosphorylation for energy, it also is subject to high levels of oxidative stress. Even basal levels of ROS in the renal cortex could potentially cause depletion of the reduced pool of GC limiting its ability to be activated by its endogenous activator, nitric oxide, or BAY 41-2272 and other GC stimulator compounds.

We then evaluated the ability of BAY 58-2667 to promote the recovery of renal and mitochondrial function following I/R-induced AKI. Mice were treated daily beginning at 24 h after I/R (time of maximal renal dysfunction) with BAY 58-2667 (100 μ g/kg) or saline vehicle until 144 h post I/R. Sildenafil was used as a positive control at a dose of 1 mg/kg. Mice treated with BAY 58-2667 or sildenafil showed accelerated recovery of renal function to sham surgical levels by 144 h, while I/R + vehicle mice failed to recover renal function (Figure 4.3). Additionally, renal mRNA and protein levels of the renal tubular injury markers, Kim-1 and NGAL, were also recovered following treatment with BAY 58-2667. Furthermore, levels of renal tubular necrosis were reduced in mice treated with BAY 58-2667 vs. I/R controls (Figure 4.4). Expression of PGC-1 α and NRF1, the mitochondrial-encoded genes, ND1 and COX1, and the nuclear-encoded mitochondrial gene, ATP5 β , all reduced following renal I/R, were increased in mice treated with BAY 58-2667, indicating a recovery of mitochondrial biogenic signaling (Figure 4.5). These signaling changes led to an increase in the mitochondrial proteins, PGC-1 α and COX1, and an increase in mitochondrial function evidenced by increased renal ATP levels (Figure 4.6). BAY 58-2667 blunted the progression of fibrosis indicated by reduced COL1A2 and α SMA expression (Figure 4.7). BAY 58-2667 also had positive effects in reducing renal inflammatory markers and oxidative DNA damage (Figure 4.8, 4.9). Finally, BAY 58-2667 recovered expression of renal cortical eNOS levels above sham controls, while tissue cGMP levels at the time of measurement were unchanged (Figure 4.10). These data strongly indicate that activation of GC promotes recovery following renal I/R through positive effects on mitochondrial content and function, reduced inflammation and oxidative stress.

Evaluation of the efficacy of mitochondrial targeted therapies, including stimulators of mitochondrial biogenesis, in humans, requires the ability to assess mitochondrial content and

function using non-invasive assays. Current methods of measuring mitochondrial function in humans are restricted to invasive tissue assays. Therefore, we evaluated two new urine biomarkers of renal mitochondrial integrity, urinary ATP synthase subunit β and urinary mtDNA, in mouse renal I/R injury and in humans following cardiac surgery.

ATPS β is a subunit of the ATP synthase located in the inner mitochondrial membrane. ATPS β was found to be elevated in the urine of rats following I/R or glycerol-induced AKI (data not shown). We evaluated urinary ATPS β levels further using a mouse I/R model. Varying degrees of renal injury were induced in mice by clamping of the renal pedicle for periods of 5, 10 or 15 min, indicative of mild, moderate or severe renal histological injury (Figure 5.2). ATPS β was detected in the urine via immunoblot, and revealed 2 prominent bands – a full length band of ~50 kDa and a cleaved band of ~25 kDa, both of which were elevated after moderate or severe I/R, preceding the elevation of traditional biomarkers of renal injury (Figure 5.1). Elevation of urinary ATPS β was associated with decreases in renal cortical expression of ATPS β , and the complex I protein, COX1 (Figure 5.3). Furthermore, changes in urinary ATPS β were associated with mitochondrial dysfunction evidenced by reduced renal tubular FCCP-uncoupled OCR and renal cortical ATP levels (Figure 5.4). Measurement of urinary ATPS β over a time course following renal I/R demonstrated continued elevation of both the full length and cleaved fragments at 72 h after I/R. Both recovered to sham control levels by 144 h after I/R mirroring the recovery of renal function in these mice (Figure 5.5). Assessment of urinary ATPS β in a non-kidney injury model, the NASH model of liver injury, revealed that only the cleaved ATPS β fragment was detected in the urine (Figure 5.6). This data indicates that the cleaved fragment is not specific for renal injury, but perhaps the full length fragment is renal specific. Mitochondrial damage in non-renal tissue could result in the systemic release of ATPS β . Due to the smaller

size of the cleaved fragment, it is likely freely filtered at the glomerulus. The larger fragment is near the size exclusion limit for filtration, and is also relatively highly charged, which would limit its ability to be filtered. The potential specificity of the full length band for renal injury highlights its potential as a renal biomarker. Lastly, urinary ATPS β was measured in human patients following cardiac surgery. Patients who developed AKI had higher urinary expression of the full length ATPS β , but not the cleaved form (Figure 5.7). This further suggests that the full length form is renal specific as the cleaved form could originate from other tissues injured during cardiac surgery including the heart and vasculature.

mtDNA is released into circulation from mitochondria in response to tissue injury [411]. Recognition of mtDNA by toll-like receptor 9 (TLR9) leads to activation of inflammatory signaling cascades [412]. Thus, mtDNA could serve as an indicator of sterile inflammation resulting from tissue injury. Several studies have examined plasma mtDNA levels following multiple pathologies, however, no studies have evaluated urinary mtDNA (UmtDNA) as either a marker of systemic or renal-specific injury [281, 413]. We evaluated UmtDNA as a biomarker of renal mitochondrial dysfunction and AKI progression/recovery in a mouse model of renal I/R and in cardiac surgery patients. Measurement of UmtDNA levels in patients following cardiac surgery demonstrated that UmtDNA was not diagnostic of AKI or AKIN stage (Figure 6.1). However, UmtDNA levels were shown to be predictive of AKI progression. Elevated UmtDNA levels were a fair predictor of progressive AKI (increase in AKIN stage following collection) vs. stable AKI (no change/reduction in AKIN stage after collection (Figure 6.2). Furthermore, UmtDNA levels were not associated with other biomarkers of renal dysfunction and injury. No correlation was observed with maximum creatinine levels, max % change in creatinine or urinary angiotensinogen levels. Additionally, UmtDNA was also not correlated with cardiac bypass

time, days to maximum creatinine or days to discharge (Figure 6.3). Failure of UmtDNA to act as a diagnostic marker of AKI and the lack of correlation with existing biomarkers of renal damage and dysfunction suggest that it is a marker of a unique biological process. Due to the role of mitochondria in tissue recovery, perhaps it is serving as a better predictive indicator of renal repair and recovery. Its ability to predict AKI progression further supports this hypothesis.

In order to further evaluate the biochemical significance of urinary mtDNA we used a mouse model of renal I/R with varying degrees of ischemia. Mice undergoing 10 or 15 min of ischemia followed by reperfusion were found to have elevated UmtDNA levels at 24 h after injury (Figure 6.4). Total 18 h output of UmtDNA was found to be significantly correlated with time of ischemia, but again failed to correlate with renal function assessed by BUN (Figure 6.5). UmtDNA levels were demonstrated to be predictive of AKI development in mice by ROC curve analysis (Figure 6.7). Correction of UmtDNA had no effect on these results (Figure 6.6). Most importantly, UmtDNA levels were found to be negatively correlated with renal mitochondrial gene expression and renal mtDNA copy number (Figure 6.8, 6.9). These data indicate that UmtDNA is serving as a biomarker of renal mitochondrial integrity and mitochondrial biogenic signaling in the kidney.

The above described studies demonstrate the importance of mitochondrial function in renal repair and recovery. Disruption of mitochondrial function after AKI can result in incomplete repair, fibrotic development and ultimately progression to CKD. Activation of MB may serve as a valuable therapeutic strategy to promote the recovery of mitochondrial content and function after AKI. Induction of cGMP through the use of phosphodiesterase inhibitors or guanylyl cyclase activators may be a valuable therapeutic strategy to activate mitochondrial biogenic signaling in the setting of AKI. Furthermore, use of new biomarkers of renal

mitochondrial integrity, urinary ATP5B and urinary mtDNA, will assist in the evaluation of these mitochondrial targeted therapies in human patients.

Unanswered questions

Mitochondrial function and tissue bioenergetics are increasingly recognized as important components of nearly all disease states, thus modulation of tissue mitochondrial content and oxidative metabolism has become an attractive target for drug development. However, there remains a significant number of unanswered questions in regards to both safety and efficacy of this therapeutic strategy. For example, could whole body activation of MB have unintended, negative consequences, including increased systemic oxidative stress and inflammation? Will MB prior to an injury, surgery or toxic drug treatment, prevent organ dysfunction or increase organ dysfunction due to the presence of “more” dysfunctional mitochondria? Additionally, what treatment strategies are required for the persistent enhancement of mitochondrial content and function in the setting of acute and chronic disease (i.e., avoidance of receptor desensitization or activation of antagonistic pathways)? Consideration of these critical questions will hasten the development of MB compounds and enhance their applicability to human disease.

Efforts to improve mitochondrial function in various disease states have targeted all aspects of mitochondrial homeostasis, including mitochondrial degradation through activation or suppression of mitophagy, mitochondrial dynamics through modulation of fission/fusion proteins, and mitochondrial synthesis through regulation of MB. Pharmacological modulation of any of these processes for therapeutic effect in a diseased organ creates the possibility of disruption of mitochondrial homeostasis in off-target tissues. For example, blocking mitochondrial fission protects against MPTP opening and apoptotic cell death in heart [414]. However, activation of mitofusin 2 (MFN2), a pro-fusion mitochondrial protein, can block

proliferation in multiple cell types, including astrocytes and vascular smooth muscle cells [415, 416]. Loss of cellular proliferation and tissue plasticity could prove problematic in the setting of injury due to impairment of angiogenesis and other critical tissue repair processes.

We can gain some insight into the safety of MB as a therapeutic strategy by examination of FDA-approved compounds subsequently identified as effectors of MB or mitochondrial function. There are examples of drugs that have subsequently been shown to affect mitochondria, including minocycline, rosiglitazone, cyclosporine A, sildenafil, captopril, formoterol, and others [143, 148, 149, 417, 418]. Many of these agents have been demonstrated to exert their effect in animal models at least in part through induction of MB in the diseased tissue. For instance, studies suggest that a component of the beneficial effects of captopril, an angiotensin converting enzyme inhibitor used extensively in treatment of hypertension and congestive heart failure, is through activation of MB in the heart [417]. This provides evidence of the chronic administration of a mitochondrial biogenic agent in a patient population with significant systemic comorbidities, suggesting the relative safety of MB as a therapeutic strategy. Despite significant promise as a therapy for an array of disease states, no specific activators of MB currently exist for treatment of a human disease. A great deal of work remains to develop more potent and specific agents for induction of MB, evaluate safety of MB in diverse patient populations, and to ultimately optimize dosing strategies for treatment of both acute and chronic conditions to maximize efficacy and avoid refractory responses.

Future directions

Both phosphodiesterase inhibition and guanylyl cyclase activation appear to be promising therapeutic strategies for the stimulation of mitochondrial biogenesis in AKI. Future studies will

seek to further characterize the mitochondrial biogenic response through the determination of the downstream signaling pathways linking cGMP to mitochondrial biogenesis. This will include examination of the activity of cGMP-dependent protein kinase (PKG) and its downstream phosphorylation targets, as well as characterization of the effects of cGMP on known regulators of MB including AMPK and SIRT1. Furthermore, in order to validate the role of NO-cGMP in the activation of MB and renal recovery, AKI studies could be performed using eNOS, GC and/or PKG knockout animals with the goal of demonstrating a clear mechanistic link between reduction of renal cGMP and impaired renal recovery.

Mitochondrial biogenesis is potently and persistently suppressed following AKI; however, the mechanisms of its suppression remain unclear. We believe that the suppression is an acute adaptive response to reduce mitochondrial generation in the setting of mitochondrial insult, thus limiting the production of ROS by damaged mitochondria. This adaptive response becomes maladaptive in the chronic setting by limiting energy-dependent tissue repair processes. To further explore the mechanisms of suppression of mitochondrial biogenesis, we performed short term I/R experiments in mice. Mice underwent 18 min of ischemia followed by reperfusion and tissues were collected at 1 and 3 h after I/R. PGC-1 α expression was reduced to ~30% of sham control levels at 3 h after I/R, but was not changed at 1 h (Figure 7.1). Expression of the mitochondrial transcription factor Tfam was also suppressed at 3 h. mtDNA copy number was decreased to ~50% of sham control levels as early as 3 h (Figure 7.2). Evaluation of the mitochondrial-encoded mitochondrial genes, COX1 and ND1, found that both were suppressed at 3 h after I/R (Figure 7.3). Finally, the nuclear-encoded mitochondrial genes, NDUFB8, NDUFS1 and ATP5B, were also all suppressed at 3 h after I/R and unchanged at 1 h (Figure 7.4).

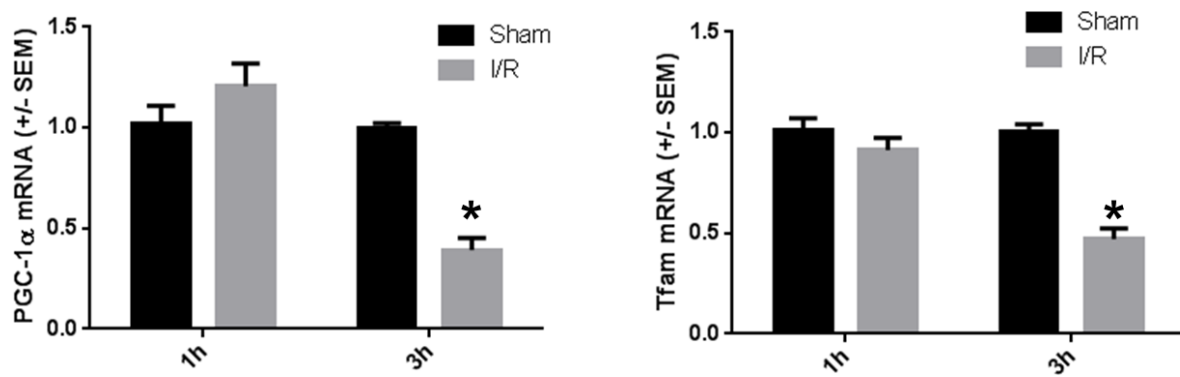


Figure 7.1. PGC-1 α and Tfam are suppressed 3 h after I/R injury. mRNA expression was assessed by qPCR. Data are expressed as mean \pm SEM. * indicates statistical significance at $p < 0.05$; $n = 6$ per group.

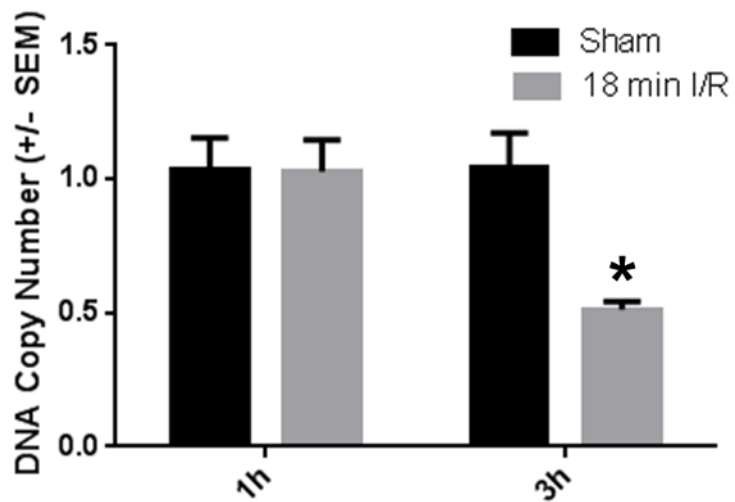


Figure 7.2. mtDNA copy number is suppressed at 3 h after I/R. mtDNA content was assessed by qPCR. Data are expressed as mean \pm SEM. * indicates statistical significance at $p < 0.05$; $n = 6$ per group.

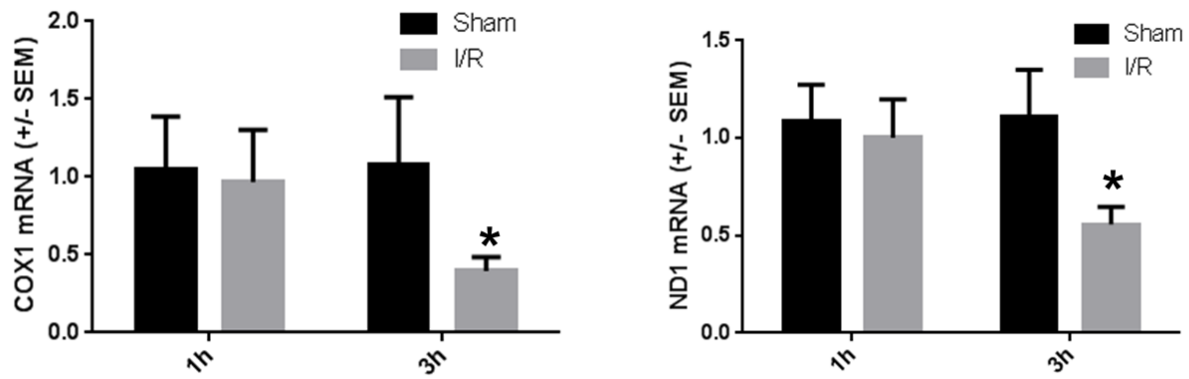


Figure 7.3. Mitochondrial-encoded mitochondrial genes are suppressed at 3 h after I/R. mRNA expression was assessed by qPCR. Data are expressed as mean +/- SEM. * indicates statistical significance at $p < 0.05$; $n = 6$ per group.

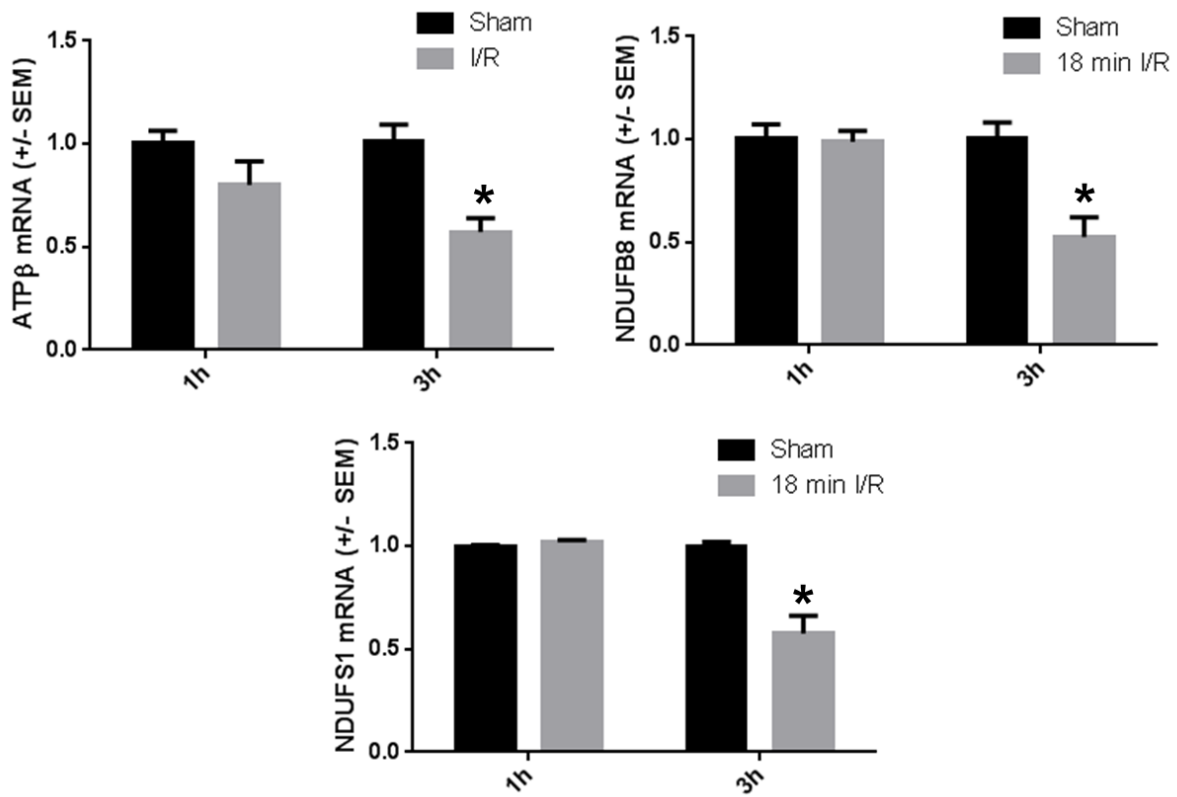


Figure 7.4. Nuclear-encoded mitochondrial genes are suppressed at 3 h after I/R. mRNA expression was assessed by qPCR. Data are expressed as mean +/- SEM. * indicates statistical significance at $p < 0.05$; $n = 6$ per group.

This data indicates that the suppression of mitochondrial biogenesis is a potent, early response after I/R injury. The signal causing the suppression is also persistent evidenced by continued reduction of renal mitochondrial biogenic signaling as late as 144 h after I/R. This rapid and persistent signal suggests that acute and chronic inflammation may be a mediator of the response. Examination of renal TNF- α levels demonstrated a 2.4-fold increase in expression by 3 h after I/R (Figure 7.5). From the BAY 58-2667 studies, TNF- α remains highly elevated in renal cortex at 144 h after I/R demonstrating that the signal is persistent. Previous studies have suggested TNF- α as a negative regulator of PGC-1 α [280, 419, 420]. Furthermore, TNF- α is known to cause suppression of eNOS expression and eNOS-dependent MB [234, 421].

In addition to inflammatory signals, microRNAs represent a novel potential regulator of mitochondrial biogenesis after AKI. Following renal I/R, expression of mir-494, a negative regulator of Tfam expression inducible by TNF- α , and mir-696, identified as a negative regulator of PGC-1 α in muscle, were upregulated as early as 1 h after injury (Figure 7.6) [422-424]. These microRNAs could be targeted therapeutically using antagomir-based strategies or inhibition of microRNA processing. While upregulation of these microRNAs is an interesting finding, further studies are needed to characterize their roles in AKI-induced suppression of MB. Additionally, each is just one in what is likely a larger cascade of mitochondrial-targeted microRNA changes after I/R.

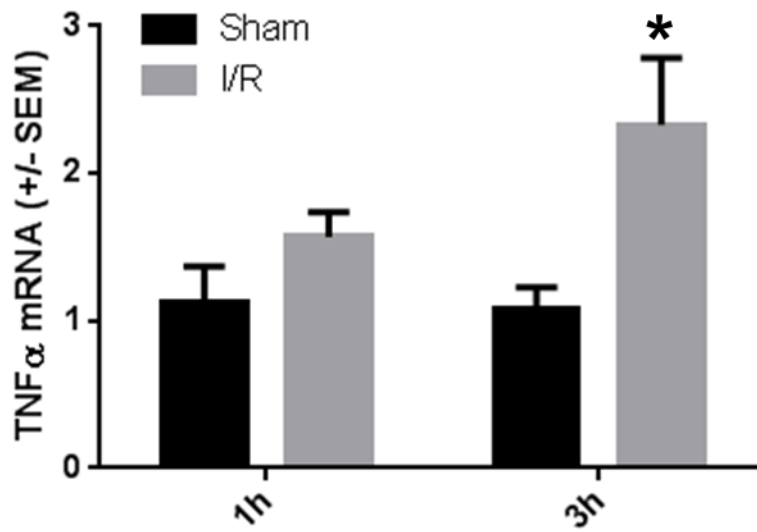


Figure 7.5. Renal cortical TNF- α is upregulated at 3 h after I/R. mRNA expression was assessed by qPCR. Data are expressed as mean \pm SEM. * indicates statistical significance at $p < 0.05$; $n = 6$ per group.

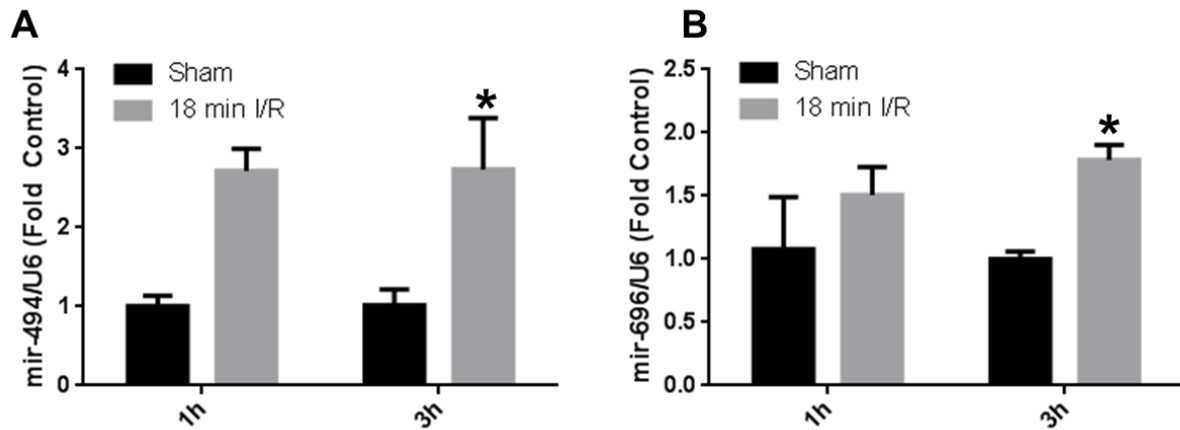


Figure 7.6. Renal mir-494 and mir-696 are upregulated after I/R. microRNA expression was assessed by qPCR. Data are expressed as mean \pm SEM. * indicates statistical significance at $p < 0.05$; $n = 6$ per group.

Results with urinary ATP synthase β and urinary mtDNA demonstrated each as promising biomarkers of renal mitochondrial dysfunction in AKI. Further validation studies are needed for each including evaluation in larger patient populations with varying degrees and etiologies of renal injury. For urinary ATPS β , the goal is to develop an ELISA or luminex-based assay for rapid and sensitive detection for use in point-of-care settings. Our results demonstrated that the full length form of ATPS β appeared specific for renal mitochondrial disruption. While this result requires further validation, assay development will require identification of antibodies that can specifically detect the full length vs. the cleaved fragment of ATPS β . We have begun procedures to develop new antibodies for ATPS β with the goal of increasing sensitivity and specificity vs. commercially available antibodies. A sampling of the immunoblot results from antibodies produced against the ATPS β recombinant protein in mice are shown below (Figure 7.7). The left lane in each blot is a sham control urine, while the right lane is urine from mouse after 15 minutes of ischemia followed by 24 h of reperfusion.

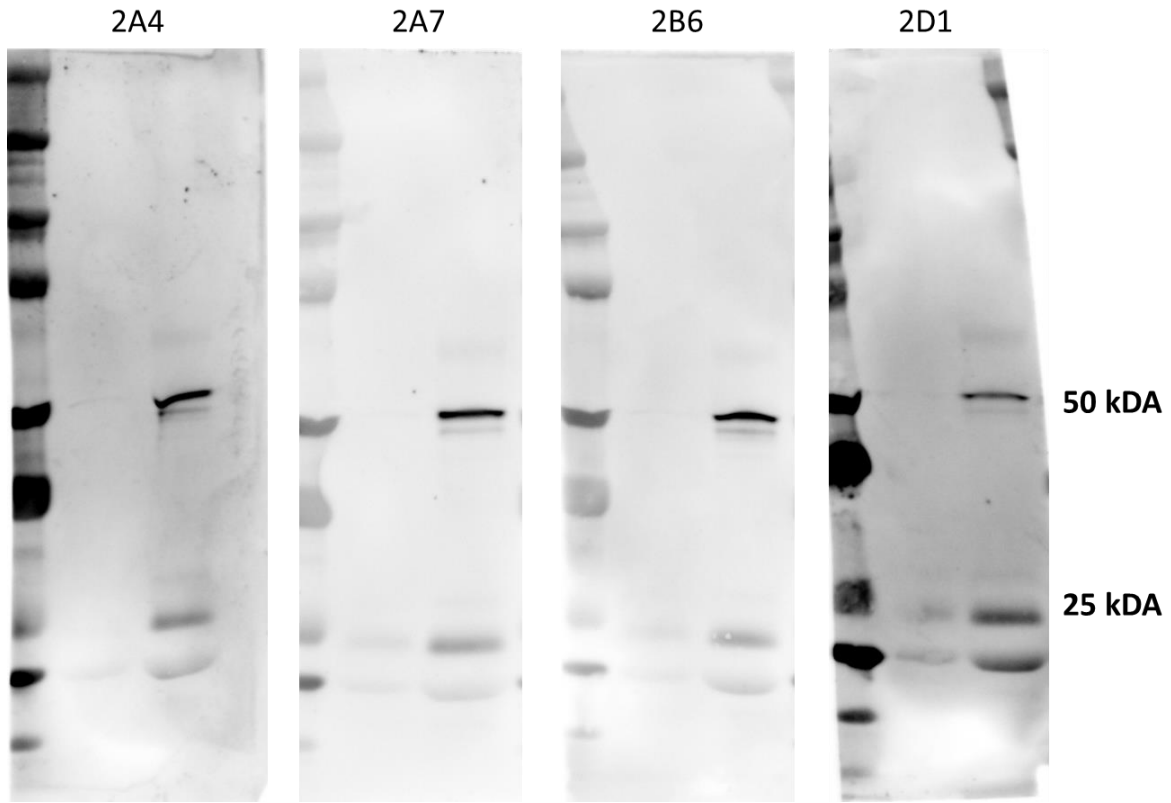


Figure 7.7. Sample of new ATPS β antibody clone immunoblot results. Each blot represents a unique antibody clone. Left lane = sham, right lane = I/R.

Urinary mtDNA was shown to be predictive marker of AKI progression that was correlated with suppression of renal mitochondrial biogenic signaling. As mtDNA is released in response to mitochondrial injury, perhaps it serves as signal to resident cells to suppress mitochondrial biogenesis. Thus, mtDNA could serve as a biostatic mechanism signaling to other cells to limit mitochondrial production to reduce further oxidative cellular damage. To evaluate this hypothesis, we first sought to determine if mtDNA is released in response to oxidant injury. Treatment of TKPTS cells with H₂O₂ demonstrated a dose-dependent release of mtDNA into the tissue culture medium, which was associated with reduction in cellular mtDNA content and PGC-1 α mRNA expression (Figure 7.8). Once released from a damaged cell, mtDNA can signal to other cells by binding and activating TLR9. To determine if TLR9 activation is involved in suppression of MB, we treated TKPTS cells with the TLR9 ligands, ODN1585, ODN1826 and ODN2395, and exogenous mtDNA (Figure 7.9). Activation of TLR9 by ODN1826 and ODN2395 caused a dose-dependent decrease in expression of ND1, NDUF β 8 and PGC-1 α . ODN1585 and exogenous mtDNA isolated from mouse kidney reduced ND1 expression, but had no effect on expression of the other two genes. Further evaluation of these effects are needed at different times and doses, as well as assessment of the requirement for fragmentation or oxidation of mtDNA for TLR9 activation.

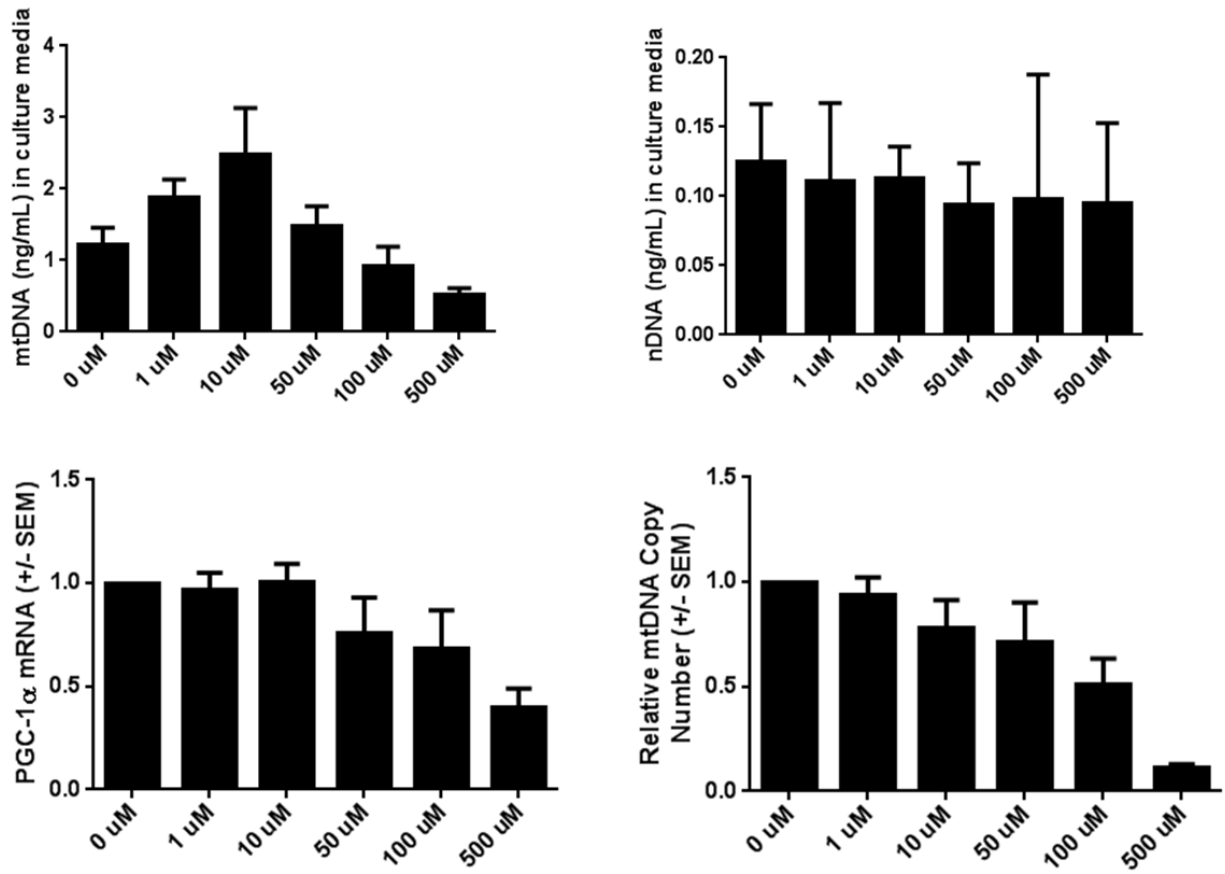


Figure 7.8. mtDNA is released after oxidant injury and is associated with suppression of cellular mtDNA content and PGC-1 α expression. TKPTS cells were treated with increasing doses of H₂O₂ for 24 h. mtDNA and nDNA were assessed in tissue culture media by qPCR. Cellular PGC-1 α mRNA expression and mtDNA copy number were measured by qPCR. n=4-6 per group.

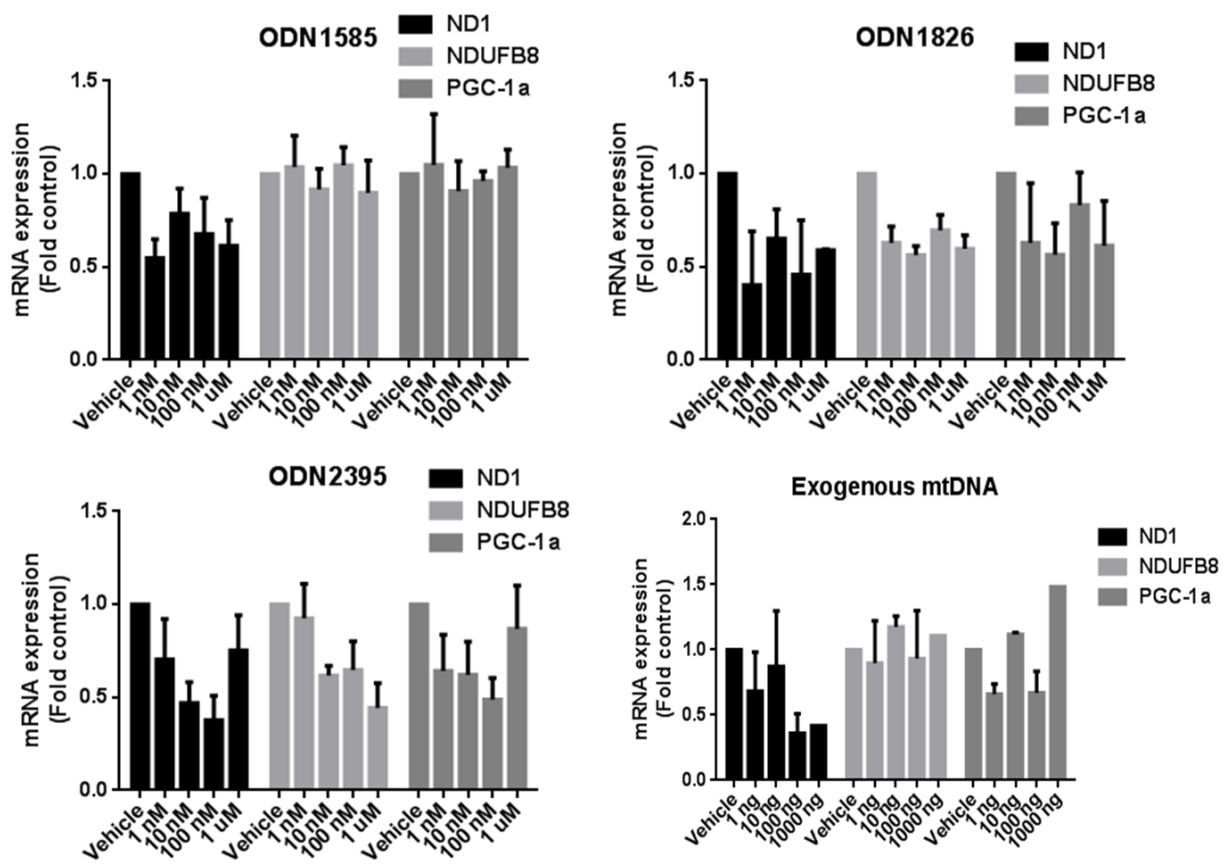


Figure 7.9. Effect of TLR9 agonists on mitochondrial gene expression in TKPTS cells. mRNA expression was measured by qPCR. n=1-3 per group.

REFERENCES

1. Kellum, J.A., N. Lameire, and K.A.G.W. Group, *Diagnosis, evaluation, and management of acute kidney injury: a KDIGO summary (Part 1)*. Crit Care, 2013. **17**(1): p. 204.
2. Kristensen, S.D., et al., *2014 ESC/ESA Guidelines on non-cardiac surgery: cardiovascular assessment and management: The Joint Task Force on non-cardiac surgery: cardiovascular assessment and management of the European Society of Cardiology (ESC) and the European Society of Anaesthesiology (ESA)*. Eur Heart J, 2014. **35**(35): p. 2383-431.
3. Kristensen, S.D., et al., *2014 ESC/ESA Guidelines on non-cardiac surgery: cardiovascular assessment and management: The Joint Task Force on non-cardiac surgery: cardiovascular assessment and management of the European Society of Cardiology (ESC) and the European Society of Anaesthesiology (ESA)*. Eur J Anaesthesiol, 2014.
4. Waikar, S.S., K.D. Liu, and G.M. Chertow, *Diagnosis, epidemiology and outcomes of acute kidney injury*. Clin J Am Soc Nephrol, 2008. **3**(3): p. 844-61.
5. Hoste, E.A. and M. Schurgers, *Epidemiology of acute kidney injury: how big is the problem?* Crit Care Med, 2008. **36**(4 Suppl): p. S146-51.
6. Rewa, O. and S.M. Bagshaw, *Acute kidney injury-epidemiology, outcomes and economics*. Nat Rev Nephrol, 2014. **10**(4): p. 193-207.
7. Wang, H.E., et al., *Acute kidney injury and mortality in hospitalized patients*. Am J Nephrol, 2012. **35**(4): p. 349-55.
8. Bagshaw, S.M., *Short- and long-term survival after acute kidney injury*. Nephrol Dial Transplant, 2008. **23**(7): p. 2126-8.
9. Chertow, G.M., et al., *Acute kidney injury, mortality, length of stay, and costs in hospitalized patients*. J Am Soc Nephrol, 2005. **16**(11): p. 3365-70.
10. Chawla, L.S., et al., *The severity of acute kidney injury predicts progression to chronic kidney disease*. Kidney Int, 2011. **79**(12): p. 1361-9.
11. Chawla, L.S., et al., *Acute kidney injury and chronic kidney disease as interconnected syndromes*. N Engl J Med, 2014. **371**(1): p. 58-66.
12. Bonventre, J.V. and L. Yang, *Cellular pathophysiology of ischemic acute kidney injury*. J Clin Invest, 2011. **121**(11): p. 4210-21.
13. Nash, K., A. Hafeez, and S. Hou, *Hospital-acquired renal insufficiency*. Am J Kidney Dis, 2002. **39**(5): p. 930-6.
14. Zarjou, A. and A. Agarwal, *Sepsis and acute kidney injury*. J Am Soc Nephrol, 2011. **22**(6): p. 999-1006.
15. Oliveira, J.F., et al., *Prevalence and risk factors for aminoglycoside nephrotoxicity in intensive care units*. Antimicrob Agents Chemother, 2009. **53**(7): p. 2887-91.
16. Park, S., S.P. Yoon, and J. Kim, *Cisplatin induces primary necrosis through poly(ADP-ribose) polymerase 1 activation in kidney proximal tubular cells*. Anat Cell Biol, 2015. **48**(1): p. 66-74.
17. Ozkok, A. and C.L. Edelstein, *Pathophysiology of cisplatin-induced acute kidney injury*. Biomed Res Int, 2014. **2014**: p. 967826.
18. Goldfarb, S., et al., *Contrast-induced acute kidney injury: specialty-specific protocols for interventional radiology, diagnostic computed tomography radiology, and interventional cardiology*. Mayo Clin Proc, 2009. **84**(2): p. 170-9.
19. Persson, P.B., *Contrast-induced nephropathy*. Eur Radiol, 2005. **15** Suppl 4: p. D65-9.
20. Ghosh, J., et al., *Acetaminophen induced renal injury via oxidative stress and TNF-alpha production: therapeutic potential of arjunolic acid*. Toxicology, 2010. **268**(1-2): p. 8-18.

21. Abraham, P., *Oxidative stress in paracetamol-induced pathogenesis: (I). Renal damage*. Indian J Biochem Biophys, 2005. **42**(1): p. 59-62.
22. Bonventre, J.V. and J.M. Weinberg, *Recent advances in the pathophysiology of ischemic acute renal failure*. J Am Soc Nephrol, 2003. **14**(8): p. 2199-210.
23. Thadhani, R., M. Pascual, and J.V. Bonventre, *Acute renal failure*. N Engl J Med, 1996. **334**(22): p. 1448-60.
24. Sharfuddin, A.A. and B.A. Molitoris, *Pathophysiology of ischemic acute kidney injury*. Nat Rev Nephrol, 2011. **7**(4): p. 189-200.
25. Conger, J.D. and J.V. Weil, *Abnormal vascular function following ischemia-reperfusion injury*. J Investig Med, 1995. **43**(5): p. 431-42.
26. Solez, K., et al., *Medullary plasma flow and intravascular leukocyte accumulation in acute renal failure*. Kidney Int, 1974. **6**(1): p. 24-37.
27. Bonventre, J.V., *Pathophysiology of AKI: injury and normal and abnormal repair*. Contrib Nephrol, 2010. **165**: p. 9-17.
28. Molitoris, B.A. and R.M. Sandoval, *Intravital multiphoton microscopy of dynamic renal processes*. Am J Physiol Renal Physiol, 2005. **288**(6): p. F1084-9.
29. Gonzalez-Flecha, B. and A. Boveris, *Mitochondrial sites of hydrogen peroxide production in reperfused rat kidney cortex*. Biochim Biophys Acta, 1995. **1243**(3): p. 361-6.
30. Vetterlein, F., et al., *Disturbances in renal microcirculation induced by myoglobin and hemorrhagic hypotension in anesthetized rat*. Am J Physiol, 1995. **268**(5 Pt 2): p. F839-46.
31. Lieberthal, W., S.A. Menza, and J.S. Levine, *Graded ATP depletion can cause necrosis or apoptosis of cultured mouse proximal tubular cells*. Am J Physiol, 1998. **274**(2 Pt 2): p. F315-27.
32. Breggia, A.C. and J. Himmelfarb, *Primary mouse renal tubular epithelial cells have variable injury tolerance to ischemic and chemical mediators of oxidative stress*. Oxid Med Cell Longev, 2008. **1**(1): p. 33-8.
33. Dong, Z., et al., *Development of porous defects in plasma membranes of adenosine triphosphate-depleted Madin-Darby canine kidney cells and its inhibition by glycine*. Lab Invest, 1998. **78**(6): p. 657-68.
34. Bonventre, J.V., *Mechanisms of ischemic acute renal failure*. Kidney Int, 1993. **43**(5): p. 1160-78.
35. Kobryn, C.E. and L.J. Mandel, *Decreased protein phosphorylation induced by anoxia in proximal renal tubules*. Am J Physiol, 1994. **267**(4 Pt 1): p. C1073-9.
36. Sutton, T.A. and B.A. Molitoris, *Mechanisms of cellular injury in ischemic acute renal failure*. Semin Nephrol, 1998. **18**(5): p. 490-7.
37. Kaushal, G.P., A.G. Basnakian, and S.V. Shah, *Apoptotic pathways in ischemic acute renal failure*. Kidney Int, 2004. **66**(2): p. 500-6.
38. Saikumar, P. and M.A. Venkatachalam, *Role of apoptosis in hypoxic/ischemic damage in the kidney*. Semin Nephrol, 2003. **23**(6): p. 511-21.
39. Burns, A.T., et al., *Apoptosis in ischemia/reperfusion injury of human renal allografts*. Transplantation, 1998. **66**(7): p. 872-6.
40. Oberbauer, R., et al., *Apoptosis of tubular epithelial cells in donor kidney biopsies predicts early renal allograft function*. J Am Soc Nephrol, 1999. **10**(9): p. 2006-13.
41. Zager, R.A., *'Biologic memory' in response to acute kidney injury: cytoresistance, toll-like receptor hyper-responsiveness and the onset of progressive renal disease*. Nephrol Dial Transplant, 2013. **28**(8): p. 1985-93.
42. Bershadsky, A.D. and V.I. Gelfand, *ATP-dependent regulation of cytoplasmic microtubule disassembly*. Proc Natl Acad Sci U S A, 1981. **78**(6): p. 3610-3.
43. Bershadsky, A.D. and V.I. Gelfand, *Role of ATP in the regulation of stability of cytoskeletal structures*. Cell Biol Int Rep, 1983. **7**(3): p. 173-87.

44. Adelstein, R.S. and E. Eisenberg, *Regulation and kinetics of the actin-myosin-ATP interaction*. Annu Rev Biochem, 1980. **49**: p. 921-56.
45. Devarajan, P., *Update on mechanisms of ischemic acute kidney injury*. J Am Soc Nephrol, 2006. **17**(6): p. 1503-20.
46. Coudrier, E., D. Kerjaschki, and D. Louvard, *Cytoskeleton organization and submembranous interactions in intestinal and renal brush borders*. Kidney Int, 1988. **34**(3): p. 309-20.
47. Niggli, V. and M.M. Burger, *Interaction of the cytoskeleton with the plasma membrane*. J Membr Biol, 1987. **100**(2): p. 97-121.
48. Mirabelli, F., et al., *Cytoskeletal alterations in human platelets exposed to oxidative stress are mediated by oxidative and Ca²⁺-dependent mechanisms*. Arch Biochem Biophys, 1989. **270**(2): p. 478-88.
49. Thor, H., et al., *Alterations in hepatocyte cytoskeleton caused by redox cycling and alkylating quinones*. Arch Biochem Biophys, 1988. **266**(2): p. 397-407.
50. Yancey, D.M., et al., *Cardiomyocyte mitochondrial oxidative stress and cytoskeletal breakdown in the heart with a primary volume overload*. Am J Physiol Heart Circ Physiol, 2015. **308**(6): p. H651-63.
51. Glaumann, B., *Effect of mannitol, dextran (macrodex), allopurinol, and methylprednisolone on the morphology of the proximal tubule of the rat kidney made ischemic in vivo*. Virchows Arch B Cell Pathol, 1977. **23**(4): p. 297-323.
52. Glaumann, B., et al., *Studies on cellular recovery from injury. II. Ultrastructural studies on the recovery of the pars convoluta of the proximal tubule of the rat kidney from temporary ischemia*. Virchows Arch B Cell Pathol, 1977. **24**(1): p. 1-18.
53. Venkatachalam, M.A., et al., *Mechanism of proximal tubule brush border loss and regeneration following mild renal ischemia*. Lab Invest, 1981. **45**(4): p. 355-65.
54. Kwon, O., et al., *Sodium reabsorption and distribution of Na⁺/K⁺-ATPase during postischemic injury to the renal allograft*. Kidney Int, 1999. **55**(3): p. 963-75.
55. Molitoris, B.A., *Na⁺-K⁺-ATPase that redistributes to apical membrane during ATP depletion remains functional*. Am J Physiol, 1993. **265**(5 Pt 2): p. F693-7.
56. Molitoris, B.A., et al., *Loss of epithelial polarity: a novel hypothesis for reduced proximal tubule Na⁺ transport following ischemic injury*. J Membr Biol, 1989. **107**(2): p. 119-27.
57. Basile, D.P., M.D. Anderson, and T.A. Sutton, *Pathophysiology of acute kidney injury*. Compr Physiol, 2012. **2**(2): p. 1303-53.
58. Nadasdy, T., et al., *Proliferative activity of intrinsic cell populations in the normal human kidney*. J Am Soc Nephrol, 1994. **4**(12): p. 2032-9.
59. Papadimou, E., et al., *Direct Reprogramming of Human Bone Marrow Stromal Cells into Functional Renal Cells Using Cell-free Extracts*. Stem Cell Reports, 2015. **4**(4): p. 685-98.
60. Lin, F., et al., *Hematopoietic stem cells contribute to the regeneration of renal tubules after renal ischemia-reperfusion injury in mice*. J Am Soc Nephrol, 2003. **14**(5): p. 1188-99.
61. Humphreys, B.D. and J.V. Bonventre, *Mesenchymal stem cells in acute kidney injury*. Annu Rev Med, 2008. **59**: p. 311-25.
62. da Silva, L.B., et al., *Evaluation of stem cell administration in a model of kidney ischemia-reperfusion injury*. Int Immunopharmacol, 2007. **7**(13): p. 1609-16.
63. Humphreys, B.D. and J.V. Bonventre, *The contribution of adult stem cells to renal repair*. Nephrol Ther, 2007. **3**(1): p. 3-10.
64. Semedo, P., et al., *Mesenchymal stem cells ameliorate tissue damages triggered by renal ischemia and reperfusion injury*. Transplant Proc, 2007. **39**(2): p. 421-3.
65. Stokman, G., et al., *Hematopoietic stem cell mobilization therapy accelerates recovery of renal function independent of stem cell contribution*. J Am Soc Nephrol, 2005. **16**(6): p. 1684-92.

66. Duffield, J.S., et al., *Conditional ablation of macrophages halts progression of crescentic glomerulonephritis*. Am J Pathol, 2005. **167**(5): p. 1207-19.
67. Hallman, M.A., S. Zhuang, and R.G. Schnellmann, *Regulation of dedifferentiation and redifferentiation in renal proximal tubular cells by the epidermal growth factor receptor*. J Pharmacol Exp Ther, 2008. **325**(2): p. 520-8.
68. Witzgall, R., et al., *Localization of proliferating cell nuclear antigen, vimentin, c-Fos, and clusterin in the postischemic kidney. Evidence for a heterogenous genetic response among nephron segments, and a large pool of mitotically active and dedifferentiated cells*. J Clin Invest, 1994. **93**(5): p. 2175-88.
69. Zhuang, S., et al., *p38 kinase-mediated transactivation of the epidermal growth factor receptor is required for dedifferentiation of renal epithelial cells after oxidant injury*. J Biol Chem, 2005. **280**(22): p. 21036-42.
70. Nony, P.A. and R.G. Schnellmann, *Interactions between collagen IV and collagen-binding integrins in renal cell repair after sublethal injury*. Mol Pharmacol, 2001. **60**(6): p. 1226-34.
71. Nony, P.A., G. Nowak, and R.G. Schnellmann, *Collagen IV promotes repair of renal cell physiological functions after toxicant injury*. Am J Physiol Renal Physiol, 2001. **281**(3): p. F443-53.
72. Nony, P.A. and R.G. Schnellmann, *Mechanisms of renal cell repair and regeneration after acute renal failure*. J Pharmacol Exp Ther, 2003. **304**(3): p. 905-12.
73. Venkatachalam, M.A., et al., *Failed Tubule Recovery, AKI-CKD Transition, and Kidney Disease Progression*. J Am Soc Nephrol, 2015.
74. Chawla, L.S., *Acute kidney injury leading to chronic kidney disease and long-term outcomes of acute kidney injury: the best opportunity to mitigate acute kidney injury?* Contrib Nephrol, 2011. **174**: p. 182-90.
75. Yang, L., et al., *Epithelial cell cycle arrest in G2/M mediates kidney fibrosis after injury*. Nat Med, 2010. **16**(5): p. 535-43, 1p following 143.
76. Humphreys, B.D., et al., *Fate tracing reveals the pericyte and not epithelial origin of myofibroblasts in kidney fibrosis*. Am J Pathol, 2010. **176**(1): p. 85-97.
77. Humphreys, B.D., et al., *Intrinsic epithelial cells repair the kidney after injury*. Cell Stem Cell, 2008. **2**(3): p. 284-91.
78. Iwano, M., et al., *Evidence that fibroblasts derive from epithelium during tissue fibrosis*. J Clin Invest, 2002. **110**(3): p. 341-50.
79. Kriz, W., B. Kaissling, and M. Le Hir, *Epithelial-mesenchymal transition (EMT) in kidney fibrosis: fact or fantasy?* J Clin Invest, 2011. **121**(2): p. 468-74.
80. Zeisberg, M. and E.G. Neilson, *Mechanisms of tubulointerstitial fibrosis*. J Am Soc Nephrol, 2010. **21**(11): p. 1819-34.
81. Zeisberg, M. and J.S. Duffield, *Resolved: EMT produces fibroblasts in the kidney*. J Am Soc Nephrol, 2010. **21**(8): p. 1247-53.
82. Delbridge, M.S., et al., *The effect of body temperature in a rat model of renal ischemia-reperfusion injury*. Transplant Proc, 2007. **39**(10): p. 2983-5.
83. Wang, H.J., et al., *Ischemia/reperfusion-induced renal failure in rats as a model for evaluating cell therapies*. Ren Fail, 2012. **34**(10): p. 1324-32.
84. Susa, D., et al., *Congenital DNA repair deficiency results in protection against renal ischemia reperfusion injury in mice*. Aging Cell, 2009. **8**(2): p. 192-200.
85. Heyman, S.N., et al., *Animal models of acute tubular necrosis*. Curr Opin Crit Care, 2002. **8**(6): p. 526-34.
86. Gupta, A., et al., *Folic acid induces acute renal failure (ARF) by enhancing renal prooxidant state*. Exp Toxicol Pathol, 2012. **64**(3): p. 225-32.

87. Fink, M., M. Henry, and J.D. Tange, *Experimental folic acid nephropathy*. Pathology, 1987. **19**(2): p. 143-9.
88. Doi, K., et al., *Attenuation of folic acid-induced renal inflammatory injury in platelet-activating factor receptor-deficient mice*. Am J Pathol, 2006. **168**(5): p. 1413-24.
89. Yang, H.C., Y. Zuo, and A.B. Fogo, *Models of chronic kidney disease*. Drug Discov Today Dis Models, 2010. **7**(1-2): p. 13-19.
90. Vaidya, V.S., et al., *Urinary biomarkers for sensitive and specific detection of acute kidney injury in humans*. Clin Transl Sci, 2008. **1**(3): p. 200-8.
91. Ichimura, T., et al., *Kidney injury molecule-1 (KIM-1), a putative epithelial cell adhesion molecule containing a novel immunoglobulin domain, is up-regulated in renal cells after injury*. J Biol Chem, 1998. **273**(7): p. 4135-42.
92. Vaidya, V.S., et al., *Kidney injury molecule-1 outperforms traditional biomarkers of kidney injury in preclinical biomarker qualification studies*. Nat Biotechnol, 2010. **28**(5): p. 478-85.
93. Hoffmann, D., et al., *Performance of novel kidney biomarkers in preclinical toxicity studies*. Toxicol Sci, 2010. **116**(1): p. 8-22.
94. Sabbisetti, V.S., et al., *Novel assays for detection of urinary KIM-1 in mouse models of kidney injury*. Toxicol Sci, 2013. **131**(1): p. 13-25.
95. Han, W.K., et al., *Urinary biomarkers in the early detection of acute kidney injury after cardiac surgery*. Clin J Am Soc Nephrol, 2009. **4**(5): p. 873-82.
96. Damman, K., et al., *Tubular damage in chronic systolic heart failure is associated with reduced survival independent of glomerular filtration rate*. Heart, 2010. **96**(16): p. 1297-302.
97. Szeto, C.C., et al., *Urinary expression of kidney injury markers in renal transplant recipients*. Clin J Am Soc Nephrol, 2010. **5**(12): p. 2329-37.
98. van Timmeren, M.M., et al., *Tubular kidney injury molecule-1 (KIM-1) in human renal disease*. J Pathol, 2007. **212**(2): p. 209-17.
99. Devarajan, P., et al., *Gene expression in early ischemic renal injury: clues towards pathogenesis, biomarker discovery, and novel therapeutics*. Mol Genet Metab, 2003. **80**(4): p. 365-76.
100. Supavekin, S., et al., *Differential gene expression following early renal ischemia/reperfusion*. Kidney Int, 2003. **63**(5): p. 1714-24.
101. Perrotti, A., et al., *Neutrophil gelatinase-associated lipocalin as early predictor of acute kidney injury after cardiac surgery in adults with chronic kidney failure*. Ann Thorac Surg, 2015. **99**(3): p. 864-9.
102. Devarajan, P., *Neutrophil gelatinase-associated lipocalin (NGAL): a new marker of kidney disease*. Scand J Clin Lab Invest Suppl, 2008. **241**: p. 89-94.
103. Wheeler, D.S., et al., *Serum neutrophil gelatinase-associated lipocalin (NGAL) as a marker of acute kidney injury in critically ill children with septic shock*. Crit Care Med, 2008. **36**(4): p. 1297-303.
104. Lassnigg, A., et al., *Lack of renoprotective effects of dopamine and furosemide during cardiac surgery*. J Am Soc Nephrol, 2000. **11**(1): p. 97-104.
105. Stone, G.W., et al., *Fenoldopam mesylate for the prevention of contrast-induced nephropathy: a randomized controlled trial*. JAMA, 2003. **290**(17): p. 2284-91.
106. Kramer, B.K., et al., *Lack of renoprotective effect of theophylline during aortocoronary bypass surgery*. Nephrol Dial Transplant, 2002. **17**(5): p. 910-5.
107. Garg, A.X., et al., *Perioperative aspirin and clonidine and risk of acute kidney injury: a randomized clinical trial*. JAMA, 2014. **312**(21): p. 2254-64.
108. Loeff, B.G., et al., *Effect of dexamethasone on perioperative renal function impairment during cardiac surgery with cardiopulmonary bypass*. Br J Anaesth, 2004. **93**(6): p. 793-8.

109. Haase, M., et al., *Phase II, randomized, controlled trial of high-dose N-acetylcysteine in high-risk cardiac surgery patients*. Crit Care Med, 2007. **35**(5): p. 1324-31.
110. Haase, M., et al., *Sodium bicarbonate to prevent increases in serum creatinine after cardiac surgery: a pilot double-blind, randomized controlled trial*. Crit Care Med, 2009. **37**(1): p. 39-47.
111. Xinwei, J., et al., *Comparison of usefulness of simvastatin 20 mg versus 80 mg in preventing contrast-induced nephropathy in patients with acute coronary syndrome undergoing percutaneous coronary intervention*. Am J Cardiol, 2009. **104**(4): p. 519-24.
112. Song, Y.R., et al., *Prevention of acute kidney injury by erythropoietin in patients undergoing coronary artery bypass grafting: a pilot study*. Am J Nephrol, 2009. **30**(3): p. 253-60.
113. Morikawa, S., et al., *Renal protective effects and the prevention of contrast-induced nephropathy by atrial natriuretic peptide*. J Am Coll Cardiol, 2009. **53**(12): p. 1040-6.
114. Morelli, A., et al., *Prophylactic fenoldopam for renal protection in sepsis: a randomized, double-blind, placebo-controlled pilot trial*. Crit Care Med, 2005. **33**(11): p. 2451-6.
115. Kaya, K., et al., *The effect of sodium nitroprusside infusion on renal function during reperfusion period in patients undergoing coronary artery bypass grafting: a prospective randomized clinical trial*. Eur J Cardiothorac Surg, 2007. **31**(2): p. 290-7.
116. Kulka, P.J., M. Tryba, and M. Zenz, *Preoperative alpha2-adrenergic receptor agonists prevent the deterioration of renal function after cardiac surgery: results of a randomized, controlled trial*. Crit Care Med, 1996. **24**(6): p. 947-52.
117. Chandel, N.S., *Mitochondria as signaling organelles*. BMC Biol, 2014. **12**: p. 34.
118. Kotiadis, V.N., M.R. Duchen, and L.D. Osellame, *Mitochondrial quality control and communications with the nucleus are important in maintaining mitochondrial function and cell health*. Biochim Biophys Acta, 2014. **1840**(4): p. 1254-65.
119. De Bock, K., M. Georgiadou, and P. Carmeliet, *Role of endothelial cell metabolism in vessel sprouting*. Cell Metab, 2013. **18**(5): p. 634-47.
120. Baker, M.J., T. Tatsuta, and T. Langer, *Quality control of mitochondrial proteostasis*. Cold Spring Harb Perspect Biol, 2011. **3**(7).
121. Youle, R.J. and D.P. Narendra, *Mechanisms of mitophagy*. Nat Rev Mol Cell Biol, 2011. **12**(1): p. 9-14.
122. Nunnari, J. and A. Suomalainen, *Mitochondria: in sickness and in health*. Cell, 2012. **148**(6): p. 1145-59.
123. Ishikawa, K., et al., *ROS-generating mitochondrial DNA mutations can regulate tumor cell metastasis*. Science, 2008. **320**(5876): p. 661-4.
124. Cohen, R.A. and X. Tong, *Vascular oxidative stress: the common link in hypertensive and diabetic vascular disease*. J Cardiovasc Pharmacol, 2010. **55**(4): p. 308-16.
125. Andreux, P.A., R.H. Houtkooper, and J. Auwerx, *Pharmacological approaches to restore mitochondrial function*. Nat Rev Drug Discov, 2013. **12**(6): p. 465-83.
126. Stallons, L.J., J.A. Funk, and R.G. Schnellmann, *Mitochondrial Homeostasis in Acute Organ Failure*. Curr Pathobiol Rep, 2013. **1**(3).
127. Sanderson, T.H., et al., *Molecular mechanisms of ischemia-reperfusion injury in brain: pivotal role of the mitochondrial membrane potential in reactive oxygen species generation*. Mol Neurobiol, 2013. **47**(1): p. 9-23.
128. Hausenloy, D.J. and D.M. Yellon, *Myocardial ischemia-reperfusion injury: a neglected therapeutic target*. J Clin Invest, 2013. **123**(1): p. 92-100.
129. McEwen, M.L., et al., *Targeting mitochondrial function for the treatment of acute spinal cord injury*. Neurotherapeutics, 2011. **8**(2): p. 168-79.

130. McGill, M.R., et al., *The mechanism underlying acetaminophen-induced hepatotoxicity in humans and mice involves mitochondrial damage and nuclear DNA fragmentation*. J Clin Invest, 2012. **122**(4): p. 1574-83.
131. Naguib, Y.M., et al., *Pleurotus ostreatus opposes mitochondrial dysfunction and oxidative stress in acetaminophen-induced hepato-renal injury*. BMC Complement Altern Med, 2014. **14**: p. 494.
132. Blake, R. and I.A. Trounce, *Mitochondrial dysfunction and complications associated with diabetes*. Biochim Biophys Acta, 2014. **1840**(4): p. 1404-12.
133. Moreira, P.I., et al., *Mitochondrial dysfunction is a trigger of Alzheimer's disease pathophysiology*. Biochim Biophys Acta, 2010. **1802**(1): p. 2-10.
134. Chaturvedi, R.K. and M. Flint Beal, *Mitochondrial diseases of the brain*. Free Radic Biol Med, 2013. **63**: p. 1-29.
135. Chaturvedi, R.K. and M.F. Beal, *Mitochondria targeted therapeutic approaches in Parkinson's and Huntington's diseases*. Mol Cell Neurosci, 2013. **55**: p. 101-14.
136. Cozzolino, M. and M.T. Carri, *Mitochondrial dysfunction in ALS*. Prog Neurobiol, 2012. **97**(2): p. 54-66.
137. Moskowitz, M.A., E.H. Lo, and C. Iadecola, *The science of stroke: mechanisms in search of treatments*. Neuron, 2010. **67**(2): p. 181-98.
138. Kalogeris, T., Y. Bao, and R.J. Korthuis, *Mitochondrial reactive oxygen species: a double edged sword in ischemia/reperfusion vs preconditioning*. Redox Biol, 2014. **2**: p. 702-14.
139. Andreadou, I., et al., *To prevent, protect and save the ischemic heart: antioxidants revisited*. Expert Opin Ther Targets, 2009. **13**(8): p. 945-56.
140. Adlam, V.J., et al., *Targeting an antioxidant to mitochondria decreases cardiac ischemia-reperfusion injury*. FASEB J, 2005. **19**(9): p. 1088-95.
141. Sun, S.Y., *N-acetylcysteine, reactive oxygen species and beyond*. Cancer Biol Ther, 2010. **9**(2): p. 109-10.
142. Skyschally, A., R. Schulz, and G. Heusch, *Cyclosporine A at reperfusion reduces infarct size in pigs*. Cardiovasc Drugs Ther, 2010. **24**(1): p. 85-7.
143. Osman, M.M., et al., *Cyclosporine-A as a neuroprotective agent against stroke: its translation from laboratory research to clinical application*. Neuropeptides, 2011. **45**(6): p. 359-68.
144. O'Connell, S., et al., *Cyclosporine A--induced oxidative stress in human renal mesangial cells: a role for ERK 1/2 MAPK signaling*. Toxicol Sci, 2012. **126**(1): p. 101-13.
145. Jiang, H.K., et al., *Aerobic interval training protects against myocardial infarction-induced oxidative injury by enhancing antioxidant system and mitochondrial biosynthesis*. Clin Exp Pharmacol Physiol, 2014. **41**(3): p. 192-201.
146. Ikeuchi, M., et al., *Overexpression of mitochondrial transcription factor a ameliorates mitochondrial deficiencies and cardiac failure after myocardial infarction*. Circulation, 2005. **112**(5): p. 683-90.
147. Hokari, M., et al., *Overexpression of mitochondrial transcription factor A (TFAM) ameliorates delayed neuronal death due to transient forebrain ischemia in mice*. Neuropathology, 2010. **30**(4): p. 401-7.
148. Jesinkey, S.R., et al., *Formoterol restores mitochondrial and renal function after ischemia-reperfusion injury*. J Am Soc Nephrol, 2014. **25**(6): p. 1157-62.
149. Whitaker, R.M., et al., *cGMP-selective phosphodiesterase inhibitors stimulate mitochondrial biogenesis and promote recovery from acute kidney injury*. J Pharmacol Exp Ther, 2013. **347**(3): p. 626-34.
150. Garrett, S.M., et al., *Agonism of the 5-hydroxytryptamine 1F receptor promotes mitochondrial biogenesis and recovery from acute kidney injury*. J Pharmacol Exp Ther, 2014. **350**(2): p. 257-64.

151. Dam, A.D., A.S. Mitchell, and J. Quadrilatero, *Induction of mitochondrial biogenesis protects against caspase-dependent and caspase-independent apoptosis in L6 myoblasts*. Biochim Biophys Acta, 2013. **1833**(12): p. 3426-35.
152. Feldkamp, T., A. Kribben, and J.M. Weinberg, *Assessment of mitochondrial membrane potential in proximal tubules after hypoxia-reoxygenation*. Am J Physiol Renal Physiol, 2005. **288**(6): p. F1092-102.
153. Hall, A.M. and R.J. Unwin, *The not so 'mighty chondrion': emergence of renal diseases due to mitochondrial dysfunction*. Nephron Physiol, 2007. **105**(1): p. p1-10.
154. Jassem, W., et al., *The role of mitochondria in ischemia/reperfusion injury*. Transplantation, 2002. **73**(4): p. 493-9.
155. Jassem, W. and N.D. Heaton, *The role of mitochondria in ischemia/reperfusion injury in organ transplantation*. Kidney Int, 2004. **66**(2): p. 514-7.
156. Weinberg, J.M., et al., *Mitochondrial dysfunction during hypoxia/reoxygenation and its correction by anaerobic metabolism of citric acid cycle intermediates*. Proc Natl Acad Sci U S A, 2000. **97**(6): p. 2826-31.
157. Plotnikov, E.Y., et al., *The role of mitochondria in oxidative and nitrosative stress during ischemia/reperfusion in the rat kidney*. Kidney Int, 2007. **72**(12): p. 1493-502.
158. Shah, S.V. and P.D. Walker, *Evidence suggesting a role for hydroxyl radical in glycerol-induced acute renal failure*. Am J Physiol, 1988. **255**(3 Pt 2): p. F438-43.
159. Zager, R.A., *Mitochondrial free radical production induces lipid peroxidation during myohemoglobinuria*. Kidney Int, 1996. **49**(3): p. 741-51.
160. Brooks, C., et al., *Regulation of mitochondrial dynamics in acute kidney injury in cell culture and rodent models*. J Clin Invest, 2009. **119**(5): p. 1275-85.
161. Funk, J.A. and R.G. Schnellmann, *Persistent disruption of mitochondrial homeostasis after acute kidney injury*. Am J Physiol Renal Physiol, 2012. **302**(7): p. F853-64.
162. Funk, J.A., S. Odejinmi, and R.G. Schnellmann, *SRT1720 induces mitochondrial biogenesis and rescues mitochondrial function after oxidant injury in renal proximal tubule cells*. J Pharmacol Exp Ther, 2010. **333**(2): p. 593-601.
163. Che, R., et al., *Mitochondrial dysfunction in the pathophysiology of renal diseases*. Am J Physiol Renal Physiol, 2014. **306**(4): p. F367-78.
164. Baker, B.M. and C.M. Haynes, *Mitochondrial protein quality control during biogenesis and aging*. Trends Biochem Sci, 2011. **36**(5): p. 254-61.
165. Baker, M.J., C.S. Palmer, and D. Stojanovski, *Mitochondrial protein quality control in health and disease*. Br J Pharmacol, 2014. **171**(8): p. 1870-89.
166. Schapira, A.H., *Mitochondria in the aetiology and pathogenesis of Parkinson's disease*. Lancet Neurol, 2008. **7**(1): p. 97-109.
167. Bezard, E., et al., *Animal models of Parkinson's disease: limits and relevance to neuroprotection studies*. Mov Disord, 2013. **28**(1): p. 61-70.
168. Luo, Y. and G.S. Roth, *The roles of dopamine oxidative stress and dopamine receptor signaling in aging and age-related neurodegeneration*. Antioxid Redox Signal, 2000. **2**(3): p. 449-60.
169. Zheng, B., et al., *PGC-1alpha, a potential therapeutic target for early intervention in Parkinson's disease*. Sci Transl Med, 2010. **2**(52): p. 52ra73.
170. Youdim, M.B. and Y.J. Oh, *Promise of neurorestoration and mitochondrial biogenesis in Parkinson's disease with multi target drugs: an alternative to stem cell therapy*. Exp Neurol, 2013. **22**(3): p. 167-72.
171. Scarpulla, R.C., *Metabolic control of mitochondrial biogenesis through the PGC-1 family regulatory network*. Biochim Biophys Acta, 2011. **1813**(7): p. 1269-78.

172. Corona, J.C. and M.R. Duchon, *PPARgamma and PGC-1alpha as Therapeutic Targets in Parkinson's*. *Neurochem Res*, 2015. **40**(2): p. 308-16.
173. St-Pierre, J., et al., *Suppression of reactive oxygen species and neurodegeneration by the PGC-1 transcriptional coactivators*. *Cell*, 2006. **127**(2): p. 397-408.
174. Dulovic, M., et al., *The protective role of AMP-activated protein kinase in alpha-synuclein neurotoxicity in vitro*. *Neurobiol Dis*, 2014. **63**: p. 1-11.
175. Martin, S.D. and S.L. McGee, *The role of mitochondria in the aetiology of insulin resistance and type 2 diabetes*. *Biochim Biophys Acta*, 2014. **1840**(4): p. 1303-12.
176. Mootha, V.K., et al., *PGC-1alpha-responsive genes involved in oxidative phosphorylation are coordinately downregulated in human diabetes*. *Nat Genet*, 2003. **34**(3): p. 267-73.
177. Calabrese, V., et al., *Oxidative stress, glutathione status, sirtuin and cellular stress response in type 2 diabetes*. *Biochim Biophys Acta*, 2012. **1822**(5): p. 729-36.
178. Robbins, N.M. and R.A. Swanson, *Opposing effects of glucose on stroke and reperfusion injury: acidosis, oxidative stress, and energy metabolism*. *Stroke*, 2014. **45**(6): p. 1881-6.
179. Ishihara, M., *Acute Hyperglycemia in Patients With Acute Myocardial Infarction*. *Circulation Journal*, 2012. **76**(3): p. 563-571.
180. Melin, J., O. Hellberg, and B. Fellstrom, *Hyperglycaemia and renal ischaemia-reperfusion injury*. *Nephrol Dial Transplant*, 2003. **18**(3): p. 460-2.
181. Attardi, G. and G. Schatz, *Biogenesis of mitochondria*. *Annu Rev Cell Biol*, 1988. **4**: p. 289-333.
182. Nisoli, E., et al., *Mitochondrial biogenesis as a cellular signaling framework*. *Biochem Pharmacol*, 2004. **67**(1): p. 1-15.
183. Puigserver, P., et al., *A cold-inducible coactivator of nuclear receptors linked to adaptive thermogenesis*. *Cell*, 1998. **92**(6): p. 829-39.
184. Yin, W., et al., *Rapidly increased neuronal mitochondrial biogenesis after hypoxic-ischemic brain injury*. *Stroke*, 2008. **39**(11): p. 3057-63.
185. Piantadosi, C.A., et al., *Heme oxygenase-1 couples activation of mitochondrial biogenesis to anti-inflammatory cytokine expression*. *J Biol Chem*, 2011. **286**(18): p. 16374-85.
186. Scarpulla, R.C., *Nucleus-encoded regulators of mitochondrial function: integration of respiratory chain expression, nutrient sensing and metabolic stress*. *Biochim Biophys Acta*, 2012. **1819**(9-10): p. 1088-97.
187. Scarpulla, R.C., *Transcriptional paradigms in mammalian mitochondrial biogenesis and function*. *Physiol Rev*, 2008. **88**(2): p. 611-38.
188. Scarpulla, R.C., R.B. Vega, and D.P. Kelly, *Transcriptional integration of mitochondrial biogenesis*. *Trends Endocrinol Metab*, 2012. **23**(9): p. 459-66.
189. Hock, M.B. and A. Kralli, *Transcriptional control of mitochondrial biogenesis and function*. *Annu Rev Physiol*, 2009. **71**: p. 177-203.
190. Rockl, K.S., C.A. Witczak, and L.J. Goodyear, *Signaling mechanisms in skeletal muscle: acute responses and chronic adaptations to exercise*. *IUBMB Life*, 2008. **60**(3): p. 145-53.
191. Cartoni, R., et al., *Mitofusins 1/2 and ERRalpha expression are increased in human skeletal muscle after physical exercise*. *J Physiol*, 2005. **567**(Pt 1): p. 349-58.
192. McClelland, G.B., et al., *Temperature- and exercise-induced gene expression and metabolic enzyme changes in skeletal muscle of adult zebrafish (Danio rerio)*. *J Physiol*, 2006. **577**(Pt 2): p. 739-51.
193. Pilegaard, H., B. Saltin, and P.D. Neuffer, *Exercise induces transient transcriptional activation of the PGC-1alpha gene in human skeletal muscle*. *J Physiol*, 2003. **546**(Pt 3): p. 851-8.
194. Russell, A.P., et al., *Regulation of metabolic transcriptional co-activators and transcription factors with acute exercise*. *FASEB J*, 2005. **19**(8): p. 986-8.

195. Chow, L.S., et al., *Impact of endurance training on murine spontaneous activity, muscle mitochondrial DNA abundance, gene transcripts, and function*. J Appl Physiol (1985), 2007. **102**(3): p. 1078-89.
196. Cao, W., et al., *p38 mitogen-activated protein kinase is the central regulator of cyclic AMP-dependent transcription of the brown fat uncoupling protein 1 gene*. Mol Cell Biol, 2004. **24**(7): p. 3057-67.
197. Puigserver, P. and B.M. Spiegelman, *Peroxisome proliferator-activated receptor-gamma coactivator 1 alpha (PGC-1 alpha): transcriptional coactivator and metabolic regulator*. Endocr Rev, 2003. **24**(1): p. 78-90.
198. Civitarese, A.E., et al., *Calorie restriction increases muscle mitochondrial biogenesis in healthy humans*. PLoS Med, 2007. **4**(3): p. e76.
199. Lopez-Lluch, G., et al., *Calorie restriction induces mitochondrial biogenesis and bioenergetic efficiency*. Proc Natl Acad Sci U S A, 2006. **103**(6): p. 1768-73.
200. Nisoli, E., et al., *Calorie restriction promotes mitochondrial biogenesis by inducing the expression of eNOS*. Science, 2005. **310**(5746): p. 314-7.
201. Borniquel, S., et al., *Nitric oxide regulates mitochondrial oxidative stress protection via the transcriptional coactivator PGC-1alpha*. FASEB J, 2006. **20**(11): p. 1889-91.
202. Gerhart-Hines, Z., et al., *Metabolic control of muscle mitochondrial function and fatty acid oxidation through SIRT1/PGC-1alpha*. EMBO J, 2007. **26**(7): p. 1913-23.
203. Jager, S., et al., *AMP-activated protein kinase (AMPK) action in skeletal muscle via direct phosphorylation of PGC-1alpha*. Proc Natl Acad Sci U S A, 2007. **104**(29): p. 12017-22.
204. Rasbach, K.A. and R.G. Schnellmann, *Signaling of mitochondrial biogenesis following oxidant injury*. J Biol Chem, 2007. **282**(4): p. 2355-62.
205. Nowak, G., et al., *Recovery of cellular functions following oxidant injury*. Am J Physiol, 1998. **274**(3 Pt 2): p. F509-15.
206. Gillissen, A. and D. Nowak, *Characterization of N-acetylcysteine and ambroxol in anti-oxidant therapy*. Respir Med, 1998. **92**(4): p. 609-23.
207. Rasbach, K.A. and R.G. Schnellmann, *PGC-1alpha over-expression promotes recovery from mitochondrial dysfunction and cell injury*. Biochem Biophys Res Commun, 2007. **355**(3): p. 734-9.
208. Kukidome, D., et al., *Activation of AMP-activated protein kinase reduces hyperglycemia-induced mitochondrial reactive oxygen species production and promotes mitochondrial biogenesis in human umbilical vein endothelial cells*. Diabetes, 2006. **55**(1): p. 120-7.
209. Golubitzky, A., et al., *Screening for active small molecules in mitochondrial complex I deficient patient's fibroblasts, reveals AICAR as the most beneficial compound*. PLoS One, 2011. **6**(10): p. e26883.
210. Komen, J.C. and D.R. Thorburn, *Turn up the power - pharmacological activation of mitochondrial biogenesis in mouse models*. Br J Pharmacol, 2014. **171**(8): p. 1818-36.
211. Canto, C., et al., *AMPK regulates energy expenditure by modulating NAD+ metabolism and SIRT1 activity*. Nature, 2009. **458**(7241): p. 1056-60.
212. Dugan, L.L., et al., *AMPK dysregulation promotes diabetes-related reduction of superoxide and mitochondrial function*. J Clin Invest, 2013. **123**(11): p. 4888-99.
213. Csiszar, A., et al., *Resveratrol induces mitochondrial biogenesis in endothelial cells*. Am J Physiol Heart Circ Physiol, 2009. **297**(1): p. H13-20.
214. Menzies, K.J., et al., *Sirtuin 1-mediated effects of exercise and resveratrol on mitochondrial biogenesis*. J Biol Chem, 2013. **288**(10): p. 6968-79.
215. Wang, B., et al., *Resveratrol preserves mitochondrial function, stimulates mitochondrial biogenesis, and attenuates oxidative stress in regulatory T cells of mice fed a high-fat diet*. J Food Sci, 2014. **79**(9): p. H1823-31.

216. Lagouge, M., et al., *Resveratrol improves mitochondrial function and protects against metabolic disease by activating SIRT1 and PGC-1alpha*. Cell, 2006. **127**(6): p. 1109-22.
217. Minor, R.K., et al., *SIRT1720 improves survival and healthspan of obese mice*. Sci Rep, 2011. **1**: p. 70.
218. Funk, J.A. and R.G. Schnellmann, *Accelerated recovery of renal mitochondrial and tubule homeostasis with SIRT1/PGC-1alpha activation following ischemia-reperfusion injury*. Toxicol Appl Pharmacol, 2013. **273**(2): p. 345-54.
219. Wills, L.P., et al., *The beta2-adrenoceptor agonist formoterol stimulates mitochondrial biogenesis*. J Pharmacol Exp Ther, 2012. **342**(1): p. 106-18.
220. Rasbach, K.A., et al., *5-hydroxytryptamine receptor stimulation of mitochondrial biogenesis*. J Pharmacol Exp Ther, 2010. **332**(2): p. 632-9.
221. Tedesco, L., et al., *Cannabinoid type 1 receptor blockade promotes mitochondrial biogenesis through endothelial nitric oxide synthase expression in white adipocytes*. Diabetes, 2008. **57**(8): p. 2028-36.
222. Sarma, S., *Use of clinically available PPAR agonists for heart failure; do the risks outweigh the potential benefits?* Curr Mol Pharmacol, 2012. **5**(2): p. 255-63.
223. Sarma, S., H. Ardehali, and M. Gheorghide, *Enhancing the metabolic substrate: PPAR-alpha agonists in heart failure*. Heart Fail Rev, 2012. **17**(1): p. 35-43.
224. Elijah, I.E., et al., *Role of the PPAR-alpha agonist fenofibrate in severe pediatric burn*. Burns, 2012. **38**(4): p. 481-6.
225. Cho, Y.R., et al., *Therapeutic effects of fenofibrate on diabetic peripheral neuropathy by improving endothelial and neural survival in db/db mice*. PLoS One, 2014. **9**(1): p. e83204.
226. Grabacka, M., M. Pierzchalska, and K. Reiss, *Peroxisome proliferator activated receptor alpha ligands as anticancer drugs targeting mitochondrial metabolism*. Curr Pharm Biotechnol, 2013. **14**(3): p. 342-56.
227. Bogacka, I., et al., *Pioglitazone induces mitochondrial biogenesis in human subcutaneous adipose tissue in vivo*. Diabetes, 2005. **54**(5): p. 1392-9.
228. Pardo, R., et al., *Rosiglitazone-induced mitochondrial biogenesis in white adipose tissue is independent of peroxisome proliferator-activated receptor gamma coactivator-1alpha*. PLoS One, 2011. **6**(11): p. e26989.
229. Kleiner, S., et al., *PPAR{delta} agonism activates fatty acid oxidation via PGC-1{alpha} but does not increase mitochondrial gene expression and function*. J Biol Chem, 2009. **284**(28): p. 18624-33.
230. Weber, K., et al., *Glucocorticoid hormone stimulates mitochondrial biogenesis specifically in skeletal muscle*. Endocrinology, 2002. **143**(1): p. 177-84.
231. Tiao, M.M., et al., *Dexamethasone decreases cholestatic liver injury via inhibition of intrinsic pathway with simultaneous enhancement of mitochondrial biogenesis*. Steroids, 2011. **76**(7): p. 660-6.
232. De Toni, L., et al., *Effects of type 5-phosphodiesterase inhibition on energy metabolism and mitochondrial biogenesis in human adipose tissue ex vivo*. J Endocrinol Invest, 2011. **34**(10): p. 738-41.
233. Nisoli, E., et al., *Mitochondrial biogenesis by NO yields functionally active mitochondria in mammals*. Proc Natl Acad Sci U S A, 2004. **101**(47): p. 16507-12.
234. Valerio, A., et al., *TNF-alpha downregulates eNOS expression and mitochondrial biogenesis in fat and muscle of obese rodents*. J Clin Invest, 2006. **116**(10): p. 2791-8.
235. Trevellin, E., et al., *Exercise training induces mitochondrial biogenesis and glucose uptake in subcutaneous adipose tissue through eNOS-dependent mechanisms*. Diabetes, 2014. **63**(8): p. 2800-11.

236. Vettor, R., et al., *Exercise training boosts eNOS-dependent mitochondrial biogenesis in mouse heart: role in adaptation of glucose metabolism*. Am J Physiol Endocrinol Metab, 2014. **306**(5): p. E519-28.
237. Salloum, F.N., et al., *Cinaciguat, a novel activator of soluble guanylate cyclase, protects against ischemia/reperfusion injury: role of hydrogen sulfide*. Am J Physiol Heart Circ Physiol, 2012. **302**(6): p. H1347-54.
238. Vandendriessche, B., et al., *The soluble guanylate cyclase activator BAY 58-2667 protects against morbidity and mortality in endotoxic shock by recoupling organ systems*. PLoS One, 2013. **8**(8): p. e72155.
239. Miyashita, K., et al., *Natriuretic peptides/cGMP/cGMP-dependent protein kinase cascades promote muscle mitochondrial biogenesis and prevent obesity*. Diabetes, 2009. **58**(12): p. 2880-92.
240. Engeli, S., et al., *Natriuretic peptides enhance the oxidative capacity of human skeletal muscle*. J Clin Invest, 2012. **122**(12): p. 4675-9.
241. Bordicchia, M., et al., *Cardiac natriuretic peptides act via p38 MAPK to induce the brown fat thermogenic program in mouse and human adipocytes*. J Clin Invest, 2012. **122**(3): p. 1022-36.
242. Rehman, H., et al., *Green tea polyphenols stimulate mitochondrial biogenesis and improve renal function after chronic cyclosporin a treatment in rats*. PLoS One, 2014. **8**(6): p. e65029.
243. Shen, W., et al., *Lipoamide or lipoic acid stimulates mitochondrial biogenesis in 3T3-L1 adipocytes via the endothelial NO synthase-cGMP-protein kinase G signalling pathway*. Br J Pharmacol, 2011. **162**(5): p. 1213-24.
244. Rasbach, K.A. and R.G. Schnellmann, *Isoflavones promote mitochondrial biogenesis*. J Pharmacol Exp Ther, 2008. **325**(2): p. 536-43.
245. Davis, J.M., et al., *Quercetin increases brain and muscle mitochondrial biogenesis and exercise tolerance*. Am J Physiol Regul Integr Comp Physiol, 2009. **296**(4): p. R1071-7.
246. Rayamajhi, N., et al., *Quercetin induces mitochondrial biogenesis through activation of HO-1 in HepG2 cells*. Oxid Med Cell Longev, 2013. **2013**: p. 154279.
247. Thomas, R.R., et al., *Recombinant human mitochondrial transcription factor A stimulates mitochondrial biogenesis and ATP synthesis, improves motor function after MPTP, reduces oxidative stress and increases survival after endotoxin*. Mitochondrion, 2011. **11**(1): p. 108-18.
248. Thomas, R.R., et al., *RhTFAM treatment stimulates mitochondrial oxidative metabolism and improves memory in aged mice*. Aging (Albany NY), 2012. **4**(9): p. 620-35.
249. Iyer, S., et al., *Mitochondrial gene therapy improves respiration, biogenesis, and transcription in G11778A Leber's hereditary optic neuropathy and T8993G Leigh's syndrome cells*. Hum Gene Ther, 2012. **23**(6): p. 647-57.
250. Hardie, D.G., *AMP-activated protein kinase: an energy sensor that regulates all aspects of cell function*. Genes Dev, 2011. **25**(18): p. 1895-908.
251. Narkar, V.A., et al., *AMPK and PPARdelta agonists are exercise mimetics*. Cell, 2008. **134**(3): p. 405-15.
252. Russell, R.R., 3rd, et al., *Translocation of myocardial GLUT-4 and increased glucose uptake through activation of AMPK by AICAR*. Am J Physiol, 1999. **277**(2 Pt 2): p. H643-9.
253. Lempiainen, J., et al., *AMPK activator AICAR ameliorates ischaemia reperfusion injury in the rat kidney*. Br J Pharmacol, 2012. **166**(6): p. 1905-15.
254. Pold, R., et al., *Long-term AICAR administration and exercise prevents diabetes in ZDF rats*. Diabetes, 2005. **54**(4): p. 928-34.
255. Morigi, M., et al., *Sirtuin 3-dependent mitochondrial dynamic improvements protect against acute kidney injury*. J Clin Invest, 2015. **125**(2): p. 715-26.

256. Canto, C. and J. Auwerx, *PGC-1alpha, SIRT1 and AMPK, an energy sensing network that controls energy expenditure*. *Curr Opin Lipidol*, 2009. **20**(2): p. 98-105.
257. Sun, A.Y., et al., *Resveratrol as a therapeutic agent for neurodegenerative diseases*. *Mol Neurobiol*, 2010. **41**(2-3): p. 375-83.
258. Ferretta, A., et al., *Effect of resveratrol on mitochondrial function: implications in parkin-associated familial Parkinson's disease*. *Biochim Biophys Acta*, 2014. **1842**(7): p. 902-15.
259. Pasinetti, G.M., et al., *Neuroprotective and metabolic effects of resveratrol: therapeutic implications for Huntington's disease and other neurodegenerative disorders*. *Exp Neurol*, 2011. **232**(1): p. 1-6.
260. Petrovski, G., N. Gurusamy, and D.K. Das, *Resveratrol in cardiovascular health and disease*. *Ann N Y Acad Sci*, 2011. **1215**: p. 22-33.
261. Kanamori, H., et al., *Resveratrol reverses remodeling in hearts with large, old myocardial infarctions through enhanced autophagy-activating AMP kinase pathway*. *Am J Pathol*, 2013. **182**(3): p. 701-13.
262. Rivera, L., et al., *Long-term resveratrol administration reduces metabolic disturbances and lowers blood pressure in obese Zucker rats*. *Biochem Pharmacol*, 2009. **77**(6): p. 1053-63.
263. Beaudeau, J.L., V. Nivet-Antoine, and P. Giral, *Resveratrol: a relevant pharmacological approach for the treatment of metabolic syndrome?* *Curr Opin Clin Nutr Metab Care*, 2010. **13**(6): p. 729-36.
264. Brasnyo, P., et al., *Resveratrol improves insulin sensitivity, reduces oxidative stress and activates the Akt pathway in type 2 diabetic patients*. *Br J Nutr*, 2011. **106**(3): p. 383-9.
265. Milne, J.C., et al., *Small molecule activators of SIRT1 as therapeutics for the treatment of type 2 diabetes*. *Nature*, 2007. **450**(7170): p. 712-6.
266. de Boer, V.C., et al., *SIRT1 stimulation by polyphenols is affected by their stability and metabolism*. *Mech Ageing Dev*, 2006. **127**(7): p. 618-27.
267. Haigis, M.C., et al., *SIRT3 is a mitochondrial tumor suppressor: a scientific tale that connects aberrant cellular ROS, the Warburg effect, and carcinogenesis*. *Cancer Res*, 2012. **72**(10): p. 2468-72.
268. Hoshino, D., et al., *Clenbuterol, a beta2-adrenergic agonist, reciprocally alters PGC-1 alpha and RIP140 and reduces fatty acid and pyruvate oxidation in rat skeletal muscle*. *Am J Physiol Regul Integr Comp Physiol*, 2012. **302**(3): p. R373-84.
269. Peterson, Y.K., et al., *beta2-Adrenoceptor agonists in the regulation of mitochondrial biogenesis*. *Bioorg Med Chem Lett*, 2013. **23**(19): p. 5376-81.
270. Nisoli, E., et al., *Mitochondrial biogenesis in mammals: the role of endogenous nitric oxide*. *Science*, 2003. **299**(5608): p. 896-9.
271. Nisoli, E. and M.O. Carruba, *Nitric oxide and mitochondrial biogenesis*. *J Cell Sci*, 2006. **119**(Pt 14): p. 2855-62.
272. Miglio, G., et al., *PPARgamma stimulation promotes mitochondrial biogenesis and prevents glucose deprivation-induced neuronal cell loss*. *Neurochem Int*, 2009. **55**(7): p. 496-504.
273. Wu, Q.Q., et al., *Bardoxolone methyl (BARD) ameliorates ischemic AKI and increases expression of protective genes Nrf2, PPARgamma, and HO-1*. *Am J Physiol Renal Physiol*, 2011. **300**(5): p. F1180-92.
274. Singh, J.P., A.P. Singh, and R. Bhatti, *Explicit role of peroxisome proliferator-activated receptor gamma in gallic acid-mediated protection against ischemia-reperfusion-induced acute kidney injury in rats*. *J Surg Res*, 2014. **187**(2): p. 631-9.
275. Stallons, L.J., R.M. Whitaker, and R.G. Schnellmann, *Suppressed mitochondrial biogenesis in folic acid-induced acute kidney injury and early fibrosis*. *Toxicol Lett*, 2014. **224**(3): p. 326-32.

276. Smith, J.A., et al., *Suppression of mitochondrial biogenesis through toll-like receptor 4-dependent mitogen-activated protein kinase kinase/extracellular signal-regulated kinase signaling in endotoxin-induced acute kidney injury*. J Pharmacol Exp Ther, 2015. **352**(2): p. 346-57.
277. Rong, J.X., et al., *Adipose mitochondrial biogenesis is suppressed in db/db and high-fat diet-fed mice and improved by rosiglitazone*. Diabetes, 2007. **56**(7): p. 1751-60.
278. Chistiakov, D.A., et al., *Mitochondrial aging and age-related dysfunction of mitochondria*. Biomed Res Int, 2014. **2014**: p. 238463.
279. Koltai, E., et al., *Age-associated declines in mitochondrial biogenesis and protein quality control factors are minimized by exercise training*. Am J Physiol Regul Integr Comp Physiol, 2012. **303**(2): p. R127-34.
280. Palomer, X., et al., *TNF-alpha reduces PGC-1alpha expression through NF-kappaB and p38 MAPK leading to increased glucose oxidation in a human cardiac cell model*. Cardiovasc Res, 2009. **81**(4): p. 703-12.
281. Zhang, Q., et al., *Circulating mitochondrial DAMPs cause inflammatory responses to injury*. Nature, 2010. **464**(7285): p. 104-7.
282. Ye, L., et al., *TRPV4 is a regulator of adipose oxidative metabolism, inflammation, and energy homeostasis*. Cell, 2012. **151**(1): p. 96-110.
283. Arany, Z., et al., *Gene expression-based screening identifies microtubule inhibitors as inducers of PGC-1alpha and oxidative phosphorylation*. Proc Natl Acad Sci U S A, 2008. **105**(12): p. 4721-6.
284. Beeson, C.C., G.C. Beeson, and R.G. Schnellmann, *A high-throughput respirometric assay for mitochondrial biogenesis and toxicity*. Anal Biochem, 2010. **404**(1): p. 75-81.
285. Wills, L.P., et al., *High-throughput respirometric assay identifies predictive toxicophore of mitochondrial injury*. Toxicol Appl Pharmacol, 2013. **272**(2): p. 490-502.
286. Choumar, A., et al., *Lipopolysaccharide-induced mitochondrial DNA depletion*. Antioxid Redox Signal, 2011. **15**(11): p. 2837-54.
287. Pundik, S., K. Xu, and S. Sundararajan, *Reperfusion brain injury: focus on cellular bioenergetics*. Neurology, 2012. **79**(13 Suppl 1): p. S44-51.
288. Bayeva, M., M. Gheorghiadu, and H. Ardehali, *Mitochondria as a therapeutic target in heart failure*. J Am Coll Cardiol, 2013. **61**(6): p. 599-610.
289. Cheng, Z. and M. Ristow, *Mitochondria and metabolic homeostasis*. Antioxid Redox Signal, 2013. **19**(3): p. 240-2.
290. Cooper, M.P., *Interplay of mitochondrial biogenesis and oxidative stress in heart failure*. Circulation, 2013. **127**(19): p. 1932-4.
291. Hwang, O., *Role of oxidative stress in Parkinson's disease*. Exp Neurobiol, 2013. **22**(1): p. 11-7.
292. Yan, M.H., X. Wang, and X. Zhu, *Mitochondrial defects and oxidative stress in Alzheimer disease and Parkinson disease*. Free Radic Biol Med, 2013. **62**: p. 90-101.
293. Weinberg, J.M., *Mitochondrial biogenesis in kidney disease*. J Am Soc Nephrol, 2011. **22**(3): p. 431-6.
294. Venkatachalam, M.A. and J.M. Weinberg, *The tubule pathology of septic acute kidney injury: a neglected area of research comes of age*. Kidney Int, 2012. **81**(4): p. 338-40.
295. Shaw, J.M. and D.R. Winge, *Shaping the mitochondrion: mitochondrial biogenesis, dynamics and dysfunction*. Conference on Mitochondrial Assembly and Dynamics in Health and Disease. EMBO Rep, 2009. **10**(12): p. 1301-5.
296. Kubli, D.A. and A.B. Gustafsson, *Mitochondria and mitophagy: the yin and yang of cell death control*. Circ Res, 2012. **111**(9): p. 1208-21.
297. Tran, M., et al., *PGC-1alpha promotes recovery after acute kidney injury during systemic inflammation in mice*. J Clin Invest, 2011. **121**(10): p. 4003-14.

298. Kang, C. and L. Li Ji, *Role of PGC-1alpha signaling in skeletal muscle health and disease*. Ann N Y Acad Sci, 2012. **1271**: p. 110-7.
299. Wenz, T., *Regulation of mitochondrial biogenesis and PGC-1alpha under cellular stress*. Mitochondrion, 2013. **13**(2): p. 134-42.
300. Wu, Z., et al., *Mechanisms controlling mitochondrial biogenesis and respiration through the thermogenic coactivator PGC-1*. Cell, 1999. **98**(1): p. 115-24.
301. Liang, H. and W.F. Ward, *PGC-1alpha: a key regulator of energy metabolism*. Adv Physiol Educ, 2006. **30**(4): p. 145-51.
302. Tadaishi, M., et al., *Effect of exercise intensity and AICAR on isoform-specific expressions of murine skeletal muscle PGC-1alpha mRNA: a role of beta(2)-adrenergic receptor activation*. Am J Physiol Endocrinol Metab, 2011. **300**(2): p. E341-9.
303. Muller, T.D., et al., *p62 links beta-adrenergic input to mitochondrial function and thermogenesis*. J Clin Invest, 2013. **123**(1): p. 469-78.
304. Francis, S.H., M.A. Blount, and J.D. Corbin, *Mammalian cyclic nucleotide phosphodiesterases: molecular mechanisms and physiological functions*. Physiol Rev, 2011. **91**(2): p. 651-90.
305. Bender, A.T. and J.A. Beavo, *Cyclic nucleotide phosphodiesterases: molecular regulation to clinical use*. Pharmacol Rev, 2006. **58**(3): p. 488-520.
306. Nowak, G. and R.G. Schnellmann, *Integrative effects of EGF on metabolism and proliferation in renal proximal tubular cells*. Am J Physiol, 1995. **269**(5 Pt 1): p. C1317-25.
307. Chida, J., et al., *An efficient extraction method for quantitation of adenosine triphosphate in mammalian tissues and cells*. Anal Chim Acta, 2012. **727**: p. 8-12.
308. Cruickshank, J.M., *Phosphodiesterase III inhibitors: long-term risks and short-term benefits*. Cardiovasc Drugs Ther, 1993. **7**(4): p. 655-60.
309. Lifshitz, J., et al., *Mitochondrial damage and dysfunction in traumatic brain injury*. Mitochondrion, 2004. **4**(5-6): p. 705-13.
310. Fernandez-Marcos, P.J. and J. Auwerx, *Regulation of PGC-1alpha, a nodal regulator of mitochondrial biogenesis*. Am J Clin Nutr, 2011. **93**(4): p. 884S-90.
311. Miura, S., et al., *An increase in murine skeletal muscle peroxisome proliferator-activated receptor-gamma coactivator-1alpha (PGC-1alpha) mRNA in response to exercise is mediated by beta-adrenergic receptor activation*. Endocrinology, 2007. **148**(7): p. 3441-8.
312. Mammadov, E., et al., *Protective effects of phosphodiesterase-4-specific inhibitor rolipram on acute ischemia-reperfusion injury in rat kidney*. Urology, 2012. **80**(6): p. 1390 e1-6.
313. Lee, K.W., et al., *Sildenafil attenuates renal injury in an experimental model of rat cisplatin-induced nephrotoxicity*. Toxicology, 2009. **257**(3): p. 137-43.
314. Sohotnik, R., et al., *Phosphodiesterase-5 inhibition attenuates early renal ischemia-reperfusion-induced acute kidney injury: assessment by quantitative measurement of urinary NGAL and KIM-1*. Am J Physiol Renal Physiol, 2013. **304**(8): p. F1099-104.
315. Bellomo, R., J.A. Kellum, and C. Ronco, *Acute kidney injury*. Lancet, 2012. **380**(9843): p. 756-66.
316. Brade, W., H. Herken, and H.J. Merker, *Regeneration of renal tubular cells after lesion by temporary ischaemia, folic acid, and 2,4,5-triamino 6-styrylpyrimidine*. Naunyn Schmiedebergs Arch Pharmacol, 1970. **266**(1): p. 95-100.
317. Long, D.A., et al., *Angiopoietin-1 therapy enhances fibrosis and inflammation following folic acid-induced acute renal injury*. Kidney Int, 2008. **74**(3): p. 300-9.
318. Schmidt, U., et al., *Acute renal failure after folate: NaK ATPase in isolated rat renal tubule. Ultramicrochemical and clinical studies*. Eur J Clin Invest, 1973. **3**(3): p. 169-78.
319. Levey, A.S. and J. Coresh, *Chronic kidney disease*. Lancet, 2012. **379**(9811): p. 165-80.
320. Fine, L.G. and J.T. Norman, *Chronic hypoxia as a mechanism of progression of chronic kidney diseases: from hypothesis to novel therapeutics*. Kidney Int, 2008. **74**(7): p. 867-72.

321. Kim, J., et al., *Reactive oxygen species/oxidative stress contributes to progression of kidney fibrosis following transient ischemic injury in mice*. *Am J Physiol Renal Physiol*, 2009. **297**(2): p. F461-70.
322. Seok, Y.M., et al., *Wen-pi-tang-Hab-Wu-ling-san attenuates kidney fibrosis induced by ischemia/reperfusion in mice*. *Phytother Res*, 2008. **22**(8): p. 1057-63.
323. Lo, L.J., et al., *Dialysis-requiring acute renal failure increases the risk of progressive chronic kidney disease*. *Kidney Int*, 2009. **76**(8): p. 893-9.
324. Leelahavanichkul, A., et al., *Angiotensin II overcomes strain-dependent resistance of rapid CKD progression in a new remnant kidney mouse model*. *Kidney Int*, 2010. **78**(11): p. 1136-53.
325. Kapitsinou, P.P., et al., *Preischemic targeting of HIF prolyl hydroxylation inhibits fibrosis associated with acute kidney injury*. *Am J Physiol Renal Physiol*, 2012. **302**(9): p. F1172-9.
326. Szeto, H.H., et al., *Mitochondria-targeted peptide accelerates ATP recovery and reduces ischemic kidney injury*. *J Am Soc Nephrol*, 2011. **22**(6): p. 1041-52.
327. Zager, R.A., A.C. Johnson, and S.Y. Hanson, *Proximal tubular cytochrome c efflux: determinant, and potential marker, of mitochondrial injury*. *Kidney Int*, 2004. **65**(6): p. 2123-34.
328. Lan, R., et al., *PTEN loss defines a TGF-beta-induced tubule phenotype of failed differentiation and JNK signaling during renal fibrosis*. *Am J Physiol Renal Physiol*, 2012. **302**(9): p. F1210-23.
329. Yuan, Y., et al., *Mitochondrial dysfunction accounts for aldosterone-induced epithelial-to-mesenchymal transition of renal proximal tubular epithelial cells*. *Free Radic Biol Med*, 2012. **53**(1): p. 30-43.
330. Wen, X., et al., *One dose of cyclosporine A is protective at initiation of folic acid-induced acute kidney injury in mice*. *Nephrol Dial Transplant*, 2012. **27**(8): p. 3100-9.
331. Korrapati, M.C., B.E. Shaner, and R.G. Schnellmann, *Recovery from glycerol-induced acute kidney injury is accelerated by suramin*. *J Pharmacol Exp Ther*, 2012. **341**(1): p. 126-36.
332. Junqueira, L.C., G. Bignolas, and R.R. Brentani, *Picrosirius staining plus polarization microscopy, a specific method for collagen detection in tissue sections*. *Histochem J*, 1979. **11**(4): p. 447-55.
333. Schrier, R.W., *Renal and electrolyte disorders*. 7th ed. 2010, Philadelphia: Wolters Kluwer Health/Lippincott Williams & Wilkins. vii, 631 p.
334. Doi, K., et al., *Pre-existing renal disease promotes sepsis-induced acute kidney injury and worsens outcome*. *Kidney Int*, 2008. **74**(8): p. 1017-25.
335. Hickey, F.B., et al., *IHG-1 promotes mitochondrial biogenesis by stabilizing PGC-1alpha*. *J Am Soc Nephrol*, 2011. **22**(8): p. 1475-85.
336. Wenz, T., et al., *Increased muscle PGC-1alpha expression protects from sarcopenia and metabolic disease during aging*. *Proc Natl Acad Sci U S A*, 2009. **106**(48): p. 20405-10.
337. Suliman, H.B., et al., *The CO/HO system reverses inhibition of mitochondrial biogenesis and prevents murine doxorubicin cardiomyopathy*. *J Clin Invest*, 2007. **117**(12): p. 3730-41.
338. Ishani, A., et al., *Acute kidney injury increases risk of ESRD among elderly*. *J Am Soc Nephrol*, 2009. **20**(1): p. 223-8.
339. Wald, R., et al., *Chronic dialysis and death among survivors of acute kidney injury requiring dialysis*. *JAMA*, 2009. **302**(11): p. 1179-85.
340. Farris, A.B., et al., *Morphometric and visual evaluation of fibrosis in renal biopsies*. *J Am Soc Nephrol*, 2011. **22**(1): p. 176-86.
341. Grgic, I., et al., *Targeted proximal tubule injury triggers interstitial fibrosis and glomerulosclerosis*. *Kidney Int*, 2012. **82**(2): p. 172-83.
342. Bechtel, W., et al., *Methylation determines fibroblast activation and fibrogenesis in the kidney*. *Nat Med*, 2010. **16**(5): p. 544-50.
343. Choudhury, D. and Z. Ahmed, *Drug-associated renal dysfunction and injury*. *Nat Clin Pract Nephrol*, 2006. **2**(2): p. 80-91.

344. Liborio, A.B., et al., *AKI complications in critically ill patients: association with mortality rates and RRT*. Clin J Am Soc Nephrol, 2015. **10**(1): p. 21-8.
345. Hall, A.M., *Maintaining mitochondrial morphology in AKI: looks matter*. J Am Soc Nephrol, 2013. **24**(8): p. 1185-7.
346. Nisoli, E., et al., *Can endogenous gaseous messengers control mitochondrial biogenesis in mammalian cells?* Prostaglandins Other Lipid Mediat, 2004. **73**(1-2): p. 9-27.
347. Straub, A., et al., *NO-independent stimulators of soluble guanylate cyclase*. Bioorg Med Chem Lett, 2001. **11**(6): p. 781-4.
348. Stasch, J.P., et al., *NO-independent regulatory site on soluble guanylate cyclase*. Nature, 2001. **410**(6825): p. 212-5.
349. Nossaman, B., E. Pankey, and P. Kadowitz, *Stimulators and activators of soluble guanylate cyclase: review and potential therapeutic indications*. Crit Care Res Pract, 2012. **2012**: p. 290805.
350. Chester, M., et al., *Cinaciguat, a soluble guanylate cyclase activator, augments cGMP after oxidative stress and causes pulmonary vasodilation in neonatal pulmonary hypertension*. Am J Physiol Lung Cell Mol Physiol, 2011. **301**(5): p. L755-64.
351. Stasch, J.P., P. Pacher, and O.V. Evgenov, *Soluble guanylate cyclase as an emerging therapeutic target in cardiopulmonary disease*. Circulation, 2011. **123**(20): p. 2263-73.
352. Radovits, T., et al., *Pre-conditioning with the soluble guanylate cyclase activator Cinaciguat reduces ischaemia-reperfusion injury after cardiopulmonary bypass*. Eur J Cardiothorac Surg, 2011. **39**(2): p. 248-55.
353. Zhuang, S., et al., *Suramin promotes recovery from renal ischemia/reperfusion injury in mice*. Kidney Int, 2009. **75**(3): p. 304-11.
354. Choi, D.E., et al., *Pretreatment of sildenafil attenuates ischemia-reperfusion renal injury in rats*. Am J Physiol Renal Physiol, 2009. **297**(2): p. F362-70.
355. Medeiros, P.J., et al., *Effect of sildenafil in renal ischemia/reperfusion injury in rats*. Acta Cir Bras, 2010. **25**(6): p. 490-5.
356. Heung, M. and L.S. Chawla, *Acute kidney injury: gateway to chronic kidney disease*. Nephron Clin Pract, 2014. **127**(1-4): p. 30-4.
357. Khairoun, M., et al., *Renal ischemia-reperfusion induces a dysbalance of angiopoietins, accompanied by proliferation of pericytes and fibrosis*. Am J Physiol Renal Physiol, 2013. **305**(6): p. F901-10.
358. Curci, C., et al., *Endothelial-to-mesenchymal transition and renal fibrosis in ischaemia/reperfusion injury are mediated by complement anaphylatoxins and Akt pathway*. Nephrol Dial Transplant, 2014. **29**(4): p. 799-808.
359. Akcay, A., Q. Nguyen, and C.L. Edelstein, *Mediators of inflammation in acute kidney injury*. Mediators Inflamm, 2009. **2009**: p. 137072.
360. Lopez-Armada, M.J., et al., *Mitochondrial dysfunction and the inflammatory response*. Mitochondrion, 2013. **13**(2): p. 106-18.
361. Zhang, J., et al., *Identification of nitric oxide as an endogenous activator of the AMP-activated protein kinase in vascular endothelial cells*. J Biol Chem, 2008. **283**(41): p. 27452-61.
362. Betz, B., et al., *Rosiglitazone affects nitric oxide synthases and improves renal outcome in a rat model of severe ischemia/reperfusion injury*. PPAR Res, 2012. **2012**: p. 219319.
363. Sivitz, W.I. and M.A. Yorek, *Mitochondrial dysfunction in diabetes: from molecular mechanisms to functional significance and therapeutic opportunities*. Antioxid Redox Signal, 2010. **12**(4): p. 537-77.
364. Federico, A., et al., *Mitochondria, oxidative stress and neurodegeneration*. J Neurol Sci, 2012. **322**(1-2): p. 254-62.
365. Griffiths, E.J., *Mitochondria and heart disease*. Adv Exp Med Biol, 2012. **942**: p. 249-67.

366. Peters, H., et al., *Expression and activity of soluble guanylate cyclase in injury and repair of anti-thy1 glomerulonephritis*. *Kidney Int*, 2004. **66**(6): p. 2224-36.
367. Wang, Y., et al., *Enhancing cGMP in experimental progressive renal fibrosis: soluble guanylate cyclase stimulation vs. phosphodiesterase inhibition*. *Am J Physiol Renal Physiol*, 2006. **290**(1): p. F167-76.
368. Kemp-Harper, B. and H.H. Schmidt, *cGMP in the vasculature*. *Handb Exp Pharmacol*, 2009(191): p. 447-67.
369. Linden, E., et al., *Endothelial dysfunction in patients with chronic kidney disease results from advanced glycation end products (AGE)-mediated inhibition of endothelial nitric oxide synthase through RAGE activation*. *Clin J Am Soc Nephrol*, 2008. **3**(3): p. 691-8.
370. Oemar, B.S., et al., *Reduced endothelial nitric oxide synthase expression and production in human atherosclerosis*. *Circulation*, 1998. **97**(25): p. 2494-8.
371. Wang, W., et al., *Endothelial nitric oxide synthase-deficient mice exhibit increased susceptibility to endotoxin-induced acute renal failure*. *Am J Physiol Renal Physiol*, 2004. **287**(5): p. F1044-8.
372. James, M.T. and R. Wald, *AKI: not just a short-term problem?* *Clin J Am Soc Nephrol*, 2014. **9**(3): p. 435-6.
373. Avula, S., et al., *Treatment of mitochondrial disorders*. *Curr Treat Options Neurol*, 2014. **16**(6): p. 292.
374. Pfeffer, G., et al., *New treatments for mitochondrial disease-no time to drop our standards*. *Nat Rev Neurol*, 2013. **9**(8): p. 474-81.
375. Alge, J.L., et al., *Urinary angiotensinogen and risk of severe AKI*. *Clin J Am Soc Nephrol*, 2013. **8**(2): p. 184-93.
376. Korrapati, M.C., et al., *Suramin: a potential therapy for diabetic nephropathy*. *PLoS One*, 2013. **8**(9): p. e73655.
377. Korrapati, M.C., et al., *Diabetes-induced renal injury in rats is attenuated by suramin*. *J Pharmacol Exp Ther*, 2012. **343**(1): p. 34-43.
378. Ball, L.E., M.N. Berkaw, and M.G. Buse, *Identification of the major site of O-linked beta-N-acetylglucosamine modification in the C terminus of insulin receptor substrate-1*. *Mol Cell Proteomics*, 2006. **5**(2): p. 313-23.
379. Nath, K.A., et al., *Intracellular targets in heme protein-induced renal injury*. *Kidney international*, 1998. **53**(1): p. 100-11.
380. Small, D.M. and G.C. Gobe, *Cytochrome c: potential as a noninvasive biomarker of drug-induced acute kidney injury*. *Expert Opin Drug Metab Toxicol*, 2012. **8**(6): p. 655-64.
381. Case, J., et al., *Epidemiology of acute kidney injury in the intensive care unit*. *Crit Care Res Pract*, 2013. **2013**: p. 479730.
382. Schiffli, H., *Severity of post-cardiac surgery acute kidney injury and long-term mortality: is chronic kidney disease the missing link?* *Crit Care*, 2014. **18**(2): p. 424.
383. Wu, V.C., et al., *Long-term outcomes after dialysis-requiring acute kidney injury*. *Biomed Res Int*, 2014. **2014**: p. 365186.
384. Rosner, M.H. and M.D. Okusa, *Acute kidney injury associated with cardiac surgery*. *Clin J Am Soc Nephrol*, 2006. **1**(1): p. 19-32.
385. Ryden, L., et al., *Acute Kidney Injury After Coronary Artery Bypass Grafting and Long-Term Risk of End-Stage Renal Disease*. *Circulation*, 2014.
386. Lopez-Delgado, J.C., et al., *Influence of acute kidney injury on short- and long-term outcomes in patients undergoing cardiac surgery: risk factors and prognostic value of a modified RIFLE classification*. *Crit Care*, 2013. **17**(6): p. R293.

387. Machado, M.N., M.A. Nakazone, and L.N. Maia, *Prognostic value of acute kidney injury after cardiac surgery according to kidney disease: improving global outcomes definition and staging (KDIGO) criteria*. PLoS One, 2014. **9**(5): p. e98028.
388. Calvert, S. and A. Shaw, *Perioperative acute kidney injury*. Perioper Med (Lond), 2012. **1**: p. 6.
389. Akcay, A., et al., *Update on the diagnosis and management of acute kidney injury*. Int J Nephrol Renovasc Dis, 2010. **3**: p. 129-40.
390. Munshi, R., C. Hsu, and J. Himmelfarb, *Advances in understanding ischemic acute kidney injury*. BMC Med, 2011. **9**: p. 11.
391. Massoudy, P., et al., *Coronary artery bypass surgery and acute kidney injury--impact of the off-pump technique*. Nephrol Dial Transplant, 2008. **23**(9): p. 2853-60.
392. Gude, D. and R. Jha, *Acute kidney injury following cardiac surgery*. Ann Card Anaesth, 2012. **15**(4): p. 279-86.
393. Mariscalco, G., et al., *Acute kidney injury: a relevant complication after cardiac surgery*. Ann Thorac Surg, 2011. **92**(4): p. 1539-47.
394. Gu, X., et al., *The plasma mitochondrial DNA is an independent predictor for post-traumatic systemic inflammatory response syndrome*. PLoS One, 2013. **8**(8): p. e72834.
395. Pinti, M., C. Mussini, and A. Cossarizza, *Mitochondrial DNA: a proinflammatory 'enemy from within' during HIV infection?* Cell Death Dis, 2012. **3**: p. 307.
396. Jesinkey, S.R., et al., *Atomoxetine prevents dexamethasone-induced skeletal muscle atrophy in mice*. J Pharmacol Exp Ther, 2014.
397. Yang, X., et al., *Urinary Angiotensinogen Level Predicts AKI in Acute Decompensated Heart Failure: A Prospective, Two-Stage Study*. J Am Soc Nephrol, 2015.
398. Whitaker, R.M., et al., *Urinary ATP synthase subunit beta is a novel biomarker of renal mitochondrial dysfunction in acute kidney injury*. Toxicol Sci, 2015.
399. Liu, K.D. and P.R. Brakeman, *Renal repair and recovery*. Crit Care Med, 2008. **36**(4 Suppl): p. S187-92.
400. Guo, J.K. and L.G. Cantley, *Cellular maintenance and repair of the kidney*. Annu Rev Physiol, 2010. **72**: p. 357-76.
401. Weinberg, J.M., et al., *Anaerobic and aerobic pathways for salvage of proximal tubules from hypoxia-induced mitochondrial injury*. Am J Physiol Renal Physiol, 2000. **279**(5): p. F927-43.
402. de Geus, H.R., M.G. Betjes, and J. Bakker, *Biomarkers for the prediction of acute kidney injury: a narrative review on current status and future challenges*. Clin Kidney J, 2012. **5**(2): p. 102-108.
403. Devarajan, P., *Biomarkers for the early detection of acute kidney injury*. Curr Opin Pediatr, 2011. **23**(2): p. 194-200.
404. Honore, P.M., et al., *Biomarkers for early diagnosis of AKI in the ICU: ready for prime time use at the bedside?* Ann Intensive Care, 2012. **2**(1): p. 24.
405. Hall, I.E., et al., *Risk of poor outcomes with novel and traditional biomarkers at clinical AKI diagnosis*. Clin J Am Soc Nephrol, 2011. **6**(12): p. 2740-9.
406. Koyner, J.L., et al., *Biomarkers predict progression of acute kidney injury after cardiac surgery*. J Am Soc Nephrol, 2012. **23**(5): p. 905-14.
407. Arthur, J.M., et al., *Evaluation of 32 urine biomarkers to predict the progression of acute kidney injury after cardiac surgery*. Kidney Int, 2014. **85**(2): p. 431-8.
408. Ralib, A.M., et al., *Test characteristics of urinary biomarkers depend on quantitation method in acute kidney injury*. J Am Soc Nephrol, 2012. **23**(2): p. 322-33.
409. Zsengeller, Z.K., et al., *Cisplatin nephrotoxicity involves mitochondrial injury with impaired tubular mitochondrial enzyme activity*. J Histochem Cytochem, 2012. **60**(7): p. 521-9.

410. Feldkamp, T., A. Kribben, and J.M. Weinberg, *F1FO-ATPase activity and ATP dependence of mitochondrial energization in proximal tubules after hypoxia/reoxygenation*. J Am Soc Nephrol, 2005. **16**(6): p. 1742-51.
411. West, A.P., G.S. Shadel, and S. Ghosh, *Mitochondria in innate immune responses*. Nat Rev Immunol, 2011. **11**(6): p. 389-402.
412. Zhang, J.Z., et al., *Mitochondrial DNA induces inflammation and increases TLR9/NF-kappaB expression in lung tissue*. Int J Mol Med, 2014. **33**(4): p. 817-24.
413. Simmons, J.D., et al., *Elevated levels of plasma mitochondrial DNA DAMPs are linked to clinical outcome in severely injured human subjects*. Ann Surg, 2013. **258**(4): p. 591-6; discussion 596-8.
414. Ong, S.B., et al., *Inhibiting mitochondrial fission protects the heart against ischemia/reperfusion injury*. Circulation, 2010. **121**(18): p. 2012-22.
415. Chen, K.H., et al., *Dysregulation of HSG triggers vascular proliferative disorders*. Nat Cell Biol, 2004. **6**(9): p. 872-83.
416. Liu, T., et al., *Overexpression of mitofusin 2 inhibits reactive astroglial proliferation in vitro*. Neurosci Lett, 2014. **579**: p. 24-9.
417. Yanagishita, T., et al., *Protective effect of captopril on ischemic myocardium*. Jpn Circ J, 1997. **61**(2): p. 161-9.
418. Monaco, E.A., 3rd, G.M. Weiner, and R.M. Friedlander, *Randomized-controlled trial of minocycline for spinal cord injury shows promise*. Neurosurgery, 2013. **72**(2): p. N17-9.
419. Tang, K., P.D. Wagner, and E.C. Breen, *TNF-alpha-mediated reduction in PGC-1alpha may impair skeletal muscle function after cigarette smoke exposure*. J Cell Physiol, 2010. **222**(2): p. 320-7.
420. Alvarez-Guardia, D., et al., *The p65 subunit of NF-kappaB binds to PGC-1alpha, linking inflammation and metabolic disturbances in cardiac cells*. Cardiovasc Res, 2010. **87**(3): p. 449-58.
421. Yan, G., et al., *Tumor necrosis factor-alpha downregulates endothelial nitric oxide synthase mRNA stability via translation elongation factor 1-alpha 1*. Circ Res, 2008. **103**(6): p. 591-7.
422. Lee, H., et al., *MicroRNA-494, upregulated by tumor necrosis factor-alpha, desensitizes insulin effect in C2C12 muscle cells*. PLoS One, 2013. **8**(12): p. e83471.
423. Yamamoto, H., et al., *MicroRNA-494 regulates mitochondrial biogenesis in skeletal muscle through mitochondrial transcription factor A and Forkhead box j3*. Am J Physiol Endocrinol Metab, 2012. **303**(12): p. E1419-27.
424. Aoi, W., et al., *The microRNA miR-696 regulates PGC-1{alpha} in mouse skeletal muscle in response to physical activity*. Am J Physiol Endocrinol Metab, 2010. **298**(4): p. E799-806.